Analysis of Trastuzumab (Tzb) Sensitivity in HER2+ PTEN-Deficient Breast Cancer Using Single Cell RNA-Seq

by

Jamie Do

A dissertation submitted in partial fulfillment
of the requirements for the degree of
Doctor of Philosophy
(Chemical Biology)
in The University of Michigan
2020

Doctoral Committee:

Professor Duxin Sun, Co-Chair
Professor Shaomeng Wang, Co-Chair
Associate Professor Tomek Cierpicki
Associate Professor Lana Garmire
Associate Professor Zaneta Nikolovska-Coleska
Professor Max Wicha

Jamie Do

jamiepdo@umich.edu

ORCID iD: 0000-0003-2198-5462

Dedication

This dissertation is dedicated to Ba, Mẹ, và Em Thy.

Acknowledgements

I would like to thank Dr. Sun for being an excellent mentor to me over the years. I learned a great deal from him about how to develop scientific questions, how to formulate scientific hypotheses, and how to critically evaluate my scientific rationale. His office door has always been open to all of his students, and I always appreciated being able to stop in his office for a quick chat about how to improve my experiments. I would like to thank my co-advisor, Dr. Shaomeng Wang, for insightful conversations for both of my drug discovery and single cell transcriptomic projects. I would also like to thank my committee members: Dr. Tomasz Cierpicki, Dr. Lana Garmire, Dr. Zaneta Nikolovska-Coleska, and Dr. Max Wicha, whose feedback during committee meetings has helped improve my approaches for data analysis and strengthened my scientific reasoning. I would also like to acknowledge Dr. Jolanta Grembecka, Dr. Monika Burness, and Dr. Anna Mapp for insightful conversations about my project during committee meetings and scientific talks. Also, I would like to thank Dr. Mapp for being incredibly supportive of all of the PCB students, having the time to listen when I felt like I was struggling in school, and for offering solutions about how to overcome my academic struggles.

I would also like to thank past and present members of the Sun Lab. I would like to acknowledge my small group leader, Dr. Joe Burnett, who provided me with the PTEN knockdown cell lines, cell lines treated previously treated with trastuzumab for 3 months, and for teaching me Drop-seq and R. Thank you to Garrett for teaching me aseptic techniques for cell culture and for the delightful conversations we shared. To Inkyung, Mady, Alek, Yudong, and Hongxiang, thanks for all of our fun conversations about science, food, and life that we shared while working in lab. I also would like to acknowledge past Sun Lab members, Dr. Mari Gasparyan and Dr. Miao-Chia Lo, who invested a significant amount of time in helping me find my footing when I first joined the Sun Lab. Also, I will always remember the warm welcome I received from former lab mate, Nick Stevers, when I first joined the lab. I would like to acknowledge Dr. Olivia Koues,

Andrea Kuligowski, and the rest of the team at the Advanced Genomics Core for answering all of my questions about Tapestation, Bioanalyzer, and sequencing runs. I would like to thank Dr. Aaron Robida for helping me with my high throughput screening campaigns when I was working towards discovering small molecule inhibitors for the protein interaction between WDR5 and Myc. I would also like to acknowledge Dr. Jeanne Stuckey from the Center of Structural Biology for her crystallization studies for my drug discovery project. I would also like to thank Laura Howe and Traci Swan for providing PCB students with plenty of support over the years and for answering all of my PCB related questions.

I also need to thank my former mentors who provided me with the analytical toolkit that helped me succeed at the University of Michigan. I would first like to thank Dr. Jacqueline Trischman from CSUSM for giving me my first opportunity to learn as an undergraduate research student and for helping develop my confidence as a researcher. To my analytical and organic chemistry professor, Dr. G, thank you for pushing me to give my absolute best and to remember to be detail-oriented in all of my experiments. I would also like to thank my mentors from UCSD: Dr. Jerry Yang, Dr. Dan Sheik, Dr. Kevin Cao, Dr. Kevin Sibucao, and Dr. John Kim. My time in the Yang Lab during my Master's studies taught me a great deal about how to thug it out when things get hard and about effective scientific communication, both of which really helped me prepare for my Ph.D. studies. All of the grilling and tough conversations we had about how to improve my science were powerful lessons that taught me the art of how to learn, unlearn, and relearn scientific fundamentals.

I would also like to thank my family and friends for supporting me on my out of state adventure for my Ph.D studies. To my West Side friends: Zach, Tyler, Anna, and Erica, thank you so much for being there for me whenever I needed an ear and time. Zach and Anna, thanks so much for checking in on my family and me repeatedly after Dad passed away during my first year. Thank you for making sure that I was staying sane, especially when grad school became a severely exhausting journey for me. Thank you, Auntie Mailyn, Uncle Luis, Maria, Lori, Matt, Raymond, Kim, Di Phin, Uncle Tavner, Bac Mao, Dr. Tsui, and Coach Wes for being supportive in all of my aspirations. I would like

to thank my family for their constant support and love for me. I would like to thank my boyfriend Jeremy for his love and support throughout my grad school journey. It was an incredibly difficult journey, and I know I wasn't always the best person to deal with so I am grateful for the continual support and care you've given to me throughout the years, Jeremy. I would also like to thank Mr. and Mrs. Felton for their love, support, and encouragement throughout the years. Next, I would like to thank my sister, Diane, who has been my bestie. Thank you, buddy, for our daily conversations and laughs and for having so much patience with me when I go absolutely bonkers. I love the little gifts and cards you pick out for me as little pieces of home away from home. Lastly, I would like to thank my mom and late dad. Thank you, Mom and Dad, for always teaching me about hard work and dedication. Mom, I appreciate your care for me and the gift packages that you, Dad, and Bear have sent to me over the years. Thank you so much, Mom, for all of your advice and for encouraging me to press forward. Dad, even though you are not here to hear about my dissertation today, you've always encouraged me to have the Mamba Mentality, take on new challenges, and to pursue my dreams. I will forever cherish our Friday phone calls during my first year where we exchanged weekly updates. I thank you and Mom for being incredibly strong about letting me have my out of state adventure. I've learned so much about myself and about the world since I've been in Michigan, and I just want to let you know I'm so grateful to have you as my parents. Thank you for everything.

Table of Contents

List of Tables

List of Figures

List of Abbreviations

ACN	Acetonitrile
AKT	Protein Kinase B
BAD	BCL2 Associated Agonist of Cell Death
CEP17	Chromosome Enumeration Probe 17
c-MET	Tyrosine Kinase Met
DGE	Differential Gene Expression
DMSO	Dimethyl Sulfoxide
EMT	Epithelial-Mesenchymal Transition
ER	Estrogen Receptor
ERBB2	Human Epidermal Receptor 2
FDBB	Fragment Based Drug Discovery
FISH	Fluorescence In-Situ Hybridization
FOXO	Forkhead Box Protein
FP	Fluorescence Polarization
GSEA	Gene Set Enrichment Analysis
GSK3B	Glycogen synthase kinase 3 β
HER2	Human Epidermal Receptor 2
HER2+ breast cancer	HER2-overexpressing breast cancer
HER3	Human Epidermal Receptor 3
HTS	High Throughput Screening
IGFR	Insulin-like Growth Factor 1 Receptor
IHC	Immunohistochemistry
k.d.	Knockdown
MSigDB	Molecular Signature Database
mTOR	Mammalian Target of Rapamycin
NMP	N-Methyl-2-pyrrolidone
OS	Overall Survival
PCA	Principal Component Analysis
PCR	Polymerase Chain Reaction
pCR	Pathological Complete Response
PFS	Progression Free Survival
PI3K	Phosphoinositide 3-kinase
PR	Progesterone Receptor
PTEN	Phosphatase and Tensin Homolog
shRNA	Short Hairpin RNA
TCGA	The Cancer Genome Atlas

T-DM1	Trastuzumab Emtansine, Kadcyla
T_m	Melting Temperature
UMAP	Uniform Manifold Approximation and Projection
UMI	Unique Molecular Identifier
wt	Wild type
ACN	Acetonitrile
Et_2O	Diethyl Ether
DCM	Dichloromethane
DIPEA	N,N-Diisopropylethylamine
HOAT	1-Hydroxy-7-azabenzotriazole
Ahx	6-Aminohexanoic acid
TFA	Trifluoroacetic Acid

Abstract

HER2+ breast cancer is marked by the overexpression and/or amplification of the HER2 protein or HER2 gene, respectively. Current standard of care is trastuzumab-based therapy, but resistance remains a huge hurdle for metastatic HER2+ breast cancer patients. The loss of tumor suppressor PTEN has been regarded to contribute to trastuzumab resistance, but the exact role of PTEN status in HER2+ breast cancer and its prognostic value remains controversial. This dissertation aims to unravel the role of PTEN expression status in HER2+ breast cancer to gain insight on its contribution to trastuzumab sensitivity. We aim to understand how PTEN deficiency alters HER2+ breast cancer subpopulations and how changes induced by PTEN deficiency could result in an aggressive cancer phenotype and/or impact response to trastuzumab. We hypothesized that PTEN deficiency in HER2+ breast cancer increases the aggressive cancer cell subpopulations that are responsible for trastuzumab resistance. To test our hypothesis, we used an unbiased single cell RNA sequencing approach called Drop-seq to profile transcriptomes of cells constituting HER2+ breast cancer *in vitro*. By profiling four different HER2+ breast cancer cell line pairs containing a parental and shPTEN cell line with Drop-seq, we were able to dissect the functional consequences of PTEN deficiency *in vitro*. Also, we investigated both the intra- and intertumoral heterogeneity effects of PTEN deficiency in HER2+ breast cancer. Comparative analyses of the transcriptomes arising from parental and shPTEN cell lines provided information about the intratumoral consequences of PTEN deficiency. These studies revealed that PTEN deficiency in HER2+ breast cancer cell lines resulted in a global increase of quiescent features in the shPTEN cell line relative to the parental cell lines for HCC1954 and SKBR3 but not for BT474. Furthermore, PTEN deficiency resulted in a 84 fold, 120 fold, and a 2.4 fold increase in a quiescent, epithelial, early EMT subpopulation in HCC1954, SKBR3, and BT474, respectively. PTEN deficiency introduced intra-subpopulation heterogeneity by altering the expression of a subset of EMT, cytokine, cell cycle, and cell adhesion genes

in HCC1954 and SKBR3 but not BT474. Comparative analyses of changes to the single cell transcriptomes resulting from PTEN deficiency between cell lines afforded insight on the intertumoral consequences of PTEN deficiency in HER2+ breast cancer. These analyses revealed that effects of PTEN deficiency were similar in HCC1954 and SKBR3 due to the similarities in magnitudes of subpopulation level changes and presence of intra-subpopulation level changes while hinted that BT474 represented a unique case for studying the consequences of PTEN deficiency. Altogether, these analyses captured the context-dependent effects that PTEN deficiency in HER2+ breast cancer.

Additionally, we aimed to elucidate how transcriptomes shaped by a pre-existing PTEN deficiency could impact trastuzumab response by performing treatment studies with two HER2+ breast cancer cell line pairs (parental and shPTEN cell line). Treatment studies of BT474 and MDA-MB-361 showed minor changes in cancer subpopulations between treated and untreated cells, and these studies remain inconclusive at this point. Collectively, studies presented in this dissertation could have important clinical implications about the consequences of PTEN deficiency in HER2+ breast cancer as we highlighted the intra- and intertumoral consequences of PTEN deficiency. This insight could contribute to the identification of biomarkers that predicts patient response to trastuzumab and facilitate the discovery of alternative therapeutic strategies for patients who acquire resistance to trastuzumab.

Chapter 1: Introduction to HER2+ Breast Cancer

1.1. Introduction to HER2+ Breast Cancer

Breast cancer is one of the most common cancer among women. In the United States, approximately 12% of women will be diagnosed with breast cancer during their lifetime.[1] Breast cancer is heterogeneous disease that presents with a variety of histological and clinical manifestations (Figure 1.1A). Breast cancer is categorized into four molecular subtypes depending on the expression of surface markers such as progesterone receptor (PR), estrogen receptor (ER), and human epidermal growth factor receptor 2 (HER2, ERBB2).[2–6] In this dissertation, I will focus on HER2+ breast cancer, which is characterized by the aberrant overamplification or overexpression of the tumor associated antigen, HER2. HER2+ breast cancer constitutes 10-30% of all breast cancer cases and is characterized by an aggressive phenotype and poor survival as exemplified by the sharp decline in the five year survival as cancer of this subtype progress from localized to distant cancer (Figure 1.1B).[1,2,5–7] In 2019, it was estimated that roughly 1M women in the United States are diagnosed and/or are survivors of HER2+ breast cancer, signifying that HER2+ breast cancer impacted 0.3% of the entire United States population.[1]

A)

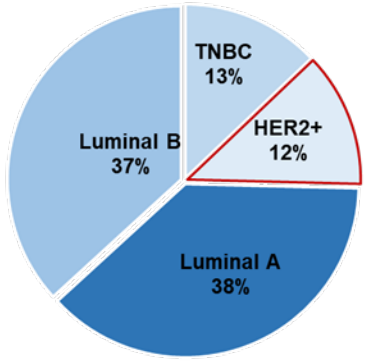

B)

Subtype	Localized	Regional	Distant
HR+/HER2+	98.7%	89.5%	43.5%
HR-/HER2+	96.1%	81.7%	36.8%

Figure 1.1. Epidemiological Perspectives of HER2+ Breast Cancer. A) Incidence rates of breast cancer by molecular subtype. Adapted from doi: 10.1038/srep11085. B) 5-year survival of HER2+ breast cancer patients. Adapted from National Cancer Institute Surveillance, Epidemiology, and End Result Program. Abbreviations: HR (hormonal receptors, e.g. estrogen receptor and/or progesterone receptor).

Clinically, the overamplification and the overexpression of HER2 has been reported to have different outcomes. Amplification of the *HER2* oncogene contributes to an aggressive cancer phenotype by enabling tumor cell proliferation, conferring invasive properties, and upregulating of the PI3K/AKT and Ras/Raf/MEK/MAPK signaling pathways.[4] Overexpression of HER2 protein has been associated with poor survival, high grade tumors, and positive-lymph node metastases.[4] In the clinic, the use of fluorescence *in situ* hybridization (FISH) and immunohistochemistry staining are used to ascertain the amplification of the HER2 oncogene and the overexpression of HER2, respectively.[4,8,9] FISH is a DNA hybridization assay that uses fluorescently labeled probes to quantify the *HER2* gene amplification status relative to the chromosome-17 centromere (CEP-17).[4] Current FDA approved FISH assays include Vetana Inform test, PathVysion, and PHarmDX.[4] To assess the expression level of HER2, IHC staining is used to determine HER2 status in the breast epithelial cells and the patient's eligibility for anti-HER2 therapies.[4] Current FDA approved IHC staining kits include Dako Hercept Test and Ventana Pathway.[4] Between FISH and IHC, IHC is the primary method to determine HER2 status.[4,10] A score of 3+ from IHC staining (i.e. high expression of HER2 protein) signifies HER2-overexpressing cancer and makes the patient eligible for anti-HER2 directed therapies.[4,10,11] According to the American Society of Clinical Oncology guidelines, IHC staining yielding a score of 2+ is termed as invasive breast cancer with moderate staining and often requires the use of the FISH assay for validation.[4,11–13] HER2+ breast cancer develops from the amplification of the HER2 oncogene and/or overexpression of the HER2 protein, both of which are assessed during diagnosis.

1.2. Trastuzumab: Standard of Care for HER2+ Breast Cancer Patients

The standard of care for HER2+ breast cancer patients features trastuzumab (commercially known as Herceptin) in combination with pertuzumab and a chemotherapeutic agent such as taxanes.[14–16] Trastuzumab is a humanized monoclonal antibody that targets the extracellular domain IV of HER2 receptor to exert its cytostatic effects on HER2-overexpressing cancer cells in breast cancer, gastric cancer, ovarian cancer, and esophageal cancer.[16–22] Upon binding to the extracellular domain of HER2 receptor, trastuzumab exerts its cytostatic action through four key mechanisms (Figure 1.2).[14,23–26] Trastuzumab is predominantly known for mediating antibody dependent cell-

mediated cytotoxicity by attracting immune effector cells to HER2 overexpressing cells (Figure 1.2A).[14,23,25–27] Secondly, trastuzumab prevents the proteolytic cleavage of the extracellular domain of HER2 (Figure 1.2A).[14,23,26,27] It can also prevent the heterodimerization of the ectodomain of the HER2 receptor with HER3/4 (Figure 1.2A).[26,27] Lastly, trastuzumab has been shown to elicit its cytostatic effects by promoting endocytosis of the HER2-trastuzumab conjugate (Figure 1.2A).[27]

The inclusion of pertuzumab (commercially known as Perjeta) in the frontline therapy (e.g. trastuzumab with docetaxel) has been shown to dramatically improve the overall survival and progression free survival of HER2+ breast cancer patients compared to patients who did not receive pertuzumab in their treatment regimen.[17] Pertuzumab is a humanized monoclonal antibody that binds to the extracellular domain II of HER2 (Figure 1.2B).[28,29] Pertuzumab binds to a different domain than trastuzumab and attenuates the HER2 signaling cascade by preventing the heterodimerization of HER2 and HER3.[4,28] The use of pertuzumab is to improve anti-HER2 targeting by dually blocking the HER2 signaling pathway.[28] Patients who develop acquired resistance to the front line therapy are given trastuzumab emtansine (referred to as T-DM1 or by its commercial name Kadcyla), which is trastuzumab conjugated to the cytotoxic agent DM1 (Figure 1.2B).[4,28,30] T-DM1 selectively targets the HER2 overexpressing cells and is internalized via endocytotic vesicles.[4,28] Once inside of the cell, the cytotoxic payload consisting of DM1 is released, which results in cell death.[4,28] Unfortunately, patients who continue to acquire resistance to the second line therapies have limited therapeutic options because there is no standard of care of advanced patients following treatment with trastuzumab, pertuzumab, and T-DM1.[28] Currently, therapeutic options for these patients include combinations of trastuzumab with different chemotherapeutic agents (e.g. vinorelbine, gemcitabine, or capecitabine) and capecitabine with lapatinib, which is a tyrosine kinase inhibitor of HER2 and HER1 (Figure 1.2B).[28]

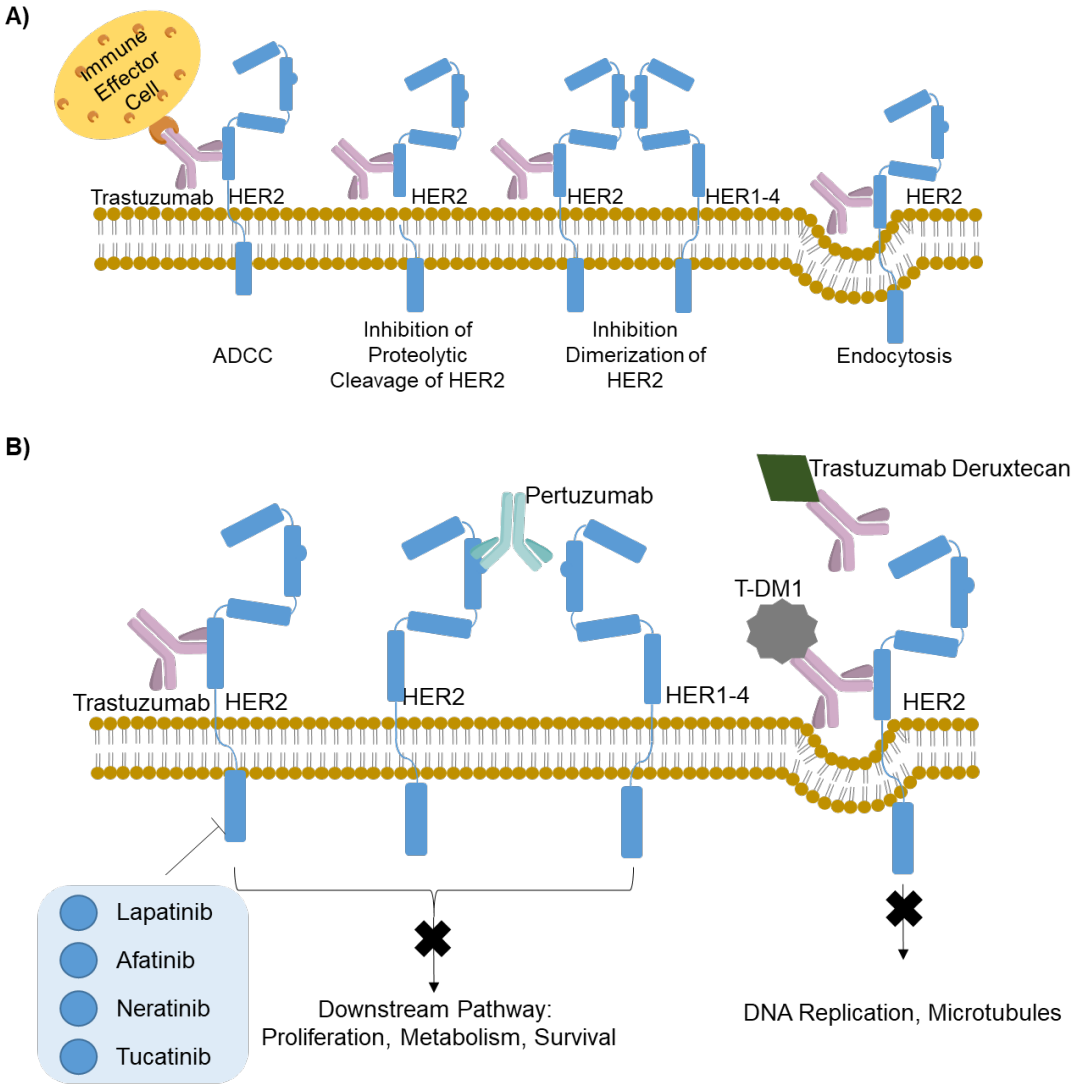

Figure 1.2. Mechanism of Action of Anti-HER2 Agents. A) Mechanism of action of trastuzumab. B) Mechanism of action of other HER2-directed therapies (pertuzumab, T-DM1, and trastuzumab deruxtecan) and tyrosine kinase inhibitors (e.g. lapatinib, afatinib, neratinib, and tucatinib).

Since its approval in 1998, trastuzumab has been used to treat early stage and HER2+ breast cancer patients with metastatic disease.[16,24,29,31–33] For early stage HER2+ breast cancer patients, the use of trastuzumab in combination with taxanes resulted in a 93% disease-free survival rate (7 years).[28,34,35] In contrast, 10-40% of HER2+ metastatic breast cancer patients initially respond to trastuzumab, and 50-70% of these patients develop acquired resistance and experience disease progression within 1 year of treatment for advanced diseased (Figure 1.3A).[36–39] Approximately 40-50% of these HER2+ metastatic breast cancer patients develop brain metastases during their disease course, which decreases the therapeutic effectiveness of trastuzumab in advanced stage

patients. Moreover, 10-12% of metastatic HER2+ breast cancer patients actually achieve clinical complete response and/or progression-free survival at 1 year when treated with trastuzumab.[19,40] Consistent with this finding, Murthy and coworkers (2016) identified a group of “exceptional responders” among HER2+ metastatic breast cancer patients, and these “exceptional responders” comprised 7% of the patients evaluated in their study.[32] The vast range in patient response to trastuzumab-based therapy among HER2+ metastatic breast cancer subgroup underscores the need to find alternative, effective therapies for these patients. At the beginning of 2020, two additional treatments were approved for HER2+ metastatic breast cancer.[18,19,41] These include tucatinib, which is a tyrosine kinase inhibitor that is more selective than lapatinib, and trastuzumab-deruxtecan, which is an antibody-drug conjugate of trastuzumab with a topoisomerase I inhibitor (Figures 1.2B and 1.3B).[18,19,41] Both of these new treatments were approved after showing clinical benefit for HER2+ metastatic breast cancer patients in the HER2CLIMB and the DESTINY-Breast01 clinical trials.[18,19,41] Both of these trials were notable because they demonstrated efficacy in HER2+ breast cancer patients with brain metastases, who in the past, were often excluded from studies.[18,19] The use of tucatinib improved progression-free survival, and the use of trastuzumab-deruxtecan improved tumor response in advanced disease (Figure 1.3B).[18,19,41] While these new treatments provide HER2+ breast cancer patients with a new hope, these new treatments are similar to standard of care agents for HER2+ breast cancer in that they all target the HER2-dependent pathway (Figure 1.2). [15,18,19,41] The development of resistance to the primary arm of trastuzumab-based treatment severely limits clinical benefit of the second and third arm treatments as evidenced by poor overall survival rates and low progression-free survival rates, especially since all lines of therapies feature trastuzumab (Figures 1.2B and 1.3B).[28] Acquired resistance to HER2-directed therapy, especially among the advanced stage and/or metastatic breast cancer patients accentuate the need for a deeper scrutiny into the development of resistance to trastuzumab, which could in turn facilitate the discovery of alternative therapeutics for patients who present acquired resistance to trastuzumab. This knowledge is critical for clinicians to effectively identify subsets of HER2+ breast cancer patients who could benefit from trastuzumab and to provide effective therapeutic solutions to patients who will develop resistance to

trastuzumab at diagnosis or shortly after diagnosis. The need for the discovery of alternative therapeutic strategies for metastatic HER2+ breast cancer patients could be addressed in two ways: by capitalizing the understanding of mechanisms driving resistance to trastuzumab and leveraging this mechanistic insight to predict how HER2+ breast cancer patients will respond to trastuzumab at the time of diagnosis.

A)

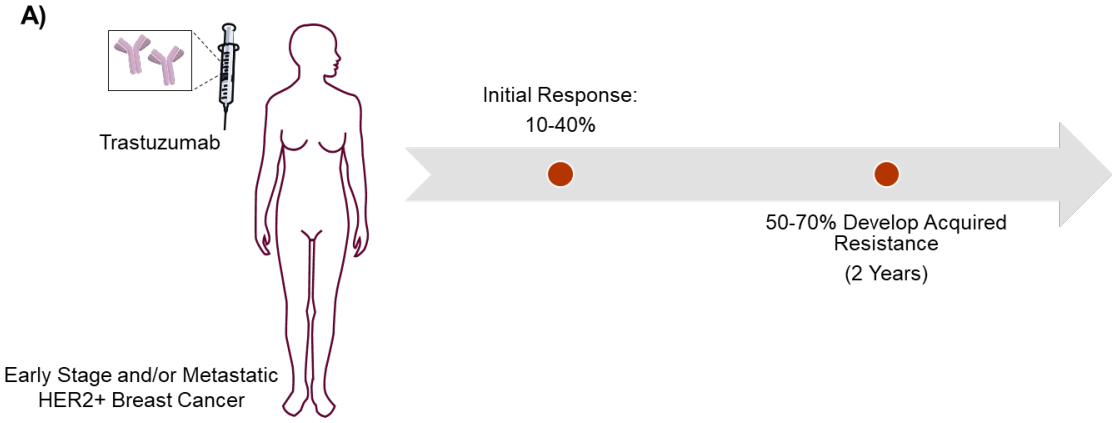

B)

HER2-Directed Therapy	Regimen	OS (months)	PFS (months)
First Line	Trastuzumab, Pertuzumab, and Taxane	32.6[1]	12-18[1]
Second Line	Contains T-DM1	30.2[2]	9.6[2]
Third Line	• Lapatinib + Capecitabine • Trastuzumab + Lapatinib (or T-DM1) • Tucatinib • Trastuzumab Deruxtecan	15.8[3], 21.4[4] (Tucatinib)	7.8[4] (Tucatinib), 21.9[5] (Trastuzumab Deruxtecan)

Figure 1.3. Lines of Therapies for HER2+ Breast Cancer Patients and Their Clinical Benefit. A) Patient journey for metastatic HER2+ breast cancer patient treated with trastuzumab-based therapies. B) Clinical benefit of first line, second line, and third line therapies for metastatic HER2+ breast cancer patients. Abbreviations: OS (overall survival), PFS (progression free survival), and mo (months). References 1: doi: 10.1016/S1470-2045(13)70130-X; 2: doi: 10.1056/NEJMoa1209124; 3: doi: 10.1016/S1470-2045(17)30313-3; 4: doi: 10.1056/NEJMoa1914609; 5: doi: 10.1056/NEJMoa1914510.

1.3. Introduction to PTEN Loss and Resistance to Trastuzumab

There is extensive literature covering mechanisms that contributes to trastuzumab resistance.[14,23–26,42–47] Three main mechanisms have been proposed: steric effects, overexpression of alternative tyrosine kinase receptors, and intracellular alterations (Figure 1.4A).[23,26,38,43] Resistance to trastuzumab by steric effects occurs as a result of the "shedding" of the extracellular domain of the HER2 receptor and prevents

trastuzumab from interacting with the HER2 receptor.[23,26,38,43] Alternatively, the overexpression of alternative tyrosine kinase receptors, such as IGFR, HER3, and c-MET, enables the cell to bypass the halted HER2-dependent pathway in the presence of trastuzumab.[23,26,38,43] Lastly, trastuzumab resistance can develop as a result of intracellular alterations, namely the upregulation of HER2 dependent intracellular signaling pathways such as PI3K/AKT signaling pathway.[23,26,38,43] Of these three mechanisms, I will focus on the aberrant intracellular alteration as the key source for trastuzumab resistance because there is extensive literature highlighting its impact on poor patient prognosis and association with trastuzumab resistance.[20,23,42,48–50]

The driving force of these intracellular alterations is governed by the loss and/or deficiency of a phosphatase and tensin homolog on chromosome 10 (PTEN).[20,23,42,48–50] PTEN is also referred to as MMAC1 (mutated in multiple advanced cancers-1) and TEP1 (tensin-like phosphatase-1).[51,52] PTEN is a cytoplasmic tumor suppressor, and it is linked to cancer through its phosphatase domain.[25,50,52–55] PTEN dephosphorylates PIP3 to PIP2, which serves to negatively regulate the PI3K/AKT signaling pathway.[25,50,52,53] This pathway is upstream various effector proteins, such as FOXO, mTOR, CyclinD, GSK3B, and BAD, which controls cell metabolism, cell survival, cell cycle control, and apoptosis (Figure 1.4B).[54,56–59] Thus, PTEN is a critical regulator of various signaling pathways linked to cell fate. In the event of PTEN loss, the PI3K/AKT pathway remains constitutively active and thus, enables the cell to bypass the HER2 pathway in presence of trastuzumab.[25,26,38,54] Thus, the loss of PTEN has been linked to cancer progression and resistance to trastuzumab through aberrant activation of PI3K/AkT/mTOR pathway.[25,26,38,54]

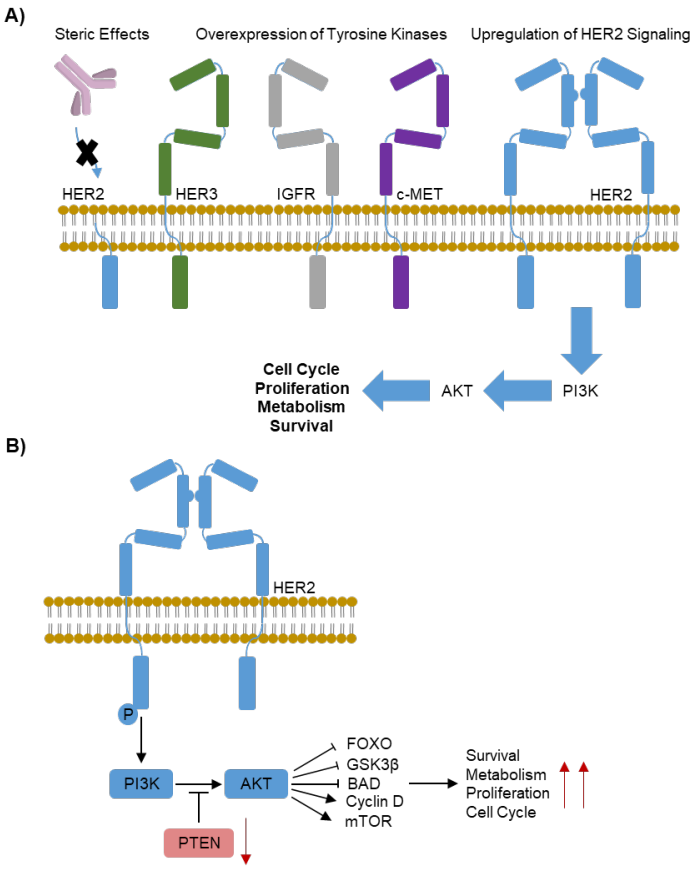

Figure 1.4. Mechanisms of Resistance to Trastuzumab. A) Three mechanisms of resistance to trastuzumab. B) Regulation and dysregulation of PI3K/AKT by PTEN loss.

In patients with HER2+ breast cancer, approximately 10-40% of these patients exhibit a loss of the PTEN tumor suppressor.[42,48,60,61] Common mechanisms for PTEN loss in various cancers include hypermethylation of the PTEN promoter and loss of heterozygosity of the PTEN locus.[51,52,61–65] In breast cancer, hypermethylation of the PTEN promoter or loss of heterozygosity occurs in 30-50% of patients.[51,52,62,63] A less common mechanism for PTEN loss in breast cancer is the somatic mutation of the *PTEN* gene, which occurs in 2-6% of patients.[52,62] Unlike the cell surface markers used to categorize the subtype of a patient's breast cancer, clinicians do not evaluate PTEN as a parameter for breast cancer diagnosis.[2–6] Interestingly, the loss of PTEN is uncommon at diagnosis.[55] However, its loss is associated with disease progression and acquired resistance to HER2-directed therapy, which highlights the need for reliable markers to identify the subset of HER2+ breast cancer patients who need alternative therapeutic solutions at the onset of diagnosis.[55]

Since resistance to anti-HER2 therapy is postulated to result from constitutive activation of effector proteins downstream of HER2 arising from PTEN loss, targeting these proteins has been explored to overcome trastuzumab resistance and to mitigate the effects of PTEN loss.[4,53,66–69] This approach includes targeting PI3K/Akt/mTOR, which are critical downstream mediators of the HER2 signaling pathway.[4,53,66–69] Feasibility studies for using PI3K/AKT/mTOR inhibitors for HER2+ breast cancer led to the evaluation of repurposing everolimus for HER2+ metastatic breast cancer and the discovery of AKT inhibitors, namely MK-2206.[34,53,66,67,69,70] Despite the significance of PI3K/AKT/mTOR to mediating the HER2 signaling pathway, various clinical trials showed that inhibitors did not significantly improve the PFS or OS of HER2+ breast cancer patients who developed resistance to frontline therapy.[53,69,70] Furthermore, studies with everolimus and PI3K/AKT inhibitors documented extensive toxicities, many of which resulted in dose interruptions or discontinuation in at least 20% of patients.[53,69,71] While there are currently ongoing clinical trials aimed at improving the efficacy of these inhibitors, none demonstrate significant clinical benefit in HER2+ breast cancer patients who developed resistance to the frontline therapies.

Since PI3K/AKT/mTOR inhibitors had limited success in overcoming resistance or restoring trastuzumab sensitivity, researchers also investigated the relationship between PTEN loss and trastuzumab resistance.[20,42,48] Stern and coworkers (2015) demonstrated that HER2+ breast cancer patients with negative PTEN staining (i.e. PTEN loss) had a significantly lower overall survival rate compared to patients whose cancer showed PTEN expression (Figure 1.5A).[42] In a separate study, Rimawi and colleagues (2018) correlated PTEN status with trastuzumab response in HER2+ breast cancer patients treated with trastuzumab and lapatinib and observed a statistically significant relationship between pCR and PTEN status (Figure 1.5C).[48] In their study, 32% of patients with high levels of PTEN experienced pCR, while 91% of patients with low PTEN did not exhibit pCR while treated with trastuzumab and lapatinib.[48] Stern and colleagues (2015), Nuciforo and coworkers (2015), Kim and colleagues (2017) also assessed the relationship of overall survival as a function of PTEN expression and presence of trastuzumab treatment in HER2+ breast cancer, as neoadjuvant therapy for HER2+ breast cancer, and gastric cancer, respectively.[20,42,60] While these studies showed a negative correlation between

overall survival rate, PTEN loss, and trastuzumab treatment, this correlation was not statistically significant.[20,42,60] The lack of the statistically significant correlation between PTEN status and trastuzumab response ignited controversy surrounding the role of PTEN in HER2+ breast cancer. Furthermore, Gschwantler-Kaulich and coworkers (2017) reported that PTEN positivity, rather than PTEN loss, was significantly correlated with progressive disease in HER2+ breast cancer.[45] While PTEN is clinically relevant to HER2+ breast cancer, the entirety of literature surrounding the relationship between PTEN deficiency and clinical parameters suggests PTEN might have a more nuanced role in HER2+ breast cancer.

A)

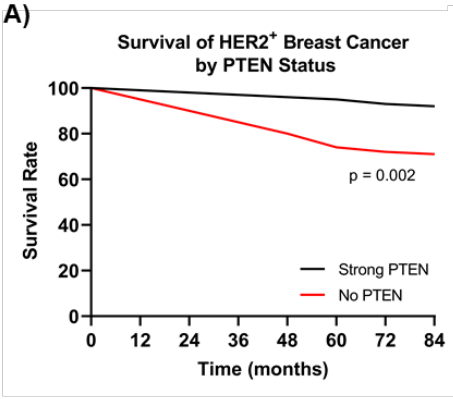

B)

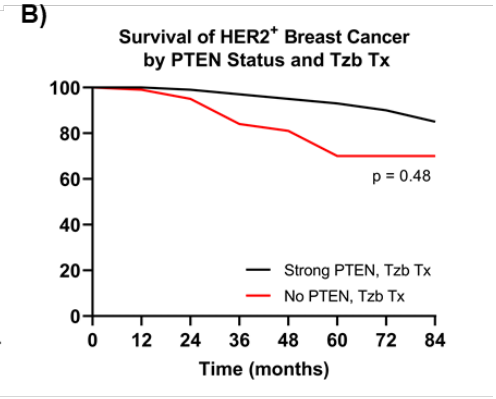

C)

PTEN Expression (n=59)	pCR (%)	No pCR (%)	P value
High PTEN	12 (32)	25 (68%)	0.04
Low PTEN	2 (9%)	20 (91%)	

Figure 1.5. Overall Survival of HER2+ Breast Cancer Patients by PTEN Status and Trastuzumab Treatment. A) Overall survival of HER2+ breast cancer patients based on PTEN expression levels. Adapted from doi: 10.1158/1078-0432.CCR-14-2993. B) Overall survival of HER2+ breast cancer patients when treated with trastuzumab based on PTEN expression levels. Adapted from doi: 10.1158/1078-0432.CCR-14-2993. C) Effect of PTEN expression levels on complete response. Adapted from doi: 10.1007/s10549-017-4533-9. Abbreviations: Tzb Tx (Trastuzumab treatment) and pCR (Pathological complete response).

The paradoxical role of PTEN as observed from the literature could stem from how the loss of PTEN affects the mosaic of cancer cells that constitute the entire cancer.[72] Within a tumor, there exists diverse subpopulations that exhibit varied growth potential, metastatic potential, and sensitivity to therapy. The phenotype of these cancer subpopulations is a direct result of the tumor's intratumoral heterogeneity, which manifests from genetic and epigenetic influences that shapes the tumor's gene

expression programs and adaptability to its environment.[10,72] For example, exposure to therapeutic agents could expand pre-existing resistant subpopulations and/or alter gene expression profiles of select subpopulations to aid the survival of those subpopulations.[72,73] Hence, intratumoral heterogeneity is thought to be a key driver in disease progression, therapeutic resistance, and poor survival in patients with metastatic disease.[72,74] Furthermore, this intratumoral heterogeneity could be at the crux of how PTEN loss shapes the phenotype of cancer subpopulations and could explain why PTEN loss produced contradictory clinical observations in the literature.

In HER2+ breast cancer, intratumoral heterogeneity manifests in a multitude of ways. Ferrari and coworkers (2016) reported that HER2+ breast cancer represents a spectrum of four additional subtypes with distinguishable gene expression programs, somatic mutations, and copy number alterations.[75] As a result, patients belonging to different subsets of HER2+ breast cancer have distinct cancer ecosystems, which explains the variation in therapeutic effect and overall survival among the HER2+ breast cancer patient population.[75] Additionally, intratumoral heterogeneity in HER2+ breast cancer could result in cells that express high levels of HER2 and cells that express low levels of HER2, which ultimately generates a heterogeneous group of cancer responsive to the HER2-directed therapies (Figure 1.6A). Lee and colleagues (2014) reported spatial heterogeneity of the HER2 gene amplification, also termed as regional heterogeneity, is common among cells that exhibit low HER2 amplification or expression within the HER2-overexpressing tumor.[73] This spatial/regional heterogeneity in the HER2 amplification was significantly associated with decreased response to trastuzumab, shorter time to cancer progression, and lower overall survival in HER2+ metastatic breast cancer patients.[73] Due to clinical importance of intratumoral heterogeneity, a wealth of studies were performed to examine HER2+ breast cancer on single cell level to account for the heterogeneity that influences the patient journey.[74,76] For example, Rye and coworkers (2018) analyzed single cells derived from biopsies of HER2+ breast cancer patients to reveal the clinical consequences of heterogeneity of HER2 gene amplification and ER status.[74] Rye and coworkers observed a statistically significant correlation between the intratumoral heterogeneity of HER2 copy number, increased frequency of relapse, and shorter disease free survival.[74] Additionally, Rye and coworkers observed the emergence

of new subpopulations of HER2+/ER+ cells following treatment. [74] In a separate study, Brady and coworkers (2018) tracked two HER2+ breast cancer patients during cancer treatment via single cell transcriptomics and uncovered significant changes to each of the patient's cancer during the course of treatment.[76] Specifically, treatment with trastuzumab-based therapies revealed mechanisms of acquired resistance in both patients: one patient had increased expression of ABC1B drug efflux pump and mutations induced by reduction of BRCA gene expression, while the other patient showed elevated expression of ESR1 and ABC1B drug efflux pump.[76] Brady and associates also revealed that these resultant subclones emerged from minor subpopulations that were expanded following a "bottleneck event" during cancer treatment, which underscores the functional consequences of intratumoral heterogeneity. Furthermore, Brady and coworkers' study highlighted the existence of therapy resistance programs present in only a subset of cancer cells, which signified that the response of the collective cancer represents the combined, varied response of the individual cells to therapy.[76] This study effectively highlighted the value of single cell transcriptomics as an unbiased approach to study subpopulations of HER2+ breast cancer on a single cell level, which enables the dissection of the evolution of resistance mechanisms to HER2-directed therapy. Specifically, this unbiased approach would afford insightful analysis of how intracellular alterations such as PTEN deficiency affects HER2+ breast cancer at the single cell level (Figure 1.6B). Previously, *in vitro* studies performed by Korkaya and coworkers (2008) using HER2+ breast cancer cells with PTEN knockdown (k.d.) indicated that trastuzumab treatment resulted in the development of an aggressive mesenchymal phenotype.[77] Furthermore, single cell colony formation studies performed by Dr. Joseph Burnett of the Sun Lab demonstrated that HER2+ breast cancer cells with PTEN k.d. generated mesenchymal colonies at a higher frequency compared to parental colonies. Furthermore, trastuzumab treatment of colonies with PTEN k.d. further increased the formation of mesenchymal colonies (unpublished data). Taken together, these studies emphasize the impact that intratumoral heterogeneity could have on the functional consequences of PTEN deficiency in HER2+ breast cancer. Importantly, these studies accentuates the need to scrutinize the functional consequences of PTEN deficiency on a

single cell level to reveal how the combined effect of intratumoral heterogeneity and PTEN deficiency ultimately governs trastuzumab sensitivity in HER2+ breast cancer.

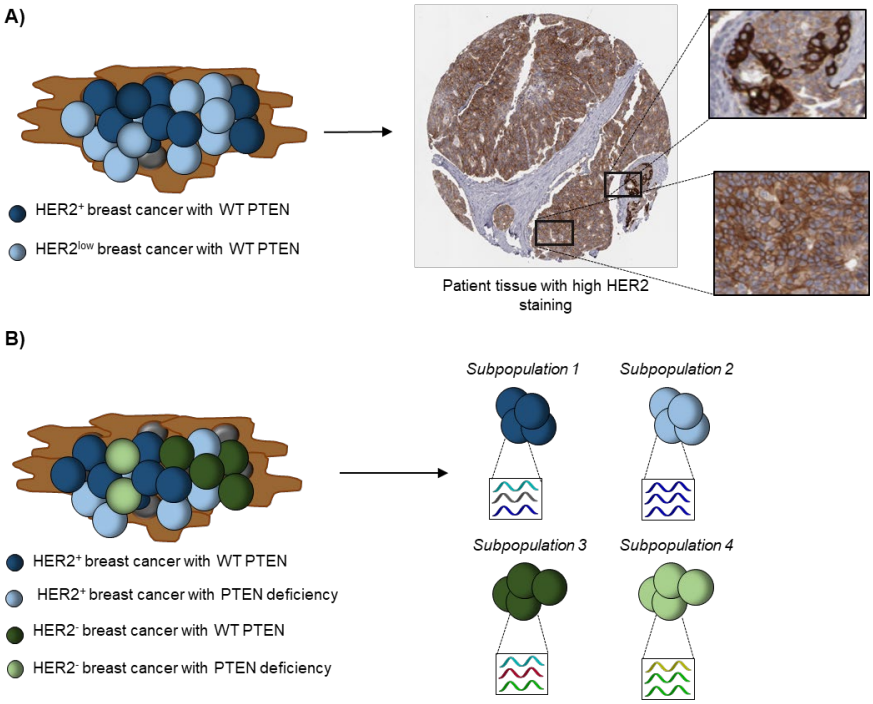

Figure 1.6. Depictions of Intratumoral Heterogeneity in HER2+ Breast Cancer Cells. A) Intratumoral heterogeneity in HER2 protein expression. Patient tissue retrieved from Protein Atlas (Patient ID: 659). B) Cartoon of intratumoral heterogeneity resulting in four distinct subpopulations based on expression of HER2 and PTEN.

1.4. Use of Drop-seq to Generate Single Cell Transcriptomic Libraries

In a clinical setting, a patient with HER2-overexpressing breast cancer could have numerous cancer subpopulations that vary in expression of critical genes and proteins, such as HER2 and PTEN. Figure 1.6B illustrates a simplified cartoon of four subpopulations of cancer cells resulting from variation in protein levels of these two genes. Based on the gene expression of these cells, these subpopulations could all behave starkly different, which collectively shape the course of the patient's cancer. Some subpopulations contribute to aggressive cancer phenotype, some are therapy-sensitive, and some are resistant to therapies. We are particularly interested in analyzing the steady-state subpopulations that constitute HER2+ breast cancer to elucidate how PTEN deficiency affects those subpopulations. To gain insight on PTEN deficiency in HER2+ breast cancer, we used single cell transcriptomics, namely Drop-seq.[78,79] While there are multiple methods for single cell transcriptomics, Drop-seq is suitable to address our research question because it has good accuracy, good statistical power to detect

differences in gene expression levels between cells, and is among the most cost effective methods.[78,80] Despite these advantages, Drop-seq is limited by high amplification noise resulting from PCR, low sensitivity (i.e. median number of genes detected per cell), high dropout probability (i.e. the fraction of cells with zero expression counts), and lower sequencing depth (i.e. genes expressed at low abundance will not be detected).[80] Drop-seq detects approximately 4,000 genes per cell and is limited to detecting high expressing genes.[80] Despite these limitations, Drop-seq is an appropriate method for analyzing large number of cells at a lower sequencing depth, which is sufficient to address our research questions and for unraveling the functional consequences resulting from PTEN deficiency.[80,81] In summary, Drop-seq is an appropriate method to evaluate the effects of PTEN deficiency to reveal subpopulation changes.

Drop-seq is a critical single cell RNA-seq technique that enables the profiling of mRNA transcripts within single cells. This technique involves the generation of nanoliter droplets containing 1 cell and 1 barcoded bead.[78] These barcoded beads contain millions of oligonucleotides on its surface, where each oligonucleotide contains four regions on it: a cell barcode, unique molecular identifier (UMI), an oligo dT sequence, and a PCR primer.[78] Cell barcodes allows mRNA transcripts originating from 1 cell to be traced to its originating cell following sequencing.[78] The UMI tags individual mRNA transcripts so that replicates of the same mRNA transcript could be tracked and quantified following sequencing.[78] The oligo-dT sequence enables mRNA transcripts from single cells to be captured onto the beads through the hybridization of the poly-A tails of the mRNA transcripts to the dT oligos of the barcoded beads.[78]Lastly, the PCR primer allows enables downstream amplification following the reverse transcription of the mRNA to cDNA.[78] Together, these components of the barcoded beads technology provides an effective way to capture mRNA from single cells and to develop single cell transcriptomic libraries. Using this technology, we would be able to profile gene expression programs derived from single cells that constitute bulk HER2+ breast cancer cell lines to reveal the functional consequences of PTEN deficiency. Furthermore, subpopulation level effects of PTEN deficiency in HER2+ breast cancer could be dissected *in vitro* to elucidate the contribution of PTEN deficiency in trastuzumab sensitivity.

Previously in Sun Lab, Dr. Joseph Burnett generated HER2+ breast cancer cell line pairs, where each pair consists of the parental cell line (wild type, wt, PTEN) and PTEN knockdown (k.d., Table 1.1). The expression of PTEN was previously knocked down using lentiviral shRNA as described by Korkaya and colleagues and provided to me for this dissertation as a gift.[77,82,83] Drop-seq analyses using these cell line pairs afforded analysis on the intertumoral heterogeneity (i.e. cancer heterogeneity arising between patients[72]), intratumoral heterogeneity (cancer heterogeneity arising within a single tumor[72]), and how those phenomena affects the functional consequences of PTEN deficiency in HER2+ breast cancer. Intertumoral heterogeneity effects of PTEN deficiency were studied using comparative analyses of the single cell transcriptomes between HER2+ breast cancer cell lines. Intratumoral heterogeneity effects of PTEN deficiency were evaluated by scrutinizing the cancer subpopulations that make up a HER2+ breast cancer cell line. Functional consequences of PTEN deficiency was elucidated in comparative transcriptomic analyses between the parental and PTEN k.d. cells for a given cell line. Single transcriptomic libraries of HCC1954, SKBR3, and BT474 (parental and PTEN k.d.) were evaluated to understand the functional consequences of PTEN deficiency in HER2+ breast cancer cells. The impact of PTEN deficiency on trastuzumab response in HER2+ breast cancer cells were evaluated in treatment studies of BT474 and MDA-MB-361 (parental and PTEN k.d.).

Table 1.1. HER2+ Breast Cancer Cell Line Pairs Used in This Dissertation.

HER2+ BC Cell Lines	Wild type PTEN	PTEN knockdown
HCC-1954	• Bulk cell line	• Bulk cell line
SKBR3	• Bulk cell line	• Bulk cell line
BT474	• Bulk cell line • Bulk cell line ± Tzb	• Bulk cell line • Bulk cell line ± Tzb
MDA-MB-361	• Bulk cell line	• Bulk cell line

1.5. Research Question, Hypothesis, and Research Aims

For this dissertation, we investigated the role of PTEN deficiency in HER2+ breast cancer to elucidate its role in trastuzumab resistance. Ultimately, we aim to contribute to the discovery of effective therapeutic solutions for HER2+ breast cancer patients who acquire resistance. To work towards this goal, we asked three key questions for this dissertation:

- What subpopulations exist in HER2+ breast cancer?
- How does PTEN deficiency affect the steady state of these subpopulations?
- How does the status of PTEN affect response to HER2-directed therapy?

To address these research questions, we proposed the following hypothesis: PTEN deficiency in HER2+ breast cancer expands aggressive subpopulations that are responsible for trastuzumab resistance. To test our hypothesis, we proposed three aims for this dissertation, which includes:

1. Characterize subpopulations in HER2+ breast cancer with wt PTEN and PTEN deficiency using Drop-seq
2. Elucidate how the transcriptomic composition of HER2+ breast cancer cells change as a result of PTEN deficiency and trastuzumab treatment
3. Identify and validate markers corresponding to subpopulations enriched by PTEN k.d. and/or trastuzumab treatment (future)

For this dissertation, we addressed Aim 1 and gathered preliminary findings for Aim 2. The bulk of this dissertation will focus on the characterization of PTEN deficiency in HER2+ breast cancer cells. Chapter 2 describes our approach and findings from analyzing the transcriptomic changes induced by PTEN k.d. in three HER2+ breast cancer cell lines: HCC1954, SKBR3, and BT474. We describe global transcriptomic changes as well as subpopulation level changes that result from PTEN k.d. in these HER2+ breast cancer cell lines. We sought to address Aim 2 in Chapter 3, but could only provide preliminary observations from trastuzumab treatment studies using BT474 and MDA-MB-361 at this time. Additional treatment studies are ongoing. The purpose of these treatment studies was to gain insight on what transcriptomic alterations resulted from trastuzumab treatment and how transcriptomes shaped by a pre-existing PTEN deficiency impact trastuzumab response. Insufficient number of treatment controls and the lack of reproducibility between biological replicates limited these treatment studies, and thus, only preliminary observations were described. No conclusive findings were identified from the treatment studies described in Chapter 3. In Chapter 4, we provide concluding remarks and thoughts about future studies. A chapter in the Appendix summarizes a drug discovery project that performed during the first 2 years of towards this dissertation. The Appendix chapter details the drug discovery efforts towards the

identification of small molecule inhibitors of the protein-protein interaction between c-MYC and WDR5 using high-throughput screening and fragment based drug discovery approaches.

1.6. Significance and Innovation

Research presented in this dissertation is significant because it elucidates the effect of PTEN deficiency on a single cell level. Previously, the role of PTEN in HER2+ breast cancer has been controversial due to the confounding contribution of intratumoral heterogeneity existing within the bulk tumor. This dissertation accounts for the contribution of intratumoral heterogeneity on the effect of PTEN deficiency in HER2+ breast cancer cells through the use of Drop-seq. We evaluated the global transcriptomic consequences of PTEN deficiency in bulk HER2+ breast cancer cells and determined how PTEN deficiency affected the intratumoral heterogeneity within each HER2+ breast cancer cell line by dissecting subpopulations that comprised the bulk cell line. We also elucidate the intertumoral consequences of PTEN deficiency by comparing transcriptomes between cell lines to gain insight about the relationship between PTEN deficiency and intertumoral heterogeneity.

This study will be the first (to our knowledge) to describe that PTEN deficiency enriches a quiescent subpopulation with an epithelial, early EMT phenotype in HER2+ breast cancer cells. Furthermore, the evaluation of PTEN deficiency in three HER2+ breast cancer cell lines revealed that PTEN deficiency also enriched/ maintained pre-existing subpopulation phenotypes, which suggested that PTEN deficiency also displayed context-dependent consequences, depending on the phenotype is enriched or maintained. Furthermore, the context dependent effects of PTEN deficiency observed *in vitro* implied that HER2+ breast cancer patients with PTEN deficiency might also endure context dependent consequences. These observations hinted of the need to evaluate HER2+ breast cancer patients on both PTEN and HER2 status. Taken together, we assessed the functional consequences of PTEN deficiency on a single cell level, which revealed an enrichment of a quiescent subpopulation with epithelial, early EMT phenotype and context dependent consequences of PTEN deficiency in remaining cancer subpopulations. Findings presented in this dissertation could contribute to shaping the personalized cancer management approaches for HER2+ breast cancer patients.

1.7. References

(1) U.S. Breast Cancer Statistics | Breastcancer.org https://www.breastcancer.org/symptoms/understand_bc/statistics (accessed Jun 1, 2020).

(2) Dai, X.; Li, T.; Bai, Z.; Yang, Y.; Liu, X.; Zhan, J.; Shi, B. *Am. J. Cancer Res.* **2015**, *5* (10), 2929–2943.

(3) Turashvili, G.; Brogi, E. *Front. Med.* **2017**, *4* (DEC).

(4) Wang, J.; Xu, B. *Signal Transduct. Target. Ther.* **2019**, *4* (1).

(5) *Am. Cancer Soc.* **2020**, 1–43.

(6) National Cancer Institute Surveillance, Epidemiology, and E. R. P. (SEER). *Natl. Cancer Inst.* **2019**.

(7) Zhang, L.; Li, J.; Xiao, Y.; Cui, H.; Du, G.; Wang, Y.; Li, Z.; Wu, T.; Li, X.; Tian, J. *Sci. Rep.* **2015**, *5*, 1–14.

(8) Godoy-Ortiz, A.; Sanchez-Muñoz, A.; Parrado, M. R. C.; Álvarez, M.; Ribelles, N.; Dominguez, A. R.; Alba, E. *Front. Oncol.* **2019**, *9* (OCT), 1124.

(9) Loibl, S.; Gianni, L. *Lancet* **2017**, *389* (10087), 2415–2429.

(10) Muller, K. E.; Marotti, J. D.; Tafe, L. J. *Am. J. Clin. Pathol.* **2019**, *152* (1), 7–16.

(11) Vandenberghe, M. E.; Scott, M. L. J.; Scorer, P. W.; Söderberg, M.; Balcerzak, D.; Barker, C. *Sci. Rep.* **2017**, *7* (1), 1–11.

(12) Zhang, X.; Bleiweiss, I.; Jaffer, S.; Nayak, A. *Clin. Breast Cancer* **2017**, *17* (6), 486–492.

(13) Wolff, A. C.; Elizabeth Hale Hammond, M.; Allison, K. H.; Harvey, B. E.; Mangu, P. B.; Bartlett, J. M. S.; Bilous, M.; Ellis, I. O.; Fitzgibbons, P.; Hanna, W.; Jenkins, R. B.; Press, M. F.; Spears, P. A.; Vance, G. H.; Viale, G.; McShane, L. M.; Dowsett, M. *J. Clin. Oncol.* **2018**, *36* (20), 2105–2122.

(14) Mastro, L. Del; Lambertini, M.; Bighin, C.; Levaggi, A.; D'Alonzo, A.; Giraudi, S.; Pronzato, P. *Expert Rev. Anticancer Ther.* **2012**, *12* (11), 1391–1405.

(15) Pernas, S.; Tolaney, S. M. *Ther. Adv. Med. Oncol.* **2019**, *11*, 1–16.

(16) Oh, D. Y.; Bang, Y. J. *Nat. Rev. Clin. Oncol.* **2020**, *17* (1), 33–48.

(17) Swain, S. M.; Kim, S. B.; Cortés, J.; Ro, J.; Semiglazov, V.; Campone, M.; Ciruelos, E.; Ferrero, J. M.; Schneeweiss, A.; Knott, A.; Clark, E.; Ross, G.; Benyunes, M. C.; Baselga, J. *Lancet Oncol.* **2013**, *14* (6), 461–471.

(18) Modi, S.; Saura, C.; Yamashita, T.; Park, Y. H.; Kim, S.-B.; Tamura, K.; Andre, F.; Iwata, H.; Ito, Y.; Tsurutani, J.; Sohn, J.; Denduluri, N.; Perrin, C.; Aogi, K.; Tokunaga, E.; Im, S.-A.; Lee, K. S.; Hurvitz, S. A.; Cortes, J.; Lee, C.; Chen, S.; Zhang, L.; Shahidi, J.; Yver, A.; Krop, I. *N. Engl. J. Med.* **2020**, *382* (7), 610–621.

(19) Murthy, R. K.; Loi, S.; Okines, A.; Paplomata, E.; Hamilton, E.; Hurvitz, S. A.; Lin, N. U.; Borges, V.; Abramson, V.; Anders, C.; Bedard, P. L.; Oliveira, M.; Jakobsen, E.; Bachelot, T.; Shachar, S. S.; Muller, V.; Braga, S.; Duhoux, F. P.; Greil, R.; Cameron, D.; Carey, L. A.; Curigliano, G.; Gelmon, K.; Hortobagyi, G.; Krop, I.; Loibl, S.; Pegram, M.; Slamon, D.; Palanca-Wessels, M. C.; Walker, L.; Feng, W.; Winer, E. P. *N. Engl. J. Med.* **2020**, *382* (7), 597–609.

(20) Kim, C.; Lee, C. K.; Chon, H. J.; Kim, J. H.; Park, H. S.; Heo, S. J.; Kim, H. J.; Kim, T. S.; Kwon, W. S.; Chung, H. C.; Rha, S. Y. *Oncotarget* **2017**, *8* (69), 113494–113501.

(21) Bang, Y. J.; Van Cutsem, E.; Feyereislova, A.; Chung, H. C.; Shen, L.; Sawaki, A.; Lordick, F.; Ohtsu, A.; Omuro, Y.; Satoh, T.; Aprile, G.; Kulikov, E.; Hill, J.; Lehle, M.; Rüschoff, J.; Kang, Y. K. *Lancet* **2010**, *376* (9742), 687–697.

(22) Sims, A. H.; Zweemer, A. J. M.; Nagumo, Y.; Faratian, D.; Muir, M.; Dodds, M.; Um, I.; Kay, C.; Hasmann, M.; Harrison, D. J.; Langdon, S. P. *Br. J. Cancer* **2012**, *106* (11), 1779–1789.

(23) Pohlmann, P. R.; Mayer, I. A.; Mernaugh, R. *Clin. Cancer Res.* **2009**, *15* (24), 7479–7491.

(24) Luque-Cabal, M.; García-Teijido, P.; Fernández-Pérez, Y.; Sánchez-Lorenzo, L.; Palacio-Vázquez, I. *Clin. Med. Insights Oncol.* **2016**, *10*, 21–30.

(25) Nagata, Y.; Lan, K. H.; Zhou, X.; Tan, M.; Esteva, F. J.; Sahin, A. A.; Klos, K. S.; Li, P.; Monia, B. P.; Nguyen, N. T.; Hortobagyi, G. N.; Hung, M. C.; Yu, D. *Cancer Cell* **2004**, *6* (2), 117–127.

(26) Nahta, R. *Int. Sch. Res. Netw.* **2012**, *2012* (428062), 1–16.

(27) Luque-Cabal, M.; García-Teijido, P.; Fernández-Pérez, Y.; Sánchez-Lorenzo, L.; Palacio-Vázquez, I. *Clin. Med. Insights Oncol.* **2016**, *10* (Suppl 1), 21–30.

(28) Pernas, S.; Tolaney, S. M. HER2-Positive Breast Cancer: New Therapeutic Frontiers and Overcoming Resistance.

(29) Chen, S.; Liang, Y.; Feng, Z.; Wang, M. *BMC Cancer* **2019**, *19* (1), 973.

(30) Verma, S.; Miles, D.; Gianni, L.; Krop, I. E.; Welslau, M.; Baselga, J.; Pegram, M.; Oh, D.-Y.; Diéras, V.; Guardino, E.; Fang, L.; Lu, M. W.; Olsen, S.; Blackwell, K. *N. Engl. J. Med.* **2012**, *367* (19), 1783–1791.

(31) Perez, E. A.; Cortés, J.; Gonzalez-angulo, A. M.; Bartlett, J. M. S. *Cancer Treat. Rev.* **2014**, *40* (2), 276–284.

(32) Murthy, P.; Kidwell, K. M.; Schott, A. F.; Merajver, S. D.; Griggs, J. J.; Smerage, J. D.; Van Poznak, C. H.; Wicha, M. S.; Hayes, D. F.; Henry, N. L. *Breast Cancer Res. Treat.* **2016**, *155* (3), 589–595.

(33) Joensuu, H. *Cancer Treat. Rev.* **2017**, *52*, 1–11.

(34) Tolaney, S. M.; Guo, H.; Pernas, S.; Barry, W. T.; Dillon, D. A.; Ritterhouse, L.;

Schneider, B. P.; Shen, F.; Fuhrman, K.; Baltay, M.; Dang, C. T.; Yardley, D. A.; Moy, B.; Kelly Marcom, P.; Albain, K. S.; Rugo, H. S.; Ellis, M. J.; Shapira, I.; Wolff, A. C.; Carey, L. A.; Overmoyer, B.; Partridge, A. H.; Hudis, C. A.; Krop, I. E.; Burstein, H. J.; Winer, E. P. *J. Clin. Oncol.* **2019**, *37* (22), 1868–1875.

(35) Gianni, L.; Pienkowski, T.; Im, Y. H.; Tseng, L. M.; Liu, M. C.; Lluch, A.; Starosławska, E.; de la Haba-Rodriguez, J.; Im, S. A.; Pedrini, J. L.; Poirier, B.; Morandi, P.; Semiglazov, V.; Srimuninnimit, V.; Bianchi, G. V.; Magazzù, D.; McNally, V.; Douthwaite, H.; Ross, G.; Valagussa, P. *Lancet Oncol.* **2016**, *17* (6), 791–800.

(36) Luque-Cabal, M.; García-Teijido, P.; Fernández-Pérez, Y.; Sánchez-Lorenzo, L.; Palacio-Vázquez, I. *Clin. Med. Insights Oncol.* **2016**, *10* (Suppl 1), 21–30.

(37) Andersson, M.; Lidbrink, E.; Bjerre, K. *J Clin Oncol* **2011**, *29* (3), 264–271.

(38) Derakhshani, A.; Rezaei, Z.; Safarpour, H.; Sabri, M.; Mir, A.; Sanati, M. A.; Vahidian, F.; Gholamiyan Moghadam, A.; Aghadoukht, A.; Hajiasgharzadeh, K.; Baradaran, B. *J. Cell. Physiol.* **2020**, *235* (4), 3142–3156.

(39) Valabrega, G.; Montemurro, F.; Sarotto, I.; Petrelli, A.; Rubini, P.; Tacchetti, C.; Aglietta, M.; Comoglio, P. M.; Giordano, S. *Oncogene* **2005**, *24* (18), 3002–3010.

(40) Takuwa, H.; Tsuji, W.; Yotsumoto, F. *Int. J. Surg. Case Rep.* **2018**, *52*, 125–131.

(41) New Treatments Emerge for Metastatic HER2+ Breast Cancer - National Cancer Institute https://www.cancer.gov/news-events/cancer-currents-blog/2020/tucatinib-trastuzumab-deruxtecan-her2-positive-metastatic-breast-cancer (accessed Jun 1, 2020).

(42) Stern, H. M.; Gardner, H.; Burzykowski, T.; Elatre, W.; O'Brien, C.; Lackner, M. R.; Pestano, G. A.; Santiago, A.; Villalobos, I.; Eiermann, W.; Pienkowski, T.; Martin, M.; Robert, N.; Crown, J.; Nuciforo, P.; Bee, V.; Mackey, J.; Slamon, D. J.; Press, M. F. *Clin. Cancer Res.* **2015**, *21* (9), 2065–2074.

(43) Vu, T.; Claret, F. X. *Front. Oncol.* **2012**, *2* (June), 62.

(44) Bartsch, R.; Wenzel, C.; Steger, G. G. *Biologics* **2007**, *1* (1), 19–31.

(45) Gschwantler-Kaulich, D.; Tan, Y. Y.; Fuchs, E.-M.; Hudelist, G.; Köstler, W. J.; Reiner, A.; Leser, C.; Salama, M.; Attems, J.; Deutschmann, C.; Zielinski, C. C.; Singer, C. F. *PLoS One* **2017**, *12* (3), e0172911.

(46) Gajria, D.; Chandarlapaty, S. *Expert Rev. Anticancer Ther.* **2011**, *11* (2), 263–275.

(47) Mercogliano, M. F.; Bruni, S.; Elizalde, P. V.; Schillaci, R. *Front. Oncol.* **2020**, *10*, 584.

(48) Rimawi, M. F.; de Angelis, C.; Contreras, A.; Pareja, F.; Geyer, F. C.; Burke, K. A.; Herrera, S.; Wang, T.; Mayer, I. A.; Forero, A.; Nanda, R.; Goetz, M. P.; Chang, J. C.; Krop, I. E.; Wolff, A. C.; Pavlick, A. C.; Fuqua, S. A. W.; Gutierrez, C.; Hilsenbeck, S. G.; Li, M. M.; Weigelt, B.; Reis-Filho, J. S.; Osborne, C. K.;

Schiff, R. *Breast Cancer Res. Treat.* **2018**, *167* (3), 731–740.

(49) Lebok, P.; Kopperschmidt, V.; Kluth, M.; Hube-Magg, C.; Özden, C.; Taskin, B.; Hussein, K.; Mittenzwei, A.; Lebeau, A.; Witzel, I.; Wölber, L.; Mahner, S.; Jänicke, F.; Geist, S.; Paluchowski, P.; Wilke, C.; Heilenkötter, U.; Simon, R.; Sauter, G.; Terracciano, L.; Krech, R.; Von, A.; Müller, V.; Burandt, E. *BMC Cancer* **2015**, *15* (1–10).

(50) Li, S.; Shen, Y.; Wang, M.; Yang, J.; Lv, M.; Li, P.; Chen, Z.; Yang, J. *Oncotarget* **2017**, *8* (19), 32043–32054.

(51) Kechagioglou, P.; Papi, R. M.; Provatopoulou, X.; Kalogera, E.; Papadimitriou, E.; Grigoropoulos, P.; Nonni, A.; Zografos, G.; Kyriakidis, D. A.; Gounaris, A. *Anticancer Res.* **2014**, *34* (3), 1387–1400.

(52) Chalhoub, N.; Baker, S. J. *Annu. Rev. Pathol. Mech. Dis.* **2009**, *4* (1), 127–150.

(53) Paplomata, E.; O'regan, R. *Ther. Adv. Med. Oncol.* **2014**, *6* (4), 154–166.

(54) Keniry, M.; Parsons, R. *Oncogene* **2008**, *27* (41), 5477–5485.

(55) Ebbesen, S. H.; Scaltriti, M.; Bialucha, C. U.; Morse, N.; Kastenhuber, E. R.; Wen, H. Y.; Dow, L. E.; Baselga, J.; Lowe, S. W. *Proc. Natl. Acad. Sci. U. S. A.* **2016**, *113* (11), 3030–3035.

(56) Luongo, F.; Colonna, F.; Calapà, F.; Vitale, S.; Fiori, M. E.; De Maria, R. *Cancers (Basel).* **2019**, *11* (8), 1076.

(57) Carracedo, A.; Pandolfi, P. P. *Oncogene* **2008**, *27* (41), 5527–5541.

(58) Crowell, J. A.; Steele, V. E.; Fay, J. R. *Mol. Cancer Ther.* **2007**, *6* (8), 2139–2148.

(59) Endersby, R.; Baker, S. J. *Oncogene* **2008**, *27* (41), 5416–5430.

(60) Nuciforo, P. G.; Aura, C.; Holmes, E.; Prudkin, L.; Jimenez, J.; Martinez, P.; Ameels, H.; de la Perna, L.; Ellis, C.; Eidtmann, H.; Piccart-Gebhart, M. J.; Scaltriti, M.; Baselga, J. *Ann. Oncol.* **2015**, *26* (7), 1494–1500.

(61) Carbognin, L.; Miglietta, F.; Paris, I.; Dieci, M. V. *Cancers (Basel).* **2019**, *11* (9), 1–18.

(62) Jones, N.; Bonnet, F.; Sfar, S.; Lafitte, M.; Lafon, D.; Sierankowski, G.; Brouste, V.; Banneau, G.; Tunon de Lara, C.; Debled, M.; MacGrogan, G.; Longy, M.; Sevenet, N. *Int. J. Cancer* **2013**, *133* (2), 323–334.

(63) Zhang, H. Y.; Liang, F.; Jia, Z. L.; Song, S. T.; Jiang, Z. F. *Oncol. Lett.* **2013**, *6* (1), 161–168.

(64) Zhu, Y.; Wloch, A.; Wu, Q.; Peters, C.; Pagenstecher, A.; Bertalanffy, H.; Sure, U. *Stroke* **2009**, *40* (3), 820–826.

(65) Kang, Y. H.; Lee, H. S.; Kim, W. H. *Lab. Investig.* **2002**, *82* (3), 285–291.

(66) Wilks, S. T. *Breast* **2015**, *24* (5), 548–555.

(67) Sangai, T.; Akcakanat, A.; Chen, H.; Tarco, E.; Wu, Y.; Do, K. A.; Miller, T. W.; Arteaga, C. L.; Mills, G. B.; Gonzalez-Angulo, A. M.; Meric-Bernstam, F. *Clin. Cancer Res.* **2012**, *18* (20), 5816–5828.

(68) Hudis, C.; Swanton, C.; Janjigian, Y. Y.; Lee, R.; Sutherland, S.; Lehman, R.; Chandarlapaty, S.; Hamilton, N.; Gajria, D.; Knowles, J.; Shah, J.; Shannon, K.; Tetteh, E.; Sullivan, D. M.; Moreno, C.; Yan, L.; Han, H. S. *Breast Cancer Res.* **2013**, *15* (6), R110.

(69) Xing, Y.; Lin, N. U.; Maurer, M. A.; Chen, H.; Mahvash, A.; Sahin, A.; Akcakanat, A.; Li, Y.; Abramson, V.; Litton, J.; Chavez-MacGregor, M.; Valero, V.; Piha-Paul, S. A.; Hong, D.; Do, K.-A.; Tarco, E.; Riall, D.; Eterovic, A. K.; Wulf, G. M.; Cantley, L. C.; Mills, G. B.; Doyle, L. A.; Winer, E.; Hortobagyi, G. N.; Gonzalez-Angulo, A. M.; Meric-Bernstam, F. *Breast Cancer Res.* **2019**, *21* (1), 78.

(70) Hurvitz, S. A.; Andre, F.; Jiang, Z.; Shao, Z.; Mano, M. S.; Neciosup, S. P.; Tseng, L. M.; Zhang, Q.; Shen, K.; Liu, D.; Dreosti, L. M.; Burris, H. A.; Toi, M.; Buyse, M. E.; Cabaribere, D.; Lindsay, M. A.; Rao, S.; Pacaud, L. B.; Taran, T.; Slamon, D. *Lancet Oncol.* **2015**, *16* (7), 816–829.

(71) Van Swearingen, A. E. D.; Siegel, M. B.; Deal, A. M.; Sambade, M. J.; Hoyle, A.; Hayes, D. N.; Jo, H.; Little, P.; Dees, E. C.; Muss, H.; Jolly, T.; Zagar, T. M.; Patel, N.; Miller, C. R.; Parker, J. S.; Smith, J. K.; Fisher, J.; Shah, N.; Nabell, L.; Nanda, R.; Dillon, P.; Abramson, V.; Carey, L. A.; Anders, C. K. *Breast Cancer Res. Treat.* **2018**, *171* (3), 637–648.

(72) Ramón y Cajal, S.; Sesé, M.; Capdevila, C.; Aasen, T.; De Mattos-Arruda, L.; Diaz-Cano, S. J.; Hernández-Losa, J.; Castellví, J. *J. Mol. Med.* **2020**, *98* (2), 161–177.

(73) Lee, H. J.; Seo, A. N.; Kim, E. J.; Jang, M. H.; Suh, K. J.; Ryu, H. S.; Kim, Y. J.; Kim, J. H.; Im, S.-A.; Gong, G.; Jung, K. H.; Park, I. A.; Park, S. Y. *Am. J. Clin. Pathol.* **2014**, *142* (6), 755–766.

(74) Rye, I. H.; Trinh, A.; Sætersdal, A. B.; Nebdal, D.; Lingjærde, O. C.; Almendro, V.; Polyak, K.; Børresen-Dale, A. L.; Helland, Å.; Markowetz, F.; Russnes, H. G. *Mol. Oncol.* **2018**, *12* (11), 1838–1855.

(75) Ferrari, A.; Vincent-Salomon, A.; Pivot, X.; Sertier, A. S.; Thomas, E.; Tonon, L.; Boyault, S.; Mulugeta, E.; Treilleux, I.; MacGrogan, G.; Arnould, L.; Kielbassa, J.; Le Texier, V.; Blanché, H.; Deleuze, J. F.; Jacquemier, J.; Mathieu, M. C.; Penault-Llorca, F.; Bibeau, F.; Mariani, O.; Mannina, C.; Pierga, J. Y.; Trédan, O.; Bachelot, T.; Bonnefoi, H.; Romieu, G.; Fumoleau, P.; Delaloge, S.; Rios, M.; Ferrero, J. M.; Tarpin, C.; Bouteille, C.; Calvo, F.; Gut, I. G.; Gut, M.; Martin, S.; Nik-Zainal, S.; Stratton, M. R.; Pauporté, I.; Saintigny, P.; Birnbaum, D.; Viari, A.; Thomas, G. *Nat. Commun.* **2016**, *7* (1), 1–9.

(76) Brady, S. W.; McQuerry, J. A.; Qiao, Y.; Piccolo, S. R.; Shrestha, G.; Jenkins, D. F.; Layer, R. M.; Pedersen, B. S.; Miller, R. H.; Esch, A.; Selitsky, S. R.; Parker, J. S.; Anderson, L. A.; Dalley, B. K.; Factor, R. E.; Reddy, C. B.; Boltax, J. P.; Li, D.

Y.; Moos, P. J.; Gray, J. W.; Heiser, L. M.; Buys, S. S.; Cohen, A. L.; Johnson, W. E.; Quinlan, A. R.; Marth, G.; Werner, T. L.; Bild, A. H. *Nat. Commun.* **2017**, *8* (1), 1–15.

(77) Korkaya, H.; Paulson, A.; Iovino, F.; Wicha, M. S. *Oncogene* **2008**, *27* (47), 6120–6130.

(78) Macosko, E. Z.; Basu, A.; Satija, R.; Nemesh, J.; Shekhar, K.; Goldman, M.; Tirosh, I.; Bialas, A. R.; Kamitaki, N.; Martersteck, E. M.; Trombetta, J. J.; Weitz, D. A.; Sanes, J. R.; Shalek, A. K.; Regev, A.; McCarroll, S. A. *Cell* **2015**, *161* (5), 1202–1214.

(79) Andrews, T. S.; Hemberg, M. *Mol. Aspects Med.* **2018**, *59*, 114–122.

(80) Ziegenhain, C.; Vieth, B.; Parekh, S.; Reinius, B.; Guillaumet-Adkins, A.; Smets, M.; Leonhardt, H.; Heyn, H.; Hellmann, I.; Enard, W. *Mol. Cell* **2017**, *65* (4), 631-643.e4.

(81) Ocasio, J.; Babcock, B.; Malawsky, D.; Weir, S. J.; Loo, L.; Simon, J. M.; Zylka, M. J.; Hwang, D.; Dismuke, T.; Sokolsky, M.; Rosen, E. P.; Vibhakar, R.; Zhang, J.; Saulnier, O.; Vladoiu, M.; El-Hamamy, I.; Stein, L. D.; Taylor, M. D.; Smith, K. S.; Northcott, P. A.; Colaneri, A.; Wilhelmsen, K.; Gershon, T. R. *Nat. Commun.* **2019**, *10* (1), 1–17.

(82) Korkaya, H.; Kim, G. II; Davis, A.; Malik, F.; Henry, N. L.; Ithimakin, S.; Quraishi, A. A.; Tawakkol, N.; D'Angelo, R.; Paulson, A. K.; Chung, S.; Luther, T.; Paholak, H. J.; Liu, S.; Hassan, K. A.; Zen, Q.; Clouthier, S. G.; Wicha, M. S. *Mol. Cell* **2012**, *47* (4), 570–584.

(83) Korkaya, H.; Paulson, A.; Charafe-Jauffret, E.; Ginestier, C.; Brown, M.; Dutcher, J.; Clouthier, S. G.; Wicha, M. S. *PLoS Biol.* **2009**, *7* (6), e1000121.

(84) Nagata, Y.; Lan, K. H.; Zhou, X.; Tan, M.; Esteva, F. J.; Sahin, A. A.; Klos, K. S.; Li, P.; Monia, B. P.; Nguyen, N. T.; Hortobagyi, G. N.; Hung, M. C.; Yu, D. *Cancer Cell* **2004**, *6* (2), 117–127.

(85) Goldman, E. M. and M. **2015**, 1–20.

(86) Nemesh, J. Drop-seq Core Computational Protocol http://mccarrolllab.org/wp-content/uploads/2016/03/Drop-seqAlignmentCookbookv1.2Jan2016.pdf (accessed Sep 1, 2020).

(87) Zappia, L.; Oshlack, A. *Gigascience* **2018**, *7* (7), 1–9.

(88) Sergushichev, A. A. *bioRxiv* **2016**, 060012.

(89) Subramanian, A.; Tamayo, P.; Mootha, V. K.; Mukherjee, S.; Ebert, B. L.; Gillette, M. A.; Paulovich, A.; Pomeroy, S. L.; Golub, T. R.; Lander, E. S.; Mesirov, J. P. *Proc. Natl. Acad. Sci. U. S. A.* **2005**, *102* (43), 15545–15550.

(90) Smith, S. E.; Mellor, P.; Ward, A. K.; Kendall, S.; McDonald, M.; Vizeacoumar, F. S.; Vizeacoumar, F. J.; Napper, S.; Anderson, D. H. *Breast Cancer Res.* **2017**, *19*

(1), 65.

(91) Jernström, S.; Hongisto, V.; Leivonen, S. K.; Due, E. U.; Tadele, D. S.; Edgren, H.; Kallioniemi, O.; Perälä, M.; Mælandsmo, G. M.; Sahlberg, K. K. *Breast Cancer Targets Ther.* **2017**, *9*, 185–198.

(92) Becht, E.; McInnes, L.; Healy, J.; Dutertre, C. A.; Kwok, I. W. H.; Ng, L. G.; Ginhoux, F.; Newell, E. W. *Nat. Biotechnol.* **2019**, *37* (1), 38–47.

(93) Luecken, M. D.; Theis, F. J. *Mol. Syst. Biol.* **2019**, *15* (6).

(94) Li, W.; Freudenberg, J.; Suh, Y. J.; Yang, Y. *Comput. Biol. Chem.* **2014**, *48*, 77–83.

(95) McDermaid, A.; Monier, B.; Zhao, J.; Liu, B.; Ma, Q. *Briefings in Bioinformatics*. Oxford University Press November 1, 2019, pp 2044–2054.

(96) Capaldo, C. T.; Nusrat, A. *Biochim. Biophys. Acta - Biomembr.* **2009**, *1788* (4), 864–871.

(97) Shen, W.-H.; Zhou, J.-H.; Broussard, S. R.; Freund, G. G.; Dantzer, R.; Kelley, K. W. *Cancer Res.* **2002**, 4746–4756.

(98) Yang, J.; Min, K.-W.; Kim, D.-H.; Son, B. K.; Moon, K. M.; Wi, Y. C.; Bang, S. S.; Oh, Y. H.; Do, S.-I.; Chae, S. W.; Oh, S.; Kim, Y. H.; Kwon, M. J. *PLoS One* **2018**, *13* (8), e0202113.

(99) Cai, X.; Cao, C.; Li, J.; Chen, F.; Zhang, S.; Liu, B.; Zhang, W.; Zhang, X.; Ye, L. *Oncotarget* **2017**, *8* (35), 58338–58352.

(100) Mostowy, S.; Shenoy, A. R. *Nat. Rev. Immunol.* **2015**, *15* (9), 559–573.

(101) Wang, W.; Eddy, R.; Condeelis, J. *Nat. Rev. Cancer* **2007**, *7* (6), 429–440.

(102) Nakayama, K. I.; Nakayama, K. *Nat. Rev. Cancer* **2006**, *6* (5), 369–381.

(103) Bassermann, F.; Eichner, R.; Pagano, M. *Biochim. Biophys. Acta - Mol. Cell Res.* **2014**, *1843* (1), 150–162.

(104) Gan, B.; DePinho, R. A. *Cell Cycle* **2009**, *8* (7), 1003–1006.

(105) Laplante, M.; Sabatini, D. M. *J. Cell Sci.* **2009**, *122* (20), 3589–3594.

(106) Kallergi, G.; Tsintari, V.; Sfakianakis, S.; Bei, E.; Lagoudaki, E.; Koutsopoulos, A.; Zacharopoulou, N.; Alkahtani, S.; Alarifi, S.; Stournaras, C.; Zervakis, M.; Georgoulias, V. *Breast Cancer Res.* **2019**, *21* (1), 86.

(107) Hasan, Z.; Koizumi, S. I.; Sasaki, D.; Yamada, H.; Arakaki, N.; Fujihara, Y.; Okitsu, S.; Shirahata, H.; Ishikawa, H. *Nat. Commun.* **2017**, *8*.

(108) Gong, C.; Shen, J.; Fang, Z.; Qiao, L.; Feng, R.; Lin, X.; Li, S. *Biosci. Rep.* **2018**, *38* (4).

(109) Sundqvist, A.; Morikawa, M.; Ren, J.; Vasilaki, E.; Kawasaki, N.; Kobayashi, M.;

Koinuma, D.; Aburatani, H.; Miyazono, K.; Heldin, C. H.; Van Dam, H.; Dijke, P. Ten. *Nucleic Acids Res.* **2018**, *46* (3), 1180–1195.

(110) Mendoza-Rodríguez, M.; Arévalo Romero, H.; Fuentes-Pananá, E. M.; Ayala-Sumuano, J. T.; Meza, I. *Cancer Lett.* **2017**, *390*, 39–44.

(111) Liu, S.; Lee, J. S.; Jie, C.; Park, M. H.; Iwakura, Y.; Patel, Y.; Soni, M.; Reisman, D.; Chen, H. *Cancer Res.* **2018**, *78* (8), 2040–2051.

(112) Korkaya, H.; Kim, G. Il; Davis, A.; Malik, F.; Henry, N. L.; Ithimakin, S.; Quraishi, A. A.; Tawakkol, N.; D'Angelo, R.; Paulson, A. K.; Chung, S.; Luther, T.; Paholak, H. J.; Liu, S.; Hassan, K. A.; Zen, Q.; Clouthier, S. G.; Wicha, M. S. *Mol. Cell* **2012**, *47* (4), 570–584.

(113) Zhang, Z.; Xu, Q.; Song, C.; Mi, B.; Zhang, H.; Kang, H.; Liu, H.; Sun, Y.; Wang, J.; Lei, Z.; Guan, H.; Li, F. *Mol. Cancer Ther.* **2020**, *19* (2), 650–660.

(114) Fagerli, U. M.; Ullrich, K.; Stühmer, T.; Holien, T.; Köchert, K.; Holt, R. U.; Bruland, O.; Chatterjee, M.; Nogai, H.; Lenz, G.; Shaughnessy, J. D.; Mathas, S.; Sundan, A.; Bargou, R. C.; Dörken, B.; Børset, M.; Janz, M. *Oncogene* **2011**, *30* (28), 3198–3206.

(115) Sahoo, S.; Brickley, D. R.; Kocherginsky, M.; Conzen, S. D. *Eur. J. Cancer* **2005**, *41* (17), 2754–2759.

(116) Mistry, P.; Deacon, K.; Mistry, S.; Blank, J.; Patel, R. *J. Biol. Chem.* **2004**, *279* (2), 1482–1490.

(117) Reymond, N.; Im, J. H.; Garg, R.; Cox, S.; Soyer, M.; Riou, P.; Colomba, A.; Muschel, R. J.; Ridley, A. J. *Mol. Oncol.* **2015**, *9* (6), 1043–1055.

(118) Tomaskovic-Crook, E.; Thompson, E. W.; Thiery, J. P. *Breast Cancer Res.* **2009**, *11* (6), 213.

(119) Kalluri, R.; Weinberg, R. A. *J. Clin. Invest.* **2009**, *119* (6), 1420–1428.

(120) Pastushenko, I.; Blanpain, C. *Trends Cell Biol.* **2019**, *29* (3), 212–226.

(121) Chu, P. G.; Weiss, L. M. *Histopathology* **2002**, *40* (5), 403–439.

(122) Xiang, X.; Deng, Z.; Zhuang, X.; Ju, S.; Mu, J.; Jiang, H.; Zhang, L.; Yan, J.; Miller, D.; Zhang, H.-G. *PLoS One* **2012**, *7* (12), e50781.

(123) Schmalhofer, O.; Brabletz, S.; Brabletz, T. *Cancer Metastasis Rev.* **2009**, *28* (1–2), 151–166.

(124) Zhang, S.; Wang, Z.; Liu, W.; Lei, R.; Shan, J.; Li, L.; Wang, X. *Sci. Rep.* **2017**, *7*.

(125) Nasser, M. W.; Qamri, Z.; Deol, Y. S.; Ravi, J.; Powell, C. A.; Trikha, P.; Schwendener, R. A.; Bai, X. F.; Shilo, K.; Zou, X.; Leone, G.; Wolf, R.; Yuspa, S. H.; Ganju, R. K. *Cancer Res.* **2012**, *72* (3), 604–615.

(126) West, N. R.; Watson, P. H. *Oncogene* **2010**, *29* (14), 2083–2092.

(127) Paruchuri, V.; Prasad, A.; McHugh, K.; Bhat, H. K.; Polyak, K.; Ganju, R. K. *PLoS One* **2008**, *3* (3), 1741.

(128) Emberley, E. D.; Murphy, L. C.; Watson, P. H. *Breast Cancer Res.* **2004**, *6* (4), 153–159.

(129) Cancemi, P.; Buttacavoli, M.; Cara, G. Di; Albanese, N. N.; Bivona, S.; Pucci-Minafra, I.; Feo, S. *Oncotarget* **2018**, *9* (49), 29064–29081.

(130) Hua, X.; Zhang, H.; Jia, J.; Chen, S.; Sun, Y.; Zhu, X. *Biomed. Pharmacother.* **2020**, *127*, 110156.

(131) Yuzugullu, H.; Von, T.; Thorpe, L. M.; Walker, S. R.; Roberts, T. M.; Frank, D. A.; Zhao, J. J. *Cell Discov.* **2016**, *2* (1), 1–13.

(132) Sadasivam, S.; DeCaprio, J. A. *Nat. Rev. Cancer* **2013**, *13* (8), 585–595.

(133) Min, M.; Spencer, S. L. *PLOS Biol.* **2019**, *17* (3), e3000178.

(134) Bracken, A. P.; Ciro, M.; Cocito, A.; Helin, K. *Trends Biochem. Sci.* **2004**, *29* (8), 409–417.

(135) Ito, T.; Teo, Y. V.; Evans, S. A.; Neretti, N.; Sedivy Correspondence, J. M. *Cell Rep.* **2018**, *22*, 3480–3492.

(136) Vizán, P.; Gutiérrez, A.; Espejo, I.; García-Montolio, M.; Lange, M.; Carretero, A.; Lafzi, A.; de Andrés-Aguayo, L.; Blanco, E.; Thambyrajah, R.; Graf, T.; Heyn, H.; Bigas, A.; Di Croce, L. *Sci. Adv.* **2020**, *6* (32), eabb2745.

(137) Doyle, L. A.; Ross, D. D. *Oncogene* **2003**, *22* (47 REV. ISS. 6), 7340–7358.

(138) Balaji, S. A.; Udupa, N.; Chamallamudi, M. R.; Gupta, V.; Rangarajan, A. *PLoS One* **2016**, *11* (5).

(139) Lucanus, A. J.; Yip, G. W. *Nat. Publ. Gr.* **2018**.

(140) Mandelkow, E.; Mandelkow, E. M. *Trends Cell Biol.* **2002**, *12* (12), 585–591.

(141) Ivanov, A. I.; McCall, I. C.; Babbin, B.; Samarin, S. N.; Nusrat, A.; Parkos, C. A. *BMC Cell Biol.* **2006**, *7* (1), 12.

(142) Li, T.-F.; Zeng, H.-J.; Shan, Z.; Ye, R.-Y.; Cheang, T.-Y.; Zhang, Y.-J.; Lu, S.-H.; Zhang, Q.; Shao, N.; Lin, Y. .

(143) Hirokawa, N.; Noda, Y.; Tanaka, Y.; Niwa, S. *Nat. Rev. Mol. Cell Biol.* **2009**, *10* (10), 682–696.

(144) Li, B.; Dou, S. X.; Yuan, J. W.; Liu, Y. R.; Li, W.; Ye, F.; Wang, P. Y.; Li, H. *Proc. Natl. Acad. Sci. U. S. A.* **2018**, *115* (48), 12118–12123.

(145) Kwon, M. J.; Park, S.; Choi, J. Y.; Oh, E.; Kim, Y. J.; Park, Y. H.; Cho, E. Y.; Kwon, M. J.; Nam, S. J.; Im, Y. H.; Shin, Y. K.; Choi, Y. L. *Br. J. Cancer* **2012**, *106* (5), 923–930.

(146) Yang, X. H.; Richardson, A. L.; Torres-Arzayus, M. I.; Zhou, P.; Sharma, C.; Kazarov, A. R.; Andzelm, M. M.; Strominger, J. L.; Brown, M.; Hemler, M. E. *Cancer Res.* **2008**, *68* (9), 3204–3213.

(147) Kumar, S.; Park, S. H.; Cieply, B.; Schupp, J.; Killiam, E.; Zhang, F.; Rimm, D. L.; Frisch, S. M. *Mol. Cell. Biol.* **2011**, *31* (19), 4036–4051.

(148) Rasiah, P. K.; Maddala, R.; Bennett, V.; Rao, P. V. *Dev. Biol.* **2019**, *446* (1), 119–131.

(149) Kurozumi, S.; Joseph, C.; Raafat, S.; Sonbul, S.; Kariri, Y.; Alsaeed, S.; Pigera, M.; Alsaleem, M.; Nolan, C. C.; Johnston, S. J.; Aleskandarany, M. A.; Ogden, A.; Fujii, T.; Shirabe, K.; Martin, S. G.; Alshankyty, I.; Mongan, N. P.; Ellis, I. O.; Green, A. R.; Rakha, E. A. *Breast Cancer Res. Treat.* **2019**, *176* (1), 63–73.

(150) Gröger, C. J.; Grubinger, M.; Waldhör, T.; Vierlinger, K.; Mikulits, W. *PLoS One* **2012**, *7* (12), e51136.

(151) Mrouj, K.; Singh, P.; Sobecki, M.; Dubra, G.; Ghoul, E. Al; Aznar, A.; Prieto, S.; Vincent, C.; Pirot, N.; Bernex, F.; Bordignon, B.; Hassen-Khodja, C.; Pouzolles, M.; Zimmerman, V.; Dardalhon, V.; Villalba, M.; Krasinska, L.; Fisher, D. *bioRxiv* **2019**, 712380.

(152) Mani, S. A.; Guo, W.; Liao, M. J.; Eaton, E. N.; Ayyanan, A.; Zhou, A. Y.; Brooks, M.; Reinhard, F.; Zhang, C. C.; Shipitsin, M.; Campbell, L. L.; Polyak, K.; Brisken, C.; Yang, J.; Weinberg, R. A. *Cell* **2008**, *133* (4), 704–715.

(153) Foroni, C.; Broggini, M.; Generali, D.; Damia, G. *Cancer Treat. Rev.* **2012**, *38* (6), 689–697.

(154) Collier, M. P.; Benesch, J. L. P. *Cell Stress Chaperones* **2020**, *25* (4), 601–613.

(155) Gunning, P. W.; Hardeman, E. C.; Lappalainen, P.; Mulvihill, D. P. *J. Cell Sci.* **2015**, *128* (16), 2965–2974.

(156) Chou, D. M.; Elledge, S. J. *Proc. Natl. Acad. Sci. U. S. A.* **2006**, *103* (48), 18143–18147.

(157) Kröger, C.; Afeyan, A.; Mraz, J.; Eaton, E. N.; Reinhardt, F.; Khodor, Y. L.; Thiru, P.; Bierie, B.; Ye, X.; Burge, C. B.; Weinberg, R. A. *Proc. Natl. Acad. Sci. U. S. A.* **2019**, *116* (15), 7353–7362.

(158) Xiao, W.; Zheng, S.; Xie, X.; Li, X.; Zhang, L.; Yang, A.; Wang, J.; Tang, H.; Xie, X. *Mol. Ther. - Oncolytics* **2020**, *17*, 118–129.

(159) Wang, C. Q.; Tang, C. H.; Wang, Y.; Jin, L.; Wang, Q.; Li, X.; Hu, G. N.; Huang, B. F.; Zhao, Y. M.; Su, C. M. *Sci. Rep.* **2017**, *7* (1).

(160) Nami, B.; Wang, Z. *Cancers (Basel).* **2018**, *10* (8), 274.

(161) Ebright, R. Y.; Lee, S.; Wittner, B. S.; Niederhoffer, K. L.; Nicholson, B. T.; Bardia, A.; Truesdell, S.; Wiley, D. F.; Wesley, B.; Li, S.; Mai, A.; Aceto, N.; Vincent-Jordan, N.; Szabolcs, A.; Chirn, B.; Kreuzer, J.; Comaills, V.; Kalinich, M.; Haas,

W.; Ting, D. T.; Toner, M.; Vasudevan, S.; Haber, D. A.; Maheswaran, S.; Micalizzi, D. S. *Science (80-.).* **2020**, *367* (6485), 1468–1473.

(162) Prashar, A.; Schnettger, L.; Bernard, E. M.; Gutierrez, M. G. *Front. Cell. Infect. Microbiol.* **2017**, *7* (SEP), 435.

(163) Barbera, S.; Nardi, F.; Elia, I.; Realini, G.; Lugano, R.; Santucci, A.; Tosi, G. M.; Dimberg, A.; Galvagni, F.; Orlandini, M. *Cell Commun. Signal.* **2019**, *17* (1), 55.

(164) Kim, S. E.; Hinoue, T.; Kim, M. S.; Sohn, K. J.; Cho, R. C.; Cole, P. D.; Weisenberger, D. J.; Laird, P. W.; Kim, Y. I. *Genes Nutr.* **2015**, *10* (1), 1–17.

(165) Maggini, S.; Pierre, A.; Calder, P. C. *Nutrients* **2018**, *10* (10).

(166) MacEyka, M.; Spiegel, S. *Nature* **2014**, *510* (7503), 58–67.

(167) Waumans, Y.; Baerts, L.; Kehoe, K.; Lambeir, A. M.; De Meester, I. *Front. Immunol.* **2015**, *6* (JUL), 387.

(168) Kingsbury, S. R.; Loddo, M.; Fanshawe, T.; Obermann, E. C.; Prevost, A. T.; Stoeber, K.; Williams, G. H. *Exp. Cell Res.* **2005**, *309* (1), 56–67.

(169) Gookin, S.; Min, M.; Phadke, H.; Chung, M.; Moser, J.; Miller, I.; Carter, D.; Spencer, S. L. *PLOS Biol.* **2017**, *15* (9), e2003268.

(170) Kabraji, S.; Solé, X.; Huang, Y.; Bango, C.; Bowden, M.; Bardia, A.; Sgroi, D.; Loda, M.; Ramaswamy, S. *Breast Cancer Res.* **2017**, *19* (1), 88.

(171) Le, X. F.; Lammayot, A.; Gold, D.; Lu, Y.; Mao, W.; Chang, T.; Patel, A.; Mills, G. B.; Bast, R. C. *J. Biol. Chem.* **2005**, *280* (3), 2092–2104.

(172) Sun, H.; Liu, K.; Huang, J.; Sun, Q.; Shao, C.; Luo, J.; Xu, L.; Shen, Y.; Ren, B. *Onco. Targets. Ther.* **2019**, *Volume 12*, 2829–2842.

(173) FAM111B gene - Genetics Home Reference - NIH https://ghr.nlm.nih.gov/gene/FAM111B (accessed Aug 8, 2020).

(174) Chung, V. Y.; Tan, T. Z.; Ye, J.; Huang, R. L.; Lai, H. C.; Kappei, D.; Wollmann, H.; Guccione, E.; Huang, R. Y. J. *Commun. Biol.* **2019**, *2* (1), 1–15.

(175) Jolly, M. K.; Tripathi, S. C.; Jia, D.; Mooney, S. M.; Celiktas, M.; Hanash, S. M.; Mani, S. A.; Pienta, K. J.; Ben-Jacob, E.; Levine, H. *Oncotarget* **2016**, *7* (19), 27067–27084.

(176) Cieply, B.; Riley IV, P.; Pifer, P. M.; Widmeyer, J.; Addison, J. B.; Ivanov, A. V.; Denvir, J.; Frisch, S. M. *Cancer Res.* **2012**, *72* (9), 2440–2453.

(177) Mooney, S. M.; Talebian, V.; Jolly, M. K.; Jia, D.; Gromala, M.; Levine, H.; McConkey, B. J. *J. Cell. Biochem.* **2017**, *118* (9), 2559–2570.

(178) Sánchez-Tilló, E.; De Barrios, O.; Siles, L.; Cuatrecasas, M.; Castells, A.; Postigo, A. *Proc. Natl. Acad. Sci. U. S. A.* **2011**, *108* (48), 19204–19209.

(179) Lee, J.; Ouh, Y.; Ahn, K. H.; Hong, S. C.; Oh, M.; Kim, J.; Cho, G. J. *PLoS One*

2017, *12* (5), 1–8.

(180) Gajria, D.; Chandarlapaty, S. *Expert Rev. Anticancer Ther.* **2011**, *11* (2), 263–275.

(181) Asgari, A.; Sharifzadeh, S.; Ghaderi, A.; Hosseini, A.; Ramezani, A. *Mol. Biol. Rep.* **2019**, *46* (6), 6205–6213.

(182) Dang, C. V. *Cell* **2012**, *149* (1), 22–35.

(183) Stine, Z. E.; Walton, Z. E.; Altman, B. J.; Hsieh, A. L.; Dang, C. V. *Cancer Discov.* **2015**, *5* (10), 1024–1039.

(184) Chen, H.; Liu, H.; Qing, G. *Signal Transduct. Target. Ther.* **2018**, *3* (1), 1–7.

(185) Gabay, M.; Li, Y.; Felsher, D. W. *Cold Spring Harb. Perspect. Med.* **2014**, *4* (6), 1–14.

(186) Richart, L.; Carrillo-de Santa Pau, E.; Río-Machín, A.; de Andrés, M. P.; Cigudosa, J. C.; Lobo, V. J. S.-A.; Real, F. X. *Nat. Commun.* **2016**, *7*, 10153.

(187) Dang, C. V. **2013**, 1–15.

(188) Bouvard, C.; Lim, S. M.; Ludka, J.; Yazdani, N.; Woods, A. K.; Chatterjee, A. K.; Schultz, P. G.; Zhu, S. *Proc. Natl. Acad. Sci. U. S. A.* **2017**, *114* (13), 3497–3502.

(189) Tawani, A.; Mishra, S. K.; Kumar, A. *Sci. Rep.* **2017**, *7* (1), 1–13.

(190) Mathad, R. I.; Hatzakis, E.; Dai, J.; Yang, D. *Nucleic Acids Res.* **2011**, *39* (20), 9023–9033.

(191) Siddiqui-Jain, A.; Grand, C. L.; Bearss, D. J.; Hurley, L. H. *Proc. Natl. Acad. Sci. U. S. A.* **2002**, *99* (18), 11593–11598.

(192) Castell, A.; Yan, Q.; Karin, F.; Hydbring, P.; Zhang, F.; Verschut, V.; Franco, M.; Zakaria, S. M.; Bazzar, W.; Goodwin, J.; Zinzalla, G.; Larson, L.-G. *Sci. Rep.* **2018**, *8* (May), 1–17.

(193) Kiessling, A.; Sperl, B.; Hollis, A.; Eick, D.; Berg, T. *Chem. Biol.* **2006**, *13* (7), 745–751.

(194) Berg, T.; Cohen, S. B.; Desharnais, J.; Sonderegger, C.; Maslyar, D. J.; Goldberg, J.; Boger, D. L.; Vogt, P. K. *Proc. Natl. Acad. Sci. U. S. A.* **2002**, *99* (6), 3830–3835.

(195) Whitfield, J. R.; Beaulieu, M. E.; Soucek, L. *Front. Cell Dev. Biol.* **2017**, *5* (FEB), 10.

(196) Castell, A.; Larsson, L. *Cancer Discov.* **2015**, *5* (7), 701–704.

(197) Carabet, L. A.; Rennie, P. S.; Cherkasov, A. *Int. J. Mol. Sci.* **2019**, *20* (1).

(198) Dang, C. V.; Reddy, E. P.; Shokat, K. M.; Soucek, L. *Nat. Rev. Cancer* **2017**, *17* (8), 502–508.

(199) McKeown, M. R.; Bradner, J. E. *Cold Spring Harb. Perspect. Med.* **2014**, *4* (10).

(200) Thomas, L. R.; Wang, Q.; Grieb, B. C.; Phan, J.; Foshage, A. M.; Sun, Q.; Olejniczak, E. T.; Clark, T.; Dey, S.; Lorey, S.; Alicie, B.; Howard, G. C.; Cawthon, B.; Ess, K. C.; Eischen, C. M.; Zhao, Z.; Fesik, S. W.; Tansey, W. P. *Mol. Cell* **2015**, *58* (3), 440–452.

(201) Thomas, L. R.; Tansey, W. P. *Open Access J. Sci. Technol.* **2015**, *3*, 1–25.

(202) Karatas, H.; Townsend, E. C.; Bernard, D.; Dou, Y.; Wang, S. *J. Med. Chem.* **2010**, *53*, 5179–5185.

(203) Odho, Z.; Southall, S. M.; Wilson, J. R. *J. Biol. Chem.* **2010**, *285* (43), 32967–32976.

(204) Dias, J.; Nguyen, N. Van; Georgiev, P.; Gaub, A.; Brettschneider, J.; Cusack, S.; Kadlec, J.; Akhtar, A. *Genes Dev.* **2014**, *28*, 929–942.

(205) Scott, D. E.; Coyne, A. G.; Hudson, S. A.; Abell, C. *Biochemistry* **2012**, *51*, 4990–5003.

(206) Murray, C. W.; Verdonk, M. L.; Rees, D. C. *Trends Pharmacol. Sci.* **2012**, *33* (5), 224–232.

(207) Huynh, K.; Partch, C. L. *Curr. Protoc. protein Sci.* **2015**, *79*, 28.9.1-28.9.14.

(208) Niesen, F. H.; Berglund, H.; Vedadi, M. *Nat. Protoc.* **2007**, *2* (9), 2212–2221.

(209) Jhoti, H.; Williams, G.; Rees, D. C.; Murray, C. W. *Nat. Publ. Gr.* **2013**, No. July.

(210) Kirsch, P.; Hartman, A. M.; Hirsch, A. K. H.; Empting, M. *Molecules* **2019**, *24* (23).

(211) Aldrich, C.; Bertozzi, C.; Georg, G. I.; Kiessling, L.; Lindsley, C.; Liotta, D.; Merz, K. M.; Schepartz, A.; Wang, S. *J. Med. Chem.* **2017**, *60* (6), 2165–2168.

(212) Zhang, Ji-hu, Chung, Thomas D.Y., Oldenburg, K. R. *J. Biomol. Screen.* **1999**, *4* (2), 67–73.

(213) Jacob, R. T.; Larsen, M. J.; Larsen, S. D.; Kirchhoff, P. D.; Sherman, D. H.; Neubig, R. R. *J. Biomol. Screen.* **2012**, *17* (8), 1080–1087.

(214) Karatas, H.; Townsend, E. C.; Cao, F.; Chen, Y.; Bernard, D.; Liu, L.; Lei, M.; Dou, Y.; Wang, S. *J. Am. Chem. Soc.* **2013**, *135* (2), 669–682.

(215) Cao, F.; Townsend, E. C.; Karatas, H.; Xu, J.; Li, L.; Lee, S.; Liu, L.; Chen, Y.; Ouillette, P.; Zhu, J.; Hess, J. L.; Atadja, P.; Lei, M.; Qin, Z. S.; Malek, S.; Wang, S.; Dou, Y. *Mol. Cell* **2014**, *53* (2), 247–261.

(216) Lea, W. A.; Simeonov, A. *Expert Opin. Drug Discov.* **2011**, *6* (1), 17–32.

(217) Rossi, A. M.; Taylor, C. W. *Nat. Protoc.* **2011**, *6* (3), 365–387.

(218) Hall, M. D.; Yasgar, A.; Peryea, T.; Braisted, J. C.; Jadhav, A.; Simeonov, A.; Coussens, N. P. *Methods Appl. Fluoresc.* **2016**, *4* (2), 022001.

(219) Koh, C. M.; Sabò, A.; Guccione, E. *BioEssays* **2016**, *38* (3), 266–275.

(220) Casey, S. C.; Tong, L.; Li, Y.; Do, R.; Walz, S.; Fitzgerald, K. N.; Gouw, A. M.; Baylot, V.; Gütgemann, I.; Eilers, M.; Felsher, D. W. *Science (80-.).* **2016**, *352* (6282), 227–231.

(221) Polivka, J.; Janku, F. *Pharmacol. Ther.* **2014**, *142* (2), 164–175.

(222) Chacón Simon, S.; Wang, F.; Thomas, L. R.; Phan, J.; Zhao, B.; Olejniczak, E. T.; MacDonald, J. D.; Shaw, J. G.; Schlund, C.; Payne, W.; Creighton, J.; Stauffer, S. R.; Waterson, A. G.; Tansey, W. P.; Fesik, S. W. *J. Med. Chem.* **2020**, *63* (8), 4315–4333.

(223) Macdonald, J. D.; Chacón Simon, S.; Han, C.; Wang, F.; Shaw, J. G.; Howes, J. E.; Sai, J.; Yuh, J. P.; Camper, D.; Alicie, B. M.; Alvarado, J.; Nikhar, S.; Payne, W.; Aho, E. R.; Bauer, J. A.; Zhao, B.; Phan, J.; Thomas, L. R.; Rossanese, O. W.; Tansey, W. P.; Waterson, A. G.; Stauffer, S. R.; Fesik, S. W. *J. Med. Chem.* **2019**, *62* (24), 11232–11259.

Chapter 2: PTEN Deficiency in HER2+ Breast Cancer Cell Lines Enriched Quiescent Subpopulation with Epithelial, Early EMT Transcriptomic Composition

Abstract

HER2+ breast cancer is a highly aggressive subtype of breast cancer and characterized by poor survival, especially among patients with advanced stage disease. Standard of care for HER2+ breast cancer is trastuzumab-based therapy in combination with taxanes and pertuzumab, which is unsuccessful for patients with late stage HER2+ breast cancer. The role of PTEN has been considered to contribute to an aggressive cancer phenotype, but the role of PTEN as it pertained to HER2+ breast cancer remains controversial. In this study, we used single cell RNA-seq to unravel the consequences of PTEN deficiency in three HER2+ breast cancer cell lines: HCC1954, SKBR3, and BT474. For all of these cell lines, we observed that PTEN k.d. by shRNA resulted in a shift in the cancer subpopulations that make up the bulk cancer cell line. Notably, PTEN k.d. in HCC1954 and SKBR3 resulted in an 84 fold and 120 fold increase in a subpopulation characterized with a quiescent, epithelial early EMT phenotype. In BT474, the magnitude of PTEN k.d. on the BT474 subpopulations changed 2-5 fold, but also enriched for the quiescent early EMT subpopulation. Furthermore, the k.d. of PTEN in these cell lines slightly increased the heterogeneity by altering the expression of genes critical phenotypes of different subpopulations.

2.1. Introduction

HER2+ breast cancer constitutes 10-30% of all breast cancer cases and is characterized by an aggressive phenotype and poor survival as exemplified by the sharp decline in the five year survival as breast cancer of this subtype progress from localized to distant cancer.[1,2,5–7] The standard of care for HER2+ breast cancer patients features trastuzumab (commercially known as Herceptin) in combination with pertuzumab and a

chemotherapeutic agent such as taxanes.[14–16] Trastuzumab has been used to target HER2-overexpressing cancer cells in breast, ovarian, gastric, and esophageal cancer.[16–22] In early stage HER2+ breast cancer patients, the use of trastuzumab in combination with taxanes resulted in 93% disease free survival rates (7 years).[28,34,35] In contrast, 10-40% of HER2+ metastatic breast cancer patients initially respond to trastuzumab, and 50-70% of these patients develop acquired resistance and experience disease progression within 1 year of treatment for advanced diseased.[36–39] The gap in efficacy between early stage and advanced stage HER2+ breast cancer patients underscores the need to dissect mechanisms that contribute to resistance of trastuzumab to facilitate the discovery of alternative therapies for patients who acquire resistance within the first 2 years of cancer management.

Among the resistance mechanisms hypothesized to contribute to trastuzumab resistance, the loss of PTEN by epigenetic silencing or by the loss of heterozygosity has been regarded as one of the driving forces for the development of a more aggressive cancer phenotype.[20,23,26,38,42,48–50,54,84] However, the exact contribution of PTEN status to the progression of HER2+ breast cancer and trastuzumab sensitivity remains controversial due to conflicting literature reports about the prognostic value of PTEN in HER2+ breast cancer.[20,42,45,48,60] The key limitation of previous studies is the use of clinical tumor samples, which are not ideal for accounting for the intratumoral heterogeneity that underlies the cancer. This heterogeneity governs the phenotype of the cells that make up the cancer, and thus, different cancer cells within a tumor responds differently to treatment and cellular stress based on the gene expression of those cells.[10,72] Thus, it is critical to evaluate the consequences of PTEN status and loss in the context of intratumoral heterogeneity. Additionally, it is critical to assess how the consequences of PTEN deficiency varies across HER2+ breast cancer patients and understand the contribution of intertumoral heterogeneity. Therefore, understanding the effects of PTEN status and loss on a single cell level would reveal how the cancer as a whole is affected by PTEN loss, and thus, enables the understanding of PTEN deficiency in the context of intertumoral heterogeneity and intratumoral heterogeneity. Herein, we describe the use of the Drop-seq pipeline to evaluate how PTEN deficiency in three HER2+ breast cancer cell lines affected the steady state subpopulations that make up

these HER2+ breast cancer cell lines. By examining the effects of PTEN deficiency on a single cell level, we determined that PTEN deficiency increased the intra-subpopulation heterogeneity by altering the expression of key genes governing the phenotype of different subpopulations. Importantly, PTEN deficiency enriched a subset of quiescent, epithelial early EMT cells, suggesting that PTEN deficiency in HER2+ could promote an aggressive phenotype.

2.2. Materials and Methods

2.2.1. Cell Culture

Cells with silenced PTEN were generated by lentiviral infection to introduce short hairpin RNA of PTEN. To target the human *PTEN* gene for silencing, the pLentilox 3.7 vector containing shPTEN was used to generate "PTEN k.d." cell lines. As a control for lentiviral infection, pLentilox 3.7 vector containing fluorescent dye DsRed, which resulted in the wild type (wt) PTEN cell line derivative. Knockdown studies were performed by Dr. Joseph Burnett as previously described by Korkaya and coworkers to yield HER2+ breast cancer cell line pairs based on PTEN status.[77,82,83]

The following HER2+ breast cancer cell lines with wild type (WT) PTEN and PTEN knockdown ("PTEN k.d." derivative) were used for this study: SKBR3, BT474, and HCC-1954. SKBR3 DsRed and PTEN k.d. cell line derivatives was maintained in RPMI 1640 and supplemented with 10% FBS, 2% Pen-Strep (Gibco cat. no. 15140122), 1% sodium pyruvate (Gibco cat. no. 11360070), and 1% of 2mM L-Glutamine. BT474 cell line derivatives were maintained in DMEM/F-12 50:50 and supplemented with 10% FBS, 1% Pen-Strep, and 1% of 2mM L-Glutamine. HCC-1954 cell line derivatives were maintained in RPMI 1640 supplemented with 10% FBS, 1% anti-anti, and 0.008% gentimycin. Cells were cultured in an incubator at 37°C and humidified with 5% CO_2.

2.2.2. Drop-seq Experiments

Drop-seq experiments were performed in accordance to the online protocol from the McCarroll lab (version 3.1, 2015).[85] Barcoded Bead SeqB beads were ordered from Chemgenes and referred henceforth as Drop-seq beads. Microfluidics devices used during this study were generous gifts from Dr. Michael Brooks from Dr. Max Wicha's group. For these devices, treatment with Aquapel was performed using instructions from the McCarroll lab to ensure a hydrophobic surface through the microfluidics devices. To

ensure high-quality droplets and maintain consistency between Drop-seq experiments, microfluidics devices were ordered from FlowJEM (PDMS Drop-seq chip, standard design, containing vaporized silane).

2.2.3. Sequencing of cDNA Libraries

Single transcriptomic libraries generated from each cell line pair (HCC1954, SKBR3, and BT474) were sequenced by Next-seq (150 cycle, MO) at the Advanced Genomics Center at the University of Michigan. Approximately 7M reads/sample (75K reads/cell) were desired for sequencing runs. The following read lengths were used for Next-seq: read 1 length: 20 bp (26 cycles), read 2 length: 50 bp (96 cycles), and index read length: 8 bp. Illumina adapters (i7) were used to discriminate single cell transcriptomic libraries derived from parental from shPTEN cell lines. The following i7 adapters (and adapter sequences) were used to prepare sequencing libraries: N701 (TCGCCTTA), N702 (CTAGTACG), N703 (TTCTGCCT), and N704 (GTTGGACA). Transcriptomic libraries pooled by equal molar pooling of cell lines and ensured equal sequencing coverage per cell line.

2.2.4. Read Alignment and Generation of Digital Expression Data

Read alignment and the generation of the digital expression data matrix were performed by Dr. Joe Burnett and in accordance to the Drop-seq Computational Cookbook.[86] Reads were de-multiplexed to separate reads corresponding to parental and shPTEN cell line based on i7 index adapters. Reads were aligned to the reference human genome (GRCh38.p13) to derive the cDNA from each read. Mapped reads were then organized into a digital count matrix based on the unique molecular identifier, which enabled the quantification of gene expression per gene for each cell represented from the single cell transcriptomic library.

2.2.5. Unsupervised Dimensionality Reduction and Clustering

Digital count matrices were imported into R for analysis using the Seurat package (version 3.1.2). The gene expression of the parental and shPTEN cell lines were normalized using the NormalizeData function, which normalized the feature (gene expression) counts of each cell relative to the total features of that cell. These normalized feature counts were transformed using a natural log transformation. In order to perform downstream analyses with the metadata for each cell line pair, the metadata

corresponding to the parental cell line and the shPTEN cell line were integrated. Integration of these metadata was performed by identifying integration anchors (FindIntegrationAnchors) with the dims and k.filter argument set to default settings. Metadata was integrated using the IntegrateData function. Cell cycle heterogeneity was minimized by regressing the difference in the expression of G2/M and S phase genes. Analyses were also performed in absence of cell cycle regression, where the data changed minimally compared to using cell cycle regression. Analyses presented in this dissertation represent data where cell cycle regression was performed. Subpopulation clusters were resolved by using principal component analysis (PCA) and Uniform Manifold Approximation and Projection (UMAP). The resolution argument within the FindClusters function was optimized for each cell line pair by clustering the metadata at each clustering resolution from 0 – 1 in increments of 0.1. The multi-resolution clusterings were evaluated using the R package clustree, which guided the selection of the optimal clustering resolution.[87] For all cell lines, clustering resolution was set to 0.7 after analysis using clustree.

2.2.6. Differential Gene Expression Analysis

Differential gene expression was performed using FindMarkers function to evaluate differentially expressed genes between cell line pairs and subpopulations using the wilcox test. This analysis was performed to scrutinize the global transcriptomic differences between parental and shPTEN cell line by specifying ident.1 as the shPTEN cell line. Additionally, differential gene expression analyses were performed to identify characteristic genes expressed by each subpopulation by specifying ident.1 as the subpopulation of interest. The FindMarkers function was used to evaluate the gene expression of PTEN and HER2 between the parental and shPTEN as well as between each subpopulation. The FindMarkers function also afforded analyses within the subpopulation to identify genes differentially expressed by the subset of cells with PTEN k.d. relative to parental cells of a given subpopulation. To identify differentially expressed genes within a subpopulation, the following arguments within the FindMarkers function was specified: ident.1 as shPTEN, group.by set to “orig.ident”, and subset.by set to subpopulation of interest. Genes identified from the FindMarkers output were considered as statistically significant if p_adj < 0.01, where p_adj accounted for the bonferroni

correction. The most statistically significant genes were exemplified by a volcano plot generated using ggplot, and gene names were labeled using ggrepel.

2.2.7. Gene Set Enrichment Analysis (GSEA)

After differential gene expression was performed to assess the genes differentially expressed by a subpopulation of cells, gene set enrichment analyses was used to elucidate the functional consequences of those differentially expressed genes. GSEA was performed using the R package fgsea.[88,89] In order to perform gsea using the fgsea package, a rank ordered list of genes from the set of differentially expressed genes was generated based on the log_avgFC of a given gene. This rank ordered list was used as the stats argument in the fgsea function. The minimum gene set size to set was 10, and the maximum gene set size to test was 500. The number of permutations to run using the fgsea function was 1M. The rank ordered list of genes was compared *a priori* to the gene sets downloaded from MSigDb (msigdb.v7.0.symbols.gmt, accessed from https://data.broadinstitute.org/gsea-msigdb/msigdb/release/7.0/). Gene sets with p_adj < 0.05 were considered statistically significant, where p_adj is the p_val adjusted using the Benjamini-Hochberg (BH) procedure. Gene sets that were identified to be statistically significant were downloaded from MSigDb and imported into R. Genes from the imported gene sets were intersected with the genes from our metadata using the Reduce function and the intersect function from the dplyr package. This step enabled the identification of genes from statistically significant gene sets that contributed to the enrichment score of those gene sets identified using fgsea. The output of the intersected list of genes were scrutinized based on avg_logFC, p_adj, pct.1, and pct.2, where avg_logFC is the natural log fold change in expression of a given gene from one subpopulation relative to another subpopulation. The p_val adjusted for BH correction and is noted as p_adj. The percentage of cells from the subpopulation of interest that expresses the gene of interest is quantified by pct.1, and the percentage of cells from the compared subpopulation that expresses the gene of interest is quantified as pct.2.

2.2.8. Quantification of Western Blot

Cell pellets isolated from cell culture were placed into -80°C freezer for at least 24 hours prior to preparation for Western blot. Cell pellets were subjected to RIPA lysis buffer containing 1x EDTA, 1x protease inhibitor, and 1x phosphatase inhibitors for 20 minutes

at 0° C. Cell pellet solutions were sonicated at 33% power with 3x3 second pulses at 0° C. After sonication, samples were maintained at 0° C for 15 minutes prior to centrifugation at 14,000 rpm and 4°C for 15 minutes. Supernatant for each sample was retained and total protein concentration was determined via Bradford assay.

The Bradford protein quantification assay was performed in accordance to the Bio-Rad instruction's manual. Briefly, a working solution of the Bradford dye concentrate was prepared by diluting 1 part of the Bio-rad dye concentrate with 4 parts of MilliQ water. Following, 200 µL of this working solution was added to 10 µL of standard BSA solution or 10 µL of diluted supernatant (1:10 in water). Contents were vortexed afterwards and optical densities were measured at 595 nm on a microplate reader (BioTek). Analyses for standards and samples were performed in triplicate.

Measurements from Bradford assay were used to determine volumes of supernatant required to load 20 µg of total protein into a well of 4-20% Mini-PROTEAN(R) TGX(tm) Precast Protein Gel (Bio-Rad cat. no. 4561094). 4x Lamelli sample buffer containing 10% mercaptoethanol and lysis buffer were added to the calculated volumes of the supernatant to provide a final volume of 20 µL and 20 µg of total protein. Proteins were separated by gel electrophoresis using 1x Tris/Glycine/SDS buffer (prepared from Bio-rad cat # 161-0734) for 80V for 20 minutes and then 100V for 45 minutes. Proteins were transferred to nitrocellulose membrane using 1x Tris/Glycine (prepared from Bio-rad cat # 161-0732) and containing 20% HPLC-grade methanol at 220 mA for 70 minutes on ice.

Successful transfer was assessed by immersing nitrocellulose membrane in Ponseau-S stain for 5 minutes with agitation and observing crude protein bands upon washing the nitrocellulose membrane with MilliQ water or 1x TBS-T (0.1% Tween-20). Following, nonspecific binding sites on proteins were blocked using 5% BSA in 1x TBS-T for 1.5 hours at room temperature with agitation. Blocking solution was removed and membranes were washed for 4x5 minutes with 1x TBS-T. Primary antibody solutions were prepared using dilutions and diluent as recommended by the manufacturer and are noted in the table below (Table 2.1).

Table 2.1. Western Blot Antibodies.

Antibody	Dilution	Diluent	MW (kDa)
CST rabbit anti-PTEN #9559	1:1000	1% BSA in 1x TBS-T	54
CST rabbit anti-pAKT (Ser473) (D9E) XP® Rabbit mAb #4060	1:2000		60
CST rabbit anti-vinculin (E1E9V) XP	1:1000		124
CST anti-rabbit HRP-linked Antibody #7074	1:1000		

Nitrocellulose membranes were incubated with primary antibody solutions for 18 hours at 4°C. Excess primary antibody solutions were discarded and membranes were washed for 4x5 minutes with 1x TBS-T. Membranes were incubated with secondary antibody solution for 1.5 hours at room temperature with agitation. Excess secondary antibody solutions were discarded and membranes were washed for 4x5 minutes with 1x TBS-T. Enhanced chemiluminescence reaction was performed in accordance to Bio-Rad Clarity protocol.

Quantification of Western was performed using ImageJ and were normalized to housekeeping gene, vinculin. The expression of vinculin in each experimental lane on the Western blot was normalized to the lane with the highest vinculin signal, which afforded the lane normalization factor. The use of lane normalization factor ensured that the signal of vinculin was constant across all lanes and ensured accurate quantification of PTEN relative to a normalized signal of vinculin. For each cell line, the reduction in PTEN expression was calculated as the quotient of normalized wild type PTEN and the normalized levels of PTEN in the shPTEN cell line.

2.3. Results and Discussion

Table 2.2. HER2+ Breast Cancer Cell Line Pairs Used to Evaluate Consequences of PTEN Deficiency. Each cell line consists of a parental cell line that expresses wild type PTEN, and the PTEN knockdown cell line has reduced expression of PTEN by shPTEN. Bulk cell line clarifies the use of cell lines that were not derived from single cell colonies or fractionation step.

HER2+ BC Cell Lines	Wild type PTEN	PTEN knockdown
HCC-1954	• Bulk cell line	• Bulk cell line
SKBR3	• Bulk cell line	• Bulk cell line
BT474	• Bulk cell line	• Bulk cell line

2.3.1. Validation of PTEN k.d. by Western and Single Cell Analysis

Using single cell transcriptomic libraries generated from these cell line pairs, we addressed the first aim of this dissertation. The first aim of this dissertation is to characterize the steady state subpopulations existing within HER2+ breast cancer cell lines and elucidate how PTEN k.d. alters those subpopulations (Table 2.2). To ensure these cell line pairs correctly reflect wt PTEN and PTEN k.d., we quantified the expression level of PTEN by Western blot and by single cell analysis in HCC1954, SKBR3, and BT474. (Figure 2.1). In HCC1954, the protein expression of PTEN was reduced by 2.7 fold after transfection with shPTEN (Figure 2.1A). Using single cell analysis, it was evident that the expression of PTEN was very low in HCC1954 as it was below the detection limit of Drop-seq in parental HCC1954 and within the six HCC1954 subpopulations (Figure 2.1A). In SKBR3, the protein expression of PTEN was reduced by 4.4 fold in SKBR3 PTEN k.d. relative to the parental cell line (Figure 2.1B). Similar to HCC1954, this cell line also harbored low levels of PTEN in its subpopulations. Levels of PTEN were observed in parental SKBR3 subpopulations 0, 2, and 3, but the difference of those levels relative to the PTEN k.d. cells were not statistically significant (Figure 2.1B). Lastly, in BT474, the expression level of PTEN was reduced by 11.4 fold in the PTEN k.d. cell line derivative (Figure 2.1C). Expression levels of PTEN were observed in parental BT474 subpopulations 1, 2, and 3, but those levels were not statistically significant relative to PTEN k.d. cells. The relatively higher levels of PTEN in BT474 compared to HCC1954 and SKBR3 observed in my findings were consistent with the literature, which also report higher protein levels of PTEN in BT474 compared to HCC1954 and SKBR3.[90,91] As a technical control, we also assessed the single cell expression levels of HER2 in these cell line pairs. For each cell line pair, HER2 was highly expressed in both the PTEN k.d. and parental cell line. Between subpopulations, the expression of HER2 was not statistically different for these cell lines. Additionally, the difference in HER2 expression between the parental and k.d. cell lines within each subpopulation was also not statistically significant (Figure 2.1).

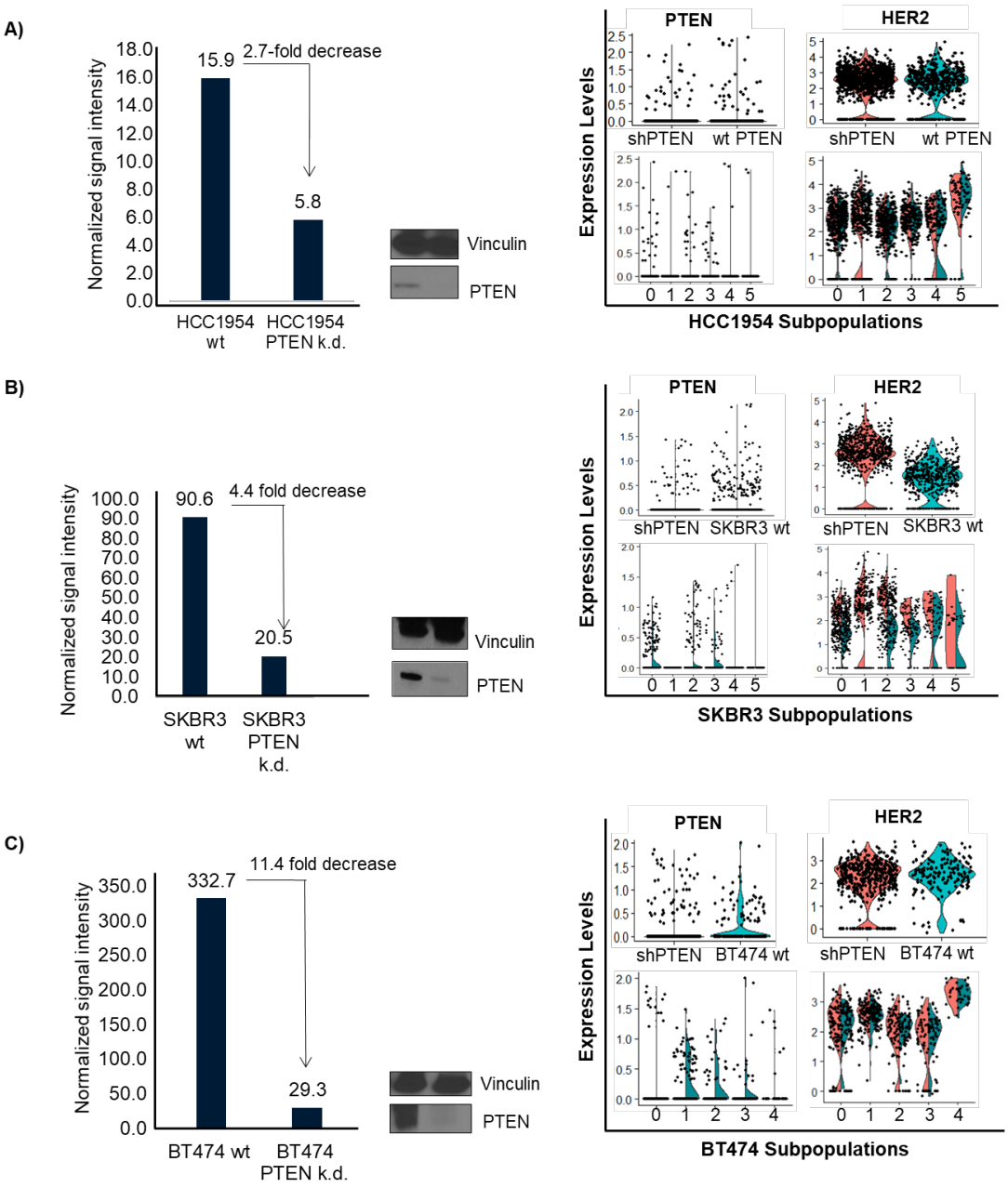

Figure 2.1. Validation of PTEN and HER2 Expression Levels in HER2+ Breast Cancer Cell Lines. Quantification of PTEN k.d. by Western for HCC1954 (A), SKBR3 (B), and BT474 (C). Protein expression levels were normalized to vinculin. Violin plots depicting PTEN levels in PTEN k.d. cells compared with parental (top) and within subpopulations (bottom) of HCC1954, SKBR3, and BT474. Violin plots depicting HER2 levels in PTEN k.d. and parental cell lines and within subpopulations of HCC1954, SKBR3, and BT474.

2.3.2. PTEN Deficiency in HCC1954 Caused Global Increase in Quiescence and Cytokine Signaling but Decreased Epithelial Phenotype

To explore the functional consequences of PTEN deficiency in HER2+ breast cancer cells, we performed Drop-seq to compare single cell transcriptomes deriving from parental and PTEN k.d. cell lines. We sought to evaluate the transcriptomic differences

in HCC1954, SKBR3, and BT474. We started our comparative analyses by elucidating the differences between parental and PTEN k.d. cell line derivatives to dissect global transcriptomic changes. Then, we scrutinized the effects of PTEN k.d. on a subpopulation level for each cell line. By dissecting the effects of PTEN k.d. on a global and subpopulation level, we ascertained how the steady state subpopulations of the HER2+ breast cancer cells were affected by PTEN k.d.

To visualize the transcriptomic composition of parental HCC1954 and HCC1954 PTEN k.d. cells, a nonlinear dimensionality reduction (uniform manifold approximation projection, UMAP) was used to analyze global transcriptomic changes resulting from PTEN k.d. Nonlinear dimensionality reduction plots, such as UMAP plots, provide a two-dimensional depiction of the spatial distribution of cells based on their transcriptomic composition.[92,93] UMAP plots represent cells with similar transcriptomic profiles as subpopulations or clusters in close proximity while cells with starkly different transcriptomic profiles as farther apart.[92,93] Thus, these plots are powerful tools that enable the visualization of the intratumoral heterogeneity existing within a cancer ecosystem by revealing the cancer cell subpopulations. With the UMAP plot, extensive spatial overlap was observed between the parental HCC1954 and HCC1954 PTEN k.d. cells (Figure 2.2). Despite this similarity between most of the cells belonging to the HCC1954 cell line pair, the knockdown of PTEN enriched a subset of cells that was not present in the wt PTEN cells (circled in Figure 2.2A).

After visualizing HCC1954 cells based on their transcriptomic composition, differential gene expression (DGE) analysis was performed to identify global transcriptomic differences between parental HCC1954 and HCC1954 PTEN k.d. cells (Figure 2.2B). This analysis identified 1,024 statistically significant genes that were differentially expressed by HCC1954 cells with PTEN k.d (padj < 0.01). From these differentially expressed genes, 476 genes were elevated (padj < 0.01), and 548 genes were lower in HCC1954 PTEN k.d. cells as depicted in the volcano plot of Figure 2.2B (padj< 0.01). A volcano plot is a scatterplot of the differentially expressed genes plotted by statistical significance ($-\log(p_{adj})$) as a function of fold change ($\log_2$(fold change)).[94,95] Thus, this plot highlights genes with different magnitudes of the fold change in the gene expression and the statistical significance of that fold change. The top 20 statistically

significant genes were prioritized for analysis and encoded cytokines and inflammatory proteins (CCL5, chemokine ligand 5; LAIR1, leukocyte associated immunoglobulin like receptor 1; LBP, lipopolysaccharide binding protein; TNIP3, TNF-α interacting protein 3, and CBF, complement factor B), which were higher in HCC1954 PTEN k.d. cells. Additionally, statistically significant genes encoded transporter proteins such as transmembrane protein TRAPPC10 and zinc transporter SLC39A8 and multidrug resistance associated protein 2, ABCC2. The k.d. of PTEN in HCC1954 appeared to upregulate inflammatory mechanisms, which was supported with findings from gene set enrichment analysis (GSEA). GSEA was performed to explore the global phenotypic differences between parental HCC1954 and HCC1954 PTEN k.d. cells. GSEA enabled the comparison of the differentially expressed genes between the HCC1954 cell line derivatives with predefined biologically relevant gene sets (obtained from the Molecular Signature Database, MSigDB.[89] GSEA of HCC1954 PTEN k.d. cells identified 387 gene sets (padj < 0.05) and low enrichment scores for cell cycle gene sets (Figure 2.2C), which suggested that PTEN k.d. resulted in an increase of quiescent properties. Additionally, GSEA also revealed high enrichment scores for gene sets critical for inflammatory response, such as cytokines signaling and interleukin signaling; these GSEA findings were consistent with differentially expressed genes represented on the volcano plot for HCC1954 PTEN k.d. cells (Figure 2.2). Interestingly, GSEA for HCC1954 PTEN k.d. cells also revealed low enrichment scores for cell adhesion/cell junction gene sets and high enrichment scores for cell motility gene sets, which suggested a loss of cell adhesion and increase of cell motility as a result of PTEN k.d (padj < 0.05). It has been well documented that cytoskeletal dynamics are governed by cytokine signaling; inflammatory signaling could trigger changes to the actin fibrils of the cytoskeleton and ultimately impact mechanisms governing the cell's motility and adhesion.[96–101] In summary, k.d. of PTEN in HCC1954 resulted in a global increase of cytokines signaling and quiescence as revealed by DGE analysis and GSEA.

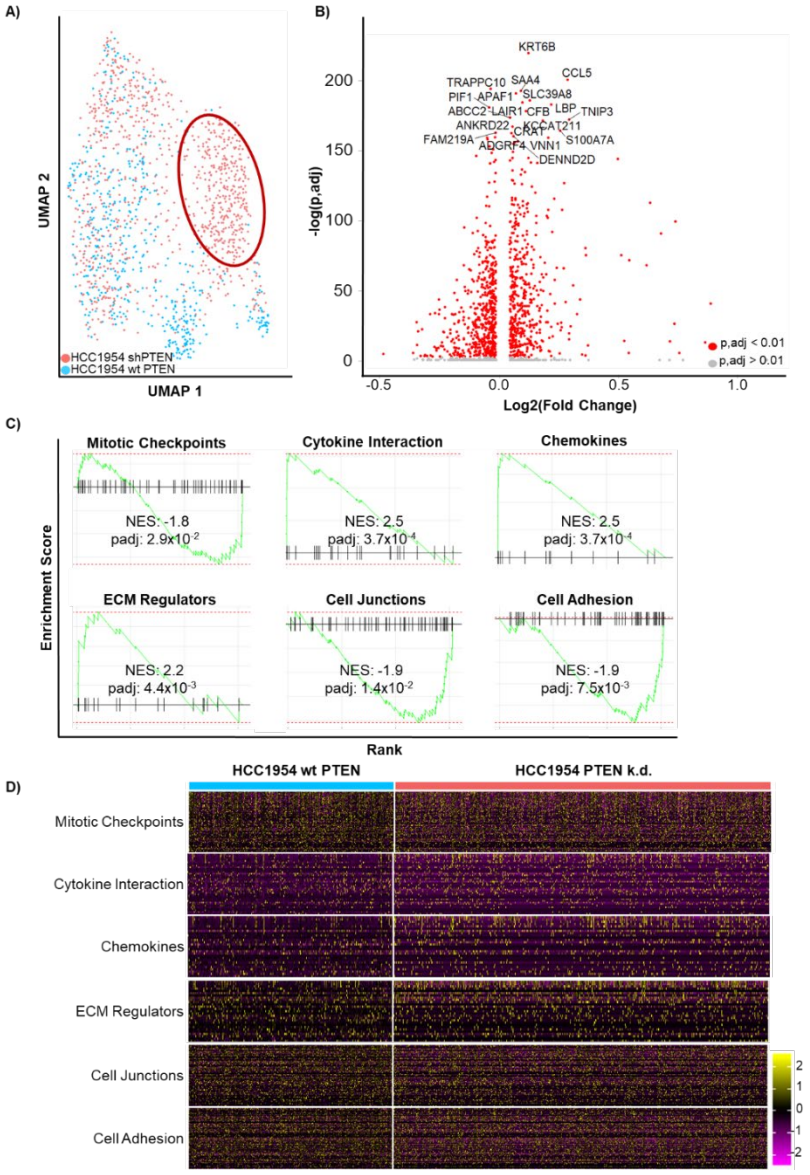

Figure 2.2. Global Comparisons of Transcriptomic Composition of Parental HCC1954 and HCC1954 PTEN k.d. A) UMAP plot depicting parental HCC1954 (cyan) and HCC1954 PTEN k.d. (pink). Circled region denotes subpopulation enriched by PTEN k.d. cells. B) Volcano plot of differentially expressed genes by HCC1954 PTEN k.d. cells. Cells in red denotes statistically significant differentially expressed genes by HCC1954 PTEN k.d. cells (padj < 0.01). Top 20 statistically significant genes are labeled. C) Gene sets identified by GSEA. Gene sets upregulated are denoted by positive normalized enrichment score (NES). Statistically significance is denoted by p-value adjusted by Benjamini-Hochberg (BH) procedure (padj < 0.05). D) Heatmap of genes identified from GSEA.

2.3.3. PTEN Deficiency in HCC1954 Resulted in an 84-Fold Enrichment of Quiescent, Epithelial Subpopulation 1

The subpopulations of HCC1954 were scrutinized to gain insight how the k.d. of PTEN affected the steady state of the subpopulations constituting HCC1954, which revealed six distinct subpopulations (Figure 2.3 and Figure 2.4A-B). The relative distribution of parental HCC1954 was the following: 35% subpopulation 0, 0.4%

subpopulation 1, 16% in subpopulation 2, 14% subpopulation 3, 27% subpopulation 4, and 8% subpopulation 5 (Figure 2.3B). After k.d. of PTEN, there was a dramatic shift in the relative distribution of HCC1954 cells, particularly in subpopulation 1, which increased by 84-fold (Figure 2.3B). HCC1954 PTEN k.d. cells consisted of 20% subpopulation 0 (1.7 fold decrease), 33% subpopulation 1 (84 fold increase), 22% subpopulation 2 (1.4 fold decrease), 14% subpopulation 3, 7.1% subpopulation 4 (3.8 fold decrease), and 2.5% subpopulation 5 (3.2 fold decrease). Notably, the relative proportion of cells in subpopulations 1, 4, and 5 underwent sizeable changes after PTEN k.d.; subpopulation 1 increased by 84 fold, while subpopulations 4 and 5 decreased by 3 fold (Figure 2.3B). Since one of the aims of this dissertation was to elucidate the mechanisms by which PTEN deficiency altered the steady state subpopulations of HER2+ breast cancer cells, we analyzed the most upregulated genes from each subpopulation to gain an overview of the phenotype of each subpopulation. These analyses only yielded high expressing subpopulation-specific genes for subpopulations 3 and 5 (Figure 2.3B). The remaining subpopulations (0, 1, 2, 4) were characterized by a combination of decreased gene expression or heterogeneous gene expression within the subpopulation (Figure 2.3C). With these highly expressed genes, it was observed that subpopulation 3 (decreased after PTEN k.d.) exhibited inflammatory signaling based on the expression of chemokines CCL2, CXCL8, and CXCL3. The expression of these cytokines were at similar expression intensities in subpopulations 1 and 2, although not as homogenous, which suggested subpopulations 1 (increased by 84 fold) and 2 (decreased by 1.4 fold) also exhibited inflammatory signaling. Subpopulation 5 appeared to be very proliferative as evidenced by the high expression of genes critical for the cell cycle and proliferation (CENPF and MKI67) and cell transport (GSDMB, ATP1B1). While these analyses revealed highly expressing genes for subpopulations 3 and 5, they revealed subpopulation level characteristics, particularly for the subpopulations with sizeable changes in the relative cell proportions after k.d. of PTEN. These analyses suggested that subpopulation 1, which increased by 84 fold after k.d. of PTEN, exhibited intra-subpopulation heterogeneity with modest high expression of chemokines. Interestingly, subpopulation 4, which decreased by 3 fold after PTEN k.d., also exhibited intra-subpopulation heterogeneity and

was not characterized by any high expressing gene. Subpopulation 5, which also decreased by 3 fold after PTEN k.d., appeared to be a proliferative subpopulation.

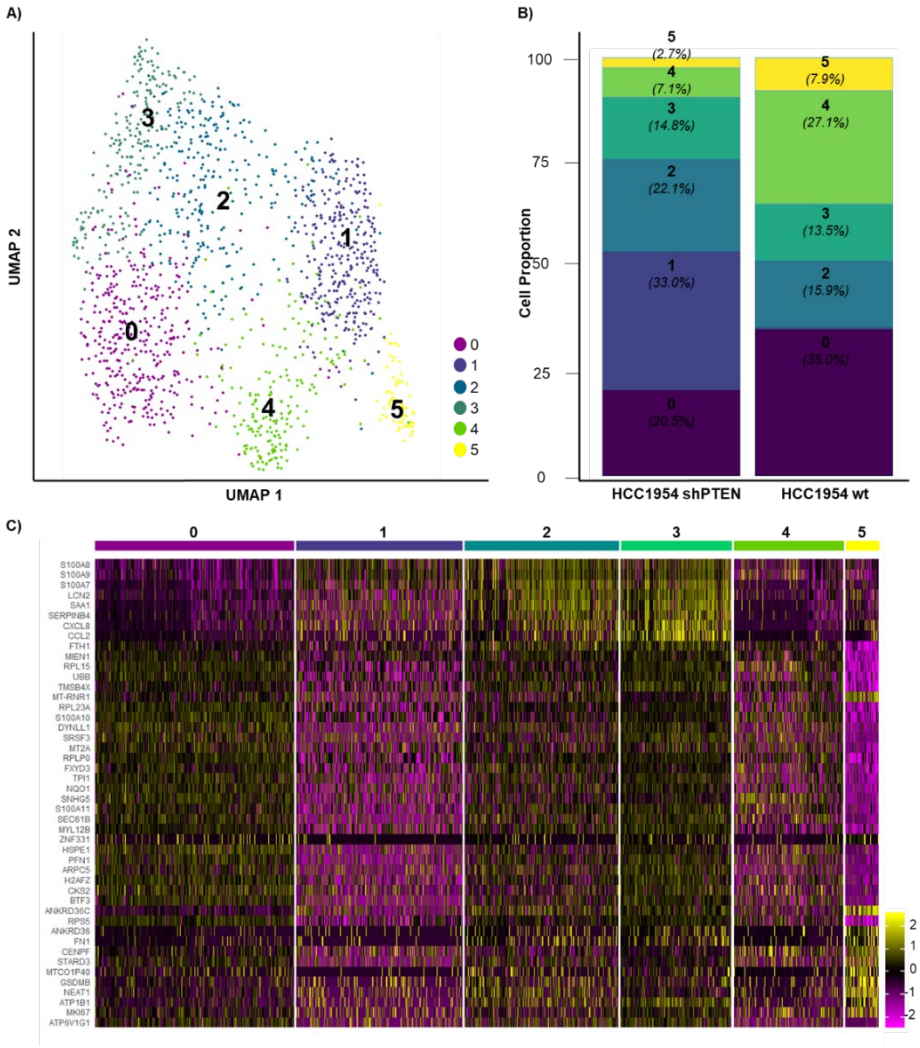

Figure 2.3. Overview of Six HCC1954 Subpopulations. A) UMAP depicting single cells organized into six HCC1954 subpopulations. B) Cell proportions of each HCC1954 subpopulation. Relative percentage of cells existing in each subpopulation relative to the total number of cells in a given cell line is noted in parentheses. C) Heatmap depicting most upregulated genes per subpopulation.

As observed previously, the analyses of upregulated genes in each subpopulation provided limited perspective to the subpopulation level changes induced by k.d of PTEN. All differentially expressed genes for each subpopulation were analyzed to characterize changes to the subpopulations after PTEN k.d. (i.e. subpopulations 1, 4, and 5). Characterization of the remaining HCC194 subpopulations are described in Section 2.3.3. Since subpopulation 1 had the largest subpopulation level change after PTEN k.d., we sought to identify genes differentially expressed by subpopulation 1 by comparing the

genes expressed by subpopulation 1 with the genes collectively expressed by the remaining clusters. This approach revealed 1,537 genes differentially expressed by subpopulation 1 and 119 statistically significant gene sets (padj < 0.05). Of these gene sets, relevant gene sets included cytokine activity and response, macromolecule catabolic process, and DNA replication (padj < 0.05). The cytokine signaling gene sets were positively enriched by subpopulation 1, suggesting high expression of inflammatory genes. Cell metabolism and cell cycle gene sets were negatively enriched in subpopulation 1, suggesting this subpopulation exhibited quiescent properties. The low quantity of relevant gene sets between subpopulation 1 and the remaining HCC1954 subpopulations suggested transcriptomic similarities between these two groups of cells, which would decrease the statistical power to identify statistically significant gene sets. Based on the heatmap shown in Figure 2.3, it appeared as though subpopulation 3 might co-express genes found in subpopulation 1. The presence of subpopulation 3 in the analyses might confound the gene expression differences between subpopulation 1 and the rest of the HCC1954 subpopulations, especially since subpopulation 1 exhibited intra-subpopulation heterogeneity in gene expression. Subpopulation 3 was removed from the differential gene expression analysis of subpopulation 1 compared with the remaining HCC1954 subpopulation to improve the statistical power to characterize subpopulation 1.

DGE analysis was performed again to identify key transcriptomic differences between HCC1954 subpopulation 1 and subpopulations 0-5 (without subpopulation 3). This analysis revealed 1,166 statistically significant differentially expressed genes (padj < 0.01). Of these 1,166 genes, 407 genes were expressed significantly higher and 759 genes were expressed significantly lower in HCC1954 subpopulation 1 (padj < 0.01, Figure 2.4C). The top 20 statistically significant genes encoded proteins that are heavily involved in DNA synthesis and repair (polymerase I and transcript release factor, *PTRF*; aurora kinase B, *AURKB*; mitotic checkpoint, *BUB3*; and DNA replication complex member, *GINS*). Other top 20 statistically significant genes encoded nuclear proteins (GRLX and EPAS), proteins involved in cellular/nucleic acid metabolism (thymidine phosphorylase, *TYMP*; monoamine oxidase A, MAOA), and proteins that regulate inflammatory response (complement factors, CFB and C1R; chemokine induced, ZC3H12A; and TNF-α interacting protein 3, TNIP3). Despite the statistical significance of

these differentially expressed genes, the fold change in their expression by subpopulation 1 was less than 2-fold (Figure 2.4C). It was possible for different subpopulations to exhibit similar expression of genes, especially ones that are critical to cellular function (i.e. metabolism and genes associated with the cell cycle), which consequentially, decrease the fold change in gene expression exhibited by cells of subpopulation 1.

GSEA identified revealed 295 statistically significant gene sets for subpopulation 1 (padj < 0.05). Of these 295 statistically significant gene sets, low enrichment in gene sets for DNA replication, and mitotic spindle were observed, suggesting an arrest from cell cycle (padj < 0.05, Figure 2.4D). Scrutiny of these gene sets revealed significant low expression of regulators of the cell cycle, such as ubiquitins, which coordinate the cell cycle by timely degradation of cyclins during distinct phases of the cell cycle.[102,103] These genes were expressed 1.5 fold lower in subpopulation 1 compared to the remaining HCC1954 subpopulations. Interestingly, the mTOR pathway was negatively enriched in subpopulation 1 relative to the other subpopulations (Figure 2.4D). The mTOR pathway is one of the pathways downstream of PI3K/AKT that governs cell growth and quiescence through the regulation of protein synthesis, transcription of cell cycle genes, and translation of cell cycle proteins.[104,105] Scrutiny of the mTOR gene set revealed reduced expression of cell cycle genes such as RRM2, TUBA4A, CDKN1A, and MAP2K3 in subpopulation 1. Low expression of these genes due to the downregulation of the mTOR pathway would result in a reduction of cell cycle proteins and quiescent characteristics for this subpopulation. Furthermore, the low expression of these genes in subpopulation 1 suggested that deficiency of PTEN might not always translate to increased mTOR signaling as suggested by the literature.[53,69] It also provided insight why mTOR inhibitors have been clinically ineffective in HER2+ breast cancer patients with PTEN loss, showing that PTEN deficiency in HER2+ breast cancer could result in unique patient cohorts that require treatment options beyond the PTEN/AKT/PI3K pathway inhibitors. GSEA also yielded a significant low enrichment in the Myc target gene set (Figure 2.4D). Analysis of the Myc target gene set revealed significantly low expression of genes encoding ribosomal subunits (RPLP0, RNPS1, RPB55), metabolic proteins (lactate dehydrogenase LDHA), and regulators of the cell cycle (mitotic checkpoint BUB3, G2/M-associated cyclin B1, and ubiquitin UBE2C). The lowered expression of these Myc targets by 1.3 – 1.7 fold

in subpopulation 1 suggested that this subpopulation exhibited quiescent properties due to reduced cell cycle activity, metabolism, and protein synthesis. From the gene sets for DNA replication, mitotic spindle, and Myc target genes, BUB3, UBE2C, PCNA, and GINS4 were expressed lowest in HCC1954 subpopulation 1 compared to the other subpopulations (padj < 0.0001, Figure 2.4E), which were expressed 1.3 – 1.6 fold lower in subpopulation 1. While these genes are lowly expressed in subpopulation 1, these genes and other cell cycle associated genes were expressed in 4-40% of HCC1954 subpopulation 1 cells (padj < 0.0001), which highlighted the intra-subpopulation heterogeneity present in this subpopulation. This intra-subpopulation heterogeneity gave rise to two groups of cells within subpopulation 1: a proliferative group and a quiescent group. Furthermore, the quiescent features of subpopulation 1 revealed by GSEA was consistent with the GSEA findings from the comparative transcriptomic analyses of HCC1954 PTEN k.d. cells and parental HCC1954 because the latter findings suggested that HCC1954 with PTEN k.d. exhibited increased quiescence. Since HCC1954 subpopulation 1 enriched after PTEN k.d., it was likely that this subpopulation contributed to the increase of quiescent features observed in cells with PTEN k.d. Taken together, PTEN k.d. in HCC1954 resulted in a 84-fold increase in subpopulation 1 that exhibited intra-subpopulation heterogeneity and was largely characterized by a quiescent phenotype.

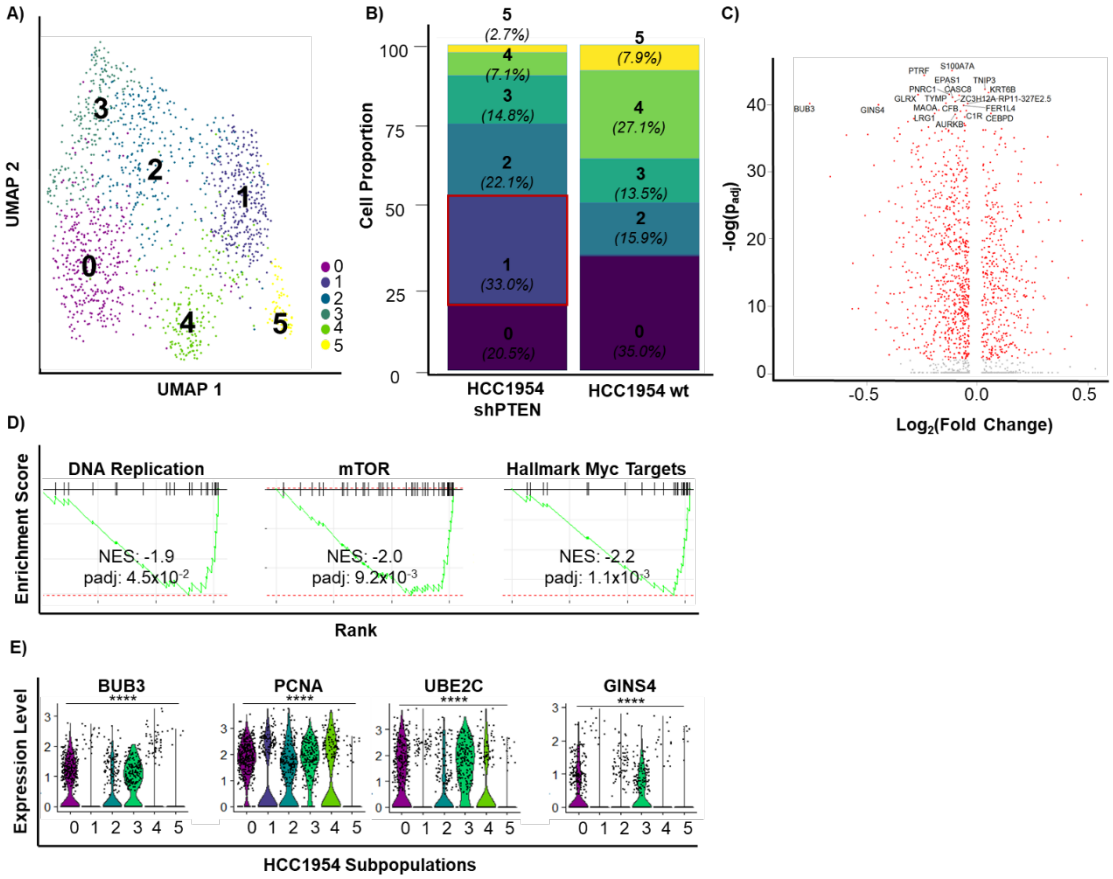

*Figure 2.4. Characterization of HCC1954 Subpopulation 1 Revealed Quiescent Properties. A) UMAP depicting single cells organized into six HCC1954 subpopulations. B) Cell proportions of each HCC1954 subpopulation. Red box emphasizes subpopulation 1, which increased by 84 fold after PTEN k.d. C) Volcano plot of differentially expressed genes by HCC1954 subpopulation 1. Cells in red denotes statistically significant differentially expressed genes by HCC1954 subpopulation 1 (padj < 0.01). Top 20 statistically significant genes are labeled. D) Gene sets identified by GSEA. Gene sets upregulated are denoted by positive normalized enrichment score (NES). Statistically significance is denoted by p-value adjusted by Benjamini-Hochberg (BH) procedure (padj < 0.05). E) Most differentially expressed genes identified from D. **** padj < 0.0001.*

2.3.4. HCC1954 Subpopulation 1 was Characterized by Heterogeneous Cytokine Signaling and Altered Cytoskeletal Dynamics

In addition to the relatively quiescent features revealed by GSEA, these analyses also showed a positive enrichment in 11 gene sets associated with inflammatory response, such as and cytokine signaling, interleukin signaling, TNF-α signaling, defense response, and chemotaxis (Figure 2.5A). Evaluation of these gene sets revealed a slightly higher yet significant expression of the CCL and CXCL families of chemokines (CCL2, CCL20, CXCL3, CXCL8, Figure 2.5). These chemokines were expressed in 10-40% of HCC1954 subpopulation 1 cells but were expressed 1.7 fold higher than the levels from the other HCC1954 subpopulations. Additionally, cytokine responsive proteins such as

NFκB inhibitor, NFκBIA; NFκB subunit 2, NFκB2; serum glycocortocoid kinase, SGK1; TNF interacting protein, TNFAIP3; AP-1 family transcription factor, JUNB, and BIRC3, were also detected. These cytokine responsive proteins were expressed in 4-24% of HCC1954 subpopulation 1 and expressed 1.1 – 1.3 fold higher than cells of subpopulations 2 – 5 (padj < 0.0001). These encoded proteins, specifically JUNB and BIRC3, have been shown to be induced by IL-1β.[106–110] The induction of these cytokines is expected in HER2-overexpressing breast cancer because the upregulated HER2 signaling has been shown to stimulate a pro-inflammatory response characterized by NFκB and STAT3 signaling.[111,112] SGK1, which has been shown to be induced by IL-6, is also a known downstream effector of AKT and has been reported to be critical for breast cancer bone metastasis.[113–115] Additionally, it has been reported that the increase of NFκB signaling via TNF-α signaling upregulates the expression of anti-apoptotic proteins that degrades inhibitors to NFκB signaling (i.e. NFκBIA) as a means to facilitate cell survival during cell cycle arrest.[116] This phenomenon could explain the enhanced cytokine signaling and overall quiescent property of HCC1954 subpopulation 1. Conversely, the increase of cytokines has been shown to inhibit the growth of breast cancer cells by preventing the G0/G1 transition.[97] The expression of cytokines and inflammatory genes in a subset of HCC1954 subpopulation 1 cells highlighted the extent of heterogeneity within HCC1954. This intratumoral heterogeneity was exemplified at the subpopulation level since only a fraction of subpopulation 1 cells expressed genes associated to inflammatory signaling, while the remaining cells of this enriched subpopulation did not express those cytokines as a response to k.d. of PTEN. Interestingly, 15% of the genes featured in the inflammatory response gene sets were cytoskeletal proteins (such as integrins, actin ACTG2, vimentin VIM, and fibronectin FN1) and cell adhesion proteins (such as claudin CLDN1 and laminin LAMB3). The detection of these encoded cytoskeletal proteins within the inflammatory response gene sets suggested the presence of cytokine-mediated changes to the cytoskeleton of cells within HCC1954 subpopulation 1 (Figure 2.5). This phenomenon was further supported by the positive enrichment of cell motility and extracellular matrix remodeling as well as a negative enrichment of cell adhesion gene sets, which further suggested that subpopulation 1 exhibited weakening cell adhesion and gain of cell motility features (Figure 2.5A). Among the genes featured

in the cell motility and adhesion gene sets included chemokines (CXCL8, CCL20, CXCL3, and CCL2) and genes regulating cell motility dynamics (Figure 2.5B). Interestingly, genes expressed lowest in cell motility and cell adhesion gene sets were genes encoding regulators of cell adhesion, such as tetraspanin CD9, actin depolymerizing protein coflin CFL1, cell adhesion laminin LAMB3, and Rho GTPase regulator of cell adhesion[117], RHOC. These encoded cell adhesion proteins, specifically CD9, LAMB3, and RHOC were expressed in 5-20% of HCC1954 subpopulation 1 cells and were expressed 1.3 fold lower in HCC1954 subpopulation 1, while actin depolymerizing protein cofilin was expressed in 48% of subpopulation 1 and expressed 1.4 fold lower. The decreased expression of these cell adhesion regulators and high expression of chemokines in subpopulation 1 suggested a deregulation of cell adhesion dynamics that was coordinated by increased cytokine signaling.

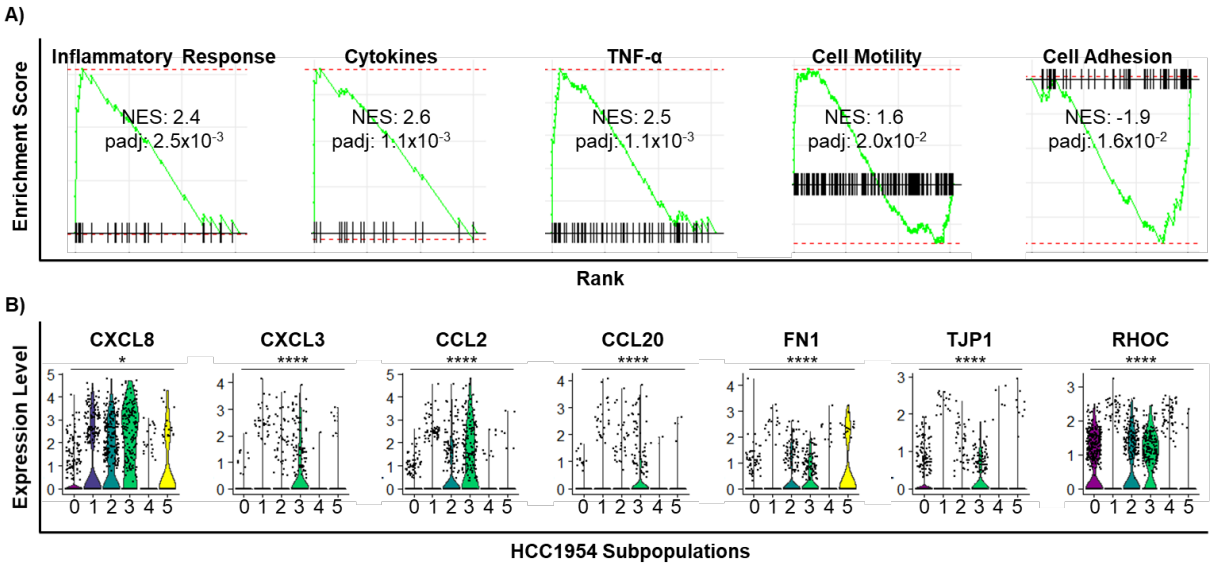

*Figure 2.5. Enrichment of Cytokine Signaling, Cell Motility, and Cell Adhesion Suggested Altered Cytoskeletal Dynamics in HCC1954 Subpopulation 1. A) Gene sets involved in inflammatory response, cell motility, and cell adhesion were identified by GSEA. Statistically significance is denoted by p-value adjusted by Benjamini-Hochberg (BH) procedure (padj < 0.05). B) Differentially expressed genes by subpopulation 1 identified by gene sets in A. Top chemokines and regulators of cell adhesion and cell motility dynamics are represented. * padj < 0.05, **** padj < 0.0001.*

2.3.5. HCC1954 Subpopulation 1 Exhibited Mixed Expression of Epithelial and Mesenchymal Markers, Hinting an Epithelial, Early EMT Phenotype

This weakened cell adhesion due to the low expression of epithelial adhesion proteins and the positive enrichment of cell motility gene sets by GSEA suggested HCC1954 subpopulation 1 harbored an epithelial early EMT phenotype. The hallmark of

epithelial cells is cell-cell adhesion between epithelial cells, which is ensured by adherens junctions, tight junctions, and desmosomes in the cytoskeletons of epithelial cells.[118,119] Proteins belonging to the claudin family and occludins are critical for maintaining tight junctions.[118–120] Cadherins, specifically E-cadherin (encoded by CDH1), is responsible for the integrity of adherens junctions.[118–120] Lastly, desmoplakins are key proteins for maintaining the cell-cell adhesions via desmosomes.[118–120] The epithelial cytoskeleton boasts of structural proteins known as keratins.[118–121] Keratins constitute the filaments of the cytoskeletons of epithelial cells, which support the apico-basal polarity established by these cells.[118–121] Together, these cytoskeletal components orchestrate the maintenance of the cell-cell adhesion between epithelial cells, and these epithelial characteristics are lost during EMT.[118–120] In HCC1954, eepithelial cell adhesion molecule EPCAM and epithelial cadherin CDH1, were detected, but the expression of CDH1 was limited to a subset of subpopulation 1 cells (Figure 2.6A). In comparison to the other subpopulations, the expression of EPCAM and CDH1 was not significantly different from the levels expressed by the remaining HCC1954 subpopulations (Figure 2.6A). The reduction of these markers have been regarded as the initial molecular switch to a mesenchymal phenotype.[120] Additionally, it has been reported that different epithelial markers are lost during distinct stages of EMT.[120] Keratins KRT14, KRT5, and KRT8 are maintained until late stages of EMT, while EPCAM and E-cadherin have been reported to be lost during the early EMT stages.[120] Consistent with the temporal parameter for EMT, epithelial keratins (KRT7, KRT8, KRT17, KRT18) were expressed in 41-63% of HCC1954 subpopulation 1 and were expressed 1.2 fold lower in subpopulation 1 compared to remaining subpopulations (Figure 2.6A). Cell adhesion proteins such as claudins (CLDN1, CLDN4, and CLDN7) were detected in up to 32% of subpopulation 1 and were expressed 1.2 fold lower than subpopulations 2 – 5 (Figure 2.6A). Other structures critical for epithelial cell adhesion, such as tight junction proteins (TJP1, aka ZO-1, and TJP3) and syndecan (SDC4 and SDCBP2) were detected in less than 15% of subpopulation 1. Additional cell adhesion molecules, such as ICAM, CEACAM1, CEACAM6 and BCAM, were also detected in less than 10% of HCC1954 subpopulation 1, which emphasized that the majority of subpopulation 1 cells did not express these cell adhesion properties. Furthermore, the expression of transcription factors that regulate epithelial genes

(GRHL1-3 and OVOL-1) and known epithelial marker MUC1 were not detected in this cell line. The high expression of epithelial structural proteins and low expression of cell adhesion markers suggested subpopulation 1 cells exhibited an epithelial phenotype with weakening cell adhesion and therefore, an early EMT hybrid phenotype.

To further support the epithelial early EMT hybrid phenotype, markers associated with EMT and the mesenchymal phenotype were investigated. Genes of interest included activators of EMT (such as MKI67, β-catennin, WNT signaling, and TGF-β signaling) and regulators of extracellular matrix interactions (such as fibronectin FN1, plasminogen activator PLAUR, tumor necrosis factor receptor TNFRSF12A, insulin growth factor binding protein IGFBP3, and S100 family protein S100A7).[98,117–120,122–125] All of these proteins contribute to development of mesenchymal phenotype through the reorganization of the extracellular matrix, weakening of epithelial cell adhesion, an increase of cell motility, and an increase of invasion characteristics.[98,117–120,122–125] These markers, specifically TNFRSF12A, FN1, PLAUR, IGFBP3, and MKI67 were expressed in 7-36% of HCC1954 subpopulation 1, while S100A7 was expressed in 84% of HCC1954 subpopulation 1 (Figure 2.6B). Interestingly, the expression of S100A7 has been reported to promote breast cancer progression through cytokine signaling and reported to correlate with HER2-overexpressing high grade tumors.[124–128] Thus, the high expression of S100A7 might be a reflection of its compounding signaling cascades in HCC1954. In addition to S100A7, subpopulation 1 expressed other S100 proteins that have been shown to be involved in reorganization of the extracellular matrix, such as S100A4, S1008, and S100A9.[124,129,130] TNF-α receptor superfamily member TNFRSF12A was detected in 16% of subpopulation 1 cells and expressed 1.5 fold higher than the cells of the other subpopulations (Figure 2.6B). Detection of this gene was particularly interesting because its expression level has been correlated with the overexpression of matrix metallopeptidase MMP9 in progressive breast cancer and thus been regarded as a prognostic marker for poor patient survival.[98] Despite the expression of genes involved in regulating the epithelial cytoskeleton and signaling that facilitate EMT, classical EMT transcription factors, such as TWIST1/2, SNAIL, SLUG, ZEB1/2, were not detected. The lack of expression of these EMT transcription factors suggested that a full EMT program was not activated. Consistent with this insight, expression of mesenchymal-specific

cytoskeletal proteins, such as N-cadherin and vimentin, and proteins that facilitate extracellular matrix degradation (MMP9 and MMP19) were not detected. Taken together, the expression of epithelial cytoskeletal proteins, low expression of proteins that maintain epithelial cell adhesion, and the low expression of proteins that promote EMT suggested that subpopulation 1 represented epithelial cells with weakened cell adhesion and thus, harbored an epithelial early EMT hybrid phenotype.

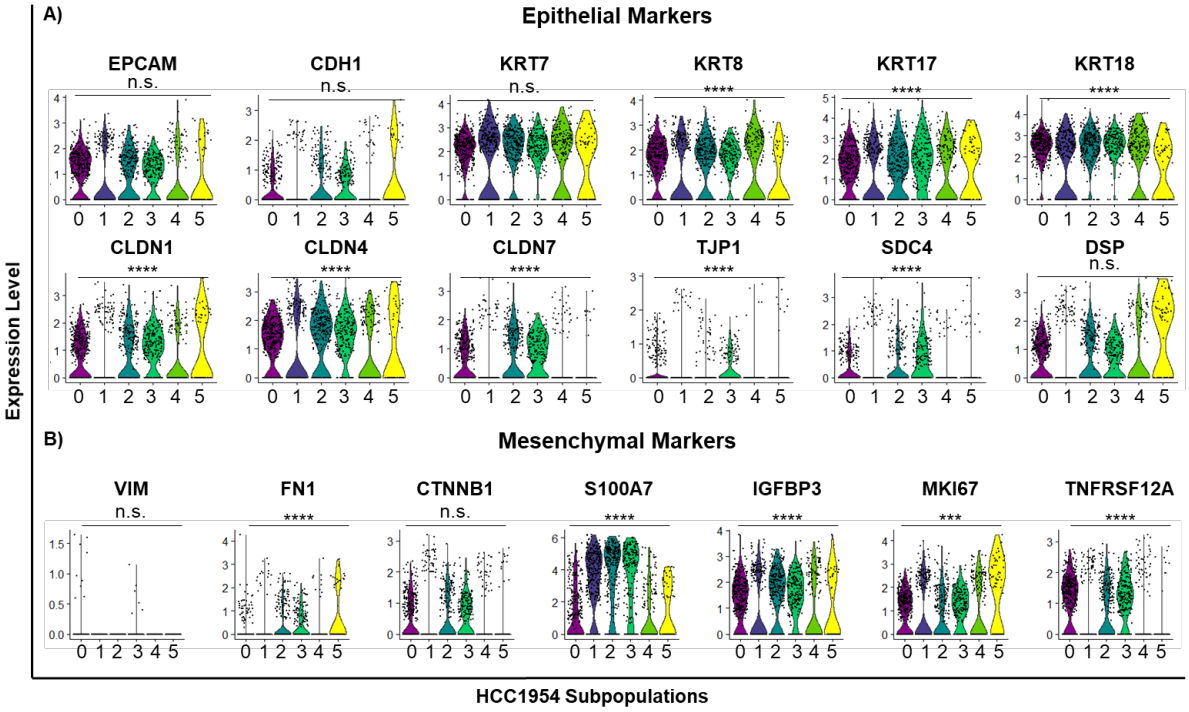

*Figure 2.6. Mixed Expression of Epithelial and Mesenchymal Markers by HCC1954 Subpopulation 1. A) Epithelial markers and B) Mesenchymal markers detected in HCC1954 Subpopulation 1. Asterisks denote statistical significance of gene expression by subpopulation 1 cells relative to remaining HCC1954 subpopulations. *** padj < 0.001, **** padj < 0.0001.*

2.3.6. PTEN k.d. in HCC1954 Slightly Increased Heterogeneity in Expression of Select Epithelial and Mesenchymal Markers

The scrutiny of epithelial and mesenchymal markers not only revealed an epithelial, early EMT phenotype for subpopulation 1, but also hinted that PTEN k.d. in HCC1954 introduced additional intratumoral heterogeneity for remaining subpopulations (Figure 2.7). PTEN k.d. did not cause significant changes in the expression of key epithelial markers, EPCAM and CDH1. In all of the subpopulations, the expression of epithelial keratins and claudins was lower in cells with PTEN k.d., but that difference was not statistically significant. In subpopulation 2, PTEN k.d. cells exhibited 1.4 fold lower

expression in CLDN1 compared to parental subpopulation 2 (Figure 2.7A). Additionally, subpopulation 4 PTEN k.d. cells expressed adhesion proteins, TJP1 and SDC4, 1.1 and 1.4 folder lower than parental subpopulation 4, respectively (padj < 0.0001, Figure 2.7A). Interestingly, within subpopulations 2, 3, and 5, the expression of S100A7 was expressed 1.2 – 1.3 fold higher in PTEN k.d. compared to the parental subpopulation (padj < 0.0001, Figure 2.7B). The expression of S100A7 has been linked to cell motility, invasion, loss of cell adhesion by stimulating pro-inflammatory response in breast cancer.[125,126,128,129] Furthermore, expression of various S100 proteins, including S100A7, have been correlated with poor overall survival and reduced relapse free survival in breast cancer patients.[124,129] Additionally, PTEN k.d. cells in subpopulation 0 and 2 expressed 1.2 fold higher levels of FN1 (fibronectin) compared to parental subpopulations (Figure 2.7B). In subpopulation 5, PTEN k.d. cells also expressed FN1 1.2 fold higher than parental cells, but this difference was not statistically significant. Taken together, this data hinted that PTEN k.d. increased intratumoral heterogeneity due to the decreased expression of tight junction proteins and increased expression of select mesenchymal markers in PTEN k.d. cells compared to parental cells of certain subpopulations.

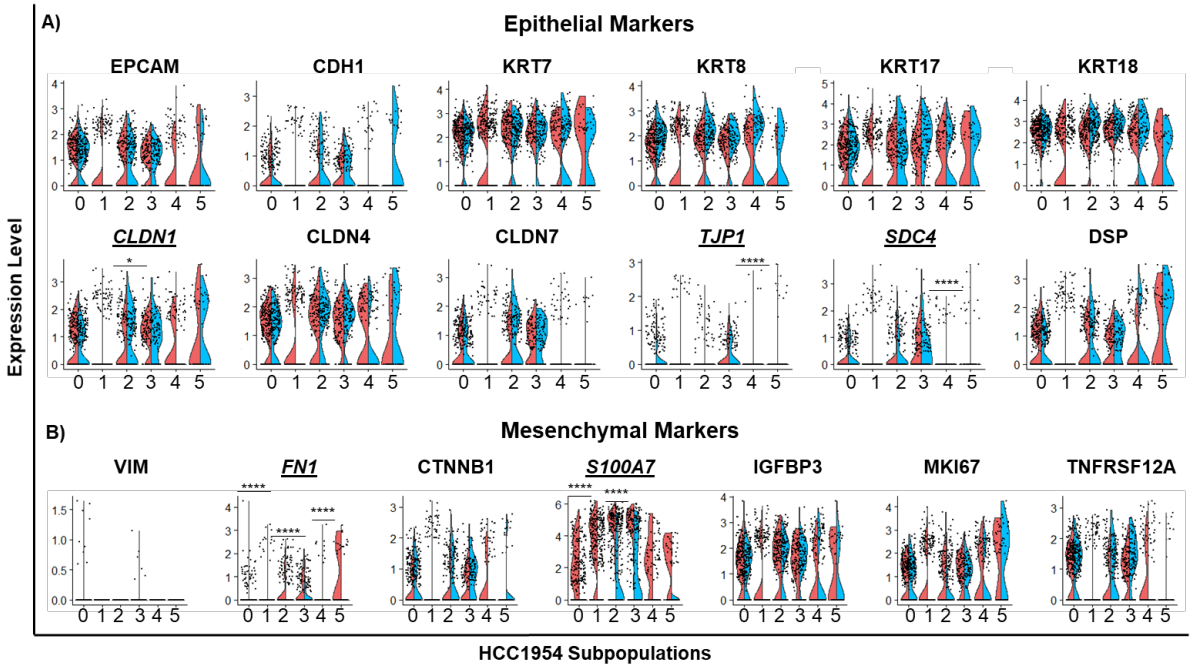

*Figure 2.7. PTEN k.d. Exerted Intra-Subpopulation Heterogeneity in Expression of Subset of Genes. A) Epithelial markers and B) Mesenchymal markers detected in HCC1954 subpopulation 1. Asterisks denote statistical significance of gene expression by subset of cells with PTEN k.d. relative to parental subpopulation. Italicized and underlined gene names are ones where gene expression was significant between PTEN k.d. cells compared with parental subpopulation. * padj < 0.05, *** padj < 0.001, **** padj < 0.0001.*

2.3.7. PTEN k.d. Increased Intra-Subpopulation Heterogeneity of Remaining HCC1954 Subpopulations

In addition to the changes to subpopulation 1, PTEN k.d. also altered relative subpopulation proportions of the remaining subpopulations. Namely, the relative subpopulation distribution of subpopulations 4 and 5 decreased by 3.2 fold after PTEN k.d. Characterization of these subpopulations by DGE and GSEA revealed both of these subpopulations were significantly enriched in cell adhesion, cell motility, and cytokine-mediated cell motility gene sets (Figures 2.8 and 2.9). HCC1954 cells from subpopulation 4 exhibited positive enrichment for cell adhesion gene sets and negative enrichment for cell motility gene sets (Figure 2.8A). Scrutiny of the cell adhesion gene sets revealed high expression of regulators of cell adhesion, such as CLDN8, NRP1, and FERMT1, which were expressed in 35-60% of subpopulation 4 cells. Interestingly, subpopulation 4 also revealed decreased expression of other known regulators of cell adhesion and epithelial polarity, such as ICAM1, AQP3, and DSC2. Furthermore, analyses of cell motility gene set revealed low expression of mediators of cell-extracellular matrix interactions, such as integrins (ITGB8 and ITGA2), collagen (COL16A1), fibroblast growth factor proteins (FGFBP2). In addition, the expression of chemokines (CXCL8, CXCL3, CXCL2, CXCL17) and cytokine modulators (SAA1 and SAA2) were low in subpopulation 4, suggesting the lack of cytokine-mediated cell motility within subpopulation 4 as a whole. Interestingly, within subpopulation 4, cells with PTEN k.d. exhibited higher cytokine signaling as evidenced in the significantly higher expression of chemokines and cytokine modulators (CXCL8, SAA1, SAA2; Figure 2.8B). Furthermore, subpopulation 4 PTEN k.d. cells also exhibited higher levels of integrins (ITGB8 and ITGA2) and collagen (COL16A1 and COL4A3BP) compared to parental subpopulation 4. The increased expression of these proteins suggested elevated cell-extracellular matrix interactions, which is an important prerequisite for gaining cell motility properties. Based on these observations, it appeared that PTEN k.d. in subpopulation 4 might facilitate the increase of cytokine expression and the acquisition of cell motility among the subset of subpopulation 4 cells with PTEN deficiency. Interestingly, certain epithelial adhesion protein, such as claudins (CLDN 7 and CLDN8), aquaporin (AQP3), desmocolin (DSC2), were expressed 1.2 fold higher in PTEN k.d. cells compared to parental subpopulation 4. Moreover, PTEN k.d. cells

exhibited decreased expression of other known regulators of epithelial adhesion and polarity, such as SDC4, SDCBP, TSPAN1, ENAH, GSN, and ATP1B1, compared to parental subpopulation 4 (padj <0.05). PTEN k.d. in subpopulation 4 distinctively expressed survivin (BIRC5), which is linked to escaping apoptosis (padj < 0.0001, Figure 2.8B). Other genes that were expressed selectively in the PTEN k.d. cells and not parental subpopulation 4 included PRC1 and matricellular protein CNN3 (Figure 2.8B). The slight but significant alterations in expression of these cell adhesion and cell motility proteins among subpopulation 4 cells with PTEN k.d. suggested a gain of cell motility properties as a result of PTEN k.d.

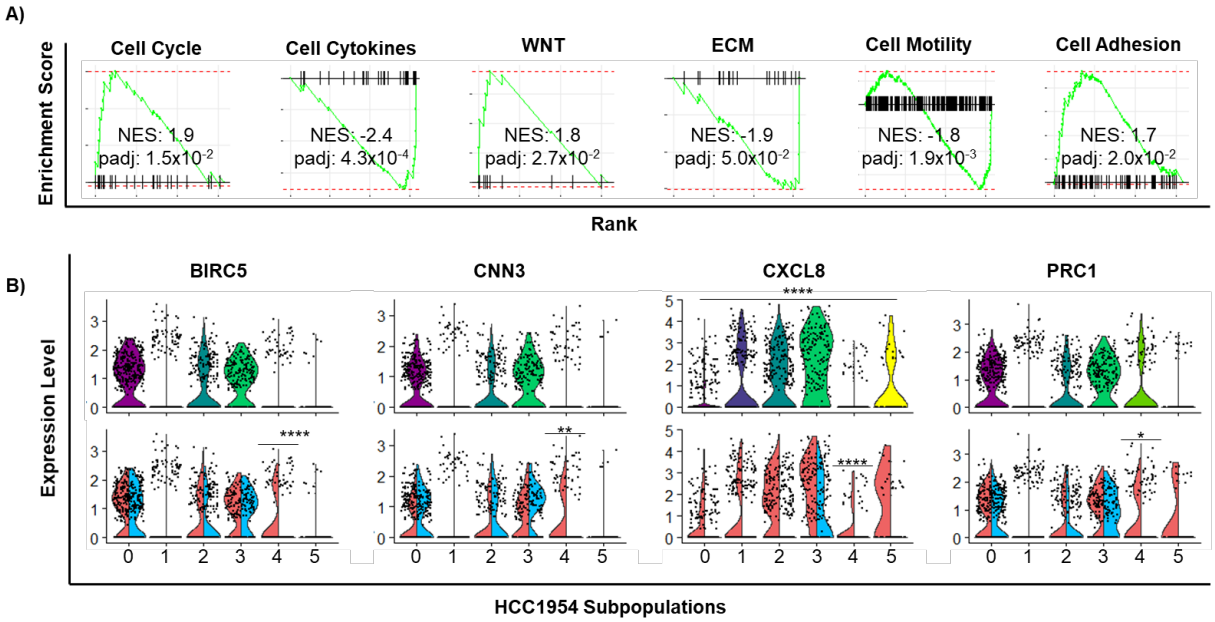

*Figure 2.8. HCC1954 Subpopulation 4 Exhibited Increased Heterogeneity with PTEN Deficiency. A) Statistically significant genes sets identified for subpopulation 4 by GSEA. Statistically significance is denoted by p-value adjusted by Benjamini-Hochberg (BH) procedure (padj < 0.05). B) Differentially expressed genes by subpopulation 4 identified by gene sets in A. Genes involved with cytokine signaling and cell growth are represented. Top: expression of genes shown for HCC1954 subpopulations with asterisk to denote statistical significance of gene expression in subpopulation 4 relative to remaining HCC1954 subpopulations. Bottom: expression of genes evaluated in parental cells and PTEN k.d. cells of each subpopulation with asterisks to denote statistical difference in gene expression between subpopulation 4 cells with PTEN k.d. compared to parental subpopulation 4. * padj < 0.05, **** padj < 0.0001.*

Besides subpopulation 4, subpopulation 5 also decreased by 3.2 fold after k.d. of PTEN. This subpopulation appeared to be largely quiescent due to the negative enrichment scores for gene sets for mitosis, DNA replication, and G1/S checkpoints, but consisted a subset of cycling cells (Figure 2.9A). The cycling phenotype of subpopulation 5 was evidenced by the expression of relatively high expression of genes critical to the G2/M transition, such as WEE1, PCNA, MKI67, and ASPM. HCC1954 subpopulation 5

was also enriched in gene sets for cell adhesion, apical cell interactions, and extracellular matrix interactions (Figure 2.9A). Analysis of these gene sets revealed expression of proteins that mediate interactions with the extracellular matrix, such as ankryins (ANKRN36C and ANKYRN36), integrins (ITGB8, ITGB2), and fibronectin (FN1). These markers were expressed in greater than 70% of subpopulation 5 cells, which suggested the occurrence of cytoskeletal remodeling in these cells. Despite the expression of regulators of extracellular matrix interactions, genes encoding cell adhesion proteins (CLDN8, TJP3, BCAM, CEACAM) were also detected in 20-50% of subpopulation 5 cells. Analysis of consequences of PTEN k.d. in subpopulation 5 revealed enhanced cytokine signaling compared to parental subpopulation 5. Cells with PTEN k.d. exhibited 1.8 fold higher expression of cytokines (CCL20, CXC3CL1, CFB, NFKB2), although these markers were expressed in 10-20% of subpopulation 5 cells with PTEN k.d. Additionally, PTEN k.d. cells within subpopulation 5 also exhibited 1.3 and 1.8 fold increase in expression of integrins ITGB2 and ITGB8, respectively, when compared to parental subpopulation 5. Furthermore, PTEN k.d. resulted in a gain of quiescent features due to a 2 fold reduction in expression of cycling markers (PCNA, ACTN1, TUBB4B, Figure 2.9B). These cycling markers were only detected in parental subpopulation 5 and not in the subset of subpopulation 5 cells with PTEN k.d (Figure 2.9B). Actins (ACTN1, ACTNG2, ACTR3, ATNR3C) were also reduced in subpopulation 5 PTEN k.d. compared to parental subpopulation 5, suggesting altered cytoskeletal actin dynamics. These changes to the cytoskeleton of subpopulation 5 PTEN k.d. cells coincides with the slight but significant increase in integrins and cytokines in these PTEN k.d. cells. It has been shown that these coupled changes cooperate to modulate actin dynamics and cell motility.[96,100,101] Taken together, PTEN k.d in subpopulation 5 introduced intra-subpopulation heterogeneity by increasing cytokine signaling and quiescence and by altering cytoskeletal dynamics for a subset of subpopulation 5 cells.

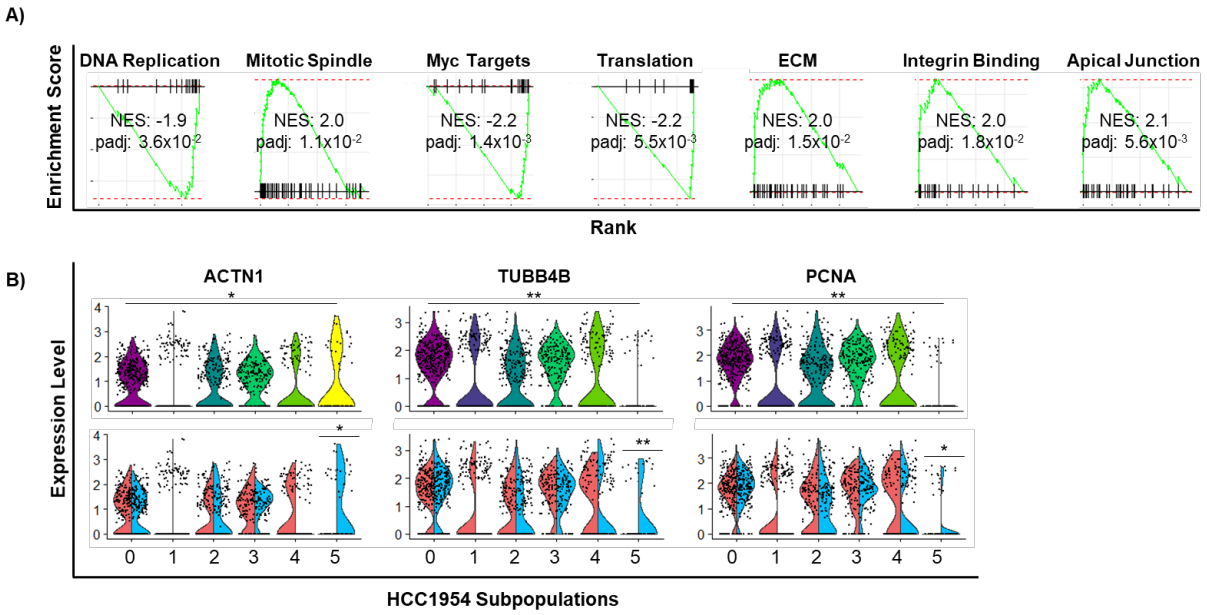

*Figure 2.9. HCC1954 Subpopulation 5 Exhibited Increased Quiescence with PTEN Deficiency. A) Statistically significant genes sets identified for subpopulation 5 by GSEA. Statistically significance was denoted by p-value adjusted by Benjamini-Hochberg (BH) procedure (padj < 0.05). B) Differentially expressed genes by subpopulation 5 identified by gene sets in A. Genes involved with cell growth are represented. Top: expression of genes shown for HCC1954 subpopulations with asterisk to denote statistical significance of gene expression in subpopulation 5 relative to remaining HCC1954 subpopulations. Bottom: expression of genes evaluated in parental cells and PTEN k.d. cells of each subpopulation with asterisks to denote statistical difference in gene expression between subpopulation 5 cells with PTEN k.d. compared to parental subpopulation 5. * padj < 0.05, ** padj < 0.01.*

Changes to the relative proportions of subpopulations 0, 2, and 3 were also observed, although those subpopulations changed by approximately 1.2 fold after k.d. of PTEN. While the changes in steady states of these subpopulations were not as dramatic as subpopulation 1, DGE analysis and GSEA that these subpopulations, particularly 2 and 3, enriched inflammatory signaling (Figure 2.10). In subpopulation 2, enhanced inflammatory signaling was evident by the high expression of SERPINB3, S100 proteins, and S100A7, which was expressed in approximately 90% of subpopulation 2 cells and expressed 1.5 fold higher than cells from other HCC1954 subpopulations. In subpopulation 3, the increased cytokine signaling was shown by elevated expression (1.5 – 3.5 fold) of inflammatory molecules (Figure 2.10). These inflammatory proteins included CCL2, CCL20, CXCL2, CXCL3, CXCL8, SERPINB3/4, S100 proteins, SAA1/2, NFKBIA, and IFI27, which were expressed in 50-90% of subpopulation 3 cells (Figures 2.8 and 2.10). Between these two subpopulations, subpopulation 3 exhibited greater inflammatory signaling compared to subpopulation 2, which demonstrated by the higher expression (2 fold) of cytokines in subpopulation 3 compared to subpopulation 2 (CCL2,

CCL20, CXCL3, CXCL8; Figures 2.8 and 2.10). Interestingly, within subpopulations 2 and 3, cells with PTEN k.d. expressed higher levels of cytokines compared to parental subpopulations 2 and 3 (Figure 2.10). Increased cytokine signaling in subpopulation 2 PTEN k.d. cells was exemplified by the elevated expression of CCL2, CXCL2, CXCL3, SAA1/2, S100A7A, TNIP3, TNFSF10, and SERPINB3/4, which expressed 1.5 – 1.7 fold higher compared to parental subpopulation 2 (padj < 0.01). In subpopulation 3, increased cytokine signaling for PTEN k.d. cells relative to parental subpopulation 3 was validated with the slightly elevated expression of SERPINE2, CCL2, CCL5, CCL28, LBP, S100A7A, CXCL5, and IL22RA2 (padj < 0.01). Despite the significantly higher expression of cytokines PTEN k.d. cells from subpopulations 2 and 3, these cytokines were expressed in 10-40% of these cells (padj < 0.01), which highlighted the heterogeneity in inflammatory signaling introduced to subpopulations 2 and 3 as a result from k.d of PTEN. In addition to cytokine signaling, both subpopulations 2 and 3 were enriched in cell adhesion and cell motility gene sets (Figure 2.10). In subpopulation 2, genes governing epithelial cell adhesion were detected and included keratins, syndecans, claudins, and regulator of epithelial polarity ATP1B1 (padj < 0.01). Of these proteins, KRT15, SDC3, and ATP1B1 were expressed approximately 1.3 fold higher in subpopulation 2 compared to the other subpopulations (padj < 0.01). Genes that regulate cell motility and interactions with the extracellular matrix were also detected in 60-90% of subpopulation 2 cells (padj < 0.01). These proteins included S100 proteins (S100A7, S100A8, S100A9, S100A11, S100P), collagen COL4A3BP, and insulin growth factor IGFBP3, which were expressed 1.2 – 2.2 fold higher in subpopulation 2 compared to the other subpopulations (padj < 0.01). Subpopulation 2 cells with PTEN k.d. were also enriched in cell motility gene sets and had slightly increased expression of integrins (ITGB2 and ITGB6) and fibronectin (padj < 0.01). Interestingly, the expression of FN1 and ITGB6 was detected only in PTEN k.d. cells of subpopulation 2 (padj < 0.01, Figures 2.8 and 2.10), which possibly hinted that PTEN k.d. enhances cell motility features through the expression of additional regulators of extracellular matrix interactions. Additionally, expression of ITGB6 was slightly yet significantly higher in subpopulation 3 than subpopulation 2 (padj < 0.0001, Figure 2.10B). Importantly, k.d. of PTEN in subpopulation 2 resulted in a slight but significant decrease in members of the claudin family (CLDN1 and CLDN8) by 1.4 and 1.2 fold, respectively,

compared to parental subpopulation 2, which suggested a decrease of epithelial character (padj < 0.01; Figure 2.8). For subpopulation 3, syndecans (SDCBP, SDCBP2, and SDC4), EPCAM, claudins (CLDN1, CLDN4, CLDN7), keratins (KRT7, KRT8, KRT17, and KRT18), and regulators of epithelial polarity (ATP1B1 and RHOC) were detected in 60-90% of subpopulation 3 cells (padj < 0.01). Of these epithelial features, syndecans, ATP1B1, and RHOC were expressed 1.2 – 1.4 fold higher in subpopulation 3 compared to the other subpopulations (padj < 0.01). Additionally, subpopulation 3 cells also expressed markers of cell motility such as MGP, S100A1, S100A8, and S100A9 that were1.2 – 2 fold higher compared to other subpopulations (padj < 0.01). Analysis of PTEN k.d. in subpopulation 3 revealed slight changes to cell adhesion and cell motility markers, such as the 1.2 fold increase in expression of ITGB2 and ACTG2 compared to parental subpopulation 3 (padj < 0.01, Figure 2.10D). Tyrosine kinase NTRK2 was expressed in 12% of subpopulation 3 PTEN k.d. cells and 1.1 fold higher compared to parental subpopulation 3 (padj < 0.01). Elevated expression of this protein has been shown to coordinate with PTEN deficiency to upregulate JAK and PI3K/AKT signaling in leukemia cells, which have some relevance in HER2-overexpressing breast cancer.[131] Taken together, subpopulations 2 and 3 were characterized by relatively high cytokine signaling and expression of genes critical to regulating cell adhesion. Analysis of PTEN k.d. in these subpopulations revealed slightly higher cytokine signaling and deregulation of cell adhesion in PTEN k.d. cells compared to parental subpopulations 2 and 3. The collective expression of cytokine signaling and deregulated cell adhesion suggested increased levels of cytokines contribute to a feedback loop that altered cell adhesion dynamics. Based on the evaluation of subpopulation 2, subpopulation 3, and the effects of PTEN k.d. within these subpopulations, it appeared that PTEN deficiency enriched for phenotypes already present in these subpopulations (i.e. high cytokine signaling and deregulated cell adhesion). Lastly, subpopulation 0 was characterized by low cytokine signaling and modest levels of cell cycle genes. Analysis of effects of PTEN k.d. in subpopulation 0 did not reveal any significant gene set that distinguished subpopulation 0 PTEN k.d. cells from parental subpopulation 0.

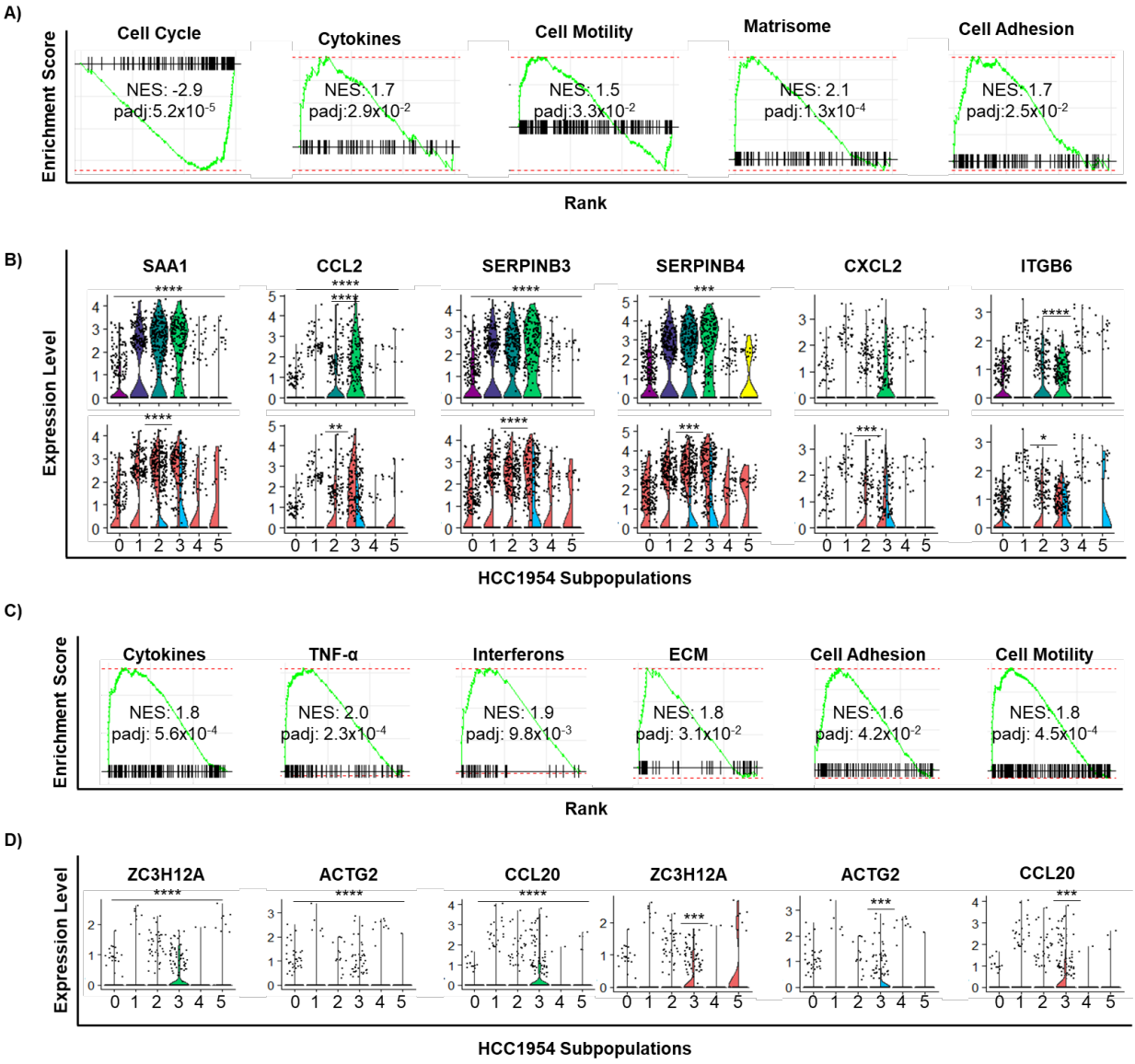

*Figure 2.10. PTEN k.d. in Subpopulations 2 and 3 Stabilized Existing Phenotypes. Statistically significant genes sets identified for A) subpopulation 2 and C) subpopulation 3 by GSEA. Statistically significance was denoted by p-value adjusted by Benjamini-Hochberg (BH) procedure (padj < 0.05). Differentially expressed genes by B) subpopulation 2 and D) subpopulation 3. Top: expression of genes shown for HCC1954 subpopulations with asterisk to denote statistical significance of gene expression in subpopulation 2 relative to remaining HCC1954 subpopulations. Gene expression differences between subpopulation 2 and 3 are also noted with asterisks. Bottom: expression of genes evaluated in parental cells and PTEN k.d. cells of each subpopulation with asterisks to denote statistical difference in gene expression between subpopulation 2 cells with PTEN k.d. compared to parental subpopulation 2. For subpopulation 3, on left, expression of genes shown for HCC1954 subpopulations with asterisk to denote statistical significance of gene expression in subpopulation 3 relative to remaining HCC1954 subpopulations. On right, expression of genes evaluated in parental cells and PTEN k.d. cells of each subpopulation with asterisks to denote statistical difference in gene expression between subpopulation 3 cells with PTEN k.d. compared to parental subpopulation 3. * padj < 0.05, ** padj < 0.01, *** padj < 0.001, **** padj < 0.0001.*

2.3.8. PTEN k.d. in SKBR3 Resulted in Global Increase of Quiescent Properties Relative to Parental SKBR3

The effects of PTEN k.d. were evaluated for SKBR3 using similar approaches as described for HCC1954. Similar to HCC1954, the SKBR3 cell line pair consisted of cells with comparable transcriptomic profiles, as evidenced by the overlap between the cells with SKBR3 PTEN k.d. cells and parental SKBR3 (Figure 2.11A). Also akin to HCC1954, SKBR3 harbored a subpopulation that was exclusively found in SKBR3 PTEN k.d. cells (circled in Figure 2.11A). DGE analysis identified 992 differentially expressed genes (padj < 0.01). Of these, 515 genes were higher, and 477 genes were lower in SKBR3 PTEN k.d. cells relative to parental SKBR3 (Figure 2.11B, padj < 0.01). GSEA of these differentially expressed genes revealed only 16 statistically significant gene sets, which included the cancer gene neighborhoods of cyclin A2 (CCNA2), cell-division protein 20 (CDC20), and mitotic checkpoint gene encoding for BUB1B (padj < 0.01, Figure 2.11C). Despite the low quantity of statistically significant gene sets between parental SKBR3 and SKBR3 PTEN k.d. cells, the low expression of gene sets associated with the cell cycle hinted of a global increase of quiescent properties resulting from k.d. of PTEN.

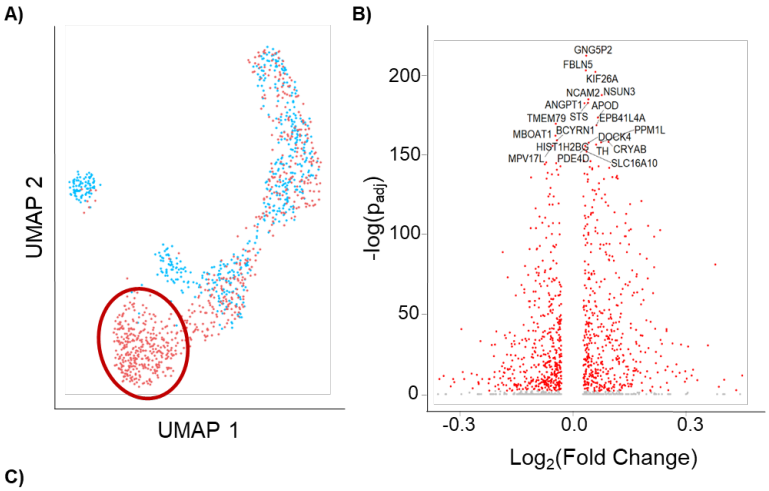

C)

Gene set	p,val	p,adj	NES
GNF2 CDC20	1.43E-05	8.80E-03	-2.09
GNF2 CCNA2	4.87E-06	4.37E-03	-2.15
GNF2 BUB1B	1.17E-05	7.86E-03	-2.17
GO CYTOSKELETON ORGANIZATION	5.96E-06	4.90E-03	-1.78

Figure 2.11. Global Comparisons of Transcriptomic Composition of Parental SKBR3 and SKBR3 PTEN k.d. A) UMAP plot depicting parental SKBR3 (cyan) and SKBR3 PTEN k.d. (pink). Circled region denotes subpopulation enriched by PTEN k.d. cells. B) Volcano plot of differentially expressed genes by SKBR3 PTEN k.d. cells. Cells in red denotes statistically significant differentially expressed genes by SKBR3 PTEN k.d. cells (padj<0.01). Top 20 statistically significant genes are labeled. C) Gene sets identified by GSEA. Statistically significance is denoted by p-value adjusted by Benjamini-Hochberg (BH) procedure (padj < 0.01).

2.3.9. PTEN Deficiency in SKBR3 Resulted in 120-Fold Enrichment of Quiescent, Early EMT Subpopulation 1

Since GSEA suggested a global increase of quiescent properties resulting from PTEN deficiency, we analyzed the effects of PTEN k.d. on the subpopulations of SKBR3 to reveal the phenotype PTEN deficiency favored. Nonlinear dimensionality reduction using UMAP revealed the intratumoral heterogeneity of SKBR3, which was manifested as six subpopulations (Figure 2.12A). Parental SKBR3 was distributed into 37% subpopulation 0, 0.3% subpopulation 1, 24% subpopulation 2, 12% subpopulation 3, 15% subpopulation 4, and 9% subpopulation 5 (Figure 2.12B). As shown in Figure 2.12B, PTEN in SKBR3 altered the cellular composition of the bulk cell line, resulting in 23% subpopulation 0 (1.5 fold decrease), 44% subpopulation 1 (120 fold increase), 23% subpopulation 2, 7.5% subpopulation 3 (1.6 fold decrease), 0.8% subpopulation 4 (18 fold decrease), and 0.4% subpopulation 5 (24 fold decrease). Interestingly, PTEN k.d. in

SKBR3 drastically enriched a minor subpopulation (i.e. subpopulation 1) akin to HCC1954.

To elucidate the phenotype of SKBR3 subpopulation 1, DGE and GSEA was performed by comparing subpopulation 1 to the rest of the subpopulations. This analysis yielded 1,154 differentially expressed genes and 9 statistically significant gene sets, most of which were involved in the electron transport chain (padj < 0.05). The low quantity of statistically significant gene sets implied extensive transcriptomic similarities between the compared subpopulations, which limited the statistical power of GSEA to identify statistically significant gene sets. As an alternative method to characterize SKBR3 subpopulation 1, we compared this subpopulation with subpopulations that were farthest on the UMAP plot (i.e. subpopulations where the transcriptomic difference between subpopulation 1 was greatest). By comparing these subpopulations (i.e. subpopulations 0 and 3) with subpopulation 1, DGE analysis revealed 1,199 genes differentially expressed by subpopulation1, despite their low fold change in gene expression (Figure 2.12C). Of these 1,199 differentially expressed genes, 440 genes were expressed higher, and 759 were expressed lower in subpopulation 1 (Figure 2.12C, padj < 0.01). Scrutiny of these genes by evaluating the top 20 statistically significant genes revealed commonalities (Figure 2.12C, padj < 0.01). The top 20 statistically significant genes encoded proteins that are critical for cell cycle (haus augmin like subunit 2, HAUS; BUB1B mitotic checkpoint serine/threonine kinase B, BUB1B; and replication factor C subunit 3, RFC3) and microtubule function (tubulin gamma 1, TUBG1; centromere protein J, CENPJ; establishment of sister chromatid cohesion N-acetyltrasferase, ESCO2; dual specificity protein kinase, TTK; and shugoshin like 1, SGOL1). Additionally, top statistically significant genes also encoded proteins involved in nucleic acid metabolism (non-SMC condensing matrix, NCAPG and cyclic nucleotide phosphodiesterase, CNP) and cellular metabolism (acetolactate synthase, ILVCL and carbonyl reductase, CBR3). These top 20 statistically significant genes were associated with cell cycle and were expressed in SKBR3 subpopulation 1, which hinted of a quiescent phenotype for this subpopulation. GSEA revealed 794 statistically significant gene sets for subpopulation 1 (padj < 0.01). SKBR3 subpopulation 1 was negatively enriched in cell cycle associated gene sets, which further supported the quiescent phenotype suggested from the analysis

of the top statistically significant genes (Figure 2.12D and E). Additionally, GSEA suggested SKBR3 subpopulation 1 harbored an epithelial phenotype as evidenced by the positive enrichment of gene sets associated with biological adhesion (Figure 2.12D). Additionally, this subpopulation exhibited a positive enrichment in cytokine signaling, specifically TNF-α signaling. Scrutiny of the gene sets was performed to determine what genes contributed to these enrichment scores and to validate the quiescent epithelial phenotype of SKBR3 subpopulation 1 as suggested by GSEA.

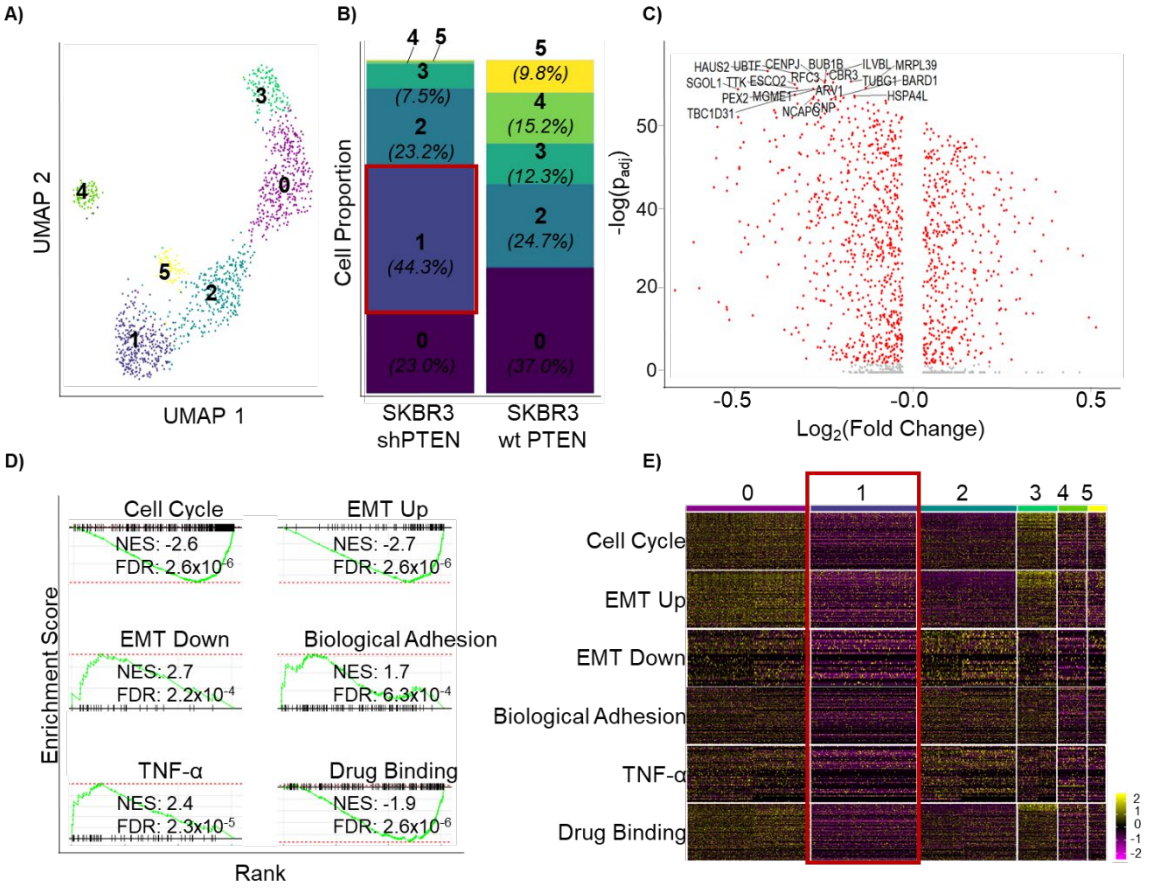

Figure 2.12. Single Cell Analysis of SKBR3 Subpopulations and Characterization of Subpopulation that Enriched After PTEN k.d. Subpopulation 1. A) UMAP plot depicting six SKBR3 subpopulations. Dots represent single cells. Subpopulations are organized by color. B) Cell Distribution using the same color scheme as shown in A. C) Volcano plot depicting genes differentially expressed by SKBR3 subpopulation 1. Grey dots represent genes with a log2FC that is not statistically significant. Red dots represent genes with a log2FC that is statistically significant. Statistical significance is denoted by p.adj < 0.01. C) Gene sets enriched by SKBR3 subpopulation 1. Normalized enrichment score (NES) and FDR (false discovery rate) adjusted p-values are displayed. FDR < 0.01 denotes statistical significance. D) Heatmap of gene sets from C. Colored scale represents normalized gene expression for each gene.

To validate the quiescent phenotype, cell cycle associated gene sets identified by GSEA were scrutinized. These gene sets included DNA replication, DNA repair, G2/M checkpoints, chromatin binding, and DNA metabolism, which were all negatively enriched

by SKBR3 subpopulation 1 and supported the quiescent phenotype of subpopulation 1 (Figure 2.13A). Furthermore, targets of E2F and the DREAM complex were also expressed lower in SKBR3 subpopulation 1, which supported the quiescent phenotype of this subpopulation since targets of E2F and the DREAM complex are repressed in quiescent cells.[132–134] Analysis of the E2F and DREAM targets gene sets revealed 74 genes expressed higher and 218 genes expressed lower in subpopulation 1. Among these high expressing genes was FOS, which was expressed in 31% of SKBR3 subpopulation 1 and expressed 1.4 fold higher (Figure 2.13A, padj < 0.01). The other genes with elevated expression in subpopulation 1 were expressed in less than 10% of subpopulation 1 (padj < 0.01). Among genes that were expressed lower in subpopulation 1 were genes associated with proliferation, such as helicase HELLS, MKI67, and geminin GMNN, which expressed in 7-31% of subpopulation 1 genes and expressed in 1.2 – 1.5 fold lower in SKBR3 subpopulation 1 (Figure 2.13B, padj < 0.01). In addition, the analysis of these genes revealed members of the PRC2 complex, such as EZH2 and RbBP8, which were expressed in 20% and 85% of subpopulation 1, respectively (Figure 2.13B, padj < 0.01). EZH2 and RbBP8 were detected 1.2 and 1.3 fold lower in subpopulation 1 compared to other SKBR3 cells (both padj < 0.0001). Decreased expression of PRC2 members has been shown to result in quiescence[135,136], which is consistent with the increase of quiescence observed from this subpopulation. Additionally, the median percent of cells that expressed genes cell cycle associated gene sets was 6%, which signified that, collectively, subpopulation 1 consisted of a quiescent group of cells. The global increase of quiescent properties revealed by the comparative analysis of parental SKBR3 and SKBR3 with PTEN k.d. cells might have stemmed from the 120 fold enrichment of subpopulation 1 (Figures 2.11 and 2.13). Together, the low expression of cell cycle gene sets observed in the collective SKBR3 PTEN k.d. cells and in SKBR3 subpopulation 1 suggested that PTEN k.d. resulted in the overall increase of quiescent features by enriching SKBR3 subpopulation 1.

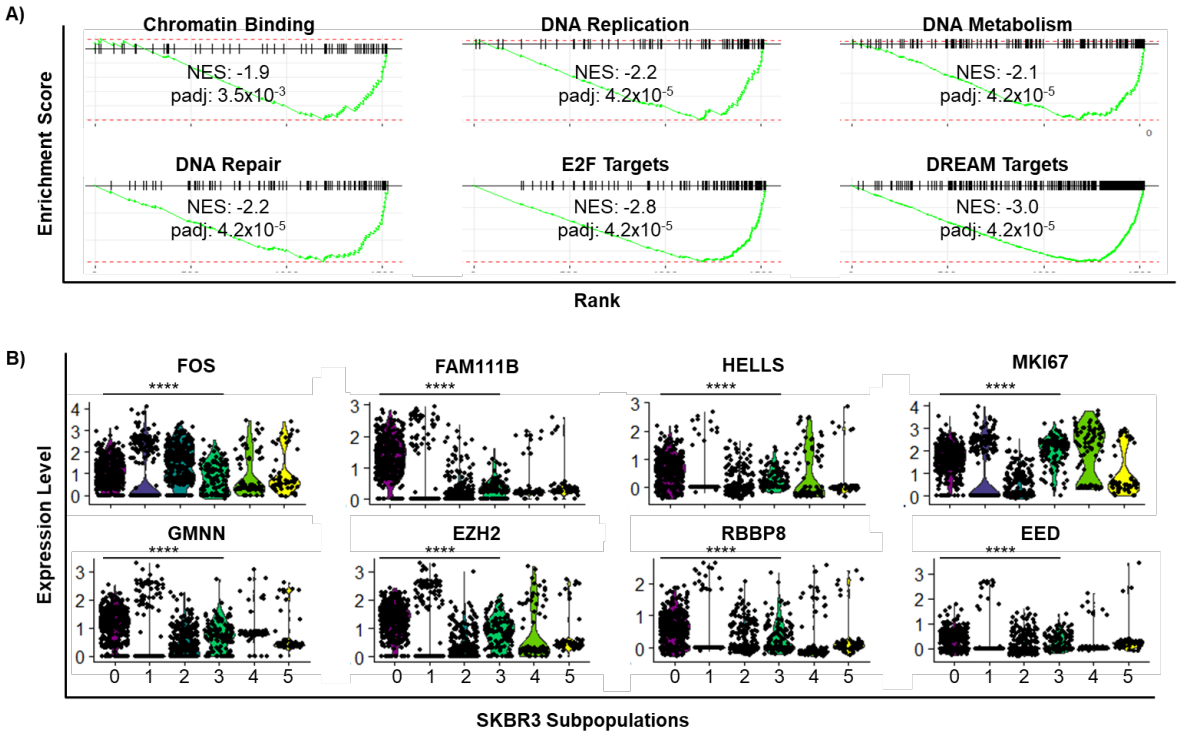

*Figure 2.13. Quiescence Properties of SKBR3 Subpopulation 1. A) Cell cycle associated gene sets identified by GSEA. Statistically significance is denoted by p-value adjusted by Benjamini-Hochberg (BH) procedure (padj < 0.01). B) Differentially expressed genes identified from gene sets from A are depicted. **** padj <0.0001.*

Interestingly, 80 of 392 genes (20%) identified from the cell cycle associated gene sets were also identified in the drug binding gene set, which was another gene set enriched by subpopulation 1 (Figure 2.12). Of the genes identified from the drug binding gene set, 80 of 135 genes (59%) overlapped with the genes identified from the cell cycle associated gene sets. The extent of the overlap underscored how the mechanisms involved in drug binding could impair cell cycle progression by disrupting the proteins that regulate it. Genes unique to the drug binding gene set were among the higher expressed genes in subpopulation 1. These top genes were are involved in cellular or nucleotide metabolism; they included receptor-interacting serine/threonine kinase RIPKA4, glutamine-ammonia ligase GLUL, purine nucleoside phosphorylase PNP, peptidyl isomerase FKBP1A, PIK3CB, calcium-independent phospholipase PNPLA8, and casein kinase CSNK1A1. These genes were expressed in 13-25% of subpopulation 1 cells and expressed 1.3 fold higher in subpopulation 1 (padj < 0.01). Interestingly, multidrug resistance protein family members, such as ABCC2 and ABCG2, were identified in SKBR3 using the drug binding gene set but were lowly expressed in SKBR3 (padj < 0.01).

In addition, ABCG2 is the nominal breast cancer resistance protein and its overexpression has been reported to contribute to a drug resistant phenotype in breast cancer cells.[137,138] The low expression of these genes in subpopulation 1 and in bulk SKBR3 suggested that PTEN k.d. would not affect the anti-HER2 sensitivity based on ABC transporter superfamily expression levels. Furthermore, the scrutiny of the drug binding exposed a reduction in the expression of genes encoding kinesins by SKBR3 subpopulation 1 compared to the other SKBR3 subpopulations (Figure 2.14). Kinesins (KIF) are a family of motor proteins that are known to coordinate the movement of spindle microtubules.[139,140] However, their functions extend beyond mitosis and they are known to rely extensively on microtubules to move cellular vesicles, organelles, mRNA, and elements of the cytoskeleton, and thus, are regarded to play a key role in cell motility.[139–143] Importantly, these proteins have been regarded to disrupt the structures that maintain the integrity of cell-cell adhesion between epithelial cells (e.g. tight junctions and adherens junctions).[141] Kinesins disrupt cell-cell adhesion by binding to the keratin filaments of the epithelial cytoskeleton to regulate the formation of contractile rings, which is a key step to dismantle tight junctions and adherens junctions present in epithelial monolayers.[141] The loss of these cell-cell adhesion structures has been regarded as a key feature of the initiation of EMT, and thus, the downregulation of these kinesins in SKBR3 subpopulations 1 corroborates its epithelial phenotype (Figure 2.14). Additionally, cells with enhanced rates of kinesin-mediated intracellular transport have been shown to exhibit early apoptosis.[144] Therefore, the reduced expression of kinesins and the concomitant decrease in kinesin activity in SKBR3 subpopulation 1 hinted of a possible mechanism to delay apoptosis induced by cellular stress from k.d. of PTEN (Figure 2.14).

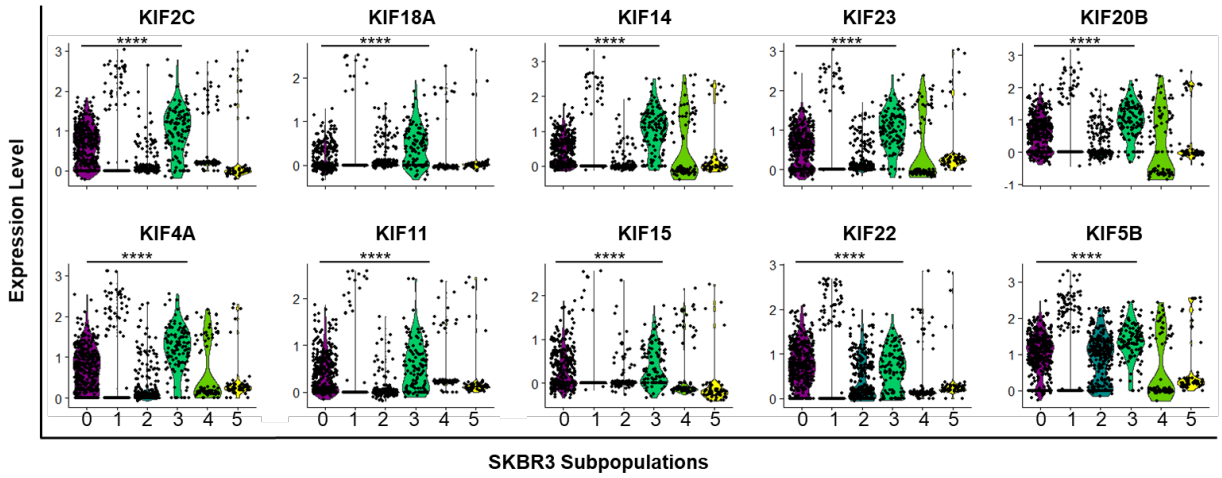

*Figure 2.14. Downregulation of Kinesins as a Possible Mechanism for Stress Response by SKBR3 Subpopulation 1. Violin plots depicting expression of known kinesins in SKBR3 subpopulation 1. Dots represent single cells expressing markers. Statistical significance was determined by comparing log2(fold change) of gene expression and differences in percentage of cells expressing genes between subpopulation 1 and subpopulations 0 and 3. **** padj < 0.0001.*

2.3.10. SKBR3 Subpopulation 1 Exhibited Mixed Expression of Epithelial Markers and Markers That Facilitate EMT

In addition, SKBR3 expressed genes characteristic of epithelial phenotype, which included EPCAM, KRT19, and CLDN4 (Figure 2.15A). These encoded proteins are critical for maintaining the cell-cell junction and polarity between the epithelial cells.[118–121] As previously shown in Figure 2.14, SKBR3 subpopulation 1 express significantly low levels of kinesins, which contributed to its epithelial phenotype since the expression of these proteins have been shown to disrupt cell-cell adhesion.[139–143] In addition to the expression of epithelial markers, SKBR3 subpopulation 1 cells expressed low levels of CD151, a tetraspanin protein that mediates integrin-dependent cell motility.[145,146] Thus, the reduced expression of this protein could compromise the ability of the subpopulation 1 cells to engage in cellular motility. Furthermore, SKBR3 subpopulation 1 cells exhibited decreased expression of ankryin G (encoded by ANK3), which is highly distributed in adherens junctions and critical for integrin signaling within the cytoskeleton.[147–149] Interestingly, ankryin 3 has been shown to interact with E-cadherin, and downregulation of ankryin 3 during EMT has been shown to interfere with the downstream signaling of E-cadherin.[147,150] While SKBR3 subpopulation 1 cells expressed a subset of epithelial-specific markers, it exhibited low expression of proteins regulating tight junction and cell adhesion, such as ANK3, CDH1, SDC1, and DSP, which suggested weakening of cell-cell adhesion and thus an early EMT phenotype (Figure 2.15A). Additionally, SKBR3

subpopulation 1 cells expressed markers associated with EMT. These markers included FN1, MKI67, S100A4, which is upregulated during EMT, metastasis, and regarded as crucial for the cytoskeletal remodeling during EMT (Figure 2.15B).[118,119,123,151–153] FN1, MKI67, and S100A4 were expressed in 4%, 31%, and 40%, respectively, were expressed by subpopulation 1 (Figure 2.15B), which not only illustrated the expression of markers that promote cell motility and interactions with the extracellular matrix but also highlighted the heterogeneity in the expression of markers that govern EMT phenotype. However, SKBR3 subpopulation 1 cells did not express classical markers of mesenchymal phenotype, such as vimentin (VIM) nor N-cadherin (CDH2). Collectively, the expression of these markers suggested SKBR3 subpopulation 1 predominantly exhibited epithelial phenotype, but the lowered expression of critical epithelial markers (CDH1 and tight junction proteins) hinted that SKBR3 subpopulation harbored an epithelial, early EMT phenotype.

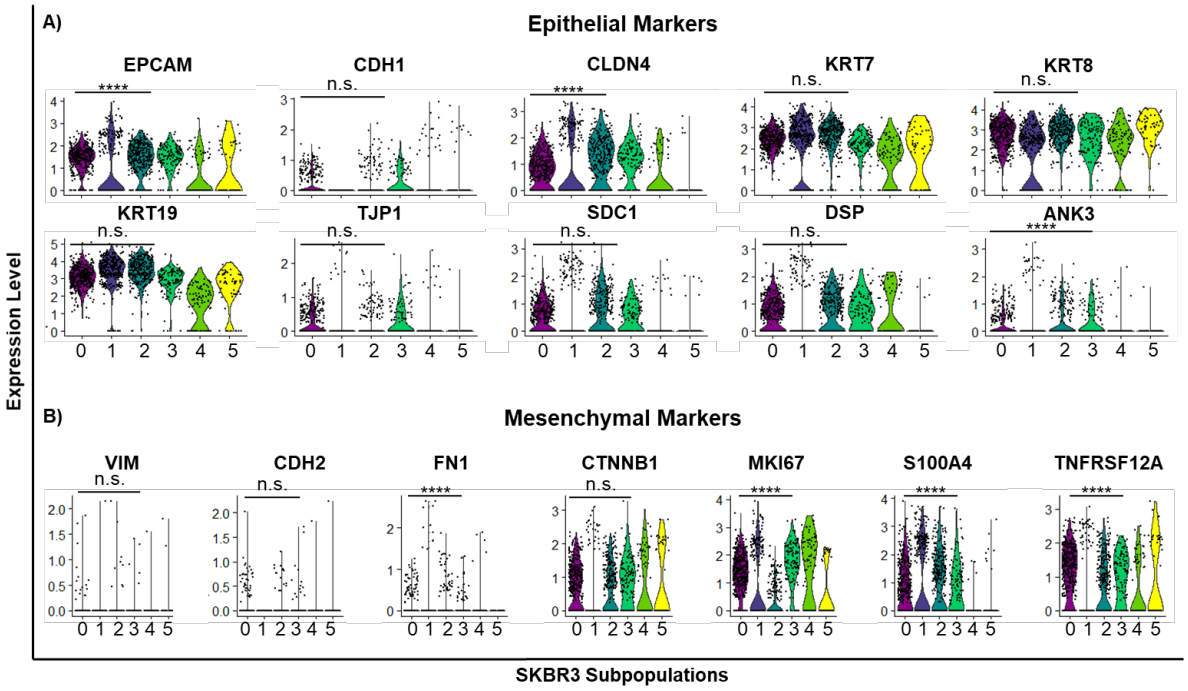

*Figure 2.15. Mixed Expression of Epithelial and Mesenchymal Markers by SKBR3 Subpopulation 1. A) Epithelial markers and B) mesenchymal markers detected in SKBR3 Subpopulation 1. Asterisks denote statistical significance of gene expression by subpopulation 1 cells relative to other subpopulations. **** padj < 0.0001.*

2.3.11. PTEN k.d. in SKBR3 Slightly Increased Heterogeneity in Expression of Markers Associated with EMT

In addition to analyzing the expression of epithelial and markers associated with EMT by SKBR3 subpopulation 1, the consequences of PTEN k.d. for each subpopulation was also analyzed for these markers. Similar to HCC1954, the expression of epithelial keratins, claudins, and tight junction proteins (TJP11 and TJP3) were not statistically different in the subset of SKBR3 cells with PTEN deficiency (Figure 2.16A). This is consistent with the literature about temporal dependence of the gained expression of EMT markers and decreased expression of epithelial markers; expression of keratins have been observed until the late stages of EMT.[120] Furthermore, syndecan binding protein 2 (SDCBP2), not SDC1, was detected in less than 20% of cells in each subpopulation (padj < 0.01), and PTEN k.d. cells of SKBR3 subpopulations 0, 2, and 3 exhibited a significantly lower expression of SDCBP2, which signified a decrease in cell adhesion based on the changes in expression of this gene (padj < 0.001). Interestingly, the expression of fibronectin (FN1) was slightly, but significantly higher in the subset of PTEN k.d. cells compared to parental SKBR3 for subpopulations 2 and 3 (padj < 0.01, Figure 2.16B). For subpopulation 0, the expression of fibronectin was slightly lower in PTEN k.d. cells compared to parental subpopulation 0 (padj < 0.01, Figure 2.16B). Taken together, PTEN k.d. in SKBR3 introduced intra-subpopulation heterogeneity by altering the expressing of markers associated with EMT.

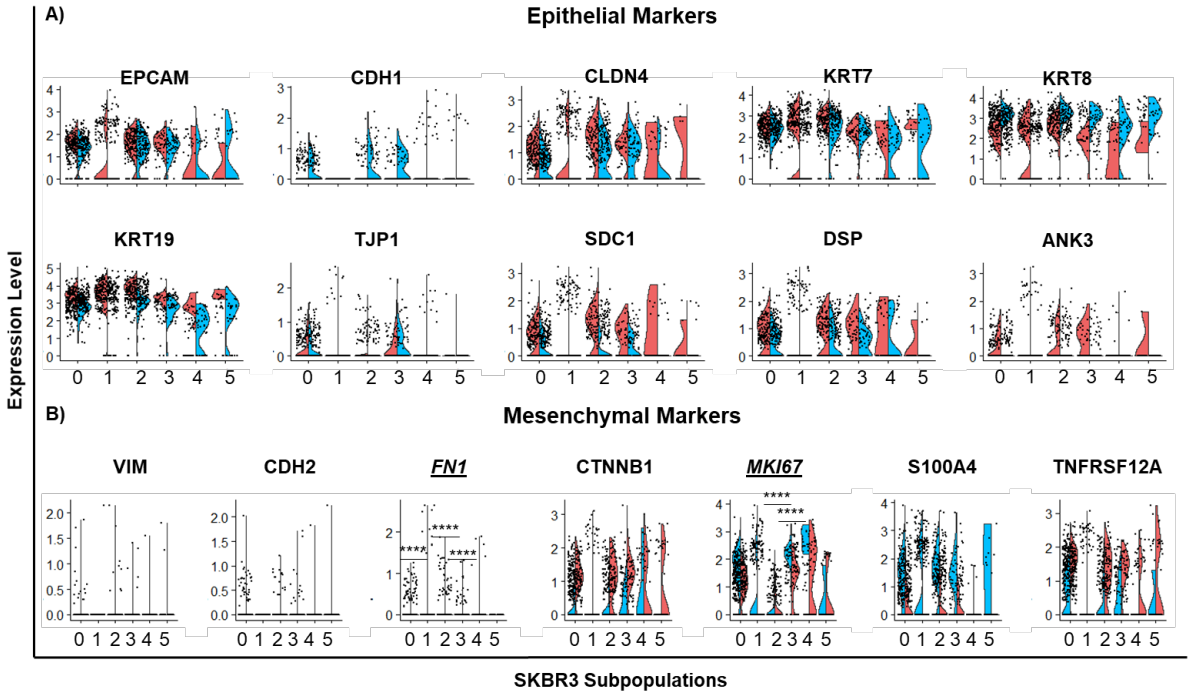

*Figure 2.16. PTEN k.d. in SKBR3 Exerted Intra-Subpopulation Heterogeneity in Expression of Subset of Genes. A) Epithelial markers and B) Mesenchymal markers detected in SKBR3 Subpopulation 1. Asterisks denote statistical significance of gene expression by subset of cells with PTEN k.d. relative to parental subpopulation. Italicized and underlined gene names (2) are ones where gene expression was significant between PTEN k.d. cells compared with parental subpopulation. **** padj < 0.0001.*

Taken together, the k.d. of PTEN in SKBR3 altered the subpopulation dynamics, which accompanied a 120 fold enrichment in quiescent, epithelial, early EMT subpopulation. This subpopulation also exhibited a kinesin-dependent mechanism to evade apoptosis induced by cellular stress. Analysis of expressed epithelial and markers associated with EMT revealed SKBR3 subpopulation 1 exhibit epithelial early EMT phenotype based on the expression of epithelial keratins, low expression of tight junction proteins, and expression of genes associated with cell motility for EMT such as FN1.

2.3.12. PTEN k.d. in SKBR3 Increased the Intra-Subpopulation Heterogeneity of Remaining SKBR3 Subpopulations

In addition to the increase of the relative SKBR3 subpopulations, PTEN k.d. also impacted other SKBR3 subpopulations (Figure 2.12). Besides subpopulation 1, the relative proportions of the remaining SKBR3 subpopulations decreased after the k.d. of PTEN relative to the parental subpopulations. Of the subpopulations that decreased, the relative proportions of subpopulations 4 and 5 decreased by the largest magnitudes (by 18 fold and 24 fold, respectively) after the k.d. of PTEN (Figure 2.12). Subpopulation 4

was constituted of 15% of parental SKBR3 and decreased to 0.8% of SKBR3 with PTEN k.d (Figure 2.12). The characterization of subpopulation 4 by DGE and GSEA revealed significantly positive enrichment for gene sets involved in the cell cycle, mitotic spindle, G2/M gene sets, and DNA replication, suggesting that subpopulation 4 cells exhibited proliferative phenotype (Figure 2.17A, padj < 0.05). This phenotype was further supported by the high expression of proliferative markers, such as CENPF, SMC4, BRCA2, CKAP5, CENPE, TOP2A, and MKI67. All of these genes were expressed in 95-100% of SKBR3 subpopulation 4 and expressed 1.5 – 2.3 fold higher in subpopulation 4 compared to other subpopulations. Additionally, subpopulation 4 was negatively enriched for inflammatory signaling, namely gene sets involved innate immune signaling, which was verified with the lowered expression of inflammatory molecules in subpopulation 4 compared to other subpopulations (Figure 2.17A, padj < 0.05). Inflammatory proteins that were lowly expressed in subpopulation 4 included S100 proteins, ILF2, NKFBIA, FTH1, DYNLL1, TNFAIP3, CCL2, CD58, and CXCL1 (Figure 2.17B, padj < 0.05); these genes were expressed 1.6-2.6 fold lower in subpopulation 4 compared to the remaining SKBR3 subpopulations. Lastly, subpopulation 4 was enriched in gene sets germane to cell adhesion and extracellular matrix interactions (Figure 2.17A, padj < 0.05). Interestingly, the expression of CLDN3, KRT8 and ACTB were expressed 2 fold lower in subpopulation 4 compared to the other subpopulations, suggesting subpopulation 4 might exhibit less epithelial phenotype compared to the other SKBR3 subpopulations (padj < 0.05). In addition, HSPB1 was identified from the cell adhesion gene set to be 3.5 fold lower in expression compared to the other SKBR3 subpopulations (padj < 0.05). This finding was interesting because the lowered expression of this heat shock protein has been shown to weaken cell adhesion and to increase cell motility in breast cancer cells.[154] Scrutiny of the consequences of PTEN k.d. in this subpopulation revealed too few subpopulation 4 cells with PTEN k.d. (6 cells) relative to parental subpopulation 4 (83 cells). This low number of SKBR3 subpopulation 4 cells with PTEN k.d. hindered the identification of differentially expressed genes and significant gene sets to distinguish the subset of subpopulation 4 cells with PTEN k.d. from the parental subpopulation 4 (padj < 0.05).

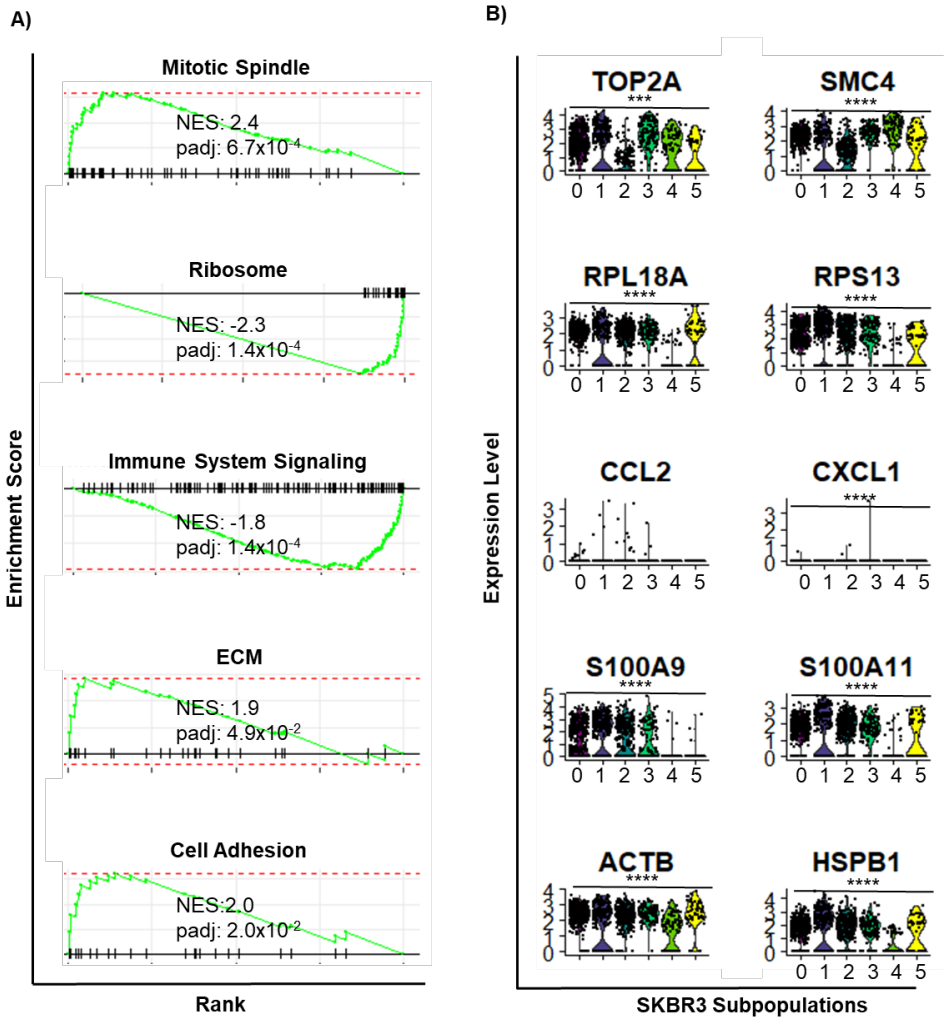

*Figure 2.17. SKBR3 Subpopulation 4 Cells were Characterized by High Cell Cycling and Cell Adhesion Properties. A) Statistically significant gene sets identified by GSEA for SKBR3 subpopulation 4. B) Genes identified from gene sets shown in A. Asterisks denote statistical significance of expression of gene in subpopulation 4 relative to expression in other subpopulations. *** pad j< 0.001, **** padj < 0.0001.*

In addition to subpopulation 4, SKBR3 subpopulation 5 was also affected by PTEN k.d.; this subpopulation constituted 10% of parental SKBR3 and was reduced by 24 fold to 0.4% in SKBR3 after k.d. of PTEN (Figure 2.12). We sought to characterize subpopulation 5 by DGE analysis and GSEA, but GSEA did not identify statistically significant gene sets for subpopulation 5 (padj > 0.05). Instead, genes differentially expressed by subpopulation 5 were analyzed. There were 926 differentially expressed genes by subpopulation 5. Among these genes were tropomyosin 1 (TPM1), which was expressed in 98% of subpopulation 5 and expressed 2.2 fold higher than cells of remaining SKBR3 subpopulations (padj < 0.05). Tropomyosin tightly regulates contraction in muscles and is known to regulate actin filaments found in the

cytoskeleton[155], and thus, its high expression in this subpopulation suggested a role in governing cell motility in this subpopulation. Interestingly, the lowest differentially expressed genes in subpopulation 5 were epithelial cell adhesion proteins, such as CLDN4, CLDN7, LAMB3, and TIPIN, all of which were expressed 1.2 – 1.4 fold lower in subpopulation 5 compared to the other SKBR3 subpopulations (padj < 0.05). These encoded proteins are critical for epithelial cell adhesion and polarity, and their relatively low expression in subpopulation 5 suggested subpopulation 5 exhibited less epithelial characteristics compared to other subpopulations. Additionally, proteins that facilitate ECM interactions and ECM degradation were also identified among the differentially expressed genes of subpopulation 5, which included ADAM17, ITGB1, and ANKRD36. Taken together, this data suggested a dysregulation of the cytoskeletal dynamics and disruption of cell-cell adhesion among subpopulation 5 cells relative to other SKBR3 subpopulations. Moreover, characterization of the subset of subpopulation 5 cells with PTEN k.d. by GSEA did not reveal significant gene sets that distinguished the subset of subpopulation 5 cells with PTEN k.d. from the parental subpopulation 5. Similarly to what was observed with the subpopulation 4 cells with PTEN k.d., the inability to distinguish parental subpopulation 5 from the cells with PTEN k.d. was due to the low number of subpopulation 5 cells with PTEN k.d. (3 cells) relative to the parental subpopulation 5 (54 cells). With 5 cells with PTEN k.d. in SKBR3 subpopulation 5, comparative analyses between these groups of cells within subpopulation 5 could not have been performed reliably to yield statistically significant gene sets.

Changes in SKBR3 subpopulations 0, 2, and 3 were also observed, although changes in the subpopulations were 1.5, 1.1, and 1.6, respectively after PTEN k.d (Figure 2.12). Subpopulation 0 was characterized with a positive enrichment in cell cycle gene sets (DNA replication, base excision, G2/M checkpoints, and proliferation), suggesting SKBR3 subpopulation 0 represented highly proliferative cells (Figure 2.18A). Scrutiny of those gene sets validated this phenotype with the high expression of genes critical for cell cycle progression and proliferation, such as CDC6, CDK1, MCM2, TOP2A, PCNA, RRM2, and ATAD2 (Figure 2.18B, padj < 0.05). These genes were among the highest expressed genes of subpopulation 0, were expressed in 90-99% of subpopulation, and were expressed 1.5 – 2 fold higher in subpopulation 0 compared to cells of other SKBR3

subpopulations (padj < 0.05). Interestingly, this subpopulation was negatively enriched for inflammation signaling gene sets, such TNF-α signaling, immune system signaling, and interleukin signaling (Figure 2.18A). The negative enrichment of these inflammatory gene sets suggested low cytokine signaling, which was supported with the low expression of various cytokines in this subpopulation (i.e. IL18, CXCL3, CCL2, CCL20, TNFAIP8L1, padj < 0.05, Figure 2.18B). In addition to being characterized as proliferative and low in cytokine signaling, subpopulation 0 was also negatively enriched in cell adhesion and cell motility gene sets (Figure 2.18A). Evaluation of these collective gene sets revealed expression of epithelial markers such as EPCAM and ACTB in approximately 90% of subpopulation 0 cells (padj < 0.05). Interestingly, markers that correspond to EMT were expressed, though at low levels, in subpopulation 0. These EMT associated genes included ADAM17 (~42% of subpopulation 0), ITGB11 (73%), FN1 (57%), S100P (94%), S100A9 (100%), and TNFRS12A (80%) (padj < 0.05). The mixed expression of epithelial markers and markers that facilitate the interaction between the extracellular matrix suggested SKBR3 subpopulation 0 exhibited both epithelial features and features associated with cytoskeletal and extracellular matrix remodeling. Aside from characterizing subpopulation 0 as a whole, we also characterized the subset of subpopulation 0 cells with k.d. of PTEN. The subset of subpopulation 0 with PTEN k.d. enriched for gene sets associated with cell cycling (padj < 0.05). However, the genes that were upregulated in subpopulation 0 PTEN k.d. cells were different from cell cycle genes that characterized the collective subpopulation 0. Instead, the cell cycle associated genes identified from subpopulation 0 PTEN k.d. cells encoded helicases, such as RMI2 and DEAD box DDX20, and stress responsive DNA replication proteins, such as TIPIN and DDIT4 (padj < 0.05). Importantly, TIPIN is known to increase DNA replication as a response to cellular stress[156], which suggested that PTEN k.d. in subpopulation 0 might engage additional mechanisms of DNA replication as a response to k.d. of PTEN. In addition, the subset of subpopulation 0 with PTEN k.d. also negatively enriched for inflammatory signaling, which was verified by the low expression of interleukins (IL18), chemokines (CXCL1), interferons (IFI27, IFIT1, and IFITM3), TNF-α interacting protein (TNFAIP3). In addition to expressing low cytokines, subpopulation 0 with PTEN k.d. also negatively enriched for cell adhesion gene sets, which mirrored the negative enrichment

of these gene sets in the collective subpopulation 0. Fibronectin (FN1) and BMP7 were detected in 15% of the subset of subpopulation 0 with k.d. of PTEN, which highlighted that PTEN k.d. resulted in a subset of SKBR3 subpopulation 0 cells exhibiting cell motility. Interestingly, canonical WNT ligand WNT7B was 1.1 fold higher in subpopulation 0 with PTEN k.d. compared to parental subpopulation 0, which revealed that PTEN k.d. altered the expression of distinct canonical WNT ligands that are critical to the EMT program. Additionally, WNT7B was identified at high expression levels in epithelial and epithelial-mesenchymal hybrid cells derived from human mammary epithelial cell line (HMLER) xenografted into mice.[157] Thus, the increased expression of WNT7B in subpopulation 0 PTEN k.d. cells suggested that PTEN k.d. might have upregulated canonical WNT signaling via increased expression of WNT7B. Another gene that was differentially expressed by subpopulation 0 PTEN k.d. cells was FSCN1 (fascin1). Fascin1 has been shown to regulate actin cytoskeletal dynamics, and its overexpression has been correlated with metastasis and cell motility.[158,159] FSCN1 was detected in parental subpopulation 0 and not in the subset of subpopulation 0 with PTEN k.d. cells (padj < 0.0001, Figure 2.18B). In summary, subpopulation 0 was largely characterized by proliferative phenotype, low cytokine signaling, slight but statistically significant deregulated cell adhesion. While PTEN k.d. in subpopulation 0 cells mirrored the phenotype of the parental subpopulation 0, consequences of PTEN k.d. in this subpopulation was revealed through the altered expression of FSCN1 and WNT7B.

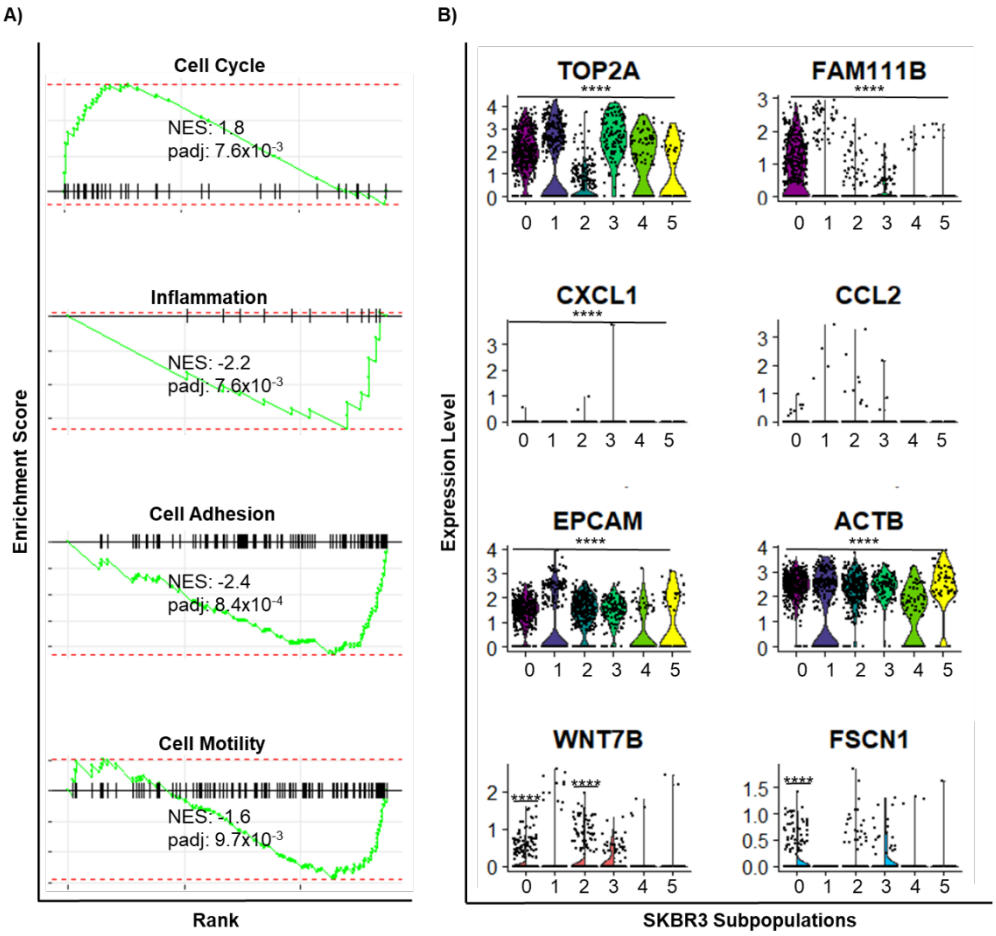

*Figure 2.18. SKBR3 Subpopulation 0 Cells were Characterized by High Cell Cycling, Low Cytokine Signaling, and Low Cell Adhesion. A) Statistically significant gene sets identified by GSEA for SKBR3 subpopulation 0. B) Genes identified from gene sets shown in A. Asterisks denote statistical significance of expression of gene in subpopulation 0 relative to expression in other subpopulations. Split violin plots (WNT7B and FSCN1) shown to compare the expression of gene in PTEN k.d. cells (pink) and parental SKBR3 (cyan), and asterisks above subpopulation denote statistical significance of gene expression by subset of cells with PTEN k.d. relative to parental subpopulation. *** padj < 0.001, **** padj < 0.0001.*

In contrast to subpopulation 0, SKBR3 subpopulation 2 exhibited low cell cycling genes, high cytokine signaling, TGF-β signaling, Myc targets, hypoxia, and regulators of cell adhesion. Scrutiny of these gene sets revealed comparably low expression of Myc target genes that are critical for cell proliferation and growth (ORC1, PCNA, CCB1, CDC6, BIRC5, TOP2A, MKI67; Figure 2.19). These genes were expressed in 1.4 – 2.3 fold lower by subpopulation 2 compared to other SKBR3 subpopulations (Figure 2.19B). Evaluation of cell adhesion gene sets revealed expression of both epithelial (EPCAM, KRT18, CLDN7, CLDN4, THBS, AQP3, ACTG1, ANK3, and HSPB1B1) and EMT promoting markers (MMP9, BMP7, TGFB, S100P, S100A11). The mixed expression of epithelial

and EMT promoting markers suggested subpopulation 2 exhibited an epithelial phenotype with cytoskeletal remodeling to possible acquire motile features that are critical for participation in EMT. Furthermore, SKBR3 subpopulation 2 also expressed inflammatory molecules (NFKBIA, JUNB, S100P, CD55, DES1, and FOS) in 60-90% of this subpopulation, which was expressed in 1.1 – 1.5 fold higher compared to other SKBR3 subpopulations (Figure 2.19B). Expression of these cytokines coincided with the mixed expression of cell adhesion and EMT associated markers because inflammatory signaling has been regarded to contribute to the activation of EMT. Furthermore, DGE analysis of the subset of subpopulation 2 with PTEN k.d. revealed 1.3 fold higher in gene expression of cleavage substrate of ADAM17, vasporsin (VASN), and WNT7B in subpopulation 2 with PTEN k.d. compared to parental subpopulation 2. This slight but significant increase in expression of these genes suggested that PTEN k.d. could increase the propensity of subpopulation 2 cells to propagate TGF-β and WNT signaling to ultimately facilitate EMT among the subset of subpopulation 2 cells with PTEN k.d.

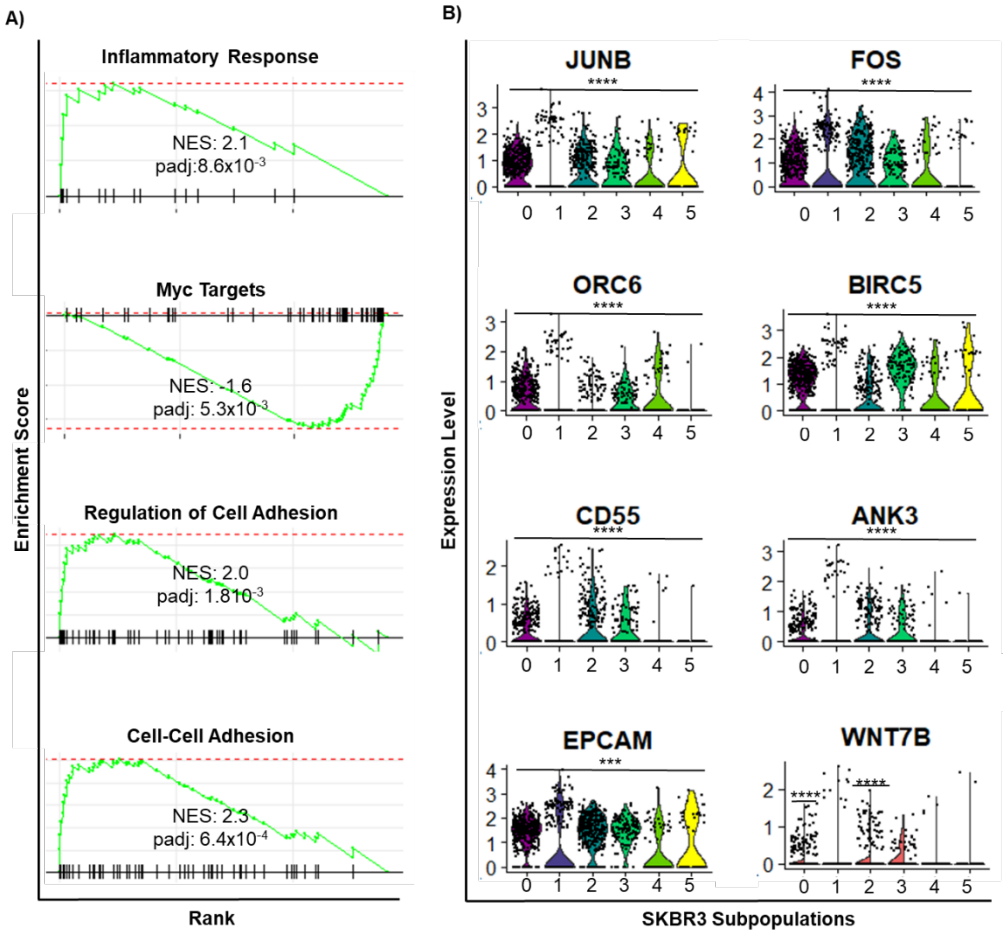

*Figure 2.19. SKBR3 Subpopulation 2 Cells were Characterized by Low Cell Cycling, High Cytokine Signaling, and High Cell Adhesion. A) Statistically significant gene sets identified by GSEA for SKBR3 subpopulation 2. B) Genes identified from gene sets shown in A. Asterisks denote statistical significance of expression of gene in subpopulation 2 relative to expression in other subpopulations. Split violin plot for WNT7B shown to compare the expression of gene in PTEN k.d. cells (pink) and parental SKBR3 (cyan), and asterisks above subpopulation denote statistical significance of gene expression by subset of cells with PTEN k.d. relative to parental subpopulation. *** padj<0.001, **** padj < 0.0001.*

Lastly, subpopulation 3 was characterized using DGE analysis and GSEA. These analyses revealed that subpopulation 3 was enriched in gene sets critical for cell cycle and motor activity (Figure 2.20). This subpopulation was negatively enriched in cytokine signaling and cell adhesion gene sets. Analysis of these gene sets revealed high expression of cyclins, survivin (BIRC5), and proteins involved in DNA transcription and replication, which indicated that subpopulation 3 cells also consisted of cycling cells. Of these cell cycling genes, CENPE, CENPF, ASPM, AURKA, TOP2A, PLK1, and TTG1 were among the most differentially expressed by subpopulation 3. These genes were expressed in 90% of subpopulation 3 and 2.5 – 3 fold higher in subpopulation 3 relative to other subpopulations (Figure 2.20B). SKBR3 subpopulation 3 was enriched in immune

system signaling, and thus, the following genes encoding inflammatory proteins were detected: S100P, JUNB, NFKBIA, IL6ST, TNFIP8L1, DYNLL1, CD58, ILF2, IFI35, S100A6, and CD55 (Figure 2.20B). However, the expression of the majority of these genes (S100P, JUNB, NFKBIA, IL6ST, TNFIP8L1, and CD58) were not differentially expressed by subpopulation 3, which suggested that cytokine signaling was not as strong characteristic of this subpopulation as compared to other SKBR3 subpopulations. In addition, subpopulation 3 was negatively enriched for cell adhesion gene sets and positively enriched for cell motility gene sets. Evaluation of these gene sets revealed expression of epithelial keratins (KRT18 and KRT19) and ANK3, which were expressed in 80% of subpopulation 3 cells. Furthermore, markers associated with EMT activation and cell motility such as matrix metalloproteinase MMP7 and MMP9 were detected in 30% and 60%, respectively. Interestingly, the subset of subpopulation 3 with PTEN k.d. did not exhibit large transcriptomic differences compared to parental subpopulation 3. For example, the proliferative property of subpopulation 3 was retained after PTEN k.d. There was no statistically significant differences in the expression of cell cycle and cell proliferative genes (TOP2A, CENPE, CENPF, AURKA), which suggested that PTEN k.d. did not significantly alter the cell cycling properties of this subpopulation. Similarly, PTEN k.d. did not appear to alter the cytokine signaling because no significant differences in cytokines were observed between parental subpopulation 3 and the subset of subpopulation 3 with k.d. of PTEN. Interestingly, the scrutiny of the effects of PTEN k.d. in this subpopulation revealed a slight, but significant difference in the expression of cell adhesion and cell motility genes. Specifically, it revealed a slightly higher expression of gap junction proteins, such as connexin (CNST), ANK1, aquaporin (AQP3) in the subset of subpopulation 3 with PTEN k.d. relative to parental subpopulation 3, but the percentage of subpopulation 3 PTEN k.d. cells that expressed these genes was approximately 10% (padj < 0.0001). In addition, PTEN k.d. cells expressed syndecan binding protein SDCBP2 and WNT inhibitor DKK1 at levels that were 1.2 fold lower than parental subpopulation 3 and in less than 5% of subpopulation PTEN k.d. cells compared to the 20% of parental subpopulations that expressed those genes. Furthermore, EMT promoting markers such as FN1 (shown in Figure 2.16), TNFAIP3, WNT9A, and FBLN5 were also expressed 1.2 fold higher in the subset of subpopulation 3 with PTEN k.d.

compared to parental subpopulation 3. These slight yet significant changes that the k.d. of PTEN introduced to the subpopulation 3 increased the intra-subpopulation heterogeneity by altering the expression of key genes critical for cell cycle and cell adhesion.

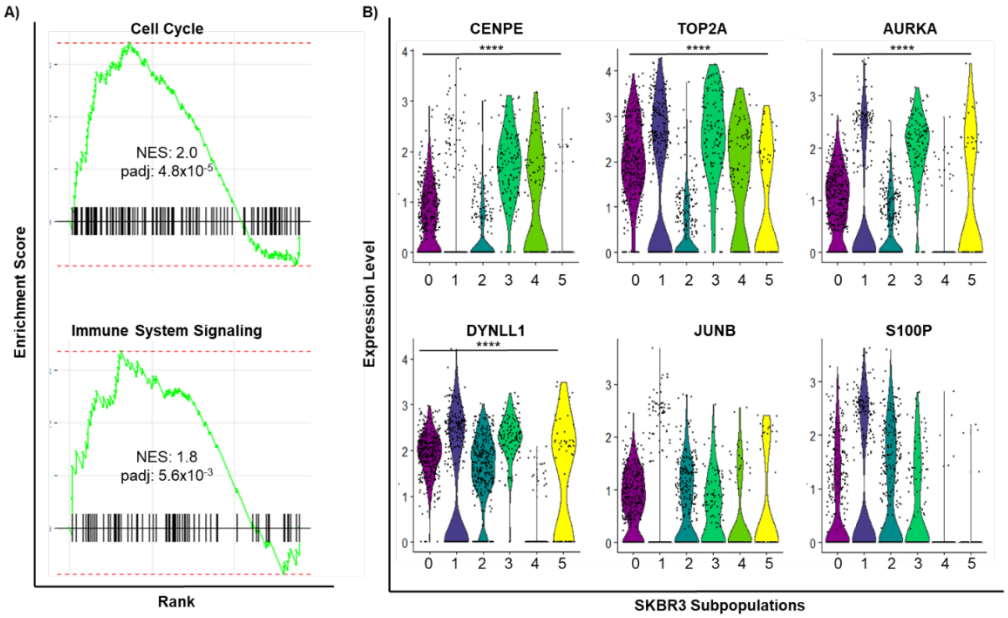

*Figure 2.20. SKBR3 Subpopulation 3 Cells were Characterized by High Cell Cycling and Immune System Signaling. A) Statistically significant gene sets identified by GSEA for SKBR3 subpopulation 3. B) Genes identified from gene sets shown in A. Asterisks denote statistical significance of expression of gene in subpopulation 3 relative to expression in other subpopulations. **** padj < 0.0001.*

2.3.13. PTEN k.d. in BT474 Increased Overall Quiescent Properties

To dissect the transcriptomic consequences of PTEN k.d. in BT474, global transcriptomic analyses were performed between parental BT474 and BT474 PTEN k.d. cells. These analyses revealed similar transcriptomic compositions for parental BT474 and BT474 with PTEN k.d. as evidenced by the overlap of single cells from both cells lines (Figure 2.21A). DGE analysis was performed between parental BT474 and BT474 PTEN k.d. cells and yielded 542 genes deregulated by BT474 PTEN k.d. cells (padj < 0.01). Of these genes, 353 were higher and 189 were lower in BT474 PTEN k.d. cells. The top 20 statistically significant genes were analyzed and revealed to encode cation-binding proteins (PCP4, C1orf101, and S100A8), proteins critical to epithelial cells (ODAM and CSTA), metabolic proteins (ATP13A5, CYP1A1, APOBE3A, and P2RY10), and proteins involved in chromosome maintenance (SMC1B and CNTLN). Interestingly, all of these 20 genes were expressed higher in PTEN k.d. cells, albeit by less than 2-fold

increase in expression (Figure 2.21B). The functions of the proteins encoded by the top 20 statistically significant genes suggested that PTEN k.d. in BT474 resulted in changes in cellular metabolism and an increase in epithelial character to adapt to the deficiency of PTEN.

To understand the functional consequences of the genes differentially expressed by BT474 PTEN k.d. cells, GSEA was performed and revealed 72 statistically significant gene sets enriched by BT474 PTEN k.d. cells (padj < 0.05). Of these, gene sets relevant to this study included genes enriched in cells with stem-like phenotypes ("Pece Stem Cell Up" from MSigDB) and genes involved in the innate immune signaling pathway (Figure 2.21C and D). From the gene set upregulated by cells with stem-like properties, tubulin TUBB2A and metallothioneins (MT1X and MT1F) were the only genes that BT474 PTEN k.d. cells expressed with a statistically significant difference (1.5 fold upregulation, padj < 0.01). Interestingly, TUBB2A has been reported to be significantly downregulated in breast cancer tissue compared to normal breast tissue and significantly upregulated in breast cancer tissue that responded to taxane compared to those that did not.[160] Additionally, 15 genes encoding ribosomal subunits were detected in BT474 PTEN k.d. cells, which constituted nearly 50% of this gene set. These ribosomal subunits were expressed in 90-100% of parental BT474 and BT474 with PTEN k.d., and thus, the expression of these genes were not significantly different between these two BT474 groups. Interestingly, aberrantly high expression of ribosomal proteins, such as RPL13, RPL15, and RPL35, have been reported to facilitate metastasis in breast cancer patients.[161] In addition to the enrichment of "stem cell up" gene set, BT474 PTEN k.d. cells were significantly enriched in genes involved in the innate immune signaling. High expressing genes detected from this gene set inflammatory-responsive cytoskeletal proteins and regulators of inflammatory response. Proteins regulating cytoskeletal activities and cell adhesion include GSN (padj < 0.0001) and RAB5C (padj < 0.01), which were both elevated by 1.4 fold in PTEN k.d. cells, despite being expressed in 28% and 36% of BT474 PTEN k.d. cells, respectively. Additional cytoskeletal proteins that were expressed by BT474 PTEN k.d. cells included cofilin COFL1 and ACTG1, although the expression of these proteins were not significant. Cytoskeletal proteins such as GSN and COFL1 are actin depolymerizing proteins that unravel the actin filaments of the

cytoskeleton to expose ACTG1 to facilitate cell motility during inflammatory responses, which highlighted the impact of inflammatory signaling to the modulation of actin dynamics in BT474 by k.d. of PTEN.[100,101,162,163] Regulators of innate immune signaling and inflammatory responses were elevated by 1.1 – 1.4 fold in BT474 PTEN k.d. cells, and these included DEGS1 (padj < 0.01), FOS (padj < 0.0001), POLR3K (padj < 0.0001), CALML5 (padj < 0.0001), GGH (padj < 0.0001), and DPP7 (padj < 0.0001). Among these regulators of the innate immune system were DEGS1, GGH, and DPP7, which encoded enzymes that modulate inflammatory responses via folate homeostasis and production of sphingolipid metabolites.[164–167] Despite their statistically significant upregulation in BT474 PTEN k.d. cells, these genes were detected in 17-38% of BT474 PTEN k.d. cells compared to their detection in 51-98% in parental BT474.

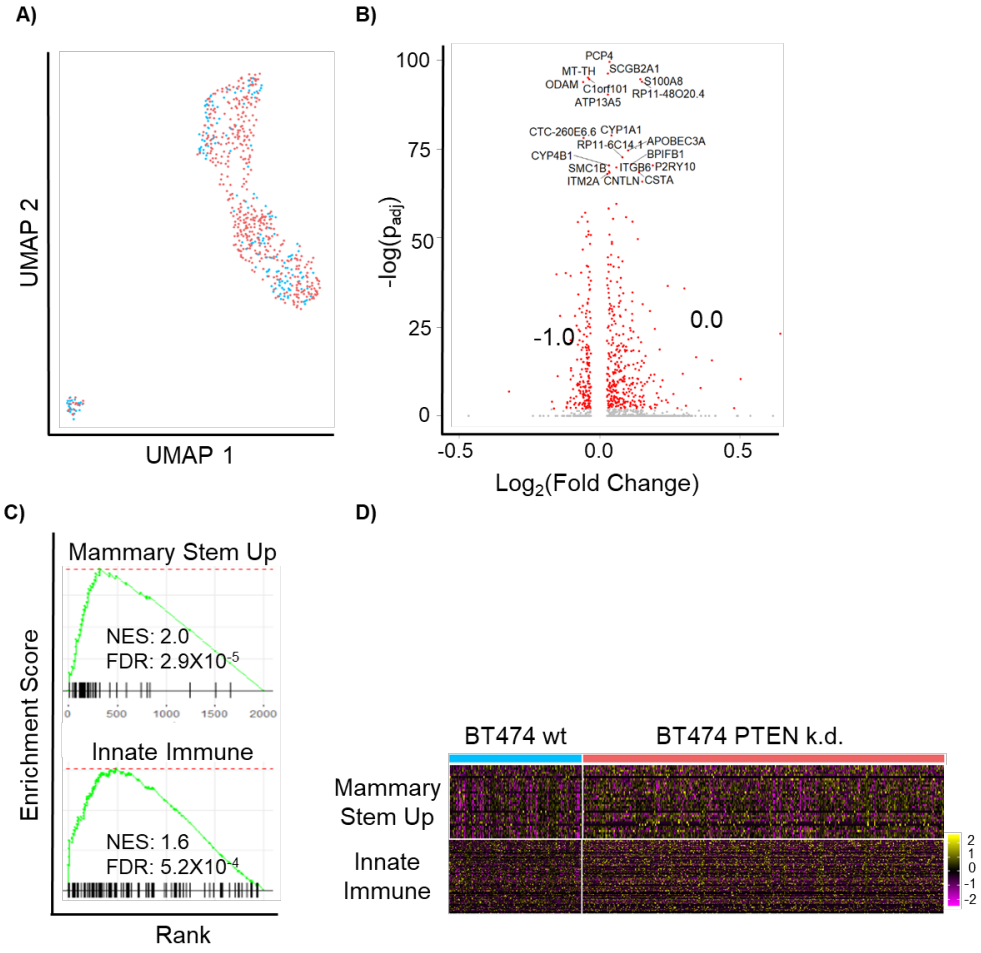

Figure 2.21. PTEN k.d. in BT474 Revealed Global Decrease of Cell Cycling Properties. A) UMAP plot depicting parental BT474 (pink) and BT474 with PTEN k.d. (blue). Dots depict single cells from each cell line. B) Volcano plot depicting genes with significant fold changes in expression in BT474 PTEN k.d. cells. Genes with statistically significant fold changes in expression are depicted in red, and genes with non-statistically significant expression are depicted in grey. Top 20 statistically significant genes are labeled. Statistical significance was denoted by padj < 0.01. C) Gene sets enriched by BT474 PTEN k.d. cells. Gene sets were identified by GSEA. Normalized gene expression (NES) and false discovery rate p-value (FDR) are shown. Statistical significance was denoted by FDR < 0.01.

2.3.14. PTEN k.d. in BT474 Induced Subpopulation Level Changes and Enriched Quiescent Subpopulation by 2 Fold

In addition to understanding the global transcriptomic changes resulting from PTEN k.d. in BT474, we analyzed how PTEN k.d. affected the steady state of BT474 subpopulations (Figure 2.22A). Parental BT474 comprised of 4 subpopulations, where 13.9% of parental BT474 was distributed into subpopulation 0, 33.0% in subpopulation 1, 15.6% in subpopulation 2, 23.1% in subpopulation 3, and 14.4% in subpopulation 4. Knockdown of PTEN changed the subpopulation composition, where 33.6% of BT474 PTEN k.d. cells were subpopulation 0 (2.4 fold increase), 24.5% were subpopulation 1

(1.3 fold decrease), 25.2% in subpopulation 2 (1.6 fold increase), 14.0% in subpopulation 3 (1.7 fold decrease), and 2.7% in subpopulation 4 (5.3 fold decrease). Interestingly, two subpopulations increased in BT474 following PTEN k.d., despite a 1.6 fold and 2.4 fold increase for subpopulations 0 and 2 (Figure 2.22B). The magnitude of the subpopulation changes induced by k.d. of PTEN in BT474 contrasted the magnitude of subpopulation level changes observed in HCC1954 and SKBR3. In the latter cell lines, the k.d. of PTEN resulted in an 84 and 120 fold increase in a subpopulation, respectively. Additionally, the observation that two subpopulations enriched in BT474 could reflect the context-dependent consequences of PTEN k.d. in these HER2+ breast cancer cell lines. Since subpopulation 0 and 2 both enriched in BT474, analyses were performed on those subpopulations.

Differential gene expression and GSEA was performed to characterize BT474 subpopulation 0. Differential gene expression of subpopulation 0 identified 499 statistically significant deregulated genes (padj < 0.01). Of these, 44 genes were higher, and 455 genes were lower in subpopulation 0 cells. The top 20 statistically significant genes of subpopulation 0 were associated with cell cycle, all of which were 2-4 fold lower in BT474 subpopulation 0 cells (padj < 0.01, Figure 2.22C). These genes encoded proteins involved in DNA replication (UBEC, CLSPN, H2AFZ, BRD8, TTF2, and TOP2A), chromatin organization (PRC1, HELLS, and SMC4), microtubule formation (MLF1IP, STMN1, TUBA1B, and ZWINT), and nucleic acid metabolism (TYMS, DUT, and RRM1). The low expression of these genes, which are heavily involved in different stages of the cell cycle, suggested BT474 subpopulation 0 exhibited a quiescent phenotype. Furthermore, this subpopulation's quiescent phenotype and the enrichment of this subpopulation due to PTEN k.d. suggested BT474 cells entered a dormant state to adapt to the cellular stress imposed by the deficiency of the PTEN tumor suppressor.

Since these differentially expressed genes provided a limited perspective to the consequences of PTEN k.d. in BT474 subpopulation 0, GSEA was performed to dissect the functional consequences of these differentially expressed genes. GSEA of BT474 subpopulation 0 revealed 849 gene sets (padj < 0.01). Among these gene sets, negative enrichment scores were observed for genes sets associated with cell cycle (padj < 0.01, Figures 2.22 and 2.23). The low expression of these gene sets was consistent with the

low expression of the top 20 statistically significant genes of BT474 subpopulation 0 (Figures 2.22 and 2.23). The negative enrichment of cell cycle associated gene sets in BT474 subpopulation supported the overall increase of a quiescent phenotype that resulted in the PTEN k.d. cells. Additionally, genes that increase with EMT (i.e. genes involved in EMT and mesenchymal genes) were identified to be negatively enriched by GSEA (Figure 2.23D). Furthermore, GSEA revealed this subpopulation was not significantly enriched in the Hallmark of EMT gene set (MsigDB systematic name: M5930, padj > 0.05), which suggested that BT474 subpopulation 0 exhibited an epithelial phenotype rather than EMT or mesenchymal characteristics. Lastly, GSEA revealed a significant attenuation in expression of genes involved in drug binding (padj < 0.01, Figure 2.22D). Together, GSEA revealed BT474 subpopulation exhibited quiescent features, epithelial phenotype, and displayed low expression of genes critical to drug binding.

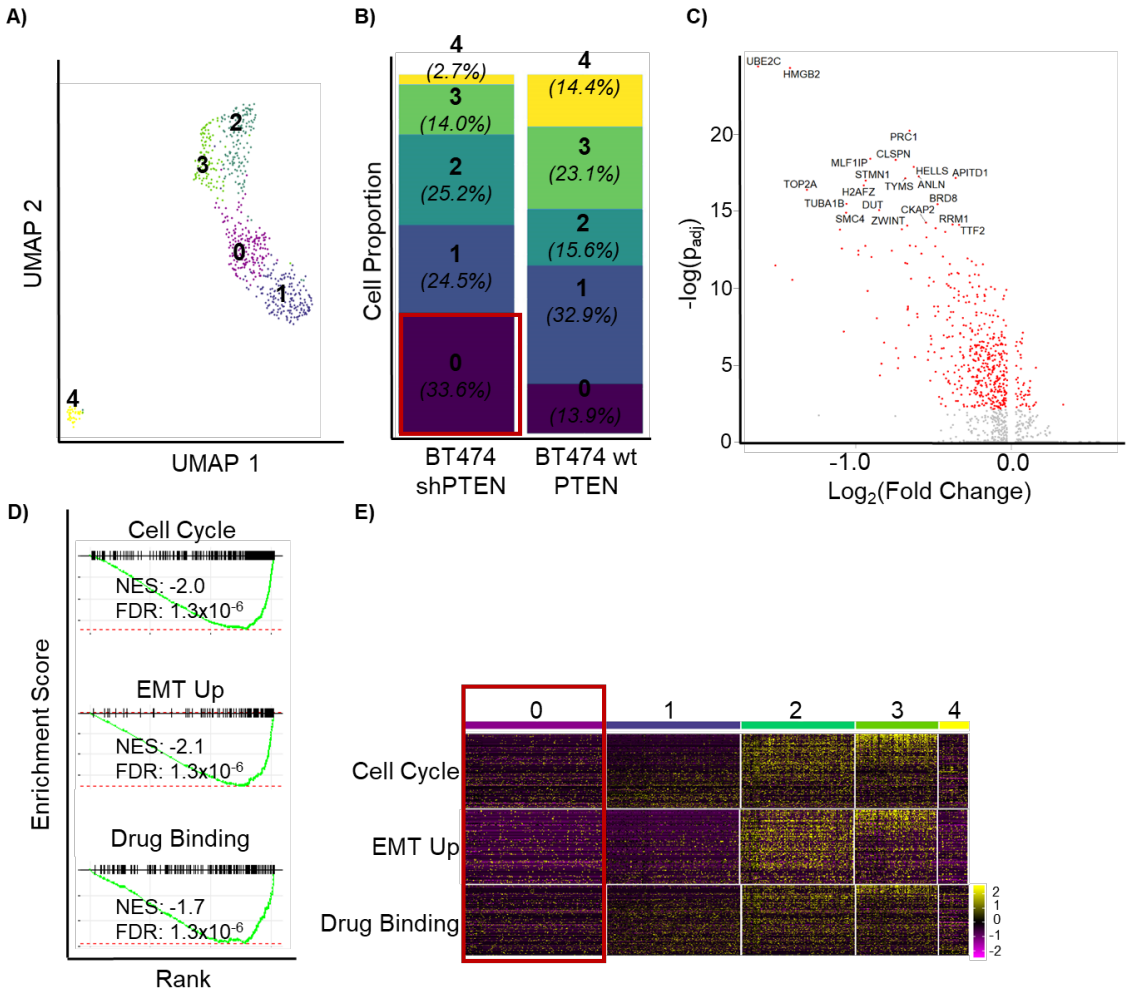

Figure 2.22. Single Cell Analysis of BT474 Subpopulations and Characterization of Subpopulation That Enriched After PTEN k.d. Subpopulation 0. A) UMAP plot depicting five BT474 subpopulations. Dots represent single cells. Subpopulations are organized by color. B) Cell Distribution using the same color scheme as shown in A. C) Volcano plot depicting genes differentially expressed by BT474 subpopulation 0. Grey dots represent genes with a log2FC that is not statistically significant. Red dots represent genes with a log2FC that is statistically significant. Statistical significance was denoted by p.adj < 0.01. C) Gene sets enriched by BT474 subpopulation 0. Normalized enrichment score (NES) and FDR (false discovery rate) adjusted p-values are displayed. FDR < 0.01 denotes statistical significance. D) Heatmap of gene sets from C. Colored scale represents normalized gene expression for each gene.

2.3.15. Decreased Cell Cycle Activity of BT474 Subpopulation 0 Coincided with Low Expression of Genes Critical for Drug Binding

In addition to exhibiting a negative enrichment score for the cell cycle gene set, GSEA of BT474 revealed negative enrichment scores for additional gene sets that are linked to cell growth and proliferation. These additional gene sets included proliferation, transcription regulated by p53, DNA replication, chromatin binding, G2/M checkpoint, DNA metabolism, DNA repair, downstream targets of E2F and DREAM complex (Figure 2.23A). Among the lowest expressed genes by BT474 subpopulation 0 were ones

encoding proteins involved in mitosis (CENPF, PRR11, ASPM, SMC4, TUB1A, and AURKA) and DNA replication (HMGB2 and TOP2A), which were expressed 2 – 3.2 fold lower in BT474 subpopulation 0 cells relative to other subpopulations (Figure 2.23B). Key proliferating genes (e.g. BIRC5, MKI67, and GMNN) were significantly lower in BT474 subpopulation 0, and the low expression of these genes is characteristic of quiescent cells (Figure 2.23B).[168–170] Interesting, epigenetic readers (EZH2 and PHF19) and non-histone binders of heterochromatin (HP1BP3 and CBX5) were also detected among the lowest expressed genes of subpopulation 0. These epigenetic modulators were detected in 13 – 37% and 37 – 48% of BT474 subpopulation 0, respectively (Figure 2.23B). Downregulation of PRC2 repressive complex subunits, such as EZH2 and PHF19, has been shown to result in an increase of quiescence in cells.[135,136] Further analysis of the genes lowly expressed by subpopulation 0 suggested that the quiescent property of BT474 subpopulation 0 could not only result from a decrease of cell cycle, but also from a decrease of regulatory proteins and transportation of cellular cargo between organelles.

Analysis of the genes identified from the cell cycle gene sets revealed an overlap of 53 genes between the cell cycle gene sets and the drug binding gene set for BT474 subpopulation 0. These 53 genes constituted 16% of the collective cell cycle gene sets and 75% of the drug binding gene set, which highlighted the integral contribution of genes involved in the cell cycle to mechanisms of drug binding. Evaluation of the shared genes between cell cycle gene sets and drug binding gene set revealed significantly low expression of ubiquitin (UBE2C and UBE2I), proteins involved in cell division (TOP2A, SMC4, RFC4, SPAG5, ZWINT, and FEN1), and proteins that regulate the cell cycle G2/M transition (AURKA, CENPE, and CDK1). Interestingly, a subset of these genes, UBE2C, AURKA, SPAG5, ZWINT, and FEN1, along with HMGB2, TYMS, and RFC4, have been shown to be downregulated in HER2+ breast cancer cells after treatment with trastuzumab, pertuzumab, and in combination.[22,171] This data highlighted how PTEN k.d. in BT474 mirrored a stress response induced by HER2-directed therapy. In addition, the genes unique to the drug binding gene set encoded specific members of ubiquitins (UBE2J2 and UBE2G1), participants of the mevalonate pathway (HMGCS1 and ACSF2), proteins involved in drug metabolism (ABCC3 and CYP4B1), metabolic proteins (GOT1, NME4, SUCLG2), proteins involved in DNA replication (EIF4A1 and ATAP1A1), histidyl-

TRNA synthetase (HARS2), calcium-dependent kinase (CAMK2G), and nuclear phosphoserine protein (KIAA0232). These genes were detected in 5-30% of BT474 subpopulation, while 25-70% of cells of remaining BT474 subpopulations expressed these genes (Figure 2.23B). All of these genes were unique to the drug binding, except HARS2, ATP13A5, CAK2G, and KIAA0232, and were lower in subpopulation 0 by 1-fold, and HARS2, ATP13A5, CAK2G, and KIAA0232 were expressed 1-fold higher in BT474 subpopulation 0. Furthermore, this subpopulation exhibited a slightly lower, yet significant expression of proteins involved in drug resistance and drug metabolism, such as multidrug resistance protein ABCC3 and cytochrome P450 proteins CYP1A1 and CYP4B1. Additionally, only a few BT474 expressed these proteins as approximately 20% of BT474 subpopulation 0 expressed these proteins whereas approximately 45% of the cells in the remaining BT474 subpopulations.

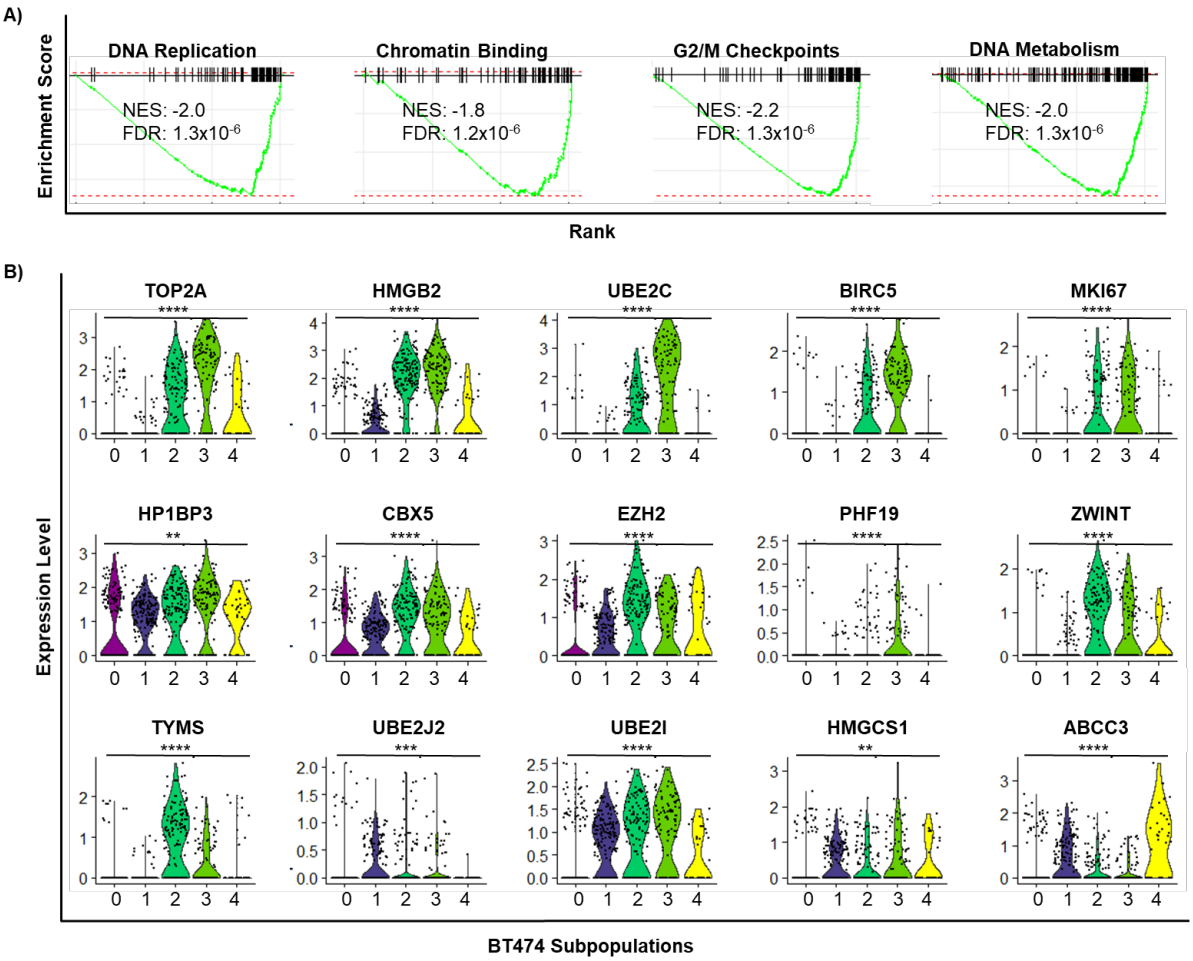

*Figure 2.23. Top Downregulated Genes Associated with Cell Cycle and Epigenetic Modulators in BT474 Subpopulation 0. A) Cell cycle associated gene sets identified for BT474 Subpopulation 0. B) Violin plots depicting genes involved in cell cycle and epigenetic modulators of gene expression. Dots denote single cells. ** $p < 0.01$, *** $p < 0.001$, **** $p < 0.0001$.*

2.3.16. BT474 Subpopulation 0 Exhibited Epithelial Early EMT Phenotype, and PTEN k.d. Did Not Introduce Intra-Subpopulation Heterogeneity

In addition to the quiescent properties, GSEA of BT474 subpopulation 0 suggested this subpopulation harbored an epithelial phenotype. Scrutiny of the genes contributing to this phenotype revealed not only of an epithelial phenotype, but an epithelial early EMT phenotype, which was consistent with the subpopulations that enriched in HCC1954 and SKBR3. This subpopulation expressed transmembrane proteins that regulate cell adhesion in epithelial cells, such as EPCAM, CLDN4, and desmosomes DSP (Figure 2.24). Additionally, BT474 subpopulation 0 expressed low levels of other cell adhesion proteins such as tight junction protein (TJP1), syndecans (SDC1), and low levels of transcription factor that suppresses EMT (GRHL2). Epithelial cytoskeletal proteins such

as keratins were detected in BT474 subpopulation 0, and the expression of these keratins in subpopulation 0 was not statistically significant from other subpopulations (Figure 2.24). Thus, the mixed expression of epithelial keratins and low expression of cell adhesion proteins suggested subpopulation 0 cells exhibited epithelial phenotype with a weakening of cell-cell adhesion. Furthermore, additional known markers of epithelial phenotype, such as E-cadherin (CDH1), keratin KRT5 and KRT14, occludin ZO1, and MUC1 were not detected in BT474 subpopulation 0. Despite the hints of an epithelial early EMT phenotype, BT474 subpopulation 0 cells did not express classical EMT markers such as EMT transcription factors (ZEB1/2, SNAIL, SLUG, or TWIST1/2), mesenchymal-specific cytoskeletal protein (VIM, FN1, or CDH2), which suggested that a full EMT program has not been activated in subpopulation 0. While classical EMT markers were not detected in BT474 subpopulation 0 cells, these cells expressed proteins that promote cytoskeletal remodeling, weaken cell-cell adhesion, and facilitate the interactions with the extracellular matrix, which included IGFBP2 and MGP. These proteins were expressed in approximately 20% of BT474 subpopulation 0 cells, which highlighted the heterogeneity in the expression of markers that govern the epithelial or the onset of an EMT program. Taken together, the mixed expression of epithelial markers, the mixed expression of cell-cell adhesion proteins, the lack of expression of classical EMT and mesenchymal markers, and the expression of proteins that promote matrix remodeling collectively suggested that BT474 subpopulation 0 exhibit an epithelial phenotype with weakened cell adhesion, and thus, an epithelial early EMT phenotype. Interestingly, the expression of these markers (presented in Figure 2.24) were not statistically significant between cells of the parental subpopulation and subset of cells with PTEN k.d. within each subpopulation. Expression of additional markers associated with cell motility and EMT (CTNNB1, WNT, BMP, and BMP7) were evaluated between parental and cells with PTEN k.d., but showed no significant difference in the expression of these genes between the parental cells and cells with PTEN k.d. within each subpopulation. Unlike HCC1954 and SKBR3, intra-subpopulation heterogeneity based on the expression of these epithelial and EMT associated markers was not detected between parental and PTEN k.d. cells of BT474. Stated differently, PTEN k.d. in BT474 subpopulation 0 did not result in increased intra-subpopulation heterogeneity.

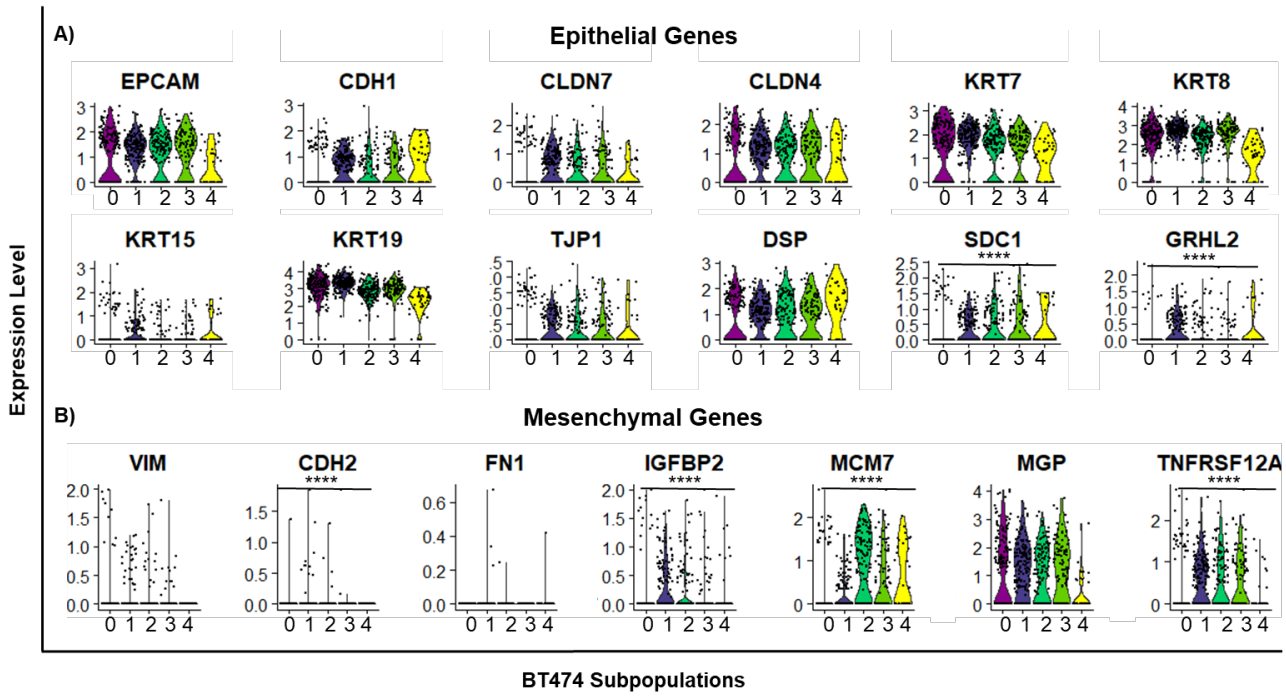

*Figure 2.24. Expression of Epithelial-Specific Markers and Markers That Promote EMT Suggested Epithelial Early EMT Phenotype for BT474 Subpopulation 0. Violin plots depicting expression of genes critical for A) epithelial phenotype and B) EMT and/or mesenchymal phenotype. Statistical significance was denoted by padj <0.05. **** p< 0.0001.*

Altogether, the data suggested that PTEN k.d. in BT474 resulted in a 2.4-fold enrichment of a quiescent, epithelial subpopulation exhibiting early EMT characteristics. However, the magnitude of PTEN k.d. in BT474 was not as large as previously observed in HCC1954 or SKBR3. Furthermore, a subset of the cell cycle genes that were significantly reduced in BT474 subpopulation 0 were identified to be critical for drug binding as well, suggesting that quiescence might be a means for these cells to evade cellular stress imposed by the k.d. of PTEN. This phenotype was supported by the lack of expression of genes involved in the cell cycle, mixed expression of epithelial cell adhesion markers, the lack of mesenchymal-specific markers, and the detection of genes involved with the weakening of epithelial cell adhesion. It is important to note that these genes, albeit their statistically significant fold changes, were expressed in a small subset of cells (7-50%), which further exemplified the consequences of intratumoral heterogeneity even within a subpopulation.

2.3.17. PTEN k.d. in BT474 Enriched for Proliferative, Mesenchymal Subpopulation by 1.6 Fold

In addition to the enrichment of subpopulation 0, BT474 also exhibited an increase in subpopulation 2 after k.d. of PTEN. Subpopulation 2 constituted 15.6% of parental BT474, and after PTEN k.d., this subpopulation consisted of 25% of BT474, which corresponded to a 1.6 fold increase in this subpopulation (Figure 2.25A). To characterize this subpopulation and gain insight on how PTEN k.d. affected BT474 subpopulation 2, we performed DGE analysis to identify significantly dysregulated genes by BT474 subpopulation 2, which revealed 237 differentially expressed genes (padj < 0.01). Of these genes, 203 genes were higher in subpopulation 2, and 34 genes were lower by subpopulation 2 relative to the other BT474 subpopulations. The top 20 statistically significant genes all contributed to the cell cycle, all of which were expressed 2-4 fold higher in subpopulation relative to the other subpopulations. Among the top 20 statistically significant genes are genes associated with DNA replication (proliferating cell nuclear antigen, PCNA; POLD3, DNA polymerase delta catalytic subunit; CCNE2, cyclin-dependent kinase 2; and DNMT1, DNA methyltransferase 1-associated protein). Also among the top 20 statistically significant genes were genes encoding nucleic acid metabolism enzymes (RRM2, ribonucleoside-diphosphate reductase subunit M2; TYMS, thymidylate synthase; and TK1, thymidine kinase), regulators of microtubules (TUBA1B, tubulin alpha 1B and STMN1, stathmin), and regulators of chromatin organization (DEK and centromere protein MLF1IP). Based the analysis of the top 20 statistically significant genes, the 2-4 fold upregulation of genes associated with the cell cycle suggested BT474 subpopulation 2 consisted of highly proliferative cells (Figure 2.25).

GSEA was performed to evaluate the functional consequences of the genes differentially expressed by subpopulation 2 (padj < 0.01, Figure 2.25C). This analysis confirmed the high expression of genes involved in the cell cycle, which reflected proliferative phenotype suggested by the top 20 statistically significant genes expressed by subpopulation 2. Furthermore, BT474 subpopulation 2 exhibited a significant upregulation of genes involved in EMT and a significant downregulation of genes that when EMT is activated (i.e. epithelial genes), which suggested BT474 subpopulation 2 exhibited a mesenchymal phenotype. Interestingly, this subpopulation was not

significantly enriched for Hallmark of EMT gene set, implying this subpopulation might not exhibit full EMT program or a complete mesenchymal phenotype. Lastly, BT474 subpopulation 2 was significantly enriched for genes involved in drug binding. Interestingly, the gene sets enriched by BT474 subpopulation 2 starkly contrasted the gene sets enriched by BT474 subpopulation 0, implying PTEN k.d. in BT474 resulted in an enrichment of distinct subpopulations.

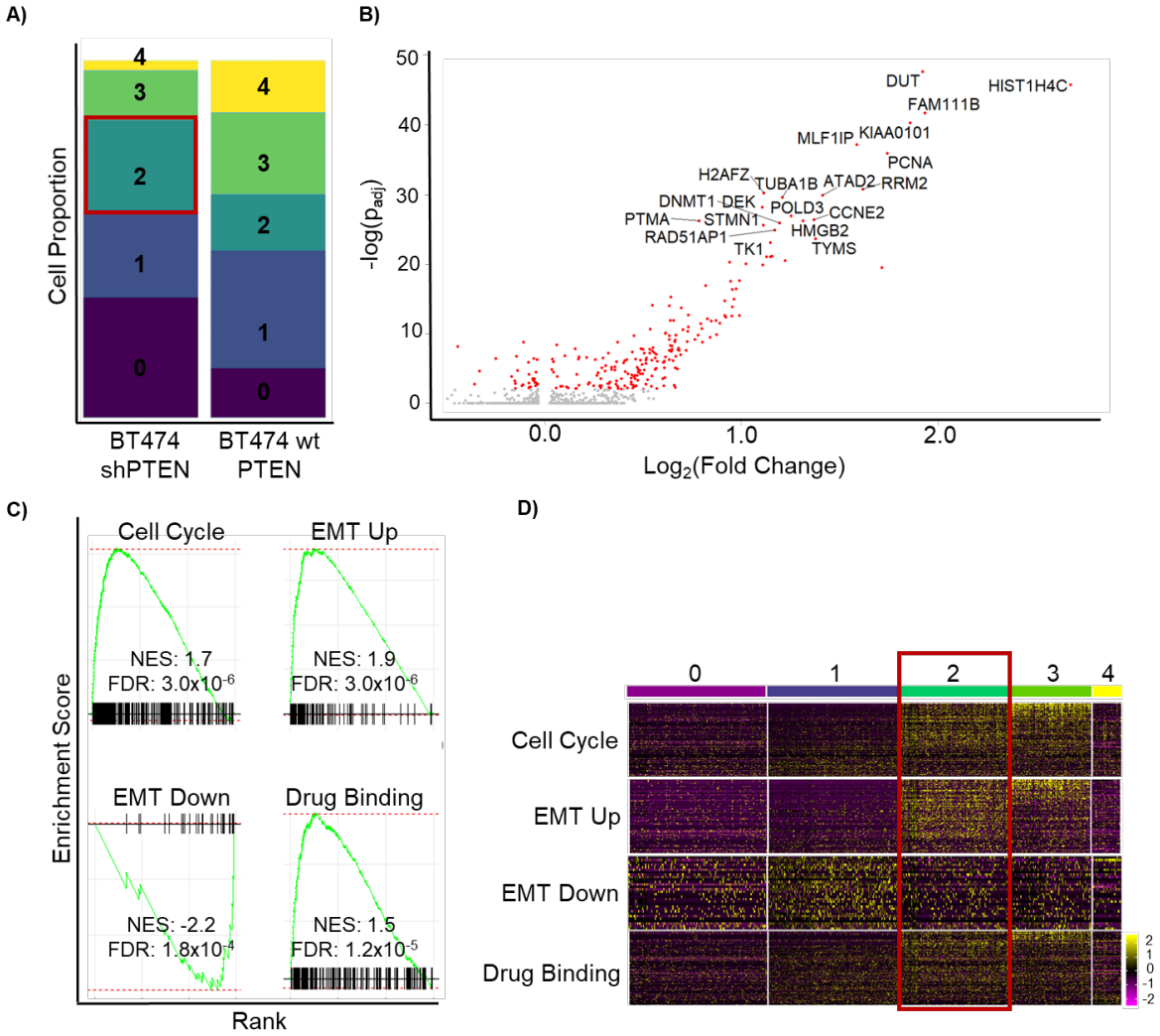

Figure 2.25. Characterization of BT474 Subpopulation 2 Revealed Proliferative Mesenchymal Properties. A) UMAP plot depicts relative distribution of parental BT474 and resultant distribution of BT474 following k.d. of PTEN. Subpopulation 2 is emphasized for clarity. B) Volcano plot depicting statistically significant genes expressed by BT474 subpopulation 2. C) Gene sets enriched by subpopulation 2. D) Heatmap of gene sets identified in C. Color scale represents normalized expression of gene.

After the general phenotype of BT474 subpopulation 2 was explored with GSEA, these gene sets evaluated to characterize subpopulation 2. This additional analysis

revealed significant upregulation in genes involved in proliferation, cell cycle checkpoints, DNA metabolism, chromatin binding, DNA replication, DNA repair, and targets of the DREAM complex (Figure 2.26A and B). Interestingly, this subpopulation showed a significant downregulation of ERK signaling. Analysis of these gene sets revealed extensive overlap between them, which was expected since they all play an integral part in the cell cycle. Between these gene sets, 174 genes were significantly expressed by subpopulation 2. The top highly expressed genes in BT474 subpopulation 2 encoded proteins involved in DNA replication (PCNA, ATAD2, HMGB2, and POLD3), DNA metabolism (DUT, RRM2, and TYMS), and regulation of G1/S phase transition (CCNE2 and CLSPN). These genes were expressed in 70-90% of BT474 subpopulation 2, while 25-60% of cells from remaining BT474 subpopulations expressed these genes (padj < 0.01, Figure 2.26C). These genes were expressed 2.3 – 3.8 fold higher in subpopulation 2 compared to cells of the remaining subpopulations (padj < 0.01). Among the top 10 highest expressed genes by subpopulation 2, FAM111B (family with sequence similarity 111 B) was the highest expressed gene and was expressed 3.8 fold higher in BT474 subpopulation 2 compared to the cells from the remaining subpopulations ($p < 0.01$, Figure 2.26C). Interestingly, the protein interactions that this encoded protein makes and its function remains to be explored.[172,173] Thus, this gene represented a potentially novel biomarker relevant to HER2+ breast cancer with deficiency in PTEN. Additionally, ATAD2, TYMS, and HMGB2 were also identified from the drug binding gene set (Figure 2.26C). Scrutiny of this drug binding gene set revealed that all the statistically significant genes were involved in the cell cycle, and thus, were already identified by the collective cell cycle gene sets. The intersection of the drug binding and cell cycle gene sets highlighted the interconnections between the effects of drug binding and its consequences to the cell cycle. Furthermore, since subpopulation 2 exhibited proliferative properties, as exhibited by the high expression of genes involved in the cell cycle, this subpopulation might represent one that can be targeted by anti-HER2 therapies, such as trastuzumab, pertuzumab, T-DM1, and the newly approved trastuzumab deruxtecan. The latter two HER2-directed therapies are antibody drug conjugates of trastuzumab and topoisomerase I inhibitor and tubulin inhibitor, respectively, and both target actively proliferating HER2-overexpressing cells. Taken together, this data highlighted the

proliferative phenotype of BT474 subpopulation 2, which starkly contrasted with the quiescent subpopulation 0.

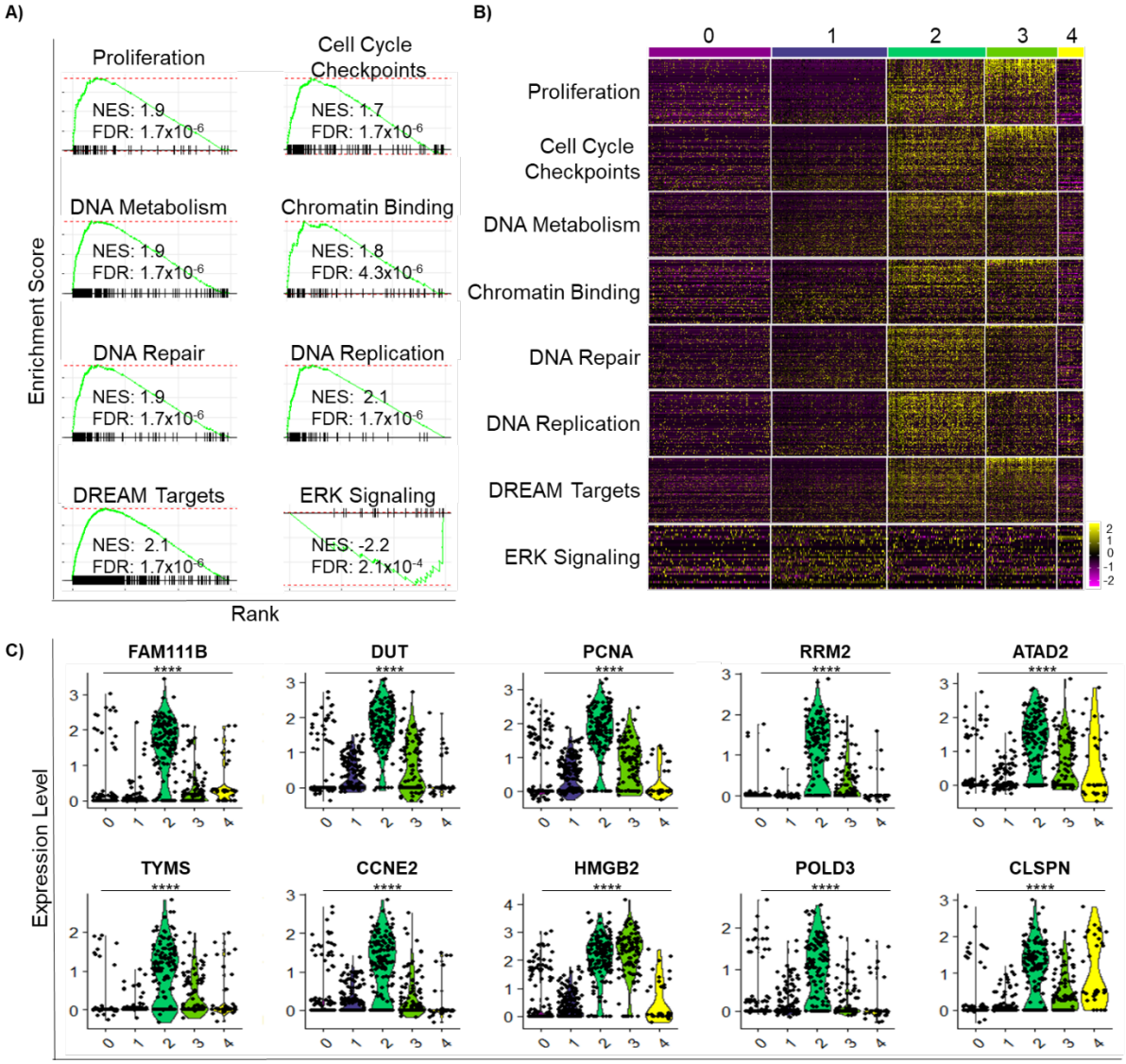

*Figure 2.26. Analysis of Proliferative Properties of Subpopulation 2. A) Gene sets identified by GSEA that supports the proliferative phenotype of BT474 subpopulation 2. B) Heatmap of gene sets identified in A. C) Differentially expressed genes identified by gene sets in A. **** padj< 0.0001.*

GSEA also suggested BT474 subpopulation 2 harbored a mesenchymal proliferative phenotype as evidenced by the upregulation of genes that increases during EMT (i.e. mesenchymal genes) and a downregulation of genes that decrease with EMT (i.e. epithelial genes). Interesting, GSEA of this subpopulation also showed a significant downregulation of genes critical for cell adhesion and cell motility, suggesting that subpopulation 2 might not be fully mesenchymal. Additionally, GSEA showed slight

enrichment in “Hallmark of EMT”, but that enrichment was not statistically significant (padj > 0.05). Analysis of genes expressed by this subpopulation revealed expression of epithelial adhesion proteins, such as EPCAM, E-cadherin, claudins (CLDN7 and CLDN4), tight junction protein (TJP1), and desmoplackin (DSP) in BT474 subpopulation 2, but the fold change in expression was not statistically significant relative to other subpopulations (Figure 2.27A). Furthermore, BT474 subpopulation 2 expressed structural proteins found in cytoskeleton of epithelial cells such as keratins (KRT7, KRT8, KRT18, and KRT19, expressed in 80-99% of subpopulation 2 cells). Certain keratins, such as KRT8 and KRT 19, were 1.3 fold lower in expression in BT474 subpopulation 2 compared to the rest of the subpopulations (pad j< 0.01, Figure 2.27A). Interestingly, subpopulation 2 did not express significantly high levels of transcription factor, GRHL2, which is known to suppress EMT in breast cancer cells by inhibiting ZEB1.[122,174–177] Aside from the expression of epithelial markers, a portion of BT474 subpopulation 2 cells exhibited proteins that are increased with EMT, such as β-catenin (encoded by CTNNB1, expressed in 36% of BT474 subpopulation 2); β-catenin is known to activate EMT transcription factor ZEB1 by binding to its promoter.[123,178] A subset of this subpopulation expressed genes needed to degrade the extracellular matrix and facilitate cell invasion, such as MGP (expressed in 70% of BT474 subpopulation 2), BMP7 (expressed in 63% of BT474 subpopulation 2), and MMP16 (expressed in 16% of BT474 subpopulation 2). Consistent with the expression of extracellular matrix remodeling genes and β-catenin, the expression of MKI67, a proliferation marker associated with EMT and invasion, was 1.6 fold higher in BT474 subpopulation 2 compared with the rest of the subpopulations (Figure 2.27B). MKI67 was expressed in 54% of BT474 subpopulation 2 cells. Interestingly, only 12% of BT474 subpopulation 2 expressed mesenchymal-specific marker vimentin (Figure 2.27B). Despite the expression of proteins that facilitate EMT, subpopulation 2 did not fully exhibit mesenchymal properties, which was supported by the lack of expression in classical EMT transcription factors (TWIST, SNAIL, SLUG, or ZEB1/2) or mesenchymal-specific marker (FN1, LOX, MMP9, MMP19, or CDH2). Rather, subpopulation 2 expressed a combination of epithelial markers and proteins involved in EMT suggested an epithelial, early EMT state. Relative to BT474 subpopulation 0, subpopulation 2 might represent an early EMT state that is later than the state BT474

subpopulation manifested based on the comparison of markers expressed by these two subpopulations.

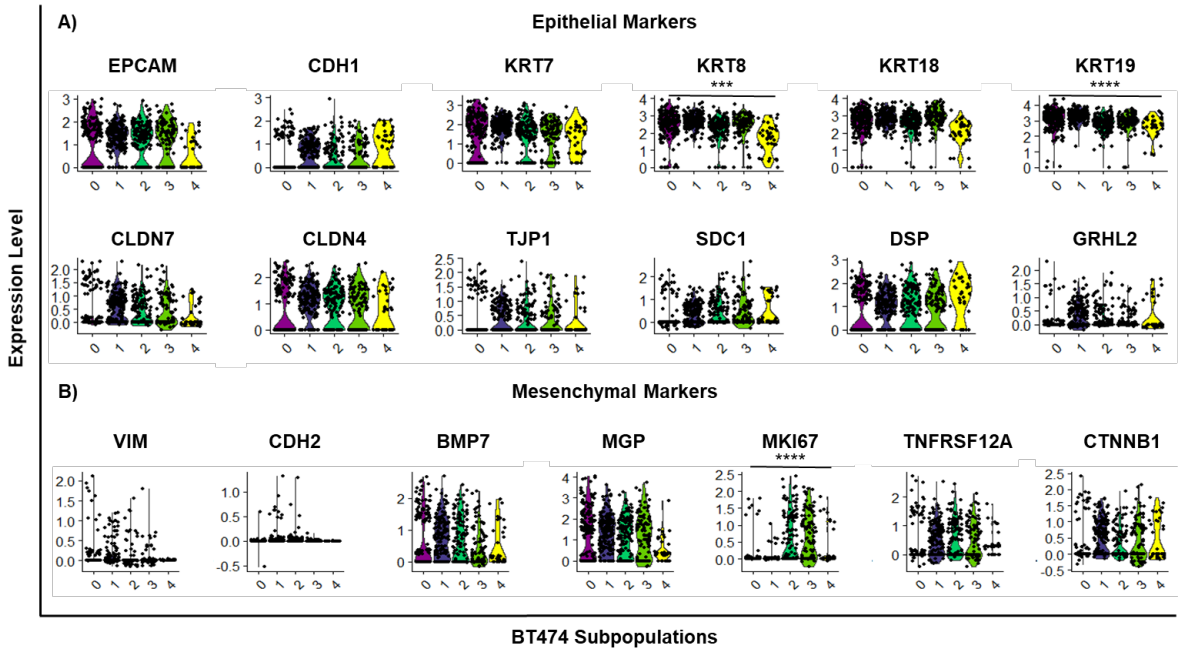

*Figure 2.27. Epithelial Early EMT (but Later than BT474 Subpopulation 0) for BT474 Subpopulation 2. Violin plots depicting A) epithelial markers and B) markers that promote EMT or mesenchymal markers. **** denotes pad j< 0.0001.*

2.4. Concluding Remarks

In this chapter, we presented the characterization of PTEN k.d. in 3 HER2+ breast cancer cell line pairs (HCC1954, SKBR3, and BT474) using the single cell transcriptomics approach, Drop-seq. This approach allowed us to dissect the single cell transcriptomes of subpopulations constituting these parental and corresponding shPTEN cell lines. Analyses using this approach provided insight about the functional consequences of PTEN deficiency in HER2+ breast cancer *in vitro*. Single cell transcriptomic profiling of these cell line pairs yielded information about the intra- and intertumoral consequences of PTEN deficiency in HER2+ breast cancer *in vitro*. We studied the consequences of intratumoral heterogeneity on PTEN deficiency by evaluating the effects of PTEN k.d. on subpopulations of a given cell line. We also studied the intertumoral heterogeneity of PTEN deficiency by comparing the phenotypic effects of PTEN deficiency between these HER2+ breast cancer cell lines. The elucidation of the intratumoral consequences of PTEN k.d. showed that PTEN k.d. in HER2+ breast cancer cell lines resulted in an enrichment in a subpopulation characterized by quiescent properties and an epithelial,

early EMT phenotype. This subpopulation increased by 84 fold, 120 fold, and 2.4 fold after k.d. of PTEN in these cell lines in HCC1954, SKBR3, and BT474, respectively. In addition, k.d. of PTEN introduced intra-subpopulation heterogeneity by altering the expression of cell cycle, cytokines, cell adhesion, and EMT genes in cells with shPTEN compared to parental cells of a given subpopulation in HCC1954 and SKBR3 but not in BT474. Taken together, it appeared that PTEN deficiency in these cell lines resulted an increase in aggressive cancer phenotype due to the enrichment of a quiescent, epithelial, early EMT subpopulation and the introduction of intra-subpopulation heterogeneity.

By evaluating the resultant consequences of PTEN deficiency between these cell lines, it appeared that the consequences of PTEN deficiency was similar in HCC1954 and SKBR3 based on the magnitude of subpopulation level changes and the introduction of intra-subpopulation heterogeneity. By these metrics, it appeared that BT474 might have represented a unique case for studying PTEN deficiency in HER2+ breast cancer *in vitro* because PTEN k.d. did not produce a substantial change in the subpopulation dynamics nor did it introduce substantial intra-subpopulation heterogeneity. Comparative analyses of the consequences of PTEN deficiency between these HER2+ breast cancer cell lines suggested an extent of context dependent effects of PTEN deficiency, which could reflect the context dependent effects of PTEN loss observed in the clinic. Altogether, our findings suggested that PTEN deficiency enhances an aggressive cancer phenotype through the enrichment of a quiescent, epithelial, early EMT subpopulation and introduction of intra-subpopulation heterogeneity.

2.5. References

(1) U.S. Breast Cancer Statistics | Breastcancer.org https://www.breastcancer.org/symptoms/understand_bc/statistics (accessed Jun 1, 2020).

(2) Dai, X.; Li, T.; Bai, Z.; Yang, Y.; Liu, X.; Zhan, J.; Shi, B. *Am. J. Cancer Res.* **2015**, *5* (10), 2929–2943.

(3) Turashvili, G.; Brogi, E. *Front. Med.* **2017**, *4* (DEC).

(4) Wang, J.; Xu, B. *Signal Transduct. Target. Ther.* **2019**, *4* (1).

(5) *Am. Cancer Soc.* **2020**, 1–43.

(6) National Cancer Institute Surveillance, Epidemiology, and E. R. P. (SEER). *Natl. Cancer Inst.* **2019**.

(7) Zhang, L.; Li, J.; Xiao, Y.; Cui, H.; Du, G.; Wang, Y.; Li, Z.; Wu, T.; Li, X.; Tian, J. *Sci. Rep.* **2015**, *5*, 1–14.

(8) Godoy-Ortiz, A.; Sanchez-Muñoz, A.; Parrado, M. R. C.; Álvarez, M.; Ribelles, N.; Dominguez, A. R.; Alba, E. *Front. Oncol.* **2019**, *9* (OCT), 1124.

(9) Loibl, S.; Gianni, L. *Lancet* **2017**, *389* (10087), 2415–2429.

(10) Muller, K. E.; Marotti, J. D.; Tafe, L. J. *Am. J. Clin. Pathol.* **2019**, *152* (1), 7–16.

(11) Vandenberghe, M. E.; Scott, M. L. J.; Scorer, P. W.; Söderberg, M.; Balcerzak, D.; Barker, C. *Sci. Rep.* **2017**, *7* (1), 1–11.

(12) Zhang, X.; Bleiweiss, I.; Jaffer, S.; Nayak, A. *Clin. Breast Cancer* **2017**, *17* (6), 486–492.

(13) Wolff, A. C.; Elizabeth Hale Hammond, M.; Allison, K. H.; Harvey, B. E.; Mangu, P. B.; Bartlett, J. M. S.; Bilous, M.; Ellis, I. O.; Fitzgibbons, P.; Hanna, W.; Jenkins, R. B.; Press, M. F.; Spears, P. A.; Vance, G. H.; Viale, G.; McShane, L. M.; Dowsett, M. *J. Clin. Oncol.* **2018**, *36* (20), 2105–2122.

(14) Mastro, L. Del; Lambertini, M.; Bighin, C.; Levaggi, A.; D'Alonzo, A.; Giraudi, S.; Pronzato, P. *Expert Rev. Anticancer Ther.* **2012**, *12* (11), 1391–1405.

(15) Pernas, S.; Tolaney, S. M. *Ther. Adv. Med. Oncol.* **2019**, *11*, 1–16.

(16) Oh, D. Y.; Bang, Y. J. *Nat. Rev. Clin. Oncol.* **2020**, *17* (1), 33–48.

(17) Swain, S. M.; Kim, S. B.; Cortés, J.; Ro, J.; Semiglazov, V.; Campone, M.; Ciruelos, E.; Ferrero, J. M.; Schneeweiss, A.; Knott, A.; Clark, E.; Ross, G.; Benyunes, M. C.; Baselga, J. *Lancet Oncol.* **2013**, *14* (6), 461–471.

(18) Modi, S.; Saura, C.; Yamashita, T.; Park, Y. H.; Kim, S.-B.; Tamura, K.; Andre, F.; Iwata, H.; Ito, Y.; Tsurutani, J.; Sohn, J.; Denduluri, N.; Perrin, C.; Aogi, K.; Tokunaga, E.; Im, S.-A.; Lee, K. S.; Hurvitz, S. A.; Cortes, J.; Lee, C.; Chen, S.; Zhang, L.; Shahidi, J.; Yver, A.; Krop, I. *N. Engl. J. Med.* **2020**, *382* (7), 610–621.

(19) Murthy, R. K.; Loi, S.; Okines, A.; Paplomata, E.; Hamilton, E.; Hurvitz, S. A.; Lin, N. U.; Borges, V.; Abramson, V.; Anders, C.; Bedard, P. L.; Oliveira, M.; Jakobsen, E.; Bachelot, T.; Shachar, S. S.; Muller, V.; Braga, S.; Duhoux, F. P.; Greil, R.; Cameron, D.; Carey, L. A.; Curigliano, G.; Gelmon, K.; Hortobagyi, G.; Krop, I.; Loibl, S.; Pegram, M.; Slamon, D.; Palanca-Wessels, M. C.; Walker, L.; Feng, W.; Winer, E. P. *N. Engl. J. Med.* **2020**, *382* (7), 597–609.

(20) Kim, C.; Lee, C. K.; Chon, H. J.; Kim, J. H.; Park, H. S.; Heo, S. J.; Kim, H. J.; Kim, T. S.; Kwon, W. S.; Chung, H. C.; Rha, S. Y. *Oncotarget* **2017**, *8* (69), 113494–113501.

(21) Bang, Y. J.; Van Cutsem, E.; Feyereislova, A.; Chung, H. C.; Shen, L.; Sawaki, A.; Lordick, F.; Ohtsu, A.; Omuro, Y.; Satoh, T.; Aprile, G.; Kulikov, E.; Hill, J.; Lehle, M.; Rüschoff, J.; Kang, Y. K. *Lancet* **2010**, *376* (9742), 687–697.

(22) Sims, A. H.; Zweemer, A. J. M.; Nagumo, Y.; Faratian, D.; Muir, M.; Dodds, M.; Um, I.; Kay, C.; Hasmann, M.; Harrison, D. J.; Langdon, S. P. *Br. J. Cancer* **2012**, *106* (11), 1779–1789.

(23) Pohlmann, P. R.; Mayer, I. A.; Mernaugh, R. *Clin. Cancer Res.* **2009**, *15* (24), 7479–7491.

(24) Luque-Cabal, M.; García-Teijido, P.; Fernández-Pérez, Y.; Sánchez-Lorenzo, L.; Palacio-Vázquez, I. *Clin. Med. Insights Oncol.* **2016**, *10*, 21–30.

(25) Nagata, Y.; Lan, K. H.; Zhou, X.; Tan, M.; Esteva, F. J.; Sahin, A. A.; Klos, K. S.; Li, P.; Monia, B. P.; Nguyen, N. T.; Hortobagyi, G. N.; Hung, M. C.; Yu, D. *Cancer Cell* **2004**, *6* (2), 117–127.

(26) Nahta, R. *Int. Sch. Res. Netw.* **2012**, *2012* (428062), 1–16.

(27) Luque-Cabal, M.; García-Teijido, P.; Fernández-Pérez, Y.; Sánchez-Lorenzo, L.; Palacio-Vázquez, I. *Clin. Med. Insights Oncol.* **2016**, *10* (Suppl 1), 21–30.

(28) Pernas, S.; Tolaney, S. M. HER2-Positive Breast Cancer: New Therapeutic Frontiers and Overcoming Resistance.

(29) Chen, S.; Liang, Y.; Feng, Z.; Wang, M. *BMC Cancer* **2019**, *19* (1), 973.

(30) Verma, S.; Miles, D.; Gianni, L.; Krop, I. E.; Welslau, M.; Baselga, J.; Pegram, M.; Oh, D.-Y.; Diéras, V.; Guardino, E.; Fang, L.; Lu, M. W.; Olsen, S.; Blackwell, K. *N. Engl. J. Med.* **2012**, *367* (19), 1783–1791.

(31) Perez, E. A.; Cortés, J.; Gonzalez-angulo, A. M.; Bartlett, J. M. S. *Cancer Treat. Rev.* **2014**, *40* (2), 276–284.

(32) Murthy, P.; Kidwell, K. M.; Schott, A. F.; Merajver, S. D.; Griggs, J. J.; Smerage, J. D.; Van Poznak, C. H.; Wicha, M. S.; Hayes, D. F.; Henry, N. L. *Breast Cancer Res. Treat.* **2016**, *155* (3), 589–595.

(33) Joensuu, H. *Cancer Treat. Rev.* **2017**, *52*, 1–11.

(34) Tolaney, S. M.; Guo, H.; Pernas, S.; Barry, W. T.; Dillon, D. A.; Ritterhouse, L.;

Schneider, B. P.; Shen, F.; Fuhrman, K.; Baltay, M.; Dang, C. T.; Yardley, D. A.; Moy, B.; Kelly Marcom, P.; Albain, K. S.; Rugo, H. S.; Ellis, M. J.; Shapira, I.; Wolff, A. C.; Carey, L. A.; Overmoyer, B.; Partridge, A. H.; Hudis, C. A.; Krop, I. E.; Burstein, H. J.; Winer, E. P. *J. Clin. Oncol.* **2019**, *37* (22), 1868–1875.

(35) Gianni, L.; Pienkowski, T.; Im, Y. H.; Tseng, L. M.; Liu, M. C.; Lluch, A.; Starosławska, E.; de la Haba-Rodriguez, J.; Im, S. A.; Pedrini, J. L.; Poirier, B.; Morandi, P.; Semiglazov, V.; Srimuninnimit, V.; Bianchi, G. V.; Magazzù, D.; McNally, V.; Douthwaite, H.; Ross, G.; Valagussa, P. *Lancet Oncol.* **2016**, *17* (6), 791–800.

(36) Luque-Cabal, M.; García-Teijido, P.; Fernández-Pérez, Y.; Sánchez-Lorenzo, L.; Palacio-Vázquez, I. *Clin. Med. Insights Oncol.* **2016**, *10* (Suppl 1), 21–30.

(37) Andersson, M.; Lidbrink, E.; Bjerre, K. *J Clin Oncol* **2011**, *29* (3), 264–271.

(38) Derakhshani, A.; Rezaei, Z.; Safarpour, H.; Sabri, M.; Mir, A.; Sanati, M. A.; Vahidian, F.; Gholamiyan Moghadam, A.; Aghadoukht, A.; Hajiasgharzadeh, K.; Baradaran, B. *J. Cell. Physiol.* **2020**, *235* (4), 3142–3156.

(39) Valabrega, G.; Montemurro, F.; Sarotto, I.; Petrelli, A.; Rubini, P.; Tacchetti, C.; Aglietta, M.; Comoglio, P. M.; Giordano, S. *Oncogene* **2005**, *24* (18), 3002–3010.

(40) Takuwa, H.; Tsuji, W.; Yotsumoto, F. *Int. J. Surg. Case Rep.* **2018**, *52*, 125–131.

(41) New Treatments Emerge for Metastatic HER2+ Breast Cancer - National Cancer Institute https://www.cancer.gov/news-events/cancer-currents-blog/2020/tucatinib-trastuzumab-deruxtecan-her2-positive-metastatic-breast-cancer (accessed Jun 1, 2020).

(42) Stern, H. M.; Gardner, H.; Burzykowski, T.; Elatre, W.; O'Brien, C.; Lackner, M. R.; Pestano, G. A.; Santiago, A.; Villalobos, I.; Eiermann, W.; Pienkowski, T.; Martin, M.; Robert, N.; Crown, J.; Nuciforo, P.; Bee, V.; Mackey, J.; Slamon, D. J.; Press, M. F. *Clin. Cancer Res.* **2015**, *21* (9), 2065–2074.

(43) Vu, T.; Claret, F. X. *Front. Oncol.* **2012**, *2* (June), 62.

(44) Bartsch, R.; Wenzel, C.; Steger, G. G. *Biologics* **2007**, *1* (1), 19–31.

(45) Gschwantler-Kaulich, D.; Tan, Y. Y.; Fuchs, E.-M.; Hudelist, G.; Köstler, W. J.; Reiner, A.; Leser, C.; Salama, M.; Attems, J.; Deutschmann, C.; Zielinski, C. C.; Singer, C. F. *PLoS One* **2017**, *12* (3), e0172911.

(46) Gajria, D.; Chandarlapaty, S. *Expert Rev. Anticancer Ther.* **2011**, *11* (2), 263–275.

(47) Mercogliano, M. F.; Bruni, S.; Elizalde, P. V.; Schillaci, R. *Front. Oncol.* **2020**, *10*, 584.

(48) Rimawi, M. F.; de Angelis, C.; Contreras, A.; Pareja, F.; Geyer, F. C.; Burke, K. A.; Herrera, S.; Wang, T.; Mayer, I. A.; Forero, A.; Nanda, R.; Goetz, M. P.; Chang, J. C.; Krop, I. E.; Wolff, A. C.; Pavlick, A. C.; Fuqua, S. A. W.; Gutierrez, C.; Hilsenbeck, S. G.; Li, M. M.; Weigelt, B.; Reis-Filho, J. S.; Osborne, C. K.;

Schiff, R. *Breast Cancer Res. Treat.* **2018**, *167* (3), 731–740.

(49) Lebok, P.; Kopperschmidt, V.; Kluth, M.; Hube-Magg, C.; Özden, C.; Taskin, B.; Hussein, K.; Mittenzwei, A.; Lebeau, A.; Witzel, I.; Wölber, L.; Mahner, S.; Jänicke, F.; Geist, S.; Paluchowski, P.; Wilke, C.; Heilenkötter, U.; Simon, R.; Sauter, G.; Terracciano, L.; Krech, R.; Von, A.; Müller, V.; Burandt, E. *BMC Cancer* **2015**, *15* (1–10).

(50) Li, S.; Shen, Y.; Wang, M.; Yang, J.; Lv, M.; Li, P.; Chen, Z.; Yang, J. *Oncotarget* **2017**, *8* (19), 32043–32054.

(51) Kechagioglou, P.; Papi, R. M.; Provatopoulou, X.; Kalogera, E.; Papadimitriou, E.; Grigoropoulos, P.; Nonni, A.; Zografos, G.; Kyriakidis, D. A.; Gounaris, A. *Anticancer Res.* **2014**, *34* (3), 1387–1400.

(52) Chalhoub, N.; Baker, S. J. *Annu. Rev. Pathol. Mech. Dis.* **2009**, *4* (1), 127–150.

(53) Paplomata, E.; O'regan, R. *Ther. Adv. Med. Oncol.* **2014**, *6* (4), 154–166.

(54) Keniry, M.; Parsons, R. *Oncogene* **2008**, *27* (41), 5477–5485.

(55) Ebbesen, S. H.; Scaltriti, M.; Bialucha, C. U.; Morse, N.; Kastenhuber, E. R.; Wen, H. Y.; Dow, L. E.; Baselga, J.; Lowe, S. W. *Proc. Natl. Acad. Sci. U. S. A.* **2016**, *113* (11), 3030–3035.

(56) Luongo, F.; Colonna, F.; Calapà, F.; Vitale, S.; Fiori, M. E.; De Maria, R. *Cancers (Basel).* **2019**, *11* (8), 1076.

(57) Carracedo, A.; Pandolfi, P. P. *Oncogene* **2008**, *27* (41), 5527–5541.

(58) Crowell, J. A.; Steele, V. E.; Fay, J. R. *Mol. Cancer Ther.* **2007**, *6* (8), 2139–2148.

(59) Endersby, R.; Baker, S. J. *Oncogene* **2008**, *27* (41), 5416–5430.

(60) Nuciforo, P. G.; Aura, C.; Holmes, E.; Prudkin, L.; Jimenez, J.; Martinez, P.; Ameels, H.; de la Perna, L.; Ellis, C.; Eidtmann, H.; Piccart-Gebhart, M. J.; Scaltriti, M.; Baselga, J. *Ann. Oncol.* **2015**, *26* (7), 1494–1500.

(61) Carbognin, L.; Miglietta, F.; Paris, I.; Dieci, M. V. *Cancers (Basel).* **2019**, *11* (9), 1–18.

(62) Jones, N.; Bonnet, F.; Sfar, S.; Lafitte, M.; Lafon, D.; Sierankowski, G.; Brouste, V.; Banneau, G.; Tunon de Lara, C.; Debled, M.; MacGrogan, G.; Longy, M.; Sevenet, N. *Int. J. Cancer* **2013**, *133* (2), 323–334.

(63) Zhang, H. Y.; Liang, F.; Jia, Z. L.; Song, S. T.; Jiang, Z. F. *Oncol. Lett.* **2013**, *6* (1), 161–168.

(64) Zhu, Y.; Wloch, A.; Wu, Q.; Peters, C.; Pagenstecher, A.; Bertalanffy, H.; Sure, U. *Stroke* **2009**, *40* (3), 820–826.

(65) Kang, Y. H.; Lee, H. S.; Kim, W. H. *Lab. Investig.* **2002**, *82* (3), 285–291.

(66) Wilks, S. T. *Breast* **2015**, *24* (5), 548–555.

(67) Sangai, T.; Akcakanat, A.; Chen, H.; Tarco, E.; Wu, Y.; Do, K. A.; Miller, T. W.; Arteaga, C. L.; Mills, G. B.; Gonzalez-Angulo, A. M.; Meric-Bernstam, F. *Clin. Cancer Res.* **2012**, *18* (20), 5816–5828.

(68) Hudis, C.; Swanton, C.; Janjigian, Y. Y.; Lee, R.; Sutherland, S.; Lehman, R.; Chandarlapaty, S.; Hamilton, N.; Gajria, D.; Knowles, J.; Shah, J.; Shannon, K.; Tetteh, E.; Sullivan, D. M.; Moreno, C.; Yan, L.; Han, H. S. *Breast Cancer Res.* **2013**, *15* (6), R110.

(69) Xing, Y.; Lin, N. U.; Maurer, M. A.; Chen, H.; Mahvash, A.; Sahin, A.; Akcakanat, A.; Li, Y.; Abramson, V.; Litton, J.; Chavez-MacGregor, M.; Valero, V.; Piha-Paul, S. A.; Hong, D.; Do, K.-A.; Tarco, E.; Riall, D.; Eterovic, A. K.; Wulf, G. M.; Cantley, L. C.; Mills, G. B.; Doyle, L. A.; Winer, E.; Hortobagyi, G. N.; Gonzalez-Angulo, A. M.; Meric-Bernstam, F. *Breast Cancer Res.* **2019**, *21* (1), 78.

(70) Hurvitz, S. A.; Andre, F.; Jiang, Z.; Shao, Z.; Mano, M. S.; Neciosup, S. P.; Tseng, L. M.; Zhang, Q.; Shen, K.; Liu, D.; Dreosti, L. M.; Burris, H. A.; Toi, M.; Buyse, M. E.; Cabaribere, D.; Lindsay, M. A.; Rao, S.; Pacaud, L. B.; Taran, T.; Slamon, D. *Lancet Oncol.* **2015**, *16* (7), 816–829.

(71) Van Swearingen, A. E. D.; Siegel, M. B.; Deal, A. M.; Sambade, M. J.; Hoyle, A.; Hayes, D. N.; Jo, H.; Little, P.; Dees, E. C.; Muss, H.; Jolly, T.; Zagar, T. M.; Patel, N.; Miller, C. R.; Parker, J. S.; Smith, J. K.; Fisher, J.; Shah, N.; Nabell, L.; Nanda, R.; Dillon, P.; Abramson, V.; Carey, L. A.; Anders, C. K. *Breast Cancer Res. Treat.* **2018**, *171* (3), 637–648.

(72) Ramón y Cajal, S.; Sesé, M.; Capdevila, C.; Aasen, T.; De Mattos-Arruda, L.; Diaz-Cano, S. J.; Hernández-Losa, J.; Castellví, J. *J. Mol. Med.* **2020**, *98* (2), 161–177.

(73) Lee, H. J.; Seo, A. N.; Kim, E. J.; Jang, M. H.; Suh, K. J.; Ryu, H. S.; Kim, Y. J.; Kim, J. H.; Im, S.-A.; Gong, G.; Jung, K. H.; Park, I. A.; Park, S. Y. *Am. J. Clin. Pathol.* **2014**, *142* (6), 755–766.

(74) Rye, I. H.; Trinh, A.; Sætersdal, A. B.; Nebdal, D.; Lingjærde, O. C.; Almendro, V.; Polyak, K.; Børresen-Dale, A. L.; Helland, Å.; Markowetz, F.; Russnes, H. G. *Mol. Oncol.* **2018**, *12* (11), 1838–1855.

(75) Ferrari, A.; Vincent-Salomon, A.; Pivot, X.; Sertier, A. S.; Thomas, E.; Tonon, L.; Boyault, S.; Mulugeta, E.; Treilleux, I.; MacGrogan, G.; Arnould, L.; Kielbassa, J.; Le Texier, V.; Blanché, H.; Deleuze, J. F.; Jacquemier, J.; Mathieu, M. C.; Penault-Llorca, F.; Bibeau, F.; Mariani, O.; Mannina, C.; Pierga, J. Y.; Trédan, O.; Bachelot, T.; Bonnefoi, H.; Romieu, G.; Fumoleau, P.; Delaloge, S.; Rios, M.; Ferrero, J. M.; Tarpin, C.; Bouteille, C.; Calvo, F.; Gut, I. G.; Gut, M.; Martin, S.; Nik-Zainal, S.; Stratton, M. R.; Pauporté, I.; Saintigny, P.; Birnbaum, D.; Viari, A.; Thomas, G. *Nat. Commun.* **2016**, *7* (1), 1–9.

(76) Brady, S. W.; McQuerry, J. A.; Qiao, Y.; Piccolo, S. R.; Shrestha, G.; Jenkins, D. F.; Layer, R. M.; Pedersen, B. S.; Miller, R. H.; Esch, A.; Selitsky, S. R.; Parker, J. S.; Anderson, L. A.; Dalley, B. K.; Factor, R. E.; Reddy, C. B.; Boltax, J. P.; Li, D.

Y.; Moos, P. J.; Gray, J. W.; Heiser, L. M.; Buys, S. S.; Cohen, A. L.; Johnson, W. E.; Quinlan, A. R.; Marth, G.; Werner, T. L.; Bild, A. H. *Nat. Commun.* **2017**, *8* (1), 1–15.

(77) Korkaya, H.; Paulson, A.; Iovino, F.; Wicha, M. S. *Oncogene* **2008**, *27* (47), 6120–6130.

(78) Macosko, E. Z.; Basu, A.; Satija, R.; Nemesh, J.; Shekhar, K.; Goldman, M.; Tirosh, I.; Bialas, A. R.; Kamitaki, N.; Martersteck, E. M.; Trombetta, J. J.; Weitz, D. A.; Sanes, J. R.; Shalek, A. K.; Regev, A.; McCarroll, S. A. *Cell* **2015**, *161* (5), 1202–1214.

(79) Andrews, T. S.; Hemberg, M. *Mol. Aspects Med.* **2018**, *59*, 114–122.

(80) Ziegenhain, C.; Vieth, B.; Parekh, S.; Reinius, B.; Guillaumet-Adkins, A.; Smets, M.; Leonhardt, H.; Heyn, H.; Hellmann, I.; Enard, W. *Mol. Cell* **2017**, *65* (4), 631-643.e4.

(81) Ocasio, J.; Babcock, B.; Malawsky, D.; Weir, S. J.; Loo, L.; Simon, J. M.; Zylka, M. J.; Hwang, D.; Dismuke, T.; Sokolsky, M.; Rosen, E. P.; Vibhakar, R.; Zhang, J.; Saulnier, O.; Vladoiu, M.; El-Hamamy, I.; Stein, L. D.; Taylor, M. D.; Smith, K. S.; Northcott, P. A.; Colaneri, A.; Wilhelmsen, K.; Gershon, T. R. *Nat. Commun.* **2019**, *10* (1), 1–17.

(82) Korkaya, H.; Kim, G. II; Davis, A.; Malik, F.; Henry, N. L.; Ithimakin, S.; Quraishi, A. A.; Tawakkol, N.; D'Angelo, R.; Paulson, A. K.; Chung, S.; Luther, T.; Paholak, H. J.; Liu, S.; Hassan, K. A.; Zen, Q.; Clouthier, S. G.; Wicha, M. S. *Mol. Cell* **2012**, *47* (4), 570–584.

(83) Korkaya, H.; Paulson, A.; Charafe-Jauffret, E.; Ginestier, C.; Brown, M.; Dutcher, J.; Clouthier, S. G.; Wicha, M. S. *PLoS Biol.* **2009**, *7* (6), e1000121.

(84) Nagata, Y.; Lan, K. H.; Zhou, X.; Tan, M.; Esteva, F. J.; Sahin, A. A.; Klos, K. S.; Li, P.; Monia, B. P.; Nguyen, N. T.; Hortobagyi, G. N.; Hung, M. C.; Yu, D. *Cancer Cell* **2004**, *6* (2), 117–127.

(85) Goldman, E. M. and M. **2015**, 1–20.

(86) Nemesh, J. Drop-seq Core Computational Protocol http://mccarrolllab.org/wp-content/uploads/2016/03/Drop-seqAlignmentCookbookv1.2Jan2016.pdf (accessed Sep 1, 2020).

(87) Zappia, L.; Oshlack, A. *Gigascience* **2018**, *7* (7), 1–9.

(88) Sergushichev, A. A. *bioRxiv* **2016**, 060012.

(89) Subramanian, A.; Tamayo, P.; Mootha, V. K.; Mukherjee, S.; Ebert, B. L.; Gillette, M. A.; Paulovich, A.; Pomeroy, S. L.; Golub, T. R.; Lander, E. S.; Mesirov, J. P. *Proc. Natl. Acad. Sci. U. S. A.* **2005**, *102* (43), 15545–15550.

(90) Smith, S. E.; Mellor, P.; Ward, A. K.; Kendall, S.; McDonald, M.; Vizeacoumar, F. S.; Vizeacoumar, F. J.; Napper, S.; Anderson, D. H. *Breast Cancer Res.* **2017**, *19*

(1), 65.

(91) Jernström, S.; Hongisto, V.; Leivonen, S. K.; Due, E. U.; Tadele, D. S.; Edgren, H.; Kallioniemi, O.; Perälä, M.; Mælandsmo, G. M.; Sahlberg, K. K. *Breast Cancer Targets Ther.* **2017**, *9*, 185–198.

(92) Becht, E.; McInnes, L.; Healy, J.; Dutertre, C. A.; Kwok, I. W. H.; Ng, L. G.; Ginhoux, F.; Newell, E. W. *Nat. Biotechnol.* **2019**, *37* (1), 38–47.

(93) Luecken, M. D.; Theis, F. J. *Mol. Syst. Biol.* **2019**, *15* (6).

(94) Li, W.; Freudenberg, J.; Suh, Y. J.; Yang, Y. *Comput. Biol. Chem.* **2014**, *48*, 77–83.

(95) McDermaid, A.; Monier, B.; Zhao, J.; Liu, B.; Ma, Q. *Briefings in Bioinformatics*. Oxford University Press November 1, 2019, pp 2044–2054.

(96) Capaldo, C. T.; Nusrat, A. *Biochim. Biophys. Acta - Biomembr.* **2009**, *1788* (4), 864–871.

(97) Shen, W.-H.; Zhou, J.-H.; Broussard, S. R.; Freund, G. G.; Dantzer, R.; Kelley, K. W. *Cancer Res.* **2002**, 4746–4756.

(98) Yang, J.; Min, K.-W.; Kim, D.-H.; Son, B. K.; Moon, K. M.; Wi, Y. C.; Bang, S. S.; Oh, Y. H.; Do, S.-I.; Chae, S. W.; Oh, S.; Kim, Y. H.; Kwon, M. J. *PLoS One* **2018**, *13* (8), e0202113.

(99) Cai, X.; Cao, C.; Li, J.; Chen, F.; Zhang, S.; Liu, B.; Zhang, W.; Zhang, X.; Ye, L. *Oncotarget* **2017**, *8* (35), 58338–58352.

(100) Mostowy, S.; Shenoy, A. R. *Nat. Rev. Immunol.* **2015**, *15* (9), 559–573.

(101) Wang, W.; Eddy, R.; Condeelis, J. *Nat. Rev. Cancer* **2007**, *7* (6), 429–440.

(102) Nakayama, K. I.; Nakayama, K. *Nat. Rev. Cancer* **2006**, *6* (5), 369–381.

(103) Bassermann, F.; Eichner, R.; Pagano, M. *Biochim. Biophys. Acta - Mol. Cell Res.* **2014**, *1843* (1), 150–162.

(104) Gan, B.; DePinho, R. A. *Cell Cycle* **2009**, *8* (7), 1003–1006.

(105) Laplante, M.; Sabatini, D. M. *J. Cell Sci.* **2009**, *122* (20), 3589–3594.

(106) Kallergi, G.; Tsintari, V.; Sfakianakis, S.; Bei, E.; Lagoudaki, E.; Koutsopoulos, A.; Zacharopoulou, N.; Alkahtani, S.; Alarifi, S.; Stournaras, C.; Zervakis, M.; Georgoulias, V. *Breast Cancer Res.* **2019**, *21* (1), 86.

(107) Hasan, Z.; Koizumi, S. I.; Sasaki, D.; Yamada, H.; Arakaki, N.; Fujihara, Y.; Okitsu, S.; Shirahata, H.; Ishikawa, H. *Nat. Commun.* **2017**, *8*.

(108) Gong, C.; Shen, J.; Fang, Z.; Qiao, L.; Feng, R.; Lin, X.; Li, S. *Biosci. Rep.* **2018**, *38* (4).

(109) Sundqvist, A.; Morikawa, M.; Ren, J.; Vasilaki, E.; Kawasaki, N.; Kobayashi, M.;

Koinuma, D.; Aburatani, H.; Miyazono, K.; Heldin, C. H.; Van Dam, H.; Dijke, P. Ten. *Nucleic Acids Res.* **2018**, *46* (3), 1180–1195.

(110) Mendoza-Rodríguez, M.; Arévalo Romero, H.; Fuentes-Pananá, E. M.; Ayala-Sumuano, J. T.; Meza, I. *Cancer Lett.* **2017**, *390*, 39–44.

(111) Liu, S.; Lee, J. S.; Jie, C.; Park, M. H.; Iwakura, Y.; Patel, Y.; Soni, M.; Reisman, D.; Chen, H. *Cancer Res.* **2018**, *78* (8), 2040–2051.

(112) Korkaya, H.; Kim, G. Il; Davis, A.; Malik, F.; Henry, N. L.; Ithimakin, S.; Quraishi, A. A.; Tawakkol, N.; D'Angelo, R.; Paulson, A. K.; Chung, S.; Luther, T.; Paholak, H. J.; Liu, S.; Hassan, K. A.; Zen, Q.; Clouthier, S. G.; Wicha, M. S. *Mol. Cell* **2012**, *47* (4), 570–584.

(113) Zhang, Z.; Xu, Q.; Song, C.; Mi, B.; Zhang, H.; Kang, H.; Liu, H.; Sun, Y.; Wang, J.; Lei, Z.; Guan, H.; Li, F. *Mol. Cancer Ther.* **2020**, *19* (2), 650–660.

(114) Fagerli, U. M.; Ullrich, K.; Stühmer, T.; Holien, T.; Köchert, K.; Holt, R. U.; Bruland, O.; Chatterjee, M.; Nogai, H.; Lenz, G.; Shaughnessy, J. D.; Mathas, S.; Sundan, A.; Bargou, R. C.; Dörken, B.; Børset, M.; Janz, M. *Oncogene* **2011**, *30* (28), 3198–3206.

(115) Sahoo, S.; Brickley, D. R.; Kocherginsky, M.; Conzen, S. D. *Eur. J. Cancer* **2005**, *41* (17), 2754–2759.

(116) Mistry, P.; Deacon, K.; Mistry, S.; Blank, J.; Patel, R. *J. Biol. Chem.* **2004**, *279* (2), 1482–1490.

(117) Reymond, N.; Im, J. H.; Garg, R.; Cox, S.; Soyer, M.; Riou, P.; Colomba, A.; Muschel, R. J.; Ridley, A. J. *Mol. Oncol.* **2015**, *9* (6), 1043–1055.

(118) Tomaskovic-Crook, E.; Thompson, E. W.; Thiery, J. P. *Breast Cancer Res.* **2009**, *11* (6), 213.

(119) Kalluri, R.; Weinberg, R. A. *J. Clin. Invest.* **2009**, *119* (6), 1420–1428.

(120) Pastushenko, I.; Blanpain, C. *Trends Cell Biol.* **2019**, *29* (3), 212–226.

(121) Chu, P. G.; Weiss, L. M. *Histopathology* **2002**, *40* (5), 403–439.

(122) Xiang, X.; Deng, Z.; Zhuang, X.; Ju, S.; Mu, J.; Jiang, H.; Zhang, L.; Yan, J.; Miller, D.; Zhang, H.-G. *PLoS One* **2012**, *7* (12), e50781.

(123) Schmalhofer, O.; Brabletz, S.; Brabletz, T. *Cancer Metastasis Rev.* **2009**, *28* (1–2), 151–166.

(124) Zhang, S.; Wang, Z.; Liu, W.; Lei, R.; Shan, J.; Li, L.; Wang, X. *Sci. Rep.* **2017**, *7*.

(125) Nasser, M. W.; Qamri, Z.; Deol, Y. S.; Ravi, J.; Powell, C. A.; Trikha, P.; Schwendener, R. A.; Bai, X. F.; Shilo, K.; Zou, X.; Leone, G.; Wolf, R.; Yuspa, S. H.; Ganju, R. K. *Cancer Res.* **2012**, *72* (3), 604–615.

(126) West, N. R.; Watson, P. H. *Oncogene* **2010**, *29* (14), 2083–2092.

(127) Paruchuri, V.; Prasad, A.; McHugh, K.; Bhat, H. K.; Polyak, K.; Ganju, R. K. *PLoS One* **2008**, *3* (3), 1741.

(128) Emberley, E. D.; Murphy, L. C.; Watson, P. H. *Breast Cancer Res.* **2004**, *6* (4), 153–159.

(129) Cancemi, P.; Buttacavoli, M.; Cara, G. Di; Albanese, N. N.; Bivona, S.; Pucci-Minafra, I.; Feo, S. *Oncotarget* **2018**, *9* (49), 29064–29081.

(130) Hua, X.; Zhang, H.; Jia, J.; Chen, S.; Sun, Y.; Zhu, X. *Biomed. Pharmacother.* **2020**, *127*, 110156.

(131) Yuzugullu, H.; Von, T.; Thorpe, L. M.; Walker, S. R.; Roberts, T. M.; Frank, D. A.; Zhao, J. J. *Cell Discov.* **2016**, *2* (1), 1–13.

(132) Sadasivam, S.; DeCaprio, J. A. *Nat. Rev. Cancer* **2013**, *13* (8), 585–595.

(133) Min, M.; Spencer, S. L. *PLOS Biol.* **2019**, *17* (3), e3000178.

(134) Bracken, A. P.; Ciro, M.; Cocito, A.; Helin, K. *Trends Biochem. Sci.* **2004**, *29* (8), 409–417.

(135) Ito, T.; Teo, Y. V.; Evans, S. A.; Neretti, N.; Sedivy Correspondence, J. M. *Cell Rep.* **2018**, *22*, 3480–3492.

(136) Vizán, P.; Gutiérrez, A.; Espejo, I.; García-Montolio, M.; Lange, M.; Carretero, A.; Lafzi, A.; de Andrés-Aguayo, L.; Blanco, E.; Thambyrajah, R.; Graf, T.; Heyn, H.; Bigas, A.; Di Croce, L. *Sci. Adv.* **2020**, *6* (32), eabb2745.

(137) Doyle, L. A.; Ross, D. D. *Oncogene* **2003**, *22* (47 REV. ISS. 6), 7340–7358.

(138) Balaji, S. A.; Udupa, N.; Chamallamudi, M. R.; Gupta, V.; Rangarajan, A. *PLoS One* **2016**, *11* (5).

(139) Lucanus, A. J.; Yip, G. W. *Nat. Publ. Gr.* **2018**.

(140) Mandelkow, E.; Mandelkow, E. M. *Trends Cell Biol.* **2002**, *12* (12), 585–591.

(141) Ivanov, A. I.; McCall, I. C.; Babbin, B.; Samarin, S. N.; Nusrat, A.; Parkos, C. A. *BMC Cell Biol.* **2006**, *7* (1), 12.

(142) Li, T.-F.; Zeng, H.-J.; Shan, Z.; Ye, R.-Y.; Cheang, T.-Y.; Zhang, Y.-J.; Lu, S.-H.; Zhang, Q.; Shao, N.; Lin, Y. .

(143) Hirokawa, N.; Noda, Y.; Tanaka, Y.; Niwa, S. *Nat. Rev. Mol. Cell Biol.* **2009**, *10* (10), 682–696.

(144) Li, B.; Dou, S. X.; Yuan, J. W.; Liu, Y. R.; Li, W.; Ye, F.; Wang, P. Y.; Li, H. *Proc. Natl. Acad. Sci. U. S. A.* **2018**, *115* (48), 12118–12123.

(145) Kwon, M. J.; Park, S.; Choi, J. Y.; Oh, E.; Kim, Y. J.; Park, Y. H.; Cho, E. Y.; Kwon, M. J.; Nam, S. J.; Im, Y. H.; Shin, Y. K.; Choi, Y. L. *Br. J. Cancer* **2012**, *106* (5), 923–930.

(146) Yang, X. H.; Richardson, A. L.; Torres-Arzayus, M. I.; Zhou, P.; Sharma, C.; Kazarov, A. R.; Andzelm, M. M.; Strominger, J. L.; Brown, M.; Hemler, M. E. *Cancer Res.* **2008**, *68* (9), 3204–3213.

(147) Kumar, S.; Park, S. H.; Cieply, B.; Schupp, J.; Killiam, E.; Zhang, F.; Rimm, D. L.; Frisch, S. M. *Mol. Cell. Biol.* **2011**, *31* (19), 4036–4051.

(148) Rasiah, P. K.; Maddala, R.; Bennett, V.; Rao, P. V. *Dev. Biol.* **2019**, *446* (1), 119–131.

(149) Kurozumi, S.; Joseph, C.; Raafat, S.; Sonbul, S.; Kariri, Y.; Alsaeed, S.; Pigera, M.; Alsaleem, M.; Nolan, C. C.; Johnston, S. J.; Aleskandarany, M. A.; Ogden, A.; Fujii, T.; Shirabe, K.; Martin, S. G.; Alshankyty, I.; Mongan, N. P.; Ellis, I. O.; Green, A. R.; Rakha, E. A. *Breast Cancer Res. Treat.* **2019**, *176* (1), 63–73.

(150) Gröger, C. J.; Grubinger, M.; Waldhör, T.; Vierlinger, K.; Mikulits, W. *PLoS One* **2012**, *7* (12), e51136.

(151) Mrouj, K.; Singh, P.; Sobecki, M.; Dubra, G.; Ghoul, E. Al; Aznar, A.; Prieto, S.; Vincent, C.; Pirot, N.; Bernex, F.; Bordignon, B.; Hassen-Khodja, C.; Pouzolles, M.; Zimmerman, V.; Dardalhon, V.; Villalba, M.; Krasinska, L.; Fisher, D. *bioRxiv* **2019**, 712380.

(152) Mani, S. A.; Guo, W.; Liao, M. J.; Eaton, E. N.; Ayyanan, A.; Zhou, A. Y.; Brooks, M.; Reinhard, F.; Zhang, C. C.; Shipitsin, M.; Campbell, L. L.; Polyak, K.; Brisken, C.; Yang, J.; Weinberg, R. A. *Cell* **2008**, *133* (4), 704–715.

(153) Foroni, C.; Broggini, M.; Generali, D.; Damia, G. *Cancer Treat. Rev.* **2012**, *38* (6), 689–697.

(154) Collier, M. P.; Benesch, J. L. P. *Cell Stress Chaperones* **2020**, *25* (4), 601–613.

(155) Gunning, P. W.; Hardeman, E. C.; Lappalainen, P.; Mulvihill, D. P. *J. Cell Sci.* **2015**, *128* (16), 2965–2974.

(156) Chou, D. M.; Elledge, S. J. *Proc. Natl. Acad. Sci. U. S. A.* **2006**, *103* (48), 18143–18147.

(157) Kröger, C.; Afeyan, A.; Mraz, J.; Eaton, E. N.; Reinhardt, F.; Khodor, Y. L.; Thiru, P.; Bierie, B.; Ye, X.; Burge, C. B.; Weinberg, R. A. *Proc. Natl. Acad. Sci. U. S. A.* **2019**, *116* (15), 7353–7362.

(158) Xiao, W.; Zheng, S.; Xie, X.; Li, X.; Zhang, L.; Yang, A.; Wang, J.; Tang, H.; Xie, X. *Mol. Ther. - Oncolytics* **2020**, *17*, 118–129.

(159) Wang, C. Q.; Tang, C. H.; Wang, Y.; Jin, L.; Wang, Q.; Li, X.; Hu, G. N.; Huang, B. F.; Zhao, Y. M.; Su, C. M. *Sci. Rep.* **2017**, *7* (1).

(160) Nami, B.; Wang, Z. *Cancers (Basel).* **2018**, *10* (8), 274.

(161) Ebright, R. Y.; Lee, S.; Wittner, B. S.; Niederhoffer, K. L.; Nicholson, B. T.; Bardia, A.; Truesdell, S.; Wiley, D. F.; Wesley, B.; Li, S.; Mai, A.; Aceto, N.; Vincent-Jordan, N.; Szabolcs, A.; Chirn, B.; Kreuzer, J.; Comaills, V.; Kalinich, M.; Haas,

W.; Ting, D. T.; Toner, M.; Vasudevan, S.; Haber, D. A.; Maheswaran, S.; Micalizzi, D. S. *Science (80-.).* **2020**, *367* (6485), 1468–1473.

(162) Prashar, A.; Schnettger, L.; Bernard, E. M.; Gutierrez, M. G. *Front. Cell. Infect. Microbiol.* **2017**, *7* (SEP), 435.

(163) Barbera, S.; Nardi, F.; Elia, I.; Realini, G.; Lugano, R.; Santucci, A.; Tosi, G. M.; Dimberg, A.; Galvagni, F.; Orlandini, M. *Cell Commun. Signal.* **2019**, *17* (1), 55.

(164) Kim, S. E.; Hinoue, T.; Kim, M. S.; Sohn, K. J.; Cho, R. C.; Cole, P. D.; Weisenberger, D. J.; Laird, P. W.; Kim, Y. I. *Genes Nutr.* **2015**, *10* (1), 1–17.

(165) Maggini, S.; Pierre, A.; Calder, P. C. *Nutrients* **2018**, *10* (10).

(166) MacEyka, M.; Spiegel, S. *Nature* **2014**, *510* (7503), 58–67.

(167) Waumans, Y.; Baerts, L.; Kehoe, K.; Lambeir, A. M.; De Meester, I. *Front. Immunol.* **2015**, *6* (JUL), 387.

(168) Kingsbury, S. R.; Loddo, M.; Fanshawe, T.; Obermann, E. C.; Prevost, A. T.; Stoeber, K.; Williams, G. H. *Exp. Cell Res.* **2005**, *309* (1), 56–67.

(169) Gookin, S.; Min, M.; Phadke, H.; Chung, M.; Moser, J.; Miller, I.; Carter, D.; Spencer, S. L. *PLOS Biol.* **2017**, *15* (9), e2003268.

(170) Kabraji, S.; Solé, X.; Huang, Y.; Bango, C.; Bowden, M.; Bardia, A.; Sgroi, D.; Loda, M.; Ramaswamy, S. *Breast Cancer Res.* **2017**, *19* (1), 88.

(171) Le, X. F.; Lammayot, A.; Gold, D.; Lu, Y.; Mao, W.; Chang, T.; Patel, A.; Mills, G. B.; Bast, R. C. *J. Biol. Chem.* **2005**, *280* (3), 2092–2104.

(172) Sun, H.; Liu, K.; Huang, J.; Sun, Q.; Shao, C.; Luo, J.; Xu, L.; Shen, Y.; Ren, B. *Onco. Targets. Ther.* **2019**, *Volume 12*, 2829–2842.

(173) FAM111B gene - Genetics Home Reference - NIH https://ghr.nlm.nih.gov/gene/FAM111B (accessed Aug 8, 2020).

(174) Chung, V. Y.; Tan, T. Z.; Ye, J.; Huang, R. L.; Lai, H. C.; Kappei, D.; Wollmann, H.; Guccione, E.; Huang, R. Y. J. *Commun. Biol.* **2019**, *2* (1), 1–15.

(175) Jolly, M. K.; Tripathi, S. C.; Jia, D.; Mooney, S. M.; Celiktas, M.; Hanash, S. M.; Mani, S. A.; Pienta, K. J.; Ben-Jacob, E.; Levine, H. *Oncotarget* **2016**, *7* (19), 27067–27084.

(176) Cieply, B.; Riley IV, P.; Pifer, P. M.; Widmeyer, J.; Addison, J. B.; Ivanov, A. V.; Denvir, J.; Frisch, S. M. *Cancer Res.* **2012**, *72* (9), 2440–2453.

(177) Mooney, S. M.; Talebian, V.; Jolly, M. K.; Jia, D.; Gromala, M.; Levine, H.; McConkey, B. J. *J. Cell. Biochem.* **2017**, *118* (9), 2559–2570.

(178) Sánchez-Tilló, E.; De Barrios, O.; Siles, L.; Cuatrecasas, M.; Castells, A.; Postigo, A. *Proc. Natl. Acad. Sci. U. S. A.* **2011**, *108* (48), 19204–19209.

(179) Lee, J.; Ouh, Y.; Ahn, K. H.; Hong, S. C.; Oh, M.; Kim, J.; Cho, G. J. *PLoS One*

2017, *12* (5), 1–8.

(180) Gajria, D.; Chandarlapaty, S. *Expert Rev. Anticancer Ther.* **2011**, *11* (2), 263–275.

(181) Asgari, A.; Sharifzadeh, S.; Ghaderi, A.; Hosseini, A.; Ramezani, A. *Mol. Biol. Rep.* **2019**, *46* (6), 6205–6213.

(182) Dang, C. V. *Cell* **2012**, *149* (1), 22–35.

(183) Stine, Z. E.; Walton, Z. E.; Altman, B. J.; Hsieh, A. L.; Dang, C. V. *Cancer Discov.* **2015**, *5* (10), 1024–1039.

(184) Chen, H.; Liu, H.; Qing, G. *Signal Transduct. Target. Ther.* **2018**, *3* (1), 1–7.

(185) Gabay, M.; Li, Y.; Felsher, D. W. *Cold Spring Harb. Perspect. Med.* **2014**, *4* (6), 1–14.

(186) Richart, L.; Carrillo-de Santa Pau, E.; Río-Machín, A.; de Andrés, M. P.; Cigudosa, J. C.; Lobo, V. J. S.-A.; Real, F. X. *Nat. Commun.* **2016**, *7*, 10153.

(187) Dang, C. V. **2013**, 1–15.

(188) Bouvard, C.; Lim, S. M.; Ludka, J.; Yazdani, N.; Woods, A. K.; Chatterjee, A. K.; Schultz, P. G.; Zhu, S. *Proc. Natl. Acad. Sci. U. S. A.* **2017**, *114* (13), 3497–3502.

(189) Tawani, A.; Mishra, S. K.; Kumar, A. *Sci. Rep.* **2017**, *7* (1), 1–13.

(190) Mathad, R. I.; Hatzakis, E.; Dai, J.; Yang, D. *Nucleic Acids Res.* **2011**, *39* (20), 9023–9033.

(191) Siddiqui-Jain, A.; Grand, C. L.; Bearss, D. J.; Hurley, L. H. *Proc. Natl. Acad. Sci. U. S. A.* **2002**, *99* (18), 11593–11598.

(192) Castell, A.; Yan, Q.; Karin, F.; Hydbring, P.; Zhang, F.; Verschut, V.; Franco, M.; Zakaria, S. M.; Bazzar, W.; Goodwin, J.; Zinzalla, G.; Larson, L.-G. *Sci. Rep.* **2018**, *8* (May), 1–17.

(193) Kiessling, A.; Sperl, B.; Hollis, A.; Eick, D.; Berg, T. *Chem. Biol.* **2006**, *13* (7), 745–751.

(194) Berg, T.; Cohen, S. B.; Desharnais, J.; Sonderegger, C.; Maslyar, D. J.; Goldberg, J.; Boger, D. L.; Vogt, P. K. *Proc. Natl. Acad. Sci. U. S. A.* **2002**, *99* (6), 3830–3835.

(195) Whitfield, J. R.; Beaulieu, M. E.; Soucek, L. *Front. Cell Dev. Biol.* **2017**, *5* (FEB), 10.

(196) Castell, A.; Larsson, L. *Cancer Discov.* **2015**, *5* (7), 701–704.

(197) Carabet, L. A.; Rennie, P. S.; Cherkasov, A. *Int. J. Mol. Sci.* **2019**, *20* (1).

(198) Dang, C. V.; Reddy, E. P.; Shokat, K. M.; Soucek, L. *Nat. Rev. Cancer* **2017**, *17* (8), 502–508.

(199) McKeown, M. R.; Bradner, J. E. *Cold Spring Harb. Perspect. Med.* **2014**, *4* (10).

(200) Thomas, L. R.; Wang, Q.; Grieb, B. C.; Phan, J.; Foshage, A. M.; Sun, Q.; Olejniczak, E. T.; Clark, T.; Dey, S.; Lorey, S.; Alicie, B.; Howard, G. C.; Cawthon, B.; Ess, K. C.; Eischen, C. M.; Zhao, Z.; Fesik, S. W.; Tansey, W. P. *Mol. Cell* **2015**, *58* (3), 440–452.

(201) Thomas, L. R.; Tansey, W. P. *Open Access J. Sci. Technol.* **2015**, *3*, 1–25.

(202) Karatas, H.; Townsend, E. C.; Bernard, D.; Dou, Y.; Wang, S. *J. Med. Chem.* **2010**, *53*, 5179–5185.

(203) Odho, Z.; Southall, S. M.; Wilson, J. R. *J. Biol. Chem.* **2010**, *285* (43), 32967–32976.

(204) Dias, J.; Nguyen, N. Van; Georgiev, P.; Gaub, A.; Brettschneider, J.; Cusack, S.; Kadlec, J.; Akhtar, A. *Genes Dev.* **2014**, *28*, 929–942.

(205) Scott, D. E.; Coyne, A. G.; Hudson, S. A.; Abell, C. *Biochemistry* **2012**, *51*, 4990–5003.

(206) Murray, C. W.; Verdonk, M. L.; Rees, D. C. *Trends Pharmacol. Sci.* **2012**, *33* (5), 224–232.

(207) Huynh, K.; Partch, C. L. *Curr. Protoc. protein Sci.* **2015**, *79*, 28.9.1-28.9.14.

(208) Niesen, F. H.; Berglund, H.; Vedadi, M. *Nat. Protoc.* **2007**, *2* (9), 2212–2221.

(209) Jhoti, H.; Williams, G.; Rees, D. C.; Murray, C. W. *Nat. Publ. Gr.* **2013**, No. July.

(210) Kirsch, P.; Hartman, A. M.; Hirsch, A. K. H.; Empting, M. *Molecules* **2019**, *24* (23).

(211) Aldrich, C.; Bertozzi, C.; Georg, G. I.; Kiessling, L.; Lindsley, C.; Liotta, D.; Merz, K. M.; Schepartz, A.; Wang, S. *J. Med. Chem.* **2017**, *60* (6), 2165–2168.

(212) Zhang, Ji-hu, Chung, Thomas D.Y., Oldenburg, K. R. *J. Biomol. Screen.* **1999**, *4* (2), 67–73.

(213) Jacob, R. T.; Larsen, M. J.; Larsen, S. D.; Kirchhoff, P. D.; Sherman, D. H.; Neubig, R. R. *J. Biomol. Screen.* **2012**, *17* (8), 1080–1087.

(214) Karatas, H.; Townsend, E. C.; Cao, F.; Chen, Y.; Bernard, D.; Liu, L.; Lei, M.; Dou, Y.; Wang, S. *J. Am. Chem. Soc.* **2013**, *135* (2), 669–682.

(215) Cao, F.; Townsend, E. C.; Karatas, H.; Xu, J.; Li, L.; Lee, S.; Liu, L.; Chen, Y.; Ouillette, P.; Zhu, J.; Hess, J. L.; Atadja, P.; Lei, M.; Qin, Z. S.; Malek, S.; Wang, S.; Dou, Y. *Mol. Cell* **2014**, *53* (2), 247–261.

(216) Lea, W. A.; Simeonov, A. *Expert Opin. Drug Discov.* **2011**, *6* (1), 17–32.

(217) Rossi, A. M.; Taylor, C. W. *Nat. Protoc.* **2011**, *6* (3), 365–387.

(218) Hall, M. D.; Yasgar, A.; Peryea, T.; Braisted, J. C.; Jadhav, A.; Simeonov, A.; Coussens, N. P. *Methods Appl. Fluoresc.* **2016**, *4* (2), 022001.

(219) Koh, C. M.; Sabò, A.; Guccione, E. *BioEssays* **2016**, *38* (3), 266–275.

(220) Casey, S. C.; Tong, L.; Li, Y.; Do, R.; Walz, S.; Fitzgerald, K. N.; Gouw, A. M.; Baylot, V.; Gütgemann, I.; Eilers, M.; Felsher, D. W. *Science (80-.).* **2016**, *352* (6282), 227–231.

(221) Polivka, J.; Janku, F. *Pharmacol. Ther.* **2014**, *142* (2), 164–175.

(222) Chacón Simon, S.; Wang, F.; Thomas, L. R.; Phan, J.; Zhao, B.; Olejniczak, E. T.; MacDonald, J. D.; Shaw, J. G.; Schlund, C.; Payne, W.; Creighton, J.; Stauffer, S. R.; Waterson, A. G.; Tansey, W. P.; Fesik, S. W. *J. Med. Chem.* **2020**, *63* (8), 4315–4333.

(223) Macdonald, J. D.; Chacón Simon, S.; Han, C.; Wang, F.; Shaw, J. G.; Howes, J. E.; Sai, J.; Yuh, J. P.; Camper, D.; Alicie, B. M.; Alvarado, J.; Nikhar, S.; Payne, W.; Aho, E. R.; Bauer, J. A.; Zhao, B.; Phan, J.; Thomas, L. R.; Rossanese, O. W.; Tansey, W. P.; Waterson, A. G.; Stauffer, S. R.; Fesik, S. W. *J. Med. Chem.* **2019**, *62* (24), 11232–11259.

Chapter 3: Preliminary Findings of Treatment Studies with Trastuzumab in HER2+ Breast Cancer Cells BT474 and MDA-MB-361

Abstract

Acquired resistance to trastuzumab is a frequent barrier to overall survival in HER2+ breast cancer patients with metastatic disease. The reduction in expression of the PTEN tumor suppressor has been hypothesized to be linked to trastuzumab resistance, but its exact contribution to the development of trastuzumab resistance remains controversial. To gain insight on the consequences of PTEN status on trastuzumab sensitivity in HER2+ breast cancer cell lines, we used single cell transcriptomics to ascertain whether the pre-existing transcriptomic alterations due to knockdown of PTEN in HER2+ breast cancer cell lines, BT474 and MDA-MB-361, affect trastuzumab response. We cultured BT474 and MDA-MB-361 (parental and shPTEN cell lines) in the presence of 10 μg/mL for 1 month prior to generating single cell transcriptomic libraries via the Drop-seq pipeline. Untreated BT474 and MDA-MB-361 (parental and shPTEN cell lines) were cultured simultaneously to serve an untreated controls for treatment studies. With BT474, successfully sequenced transcriptomic libraries included parental BT474, BT474 shPTEN, and BT474 shPTEN+treatment. Global transcriptomic analyses between treated and untreated BT474 shPTEN revealed that treated BT474 shPTEN significantly downregulated genes critical for cell growth (padj < 0.01). However, the distribution of BT474 subpopulations between parental BT474, BT474 shPTEN, and BT474 shPTEN+treatment remained constant and did not reproduce the 2 fold increase in the quiescent subpopulation as observed from a previous biological replicate. With MDA-MB-361, successfully sequenced transcriptomic libraries included MDA-MB-361 (± treatment) and MDA-MB-361 shPTEN. Comparative transcriptomic analyses between parental MDA-MB-361 and MDA-MB-361 shPTEN revealed no statistically significant gene sets

based on PTEN status. Treatment of parental MDA-MB-361 revealed significant downregulation of gene sets critical for cell growth relative to untreated parental MDA-MB-361 (padj < 0.05). Due to the insufficient number of treatment controls from both BT474 and MDA-MB-361, no conclusions were made from these treatment studies. It is possible that BT474 and MDA-MB-361 might not represent appropriate models for combined analyses of PTEN knockdown and trastuzumab treatment because the magnitude of changes resulting in PTEN knockdown might be too small. It might be more appropriate to consider alternative HER2+ breast cancer cell line models, such as HCC1954 and SKBR3, for studying how PTEN deficiency affects trastuzumab response.

3.1. Introduction

Trastuzumab resistance among HER2-overexpressing (HER2+) breast cancer remains a barrier to patient survival and outcome.[36–39] Resistance to anti-HER2 therapies is prevalent among patients with advanced, metastatic disease and less common among early stage HER2+ breast cancer patients.[28,34,35] There are many mechanisms hypothesized to governed the onset of trastuzumab resistance, such as proteolytic cleavage of the extracellular domain of HER2; the overexpression of tyrosine kinases, such as HER3, IGFR, and c-MET; and aberrant PI3K/AKT signaling due to PTEN deficiency.[23,26,38,43]

PTEN is a tumor suppressor that regulates the PI3K/AKT signaling pathway through the dephosphorylation of PIP3 → PIP2 and thus controls cell survival, cell metabolism, and tumorigenesis.[25,50,52,53] Aberrant downregulation due epigenetic silencing or loss of heterozygosity has been shown to result in constitutive activation of PI3K/AKT and its effector proteins such as FOXO, mTOR, and GSK-β.[54,56–59] Deficiency of PTEN occurs in 40% of HER2+ breast cancer patients and is significantly correlated with decreased survival rates among these patients.[42,48,60,61] The role of PTEN deficiency and its contribution to trastuzumab resistance remains controversial.[20,42,45,48,179] *In vitro* studies with HER2+ breast cancer cells with PTEN knockdown (k.d.) indicated that trastuzumab treatment resulted in the development of an aggressive mesenchymal phenotype.[112] Furthermore, previous single cell colony formation studies from the Sun Lab demonstrated that HER2+ breast cancer cells with PTEN k.d. generated mesenchymal colonies at a higher frequency compared to parental colonies.

Furthermore, trastuzumab treatment of these colonies with PTEN k.d. further increased the formation of mesenchymal colonies (unpublished data). Despite being phenotypically different from the parental cells, the subset of HER2+ breast cancer cells with PTEN k.d. that increased mesenchymal colonies were unable to be characterized by traditional stem cell markers, such as CD44, CD24, and ALDH, which exemplified the limitation of these assays in classifying these aggressive colonies that resulted from PTEN k.d. and trastuzumab treatment. These previous findings emphasized the need for alternative, unbiased strategies to characterizing these aggressive colonies that were enriched by PTEN k.d. and trastuzumab treatment. These previous findings suggested that PTEN deficiency in patients could worsen the patient outcome when they are treated with trastuzumab. Despite these implied consequences of PTEN deficiency in HER2+ breast cancer, PTEN is not routinely assessed for HER2+ breast cancer patients, and HER2+ breast cancer patients are treated with trastuzumab-based therapy regardless of PTEN status.

There is a critical need to elucidate the mechanisms by which HER2+ breast cancer cells with PTEN deficiency responds to trastuzumab to generate a cancer phenotype with increased aggressiveness. Furthermore, it is critical to determine how the phenotype that result from PTEN deficiency and trastuzumab treatment ultimately impact the long term response to trastuzumab. This insight could guide the discovery of effective, alternative therapeutic solutions for HER2+ metastatic breast cancer who experience trastuzumab resistance. Deeper knowledge about how PTEN deficiency impacts trastuzumab sensitivity could have clinical significance since PTEN deficiency occurs in 40% of HER2+ breast cancer patients. Additionally, understanding the relationship between PTEN deficiency and trastuzumab treatment could reveal characteristics of subsets of HER2+ breast cancer patients who are predisposed to respond poorly to trastuzumab-based therapies based on PTEN deficiency. Ideally, those patients could be identified at the beginning of their cancer management journey and could be treated with alternative therapies. Herein, we described preliminary findings using single cell RNA-seq to scrutinize the transcriptomic alterations that arise in HER2+ breast cancer cells with PTEN deficiency when treated with trastuzumab.

3.2. Materials and Methods

3.2.1. Cell Culture

Cells with silenced PTEN were generated by lentiviral infection to introduce short hairpin RNA of PTEN. To target the human *PTEN* gene for silencing, the pLentilox 3.7 vector containing shPTEN was used to generate "PTEN k.d." cell lines. As a control for lentiviral infection, pLentilox 3.7 vector containing fluorescent dye DsRed, which resulted in the wild type (wt) PTEN cell line derivative. Knockdown studies were performed by Dr. Joseph Burnett as previously described by Korkaya and coworkers to yield HER2+ breast cancer cell line pairs based on PTEN status.[77,82,83]

The following $HER2^+$ breast cancer cell lines with wild type (WT) PTEN and PTEN knockdown ("PTEN k.d." derivative) were used during the course of this study: BT474 and MDA-MB-361. BT474 cell line derivatives were maintained in DMEM/F-12 50:50 and supplemented with 10% FBS, 1% Pen-Strep, and 1% of 2mM L-Glutamine. MDA-MB-361 cell line derivatives were maintained in DMEM supplemented with 1% anti-anti (Gibco cat. no. 15240062) and 20% FBS. MDA-MB-361 and BT474 were cultured with 10 µg/mL trastuzumab in complete media for 4 weeks prior to use for Drop-seq experiments. Complete media with trastuzumab was prepared fresh by reconstituting trastuzumab powder into complete media to a final concentration of 10 µg/mL. All concentrations noted are final concentrations in media. Cells were cultured in an incubator at 37°C and humidified with 5% CO_2.

3.2.2. Drop-seq Experiments

Drop-seq experiments were performed in accordance to the online protocol from the McCarroll lab (version 3.1, 2015).[85] Barcoded Bead SeqB beads were ordered from Chemgenes and will be referred as Drop-seq beads. Microfluidics devices used were generous gifts from Dr. Michael Brooks from Dr. Max Wicha's group. For these devices, treatment with Aquapel was performed using instructions from the McCarroll lab to ensure a hydrophobic surface through the microfluidics devices. To ensure high-quality droplets and maintain consistency between Drop-seq experiments, microfluidics devices were ordered from FlowJEM (PDMS Drop-seq chip, standard design, containing vaporized silane).

3.2.3. Sequencing of cDNA libraries

Single transcriptomic libraries generated from each cell line pair (BT474 and MDA-MB-361) were sequenced by Next-seq (150 cycle, MO) at the Advanced Genomics Center at the University of Michigan. Approximately 7M reads/sample (75K reads/cell) were desired for sequencing runs. The following read lengths were used for Next-seq: read 1 length: 20 bp (26 cycles), read 2 length: 50 bp (96 cycles), and index read length: 8 bp. Illumina adapters (i7) were used to discriminate single cell transcriptomic libraries derived from parental from shPTEN cell lines. The following i7 adapters (and adapter sequences) were used to prepare sequencing libraries: N701 (TCGCCTTA), N702 (CTAGTACG), N703 (TTCTGCCT), and N704 (GTTGGACA). Transcriptomic libraries pooled by equal molar pooling of cell lines and ensured equal sequencing coverage per cell line.

3.2.4. Read Alignment and Generation of Digital Expression Data

Read alignment and the generation of the digital expression data matrix was performed by Dr. Joe Burnett and in accordance to the Drop-seq Computational Cookbook.[86] Reads were de-multiplexed to separate reads corresponding to parental and shPTEN cell line based on i7 index adapters. Reads were aligned to the reference human genome (GRCh38.p13) to derive the cDNA from each read. Mapped reads were then organized into a digital count matrix based on the unique molecular identifier, which enabled the quantification of gene expression per gene for each cell represented from the single cell transcriptomic library.

3.2.5. Unsupervised Dimensionality Reduction and Clustering

Digital count matrices were imported into R for analysis using the Seurat package (version 3.1.2). The gene expression for treatment conditions of the parental and shPTEN cell lines were normalized using the NormalizeData function, which normalizes the feature (gene expression) counts of each cell relative to the total features of that cell. These normalized feature counts were then transformed using a natural log transformation. In order to perform downstream analyses with the metadata for each cell line pair, the metadata corresponding to the parental cell line and the shPTEN cell line were integrated. Integration of these metadata was performed by identifying integration anchors (FindIntegrationAnchors) with the dims and k.filter argument set to default settings.

Metadata was integrated using the IntegrateData function. Cell cycle heterogeneity was minimized by regressing the difference in the expression of G2/M and S phase genes. Analyses were also performed in absence of cell cycle regression, where the data changed minimally compared to using cell cycle regression. Analyses presented in this dissertation represent data where cell cycle regression was performed. Subpopulation clusters were resolved by using principal component analysis (PCA) and Uniform Manifold Approximation and Projection (UMAP). The resolution argument within the FindClusters function was optimized for each cell line pair by clustering the metadata at each clustering resolution from 0 – 1 in increments of 0.1. The multi-resolution clusterings were evaluated using the R package clustree, which guided the selection of the optimal clustering resolution.[87]

3.2.6. Differential Gene Expression Analysis

Differential gene expression was performed using FindMarkers function to evaluate differentially expressed genes between cell line pairs and subpopulations using the wilcox test. This analysis was performed to scrutinize the global transcriptomic differences between parental and shPTEN cell line by specifying ident.1 as the shPTEN cell line. Similarly, this analysis was performed to compare transcriptomes of treated and corresponding untreated condition. Additionally, differential gene expression analyses were performed to identify characteristic gene expressed by each subpopulation by specifying ident.1 as the subpopulation of interest. The FindMarkers function was used to evaluate the gene expression of PTEN and HER2 in all cell lines and between each subpopulation. Genes identified from the FindMarkers output were considered as statistically significant if p_adj < 0.01, where p_adj accounted for the bonferroni correction.

3.2.7. Gene Set Enrichment Analysis (GSEA)

After differential gene expression was performed to assess the genes differentially expressed by a subpopulation of cells, gene set enrichment analyses was used to elucidate the functional consequences of those differentially expressed genes. GSEA was performed using the R package fgsea.[88,89] In order to perform gsea using the fgsea package, a rank ordered list of genes from the set of differentially expressed genes was generated based on the log_avgFC of a given gene. This rank ordered list was used as

the stats argument within the fgsea function. The minimum gene set size was set to 10, and the maximum gene set size to test was 500. The number of permutations to run using the fgsea function was 1M. The rank ordered list of genes was compared a priori to the gene sets downloaded from MSigDb (msigdb.v7.0.symbols.gmt, accessed from https://data.broadinstitute.org/gsea-msigdb/msigdb/release/7.0/). Gene sets with p_adj < 0.05 were considered statistically significant, where p_adj is the p_val adjusted using the Benjamini-Hochberg (BH) procedure. Gene sets that were identified to be statistically significant were downloaded from MSigDb and imported into R. Genes from the imported gene sets were intersected with the genes from our metadata using the Reduce function and the intersect function from the dplyr package; this enabled the identification of genes from statistically significant gene sets that contributed to the enrichment score of those gene sets. The output of the intersected list of genes were scrutinized based on avg_logFC, p_adj, pct.1, and pct.2, where avg_logFC is the natural log fold change in expression of a given gene from one subpopulation relative to another subpopulation. The p_val adjusted for BH correction and is noted as p_adj. The percentage of cells from the subpopulation of interest that expressed the gene of interest is quantified by pct.1, and the percentage of cells from the compared subpopulation that expressed the gene of interest is quantified as pct.2.

3.3. Results and Discussion

To elucidate how PTEN k.d. affected the sensitivity of HER2+ breast cancer cells to trastuzumab, we performed single cell RNA-seq using the Drop-seq pipeline with two HER2+ breast cancer cell lines, BT474 and MDA-MB-361. With the treatment studies using these cell lines, we aimed to understand how the transcriptomic profiles of parental HER2+ breast cancer cells and the PTEN k.d. cells were altered when treated with trastuzumab. Findings from these *in vitro* studies could reveal how transcriptomes shaped by pre-existing PTEN deficiency affects the response of HER2+ breast cancer to trastuzumab.

For these treatment studies, both BT474 and MDA-MB-361 were previously treated for 3 months to develop trastuzumab resistance and provided to me as a gift for additional 1 month treatment with trastuzumab prior to sequencing. We integrated previous data for BT474 (data presented in Ch. 2, referred here as “batch 1”, noted with

“2” at end of sample name designations in this chapter) into the current treatment data. Data from the treatment studies belong to batch 2 and are referred as “BT474 wt” and “BT474 shPTEN,” respectively. Among the treatment set for BT474, we aimed to sequence parental and BT474 PTEN k.d. in the presence and absence of trastuzumab treatment (i.e. 4 treatment conditions in total). However, we were only able to sequence parental BT474 (no treatment), BT474 shPTEN (no treatment), and shPTEN (with treatment). Thus, with BT474, we were only able to glean insight about transcriptomic changes arising from trastuzumab treatment using BT474 shPTEN in the presence and absence of trastuzumab. Additionally, we used the second biological replicate of BT474 wt 2 and BT474 shPTEN shPTEN to validate the 2 fold increase of a quiescence subpopulation after k.d. of PTEN. A similar experimental limitation was observed for the treatment studies using MDA-MB-361. We sought to sequence 4 treatment conditions using MDA-MB-361 (parental MDA-MB-361 and PTEN k.d., in presence and absence of trastuzumab). However, only parental MDA-MB-361 ($\pm$ treatment) and MDA-MB-361 PTEN k.d. (no treatment) were successfully sequenced. Thus, treatment-induced changes could only be derived from the parental cell lines. Elucidation of the consequences of PTEN k.d. in MDA-MB-361 were also afforded using this cell line. Only preliminary observations will be presented in this chapter, and observations will need to be validated using the proper number of controls per cell line.

3.3.1. Preliminary Findings for Treatment Studies Using Parental BT474 and BT474 PTEN k.d. Cells

Prior to downstream analyses, we verified protein expression levels of HER2 and PTEN between the three treatment conditions and within each subpopulation. As expected for BT474, the three treatment conditions of BT474 (denoted as “BT474 wt,” “BT474 shPTEN,” and “BT474 shPTEN + tx” from batch 2) expressed similarly high protein levels of HER2, which were not statistically significant between treatment conditions. The protein expression level of PTEN was significantly higher in parental BT474 compared to BT474 shPTEN ($\pm$ treatment, padj < 0.0001), although more cells were detected in both PTEN k.d. conditions compared to parental cell line. Between each of the BT474 subpopulations, the expression levels of HER2 and PTEN exhibited statistically significant differences. The expression of HER2 in subpopulations 0 (padj <

0.01) and 2 (padj < 0.0001) was significantly lower compared to other subpopulations (Figure 3.1A). In addition, the expression of HER2 in subpopulations 1 and 5 were significantly higher compared to other subpopulations (padj < 0.0001, Figure 3.1A). The expression of HER2 within each subpopulation was not statistically different between the treatment groups. The expression of PTEN was significantly lower in subpopulations 0 and 4 compared to the other subpopulations (padj < 0.0001), while the expression of PTEN was significantly higher in subpopulation 5 compared to the other subpopulations (padj < 0.0001, Figure 3.1B).

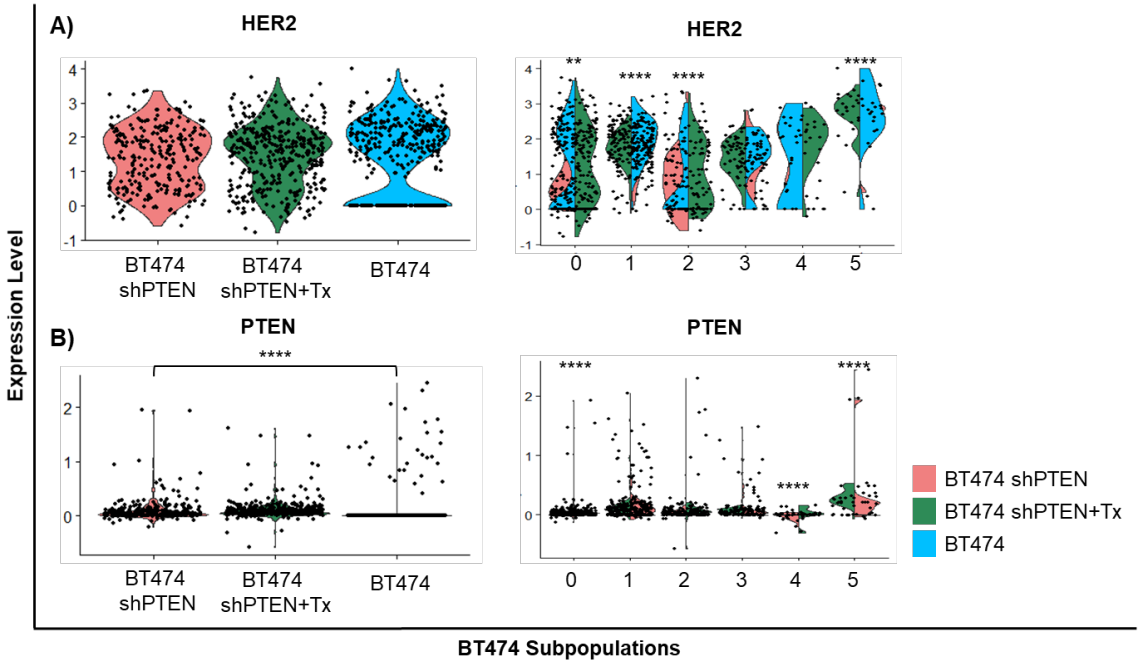

*Figure 3.1. Evaluation of Expression Levels of HER2 and PTEN in BT474 (Batch 2) Revealed Heterogeneous Expression. Expression levels of A) HER2 and B) PTEN between treatment groups (left) and between subpopulations (right). Dots represent single cells from each treatment group, and the expression levels are normalized log transformed values. Asterisks above subpopulations denote statistical significance of HER2 or PTEN expression between subpopulations by Wilcox test. ** p < 0.01, **** p < 0.0001.*

After relative levels of HER2 and PTEN were verified between treatment groups of BT474, between subpopulations, and within subpopulations, we evaluated how trastuzumab treatment induced global transcriptomic changes. The global transcriptomic profiles of parental BT474, BT474 shPTEN, and and BT474 shPTEN with treatment were analyzed using differential gene expression and GSEA. First, we sought to replicate the global transcriptomic differences that we previously observed by GSEA using parental BT474 and BT474 shPTEN (batch 2). This analysis yielded 36 significant gene sets and

revealed opposite phenotypes than what we previously observed for the global transcriptomic comparison between parental BT474 and BT474 shPTEN (padj < 0.01, Table 3.1). As detailed in Ch. 2, we previously observed an enrichment in innate immune signaling and stem cell gene sets by BT474 shPTEN. However, those gene sets were negatively enriched in BT474 shPTEN from batch 2 (padj < 0.01, Table 3.1).

The global transcriptomic comparisons between BT474 shPTEN and BT474 shPTEN+treatment revealed 175 significant gene sets. Relative to BT474 shPTEN, BT474 shPTEN+treatment was negatively enriched DREAM complex targets, E2F targets, cycling genes, mitotic spindle, and cell division (padj < 0.01, Table 3.1), which suggested that trastuzumab treatment of BT474 PTEN k.d. cells reduced proliferation and cell growth. This treatment-induced reduction of cell growth was expected because it was consistent with the cytostatic effect of trastuzumab treatment.[43,180,181]

Table 3.1. Gene Sets Identified from Comparative Transcriptomic Analyses of Parental BT474, BT474 shPTEN, and BT474 shPTEN+Treatment (Batch 2). pval represents unadjusted pval. padj represents the pval adjusted with BH correction. NES signifies the normalized enrichment score of the gene sets. Gene sets considered to be statistically significant if padj < 0.01.

GSEA Comparisons	Identified Gene Sets	pval	padj	NES
BT474 shPTEN vs BT474	Mammary Stem Cell Up	1.44E-05	2.87E-05	-1.98
	Innate Immune System	5.16E-04	5.16E-04	-1.61
BT474 shPTEN+Tx vs BT474 shPTEN	Dream Targets	1.43E-06	3.38E-04	-2.26
	Hallmark E2F Targets	1.59E-06	3.38E-04	-2.26
	Proliferation	3.30E-06	5.45E-04	-2.50
	Mitotic Cell Cycle	7.48E-06	8.95E-04	-2.00
	Cycling Genes	7.55E-06	8.95E-04	-2.03
	Hallmark G2/M Chekcpoint	9.65E-06	1.05E-03	-2.25
	Hallmark Mitotic Spindle	1.36E-05	1.31E-03	-2.29
	Cell Division	1.57E-05	1.41E-03	-2.07
	Apoptosis by CDKN1A via p53	2.20E-04	8.53E-03	-2.12

Next, we aimed to verify our previous findings that PTEN k.d. in BT474 resulted in changes in the relative subpopulation proportions. Specifically, we wanted to verify the 2 fold increase in a quiescent early EMT subpopulation, the 1.6 fold increase of a proliferative subpopulation, and the 5 fold decrease of a quiescent subpopulation marked

by high expression levels of HER2 and NEAT1. In order to make these comparisons between the experimental batches of BT474, we needed to determine how the subpopulations corresponded to each other across experimental batches. After integrating BT474 (batch 1) with the newly sequenced data (batch 2), we used different clustering parameters to accommodate the entire integrated BT474 dataset, which identified 6 subpopulations for both batch 1 and batch 2. Integrating the collective BT474 datasets normalized the data relative to each other and lessened the batch variation between experiments. To characterize the subpopulations from this integrated dataset relative to BT474 wt 2 and BT474 shPTEN 2 from batch 1, we identified top differentially expressed genes for each subpopulation for each experimental batch (Figure 3.2). By using the differentially expressed genes from each subpopulation, we would be able to verify the previously observed subpopulation changes induced by k.d. of PTEN, and we would be able to evaluate what subpopulation level changes arose from trastuzumab treatment. As shown in Figure 3.2, the subpopulation identified between the two batches were fairly conserved, except for subpopulation 0 and 1. Based on the expression of PCNA, DUT, PRR11, PTTG1, SMC4, UBE2C, ARI61P1, TUBA1B, and HMGB2, subpopulation 0 from batch 1 corresponded to subpopulation 1 from batch 2. We previously observed subpopulation 0 (batch 1) increased by 2 fold after k.d. of PTEN. Additionally, subpopulation 1 from batch 1 corresponded to subpopulation 0 of batch 2 based on the expression of those markers as well. Subpopulations 2 and 3 from both batches have the same respective subpopulation designation. Subpopulation 4 from batch 2 appeared to be quiescent due to the low and heterogeneous expression of a mixture of genes. Lastly, subpopulation 5 from batch 2 corresponded to subpopulation 4 from batch 1 of BT474 due to the characteristically high expression levels of NEAT1 and HER2. Now that the subpopulations between the experimental batches have been identified, we can proceed to verify subpopulation level changes induced by PTEN k.d. (no treatment) and scrutinize how trastuzumab treatment altered the transcriptomic composition of BT474.

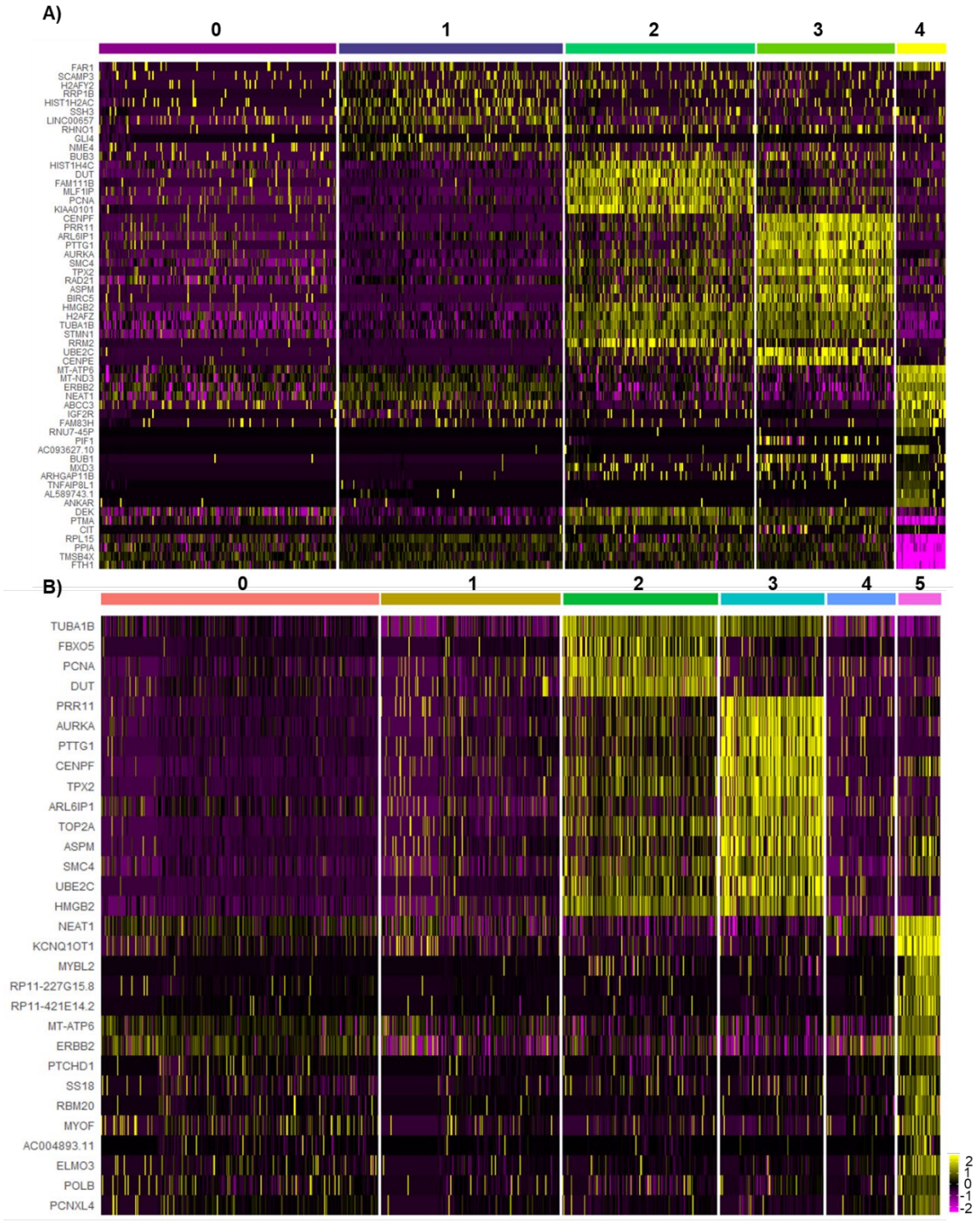

Figure 3.2. Comparison of BT474 Subpopulations Between Experimental Batch 1 and 2. Heatmap depicting differentially expressed markers for each BT474 subpopulation in A) batch 1 (data presented in Chapter 2) and B) batch 2 (consisting of treatment studies) of BT474.

Firstly, we were unable to verify the previously observed changed induced by k.d. of PTEN in BT474 wt and BT474 shPTEN from batch 2. Specifically, we sought to verify

the 2 fold increase of the quiescent subpopulation 1 in batch 2 (corresponded to subpopulation 0 of batch 1), the 1.6 fold increase of the proliferative subpopulation 2, and the 4 fold decrease in subpopulation 5 (corresponded to subpopulation 4 from batch 1). However, the magnitude of these subpopulation changes were not reproduced in batch 2 for subpopulations 1 and 5 (corresponded to subpopulations 0 and 4 from batch 1, Figure 3.3). Interestingly, subpopulation 2 from batch exhibited a 1.5 fold increase after k.d. of PTEN relative to parental subpopulation 2, which mirrored the 1.6 fold increase of subpopulation 2 after PTEN k.d. in BT474 from batch 1 (Figure 3.3). Using the biological replicates for parental BT474 and BT474 with PTEN k.d. from batch 1 and 2, we only reproduced the 1.5 fold increase of the proliferative subpopulation 2 after PTEN k.d. relative to parental BT474. We were unable to detect a 2 fold increase in the quiescence epithelial, early EMT subpopulation 1. Furthermore, we were unable to reproduce the 4 fold decrease of the quiescent subpopulation marked by high expression of HER2 and NEAT1.

Despite the inconsistencies between experimental batches, we also made preliminary assessments of subpopulation level changes using comparative analyses of BT474 shPTEN and BT474 shPTEN+treatment. Based on the relative distribution of subpopulations, trastuzumab treatment appeared to increase subpopulation 5 by 1.7 fold. Since the previously observed subpopulation level changes induced by k.d. of PTEN were not fully observed in BT474 shPTEN (batch 2), the treatment induced changes to subpopulation 5 can only be regarded as a preliminary observation. For BT474, it is possible that the additive effects of trastuzumab treatment to PTEN deficiency could not be assessed due to the relatively small magnitude of transcriptomic change that PTEN k.d. induced in this cell line compared to others (i.e. HCC1954 and SKBR3). Thus, it is critical to repeat the treatment studies using those cell lines sine the magnitude of PTEN k.d. was larger in order to study how the consequences of PTEN deficiency in the presence of trastuzumab treatment. Choosing an appropriate cell line is critical to ascertaining whether PTEN deficiency primes the HER2+ breast cancer to respond poorly to trastuzumab, and if so, by what transcriptomic changes and mechanisms.

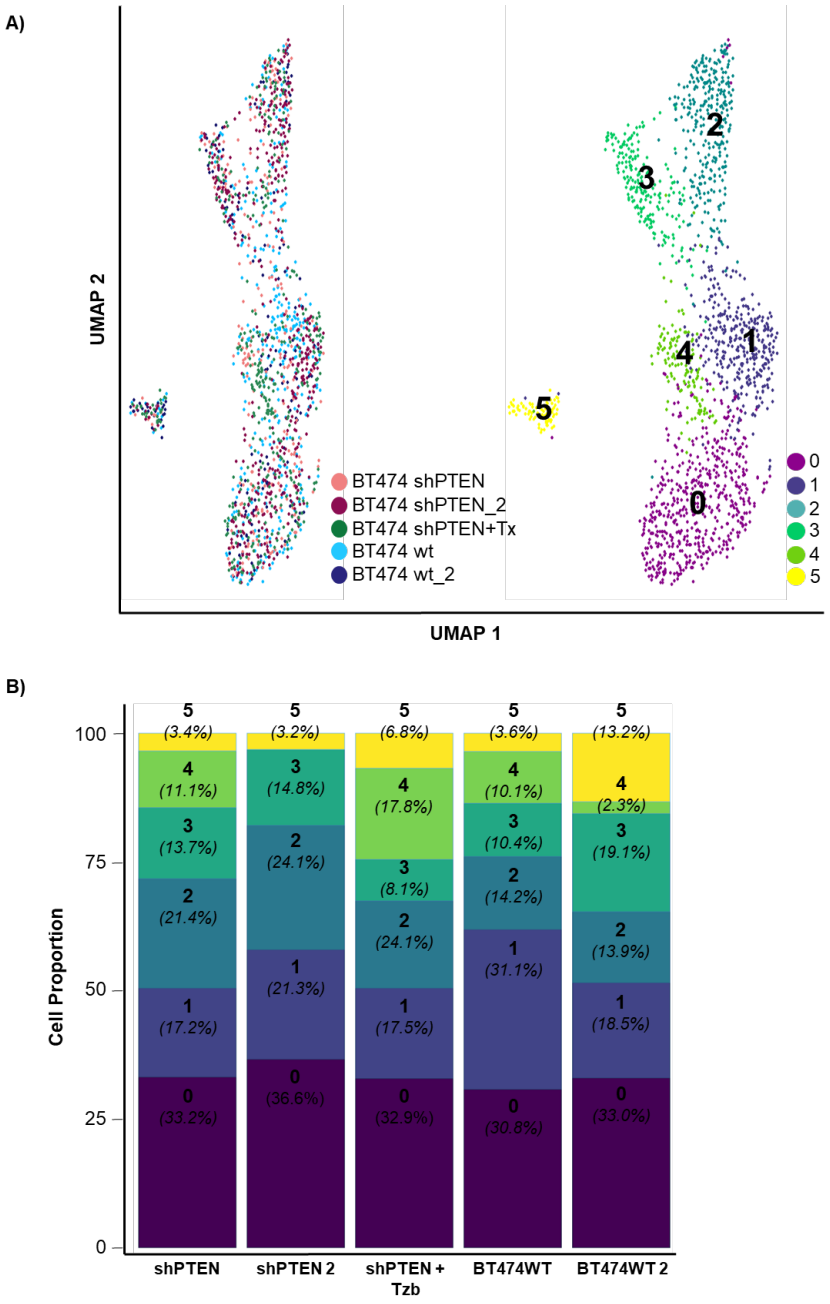

Figure 3.3. Single Cell Characterization of BT474 Datasets (Batch 1 and Batch 2). A) The left UMAP plot depicts single cells of each treatment group. Sample name followed with "2" denotes data from batch 1 (presented in Chapter 2). The right UMAP plot depicts single cells categorized into five BT474 subpopulations. B) Relative cell distribution of each treatment group/cell line into five BT474 subpopulations. Subpopulations colored using the same color scheme as right UMAP plot in A. Subpopulations are noted in bold and relative percentage of cells in given subpopulation relative to entire cell line is noted in parentheses.

3.3.2. Preliminary Observations from Treatment Studies Using MDA-MB-361

Similar to the treatment studies with BT474, preliminary observations were only made with MDA-MB-361 due to the insufficient number of controls. Treatment studies using MDA-MB-361 featured 3 treatment conditions: parental MDA-MB-361 (± treatment)

and MDA-MB-361 shPTEN (no treatment). In this cell line, comparative analyses were performed with parental MDA-MB-361 and MDA-MB-361 with PTEN k.d. to ascertain how PTEN k.d. altered the transcriptome of MDA-MB-361. Additionally, we sought to determine how trastuzumab treatment induced transcriptomic alterations by comparing parental MDA-MB-361 in the presence and absence of trastuzumab treatment.

We first verified the protein expression levels of HER2 and PTEN levels between the treatment groups, between subpopulations, and within a subpopulation. Cells from each treatment group exhibited high expression levels of HER2, which were not significantly different between the groups (Figure 3.4). Furthermore, HER2 was expressed in all five of the subpopulations that comprised MDA-MB-361 and within each subpopulation. The expression levels of HER2 was not significantly different between each of the treatment group (Figure 3.4). Regarding PTEN, the expression of PTEN was low in this cell line, and the expression levels of PTEN were not significantly different between each treatment group (Figure 3.4). Within each subpopulation, the levels of PTEN was not significant between the treatment groups (Figure 3.4). Lack of significant difference in PTEN expression levels might reflect the low levels of PTEN in this cell line and this difference in PTEN expression levels might be too low for Drop-seq to discriminate between parental MDA-MB-361 and MDA-MB-361 with PTEN k.d.

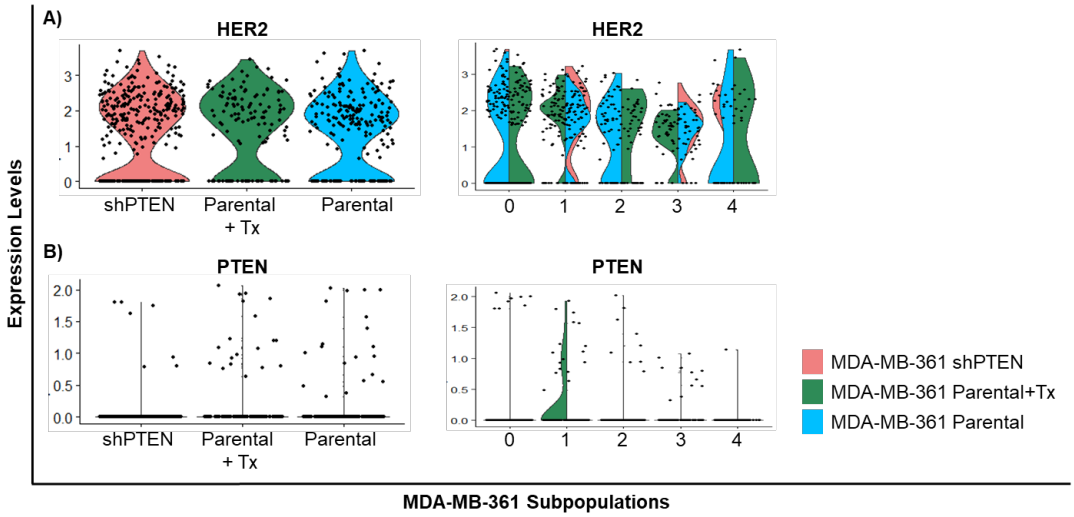

Figure 3.4. Evaluation of Expression Levels of HER2 and PTEN in MDA-MB-361. Expression levels of A) HER2 and B) PTEN between treatment groups (left) and between subpopulations (right). Dots represent single cells from each treatment group, and the expression levels are normalized log transformed values. Asterisks above subpopulations denote statistical significance of HER2 or PTEN expression between subpopulations by Wilcox test.

Due to the insufficient number of controls for the treatment studies of MDA-MB-361, we only presented preliminary observations, which require further follow-up studies for validation. We used DGE analysis and GSEA to evaluate the global transcriptomic differences between parental MDA-MB-361 and PTEN k.d. cells. GSEA identified 139 gene sets (padj < 0.01), which included negative enrichment scores for drug binding and drug responses gene sets (Table 3.2). Furthermore, MDA-MB-361 shPTEN were also negatively enriched for cell motility and cell adhesion gene sets (Table 3.2). In addition, MDA-MB-361 PTEN k.d. cells were positively enriched for cell cycle gene sets, such as nuclear division, regulation of cell cycle, and cell cycle transition (Table 3.2), which suggested these cells actively progress through the cell cycle. Interestingly, MDA-MB-361 PTEN k.d. cells were positively enriched in p53 signaling pathway (Table 3.2). Comparative analyses of parental MDA-MB-361 and MDA-MB-361 with PTEN k.d. revealed global transcriptomic differences. The reduction in PTEN expression increased cell cycling and p53 pathway relative to parental MDA-MB-361.

Differential gene expression and GSEA was also used to assess the global transcriptomic alternations due to trastuzumab treatment using parental MDA-MB-361. These comparative analyses were performed using pval < 0.01 rather than padj < 0.01 or padj < 0.05 as the parameter for statistical significance because 0 and 5 statistically significant gene sets were identified using the latter statistical significance cut offs, respectively. Previously, only BH-adjusted (Benjamini-Hochberg) p-values (padj) were used to determine statistical significance of gene sets because padj considers the gene set size and multiple hypothesis treating and thus represented a more stringent parameter for statistical significance cut offs. Only negative enrichment for cycling genes and vesicle mediated cell transport, hinting that treatment of parental cells reduced cell activity, which is consistent with the cytostatic mechanism of trastuzumab (padj < 0.05).[43,180,181] Using the less stringent pval < 0.01 rather than padj as the parameter for statistical significance, GSEA revealed 313 gene sets (pval < 0.01). At this level of statistical significance, negative enrichment scores were identified for drug responses and drug binding gene sets. Furthermore, treated parental cells were also negatively enriched in cell cycle gene sets, such as cell division, cycling genes, proliferation, mitotic spindle, and chromosome remodeling. Taken together, trastuzumab treatment did not appear to result in significant

transcriptomic changes between the treated parental and untreated parental MDA-Mb-361 as evidenced by the low number of significant gene sets (padj < 0.05) and the need to use the less stringent statistical significance parameter (pval < 0.01).

Table 3.2. Gene Sets Identified from Comparative Transcriptomic Analyses of Parental MDA-MB-361, MDA-MB-361 shPTEN, and Parental MDA-MB-361 +Treatment. pval represents unadjusted pval. padj represents the pval adjusted with BH correction. NES signifies the normalized enrichment score of the gene sets. Gene sets considered to be statistically significant if padj < 0.01.

GSEA Comparisons	Identified Gene Sets	pval	padj	NES
MDA-MB-361 PTEN vs WT	Response to Drug	5.70E-04	3.50E-01	-1.79
	Extracellular Matrix	5.04E-04	3.50E-01	-1.96
	Drug Binding	3.92E-03	5.10E-01	-1.57
	Collagen Containing Extracellular Matrix	9.53E-04	4.06E-01	-1.92
	Cell-Cell Adhesion	5.43E-03	5.10E-01	-1.70
	Kegg p53 Signaling Pathway	4.57E-04	3.50E-01	2.24
	Mitotic Nuclear Division	7.43E-03	5.21E-01	1.62
MDA-MB-361 Parental+Tx vs Parental	Cycling Genes	1.50E-05	4.34E-02	-1.73
	CTNNB1 Targets Down	9.06E-06	4.34E-02	-1.83
	Reactome Vesicle Mediated Transport	1.93E-05	4.34E-02	-1.87
	Cell Cycle G2/M	9.24E-05	5.43E-02	-1.90
	Drug Binding	2.59E-04	7.51E-02	-1.62

After the evaluation of the global transcriptomic composition of the untreated, treated parental, and PTEN k.d. of MDA-MB-361, we evaluated the steady state subpopulations of each treatment condition for MDA-MB-361. We observed minimal differences in all of the subpopulations between the three treatment groups. Each treatment group consisted of the following subpopulation composition: 34-40% of subpopulation 0, 21-28% of subpopulation 1, 11-17% of subpopulation 2, 12-15% of subpopulation 3, and 8-11% of subpopulation 4 (Figure 3.5). Based on the relative distribution of MDA-MB-361 cells in each subpopulation, no significant change in the subpopulations were observed between untreated parental and MDA-MB-361 with PTEN k.d., which implied that PTEN k.d. might not induce observable changes at the subpopulation levels in this cell line. While GSEA revealed that PTEN k.d. in MDA-MB-361 expressed more cell cycling genes, the reduction of PTEN did not result in changes to the subpopulation steady state of MDA-MB-361. In HER2+ breast cancer cell lines, it

is possible that PTEN k.d. causes a global increase of quiescent features, and this global increase in quiescent features cause noticeable subpopulation level changes within the bulk cell line. If this is the case, it is possible that the subpopulation composition of MDA-MB-361 did not change as a result of PTEN k.d. because PTEN k.d. caused a global increase of cell cycling gene expression, rather than a global increase of quiescent features. Similarly, treatment induced changes were also not detected between the treated and untreated parental MDA-MB-361 at the subpopulation level. Thus, downstream analyses and the characterization of MDA-MB-361 subpopulations were not performed using this cell line due to the lack of subpopulation level changes resulting from both k.d of PTEN and trastuzumab treatment.

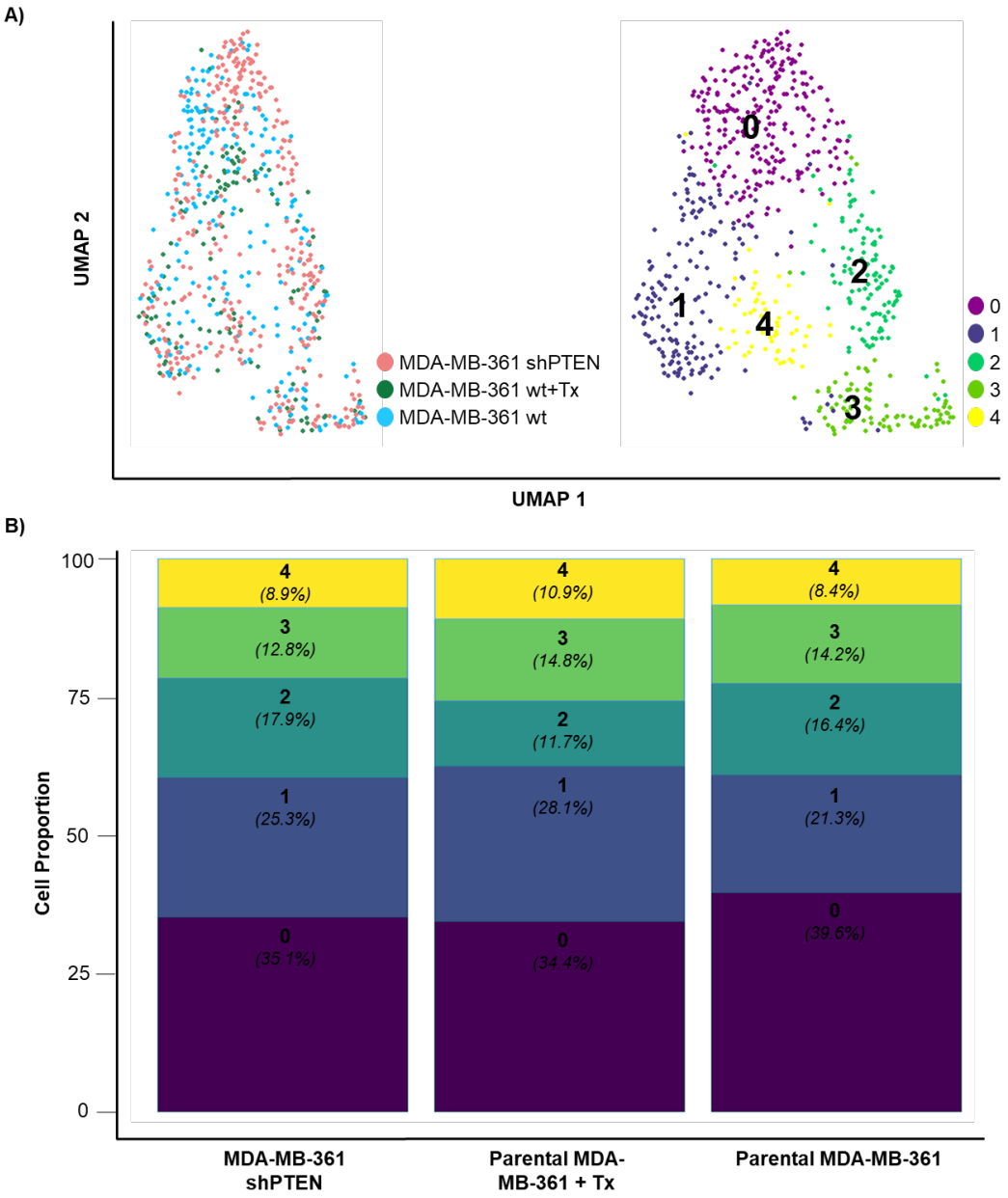

Figure 3.5. Single Cell Characterization of MDA-MB-361. A) UMAP plot depicting single cells of each treatment group (left) and single cells categorized into five MDA-MB-361 subpopulations (right). B) Relative cell distribution of each treatment group/cell line into five MDA-MB-361 subpopulations. Subpopulations colored using the same color scheme as UMAP plot in A. Subpopulations are noted in bold and relative percentage of cells in given subpopulation relative to entire cell line is noted in parentheses.

3.4. Concluding Remarks

Treatment studies yielded inconclusive results from both BT474 and MDA-MB-361. In BT474, the previously observed 2 fold increase of the quiescent early EMT subpopulation was not reproduced in the current datasets. Furthermore, the 4 fold decrease of the quiescent subpopulation characterized by high expression of HER2 and

NEAT1 were also not reproduced using the biological replicate of parental BT474 and BT474 shPTEN from the treatment studies (BT474 batch 2). Regarding MDA-MB-361, similar observations were made after analyzing the effects of PTEN k.d. and trastuzumab treatment. While GSEA revealed that MDA-MB-361 with PTEN k.d. exhibited more cell cycling features, k.d. of PTEN did not result in changes to the subpopulation level steady states. In addition, GSEA of treated parental and untreated parental only suggested that treated parental cells exhibited less cell cycling compared to untreated parental MDA-MB-361, which is reflective of the cytostatic mechanism of trastuzumab.[43,180,181] Furthermore, trastuzumab treatment did not induce changes at the subpopulation level of MDA-MB-361 as the subpopulation distribution remained constant regardless of PTEN status and trastuzumab treatment.

It is possible that BT474 and MDA-MB-361 represented inappropriate models to observe subpopulation level changes that result from PTEN k.d. and trastuzumab treatment. For BT474, changes of 2-4 fold were observed in the subpopulations once, whereas, in other cell lines, such as HCC1954 and SKBR3, the subpopulations changed by a magnitude of 80 and 120 fold after k.d. of PTEN in those cell lines. Thus, the magnitude of change induced by PTEN k.d. in BT474 might be too small to be reliably observed and thus, this cell line might represent an inappropriate model for studying the consequences of PTEN k.d. at the subpopulation level. Instead, alternative HER2+ breast cancer cell lines such as HCC1954 or SKBR3 might reliably capture the functional consequences of PTEN k.d. on a subpopulation level and thus might be more appropriate models to scrutinize the added effect of trastuzumab treatment in the context of HER2+ breast cancer with PTEN deficiency. The differences in the global transcriptomic changes and the magnitude of subpopulation level changes that resulted from k.d. of PTEN also highlighted the context-dependency of PTEN deficiency. These context-dependent consequences of PTEN deficiency might mirror the intertumoral heterogeneity faced in the clinical management of HER2+ breast cancer among patients. Thus, these context-dependent effects of PTEN deficiency might suggest that some patients with PTEN deficiency might be unaffected by PTEN deficiency as modeled by our preliminary findings using MDA-MB-361, whereas in other patients, the deficiency of PTEN might enrich for a quiescent epithelial early EMT subpopulation as suggested our findings from

Chapter 2 using HCC1954 and SKBR3. Taken together, the preliminary findings from the treatment studies using BT474 and MDA-MB-361 highlighted the inter- and intratumoral heterogeneity elicited by PTEN k.d. alone and hinted at the need for methods to subset patients based on PTEN status as another diagnostic and treatment parameter.

3.5. References

(1) U.S. Breast Cancer Statistics | Breastcancer.org https://www.breastcancer.org/symptoms/understand_bc/statistics (accessed Jun 1, 2020).

(2) Dai, X.; Li, T.; Bai, Z.; Yang, Y.; Liu, X.; Zhan, J.; Shi, B. *Am. J. Cancer Res.* **2015**, *5* (10), 2929–2943.

(3) Turashvili, G.; Brogi, E. *Front. Med.* **2017**, *4* (DEC).

(4) Wang, J.; Xu, B. *Signal Transduct. Target. Ther.* **2019**, *4* (1).

(5) *Am. Cancer Soc.* **2020**, 1–43.

(6) National Cancer Institute Surveillance, Epidemiology, and E. R. P. (SEER). *Natl. Cancer Inst.* **2019**.

(7) Zhang, L.; Li, J.; Xiao, Y.; Cui, H.; Du, G.; Wang, Y.; Li, Z.; Wu, T.; Li, X.; Tian, J. *Sci. Rep.* **2015**, *5*, 1–14.

(8) Godoy-Ortiz, A.; Sanchez-Muñoz, A.; Parrado, M. R. C.; Álvarez, M.; Ribelles, N.; Dominguez, A. R.; Alba, E. *Front. Oncol.* **2019**, *9* (OCT), 1124.

(9) Loibl, S.; Gianni, L. *Lancet* **2017**, *389* (10087), 2415–2429.

(10) Muller, K. E.; Marotti, J. D.; Tafe, L. J. *Am. J. Clin. Pathol.* **2019**, *152* (1), 7–16.

(11) Vandenberghe, M. E.; Scott, M. L. J.; Scorer, P. W.; Söderberg, M.; Balcerzak, D.; Barker, C. *Sci. Rep.* **2017**, *7* (1), 1–11.

(12) Zhang, X.; Bleiweiss, I.; Jaffer, S.; Nayak, A. *Clin. Breast Cancer* **2017**, *17* (6), 486–492.

(13) Wolff, A. C.; Elizabeth Hale Hammond, M.; Allison, K. H.; Harvey, B. E.; Mangu, P. B.; Bartlett, J. M. S.; Bilous, M.; Ellis, I. O.; Fitzgibbons, P.; Hanna, W.; Jenkins, R. B.; Press, M. F.; Spears, P. A.; Vance, G. H.; Viale, G.; McShane, L. M.; Dowsett, M. *J. Clin. Oncol.* **2018**, *36* (20), 2105–2122.

(14) Mastro, L. Del; Lambertini, M.; Bighin, C.; Levaggi, A.; D'Alonzo, A.; Giraudi, S.; Pronzato, P. *Expert Rev. Anticancer Ther.* **2012**, *12* (11), 1391–1405.

(15) Pernas, S.; Tolaney, S. M. *Ther. Adv. Med. Oncol.* **2019**, *11*, 1–16.

(16) Oh, D. Y.; Bang, Y. J. *Nat. Rev. Clin. Oncol.* **2020**, *17* (1), 33–48.

(17) Swain, S. M.; Kim, S. B.; Cortés, J.; Ro, J.; Semiglazov, V.; Campone, M.; Ciruelos, E.; Ferrero, J. M.; Schneeweiss, A.; Knott, A.; Clark, E.; Ross, G.; Benyunes, M. C.; Baselga, J. *Lancet Oncol.* **2013**, *14* (6), 461–471.

(18) Modi, S.; Saura, C.; Yamashita, T.; Park, Y. H.; Kim, S.-B.; Tamura, K.; Andre, F.; Iwata, H.; Ito, Y.; Tsurutani, J.; Sohn, J.; Denduluri, N.; Perrin, C.; Aogi, K.; Tokunaga, E.; Im, S.-A.; Lee, K. S.; Hurvitz, S. A.; Cortes, J.; Lee, C.; Chen, S.; Zhang, L.; Shahidi, J.; Yver, A.; Krop, I. *N. Engl. J. Med.* **2020**, *382* (7), 610–621.

(19) Murthy, R. K.; Loi, S.; Okines, A.; Paplomata, E.; Hamilton, E.; Hurvitz, S. A.; Lin, N. U.; Borges, V.; Abramson, V.; Anders, C.; Bedard, P. L.; Oliveira, M.; Jakobsen, E.; Bachelot, T.; Shachar, S. S.; Muller, V.; Braga, S.; Duhoux, F. P.; Greil, R.; Cameron, D.; Carey, L. A.; Curigliano, G.; Gelmon, K.; Hortobagyi, G.; Krop, I.; Loibl, S.; Pegram, M.; Slamon, D.; Palanca-Wessels, M. C.; Walker, L.; Feng, W.; Winer, E. P. *N. Engl. J. Med.* **2020**, *382* (7), 597–609.

(20) Kim, C.; Lee, C. K.; Chon, H. J.; Kim, J. H.; Park, H. S.; Heo, S. J.; Kim, H. J.; Kim, T. S.; Kwon, W. S.; Chung, H. C.; Rha, S. Y. *Oncotarget* **2017**, *8* (69), 113494–113501.

(21) Bang, Y. J.; Van Cutsem, E.; Feyereislova, A.; Chung, H. C.; Shen, L.; Sawaki, A.; Lordick, F.; Ohtsu, A.; Omuro, Y.; Satoh, T.; Aprile, G.; Kulikov, E.; Hill, J.; Lehle, M.; Rüschoff, J.; Kang, Y. K. *Lancet* **2010**, *376* (9742), 687–697.

(22) Sims, A. H.; Zweemer, A. J. M.; Nagumo, Y.; Faratian, D.; Muir, M.; Dodds, M.; Um, I.; Kay, C.; Hasmann, M.; Harrison, D. J.; Langdon, S. P. *Br. J. Cancer* **2012**, *106* (11), 1779–1789.

(23) Pohlmann, P. R.; Mayer, I. A.; Mernaugh, R. *Clin. Cancer Res.* **2009**, *15* (24), 7479–7491.

(24) Luque-Cabal, M.; García-Teijido, P.; Fernández-Pérez, Y.; Sánchez-Lorenzo, L.; Palacio-Vázquez, I. *Clin. Med. Insights Oncol.* **2016**, *10*, 21–30.

(25) Nagata, Y.; Lan, K. H.; Zhou, X.; Tan, M.; Esteva, F. J.; Sahin, A. A.; Klos, K. S.; Li, P.; Monia, B. P.; Nguyen, N. T.; Hortobagyi, G. N.; Hung, M. C.; Yu, D. *Cancer Cell* **2004**, *6* (2), 117–127.

(26) Nahta, R. *Int. Sch. Res. Netw.* **2012**, *2012* (428062), 1–16.

(27) Luque-Cabal, M.; García-Teijido, P.; Fernández-Pérez, Y.; Sánchez-Lorenzo, L.; Palacio-Vázquez, I. *Clin. Med. Insights Oncol.* **2016**, *10* (Suppl 1), 21–30.

(28) Pernas, S.; Tolaney, S. M. HER2-Positive Breast Cancer: New Therapeutic Frontiers and Overcoming Resistance.

(29) Chen, S.; Liang, Y.; Feng, Z.; Wang, M. *BMC Cancer* **2019**, *19* (1), 973.

(30) Verma, S.; Miles, D.; Gianni, L.; Krop, I. E.; Welslau, M.; Baselga, J.; Pegram, M.; Oh, D.-Y.; Diéras, V.; Guardino, E.; Fang, L.; Lu, M. W.; Olsen, S.; Blackwell, K. *N. Engl. J. Med.* **2012**, *367* (19), 1783–1791.

(31) Perez, E. A.; Cortés, J.; Gonzalez-angulo, A. M.; Bartlett, J. M. S. *Cancer Treat. Rev.* **2014**, *40* (2), 276–284.

(32) Murthy, P.; Kidwell, K. M.; Schott, A. F.; Merajver, S. D.; Griggs, J. J.; Smerage, J. D.; Van Poznak, C. H.; Wicha, M. S.; Hayes, D. F.; Henry, N. L. *Breast Cancer Res. Treat.* **2016**, *155* (3), 589–595.

(33) Joensuu, H. *Cancer Treat. Rev.* **2017**, *52*, 1–11.

(34) Tolaney, S. M.; Guo, H.; Pernas, S.; Barry, W. T.; Dillon, D. A.; Ritterhouse, L.;

Schneider, B. P.; Shen, F.; Fuhrman, K.; Baltay, M.; Dang, C. T.; Yardley, D. A.; Moy, B.; Kelly Marcom, P.; Albain, K. S.; Rugo, H. S.; Ellis, M. J.; Shapira, I.; Wolff, A. C.; Carey, L. A.; Overmoyer, B.; Partridge, A. H.; Hudis, C. A.; Krop, I. E.; Burstein, H. J.; Winer, E. P. *J. Clin. Oncol.* **2019**, *37* (22), 1868–1875.

(35) Gianni, L.; Pienkowski, T.; Im, Y. H.; Tseng, L. M.; Liu, M. C.; Lluch, A.; Starosławska, E.; de la Haba-Rodriguez, J.; Im, S. A.; Pedrini, J. L.; Poirier, B.; Morandi, P.; Semiglazov, V.; Srimuninnimit, V.; Bianchi, G. V.; Magazzù, D.; McNally, V.; Douthwaite, H.; Ross, G.; Valagussa, P. *Lancet Oncol.* **2016**, *17* (6), 791–800.

(36) Luque-Cabal, M.; García-Teijido, P.; Fernández-Pérez, Y.; Sánchez-Lorenzo, L.; Palacio-Vázquez, I. *Clin. Med. Insights Oncol.* **2016**, *10* (Suppl 1), 21–30.

(37) Andersson, M.; Lidbrink, E.; Bjerre, K. *J Clin Oncol* **2011**, *29* (3), 264–271.

(38) Derakhshani, A.; Rezaei, Z.; Safarpour, H.; Sabri, M.; Mir, A.; Sanati, M. A.; Vahidian, F.; Gholamiyan Moghadam, A.; Aghadoukht, A.; Hajiasgharzadeh, K.; Baradaran, B. *J. Cell. Physiol.* **2020**, *235* (4), 3142–3156.

(39) Valabrega, G.; Montemurro, F.; Sarotto, I.; Petrelli, A.; Rubini, P.; Tacchetti, C.; Aglietta, M.; Comoglio, P. M.; Giordano, S. *Oncogene* **2005**, *24* (18), 3002–3010.

(40) Takuwa, H.; Tsuji, W.; Yotsumoto, F. *Int. J. Surg. Case Rep.* **2018**, *52*, 125–131.

(41) New Treatments Emerge for Metastatic HER2+ Breast Cancer - National Cancer Institute https://www.cancer.gov/news-events/cancer-currents-blog/2020/tucatinib-trastuzumab-deruxtecan-her2-positive-metastatic-breast-cancer (accessed Jun 1, 2020).

(42) Stern, H. M.; Gardner, H.; Burzykowski, T.; Elatre, W.; O'Brien, C.; Lackner, M. R.; Pestano, G. A.; Santiago, A.; Villalobos, I.; Eiermann, W.; Pienkowski, T.; Martin, M.; Robert, N.; Crown, J.; Nuciforo, P.; Bee, V.; Mackey, J.; Slamon, D. J.; Press, M. F. *Clin. Cancer Res.* **2015**, *21* (9), 2065–2074.

(43) Vu, T.; Claret, F. X. *Front. Oncol.* **2012**, *2* (June), 62.

(44) Bartsch, R.; Wenzel, C.; Steger, G. G. *Biologics* **2007**, *1* (1), 19–31.

(45) Gschwantler-Kaulich, D.; Tan, Y. Y.; Fuchs, E.-M.; Hudelist, G.; Köstler, W. J.; Reiner, A.; Leser, C.; Salama, M.; Attems, J.; Deutschmann, C.; Zielinski, C. C.; Singer, C. F. *PLoS One* **2017**, *12* (3), e0172911.

(46) Gajria, D.; Chandarlapaty, S. *Expert Rev. Anticancer Ther.* **2011**, *11* (2), 263–275.

(47) Mercogliano, M. F.; Bruni, S.; Elizalde, P. V.; Schillaci, R. *Front. Oncol.* **2020**, *10*, 584.

(48) Rimawi, M. F.; de Angelis, C.; Contreras, A.; Pareja, F.; Geyer, F. C.; Burke, K. A.; Herrera, S.; Wang, T.; Mayer, I. A.; Forero, A.; Nanda, R.; Goetz, M. P.; Chang, J. C.; Krop, I. E.; Wolff, A. C.; Pavlick, A. C.; Fuqua, S. A. W.; Gutierrez, C.; Hilsenbeck, S. G.; Li, M. M.; Weigelt, B.; Reis-Filho, J. S.; Osborne, C. K.;

Schiff, R. *Breast Cancer Res. Treat.* **2018**, *167* (3), 731–740.

(49) Lebok, P.; Kopperschmidt, V.; Kluth, M.; Hube-Magg, C.; Özden, C.; Taskin, B.; Hussein, K.; Mittenzwei, A.; Lebeau, A.; Witzel, I.; Wölber, L.; Mahner, S.; Jänicke, F.; Geist, S.; Paluchowski, P.; Wilke, C.; Heilenkötter, U.; Simon, R.; Sauter, G.; Terracciano, L.; Krech, R.; Von, A.; Müller, V.; Burandt, E. *BMC Cancer* **2015**, *15* (1–10).

(50) Li, S.; Shen, Y.; Wang, M.; Yang, J.; Lv, M.; Li, P.; Chen, Z.; Yang, J. *Oncotarget* **2017**, *8* (19), 32043–32054.

(51) Kechagioglou, P.; Papi, R. M.; Provatopoulou, X.; Kalogera, E.; Papadimitriou, E.; Grigoropoulos, P.; Nonni, A.; Zografos, G.; Kyriakidis, D. A.; Gounaris, A. *Anticancer Res.* **2014**, *34* (3), 1387–1400.

(52) Chalhoub, N.; Baker, S. J. *Annu. Rev. Pathol. Mech. Dis.* **2009**, *4* (1), 127–150.

(53) Paplomata, E.; O'regan, R. *Ther. Adv. Med. Oncol.* **2014**, *6* (4), 154–166.

(54) Keniry, M.; Parsons, R. *Oncogene* **2008**, *27* (41), 5477–5485.

(55) Ebbesen, S. H.; Scaltriti, M.; Bialucha, C. U.; Morse, N.; Kastenhuber, E. R.; Wen, H. Y.; Dow, L. E.; Baselga, J.; Lowe, S. W. *Proc. Natl. Acad. Sci. U. S. A.* **2016**, *113* (11), 3030–3035.

(56) Luongo, F.; Colonna, F.; Calapà, F.; Vitale, S.; Fiori, M. E.; De Maria, R. *Cancers (Basel).* **2019**, *11* (8), 1076.

(57) Carracedo, A.; Pandolfi, P. P. *Oncogene* **2008**, *27* (41), 5527–5541.

(58) Crowell, J. A.; Steele, V. E.; Fay, J. R. *Mol. Cancer Ther.* **2007**, *6* (8), 2139–2148.

(59) Endersby, R.; Baker, S. J. *Oncogene* **2008**, *27* (41), 5416–5430.

(60) Nuciforo, P. G.; Aura, C.; Holmes, E.; Prudkin, L.; Jimenez, J.; Martinez, P.; Ameels, H.; de la Perna, L.; Ellis, C.; Eidtmann, H.; Piccart-Gebhart, M. J.; Scaltriti, M.; Baselga, J. *Ann. Oncol.* **2015**, *26* (7), 1494–1500.

(61) Carbognin, L.; Miglietta, F.; Paris, I.; Dieci, M. V. *Cancers (Basel).* **2019**, *11* (9), 1–18.

(62) Jones, N.; Bonnet, F.; Sfar, S.; Lafitte, M.; Lafon, D.; Sierankowski, G.; Brouste, V.; Banneau, G.; Tunon de Lara, C.; Debled, M.; MacGrogan, G.; Longy, M.; Sevenet, N. *Int. J. Cancer* **2013**, *133* (2), 323–334.

(63) Zhang, H. Y.; Liang, F.; Jia, Z. L.; Song, S. T.; Jiang, Z. F. *Oncol. Lett.* **2013**, *6* (1), 161–168.

(64) Zhu, Y.; Wloch, A.; Wu, Q.; Peters, C.; Pagenstecher, A.; Bertalanffy, H.; Sure, U. *Stroke* **2009**, *40* (3), 820–826.

(65) Kang, Y. H.; Lee, H. S.; Kim, W. H. *Lab. Investig.* **2002**, *82* (3), 285–291.

(66) Wilks, S. T. *Breast* **2015**, *24* (5), 548–555.

(67) Sangai, T.; Akcakanat, A.; Chen, H.; Tarco, E.; Wu, Y.; Do, K. A.; Miller, T. W.; Arteaga, C. L.; Mills, G. B.; Gonzalez-Angulo, A. M.; Meric-Bernstam, F. *Clin. Cancer Res.* **2012**, *18* (20), 5816–5828.

(68) Hudis, C.; Swanton, C.; Janjigian, Y. Y.; Lee, R.; Sutherland, S.; Lehman, R.; Chandarlapaty, S.; Hamilton, N.; Gajria, D.; Knowles, J.; Shah, J.; Shannon, K.; Tetteh, E.; Sullivan, D. M.; Moreno, C.; Yan, L.; Han, H. S. *Breast Cancer Res.* **2013**, *15* (6), R110.

(69) Xing, Y.; Lin, N. U.; Maurer, M. A.; Chen, H.; Mahvash, A.; Sahin, A.; Akcakanat, A.; Li, Y.; Abramson, V.; Litton, J.; Chavez-MacGregor, M.; Valero, V.; Piha-Paul, S. A.; Hong, D.; Do, K.-A.; Tarco, E.; Riall, D.; Eterovic, A. K.; Wulf, G. M.; Cantley, L. C.; Mills, G. B.; Doyle, L. A.; Winer, E.; Hortobagyi, G. N.; Gonzalez-Angulo, A. M.; Meric-Bernstam, F. *Breast Cancer Res.* **2019**, *21* (1), 78.

(70) Hurvitz, S. A.; Andre, F.; Jiang, Z.; Shao, Z.; Mano, M. S.; Neciosup, S. P.; Tseng, L. M.; Zhang, Q.; Shen, K.; Liu, D.; Dreosti, L. M.; Burris, H. A.; Toi, M.; Buyse, M. E.; Cabaribere, D.; Lindsay, M. A.; Rao, S.; Pacaud, L. B.; Taran, T.; Slamon, D. *Lancet Oncol.* **2015**, *16* (7), 816–829.

(71) Van Swearingen, A. E. D.; Siegel, M. B.; Deal, A. M.; Sambade, M. J.; Hoyle, A.; Hayes, D. N.; Jo, H.; Little, P.; Dees, E. C.; Muss, H.; Jolly, T.; Zagar, T. M.; Patel, N.; Miller, C. R.; Parker, J. S.; Smith, J. K.; Fisher, J.; Shah, N.; Nabell, L.; Nanda, R.; Dillon, P.; Abramson, V.; Carey, L. A.; Anders, C. K. *Breast Cancer Res. Treat.* **2018**, *171* (3), 637–648.

(72) Ramón y Cajal, S.; Sesé, M.; Capdevila, C.; Aasen, T.; De Mattos-Arruda, L.; Diaz-Cano, S. J.; Hernández-Losa, J.; Castellví, J. *J. Mol. Med.* **2020**, *98* (2), 161–177.

(73) Lee, H. J.; Seo, A. N.; Kim, E. J.; Jang, M. H.; Suh, K. J.; Ryu, H. S.; Kim, Y. J.; Kim, J. H.; Im, S.-A.; Gong, G.; Jung, K. H.; Park, I. A.; Park, S. Y. *Am. J. Clin. Pathol.* **2014**, *142* (6), 755–766.

(74) Rye, I. H.; Trinh, A.; Sætersdal, A. B.; Nebdal, D.; Lingjærde, O. C.; Almendro, V.; Polyak, K.; Børresen-Dale, A. L.; Helland, Å.; Markowetz, F.; Russnes, H. G. *Mol. Oncol.* **2018**, *12* (11), 1838–1855.

(75) Ferrari, A.; Vincent-Salomon, A.; Pivot, X.; Sertier, A. S.; Thomas, E.; Tonon, L.; Boyault, S.; Mulugeta, E.; Treilleux, I.; MacGrogan, G.; Arnould, L.; Kielbassa, J.; Le Texier, V.; Blanché, H.; Deleuze, J. F.; Jacquemier, J.; Mathieu, M. C.; Penault-Llorca, F.; Bibeau, F.; Mariani, O.; Mannina, C.; Pierga, J. Y.; Trédan, O.; Bachelot, T.; Bonnefoi, H.; Romieu, G.; Fumoleau, P.; Delaloge, S.; Rios, M.; Ferrero, J. M.; Tarpin, C.; Bouteille, C.; Calvo, F.; Gut, I. G.; Gut, M.; Martin, S.; Nik-Zainal, S.; Stratton, M. R.; Pauporté, I.; Saintigny, P.; Birnbaum, D.; Viari, A.; Thomas, G. *Nat. Commun.* **2016**, *7* (1), 1–9.

(76) Brady, S. W.; McQuerry, J. A.; Qiao, Y.; Piccolo, S. R.; Shrestha, G.; Jenkins, D. F.; Layer, R. M.; Pedersen, B. S.; Miller, R. H.; Esch, A.; Selitsky, S. R.; Parker, J. S.; Anderson, L. A.; Dalley, B. K.; Factor, R. E.; Reddy, C. B.; Boltax, J. P.; Li, D.

Y.; Moos, P. J.; Gray, J. W.; Heiser, L. M.; Buys, S. S.; Cohen, A. L.; Johnson, W. E.; Quinlan, A. R.; Marth, G.; Werner, T. L.; Bild, A. H. *Nat. Commun.* **2017**, *8* (1), 1–15.

(77) Korkaya, H.; Paulson, A.; Iovino, F.; Wicha, M. S. *Oncogene* **2008**, *27* (47), 6120–6130.

(78) Macosko, E. Z.; Basu, A.; Satija, R.; Nemesh, J.; Shekhar, K.; Goldman, M.; Tirosh, I.; Bialas, A. R.; Kamitaki, N.; Martersteck, E. M.; Trombetta, J. J.; Weitz, D. A.; Sanes, J. R.; Shalek, A. K.; Regev, A.; McCarroll, S. A. *Cell* **2015**, *161* (5), 1202–1214.

(79) Andrews, T. S.; Hemberg, M. *Mol. Aspects Med.* **2018**, *59*, 114–122.

(80) Ziegenhain, C.; Vieth, B.; Parekh, S.; Reinius, B.; Guillaumet-Adkins, A.; Smets, M.; Leonhardt, H.; Heyn, H.; Hellmann, I.; Enard, W. *Mol. Cell* **2017**, *65* (4), 631-643.e4.

(81) Ocasio, J.; Babcock, B.; Malawsky, D.; Weir, S. J.; Loo, L.; Simon, J. M.; Zylka, M. J.; Hwang, D.; Dismuke, T.; Sokolsky, M.; Rosen, E. P.; Vibhakar, R.; Zhang, J.; Saulnier, O.; Vladoiu, M.; El-Hamamy, I.; Stein, L. D.; Taylor, M. D.; Smith, K. S.; Northcott, P. A.; Colaneri, A.; Wilhelmsen, K.; Gershon, T. R. *Nat. Commun.* **2019**, *10* (1), 1–17.

(82) Korkaya, H.; Kim, G. II; Davis, A.; Malik, F.; Henry, N. L.; Ithimakin, S.; Quraishi, A. A.; Tawakkol, N.; D'Angelo, R.; Paulson, A. K.; Chung, S.; Luther, T.; Paholak, H. J.; Liu, S.; Hassan, K. A.; Zen, Q.; Clouthier, S. G.; Wicha, M. S. *Mol. Cell* **2012**, *47* (4), 570–584.

(83) Korkaya, H.; Paulson, A.; Charafe-Jauffret, E.; Ginestier, C.; Brown, M.; Dutcher, J.; Clouthier, S. G.; Wicha, M. S. *PLoS Biol.* **2009**, *7* (6), e1000121.

(84) Nagata, Y.; Lan, K. H.; Zhou, X.; Tan, M.; Esteva, F. J.; Sahin, A. A.; Klos, K. S.; Li, P.; Monia, B. P.; Nguyen, N. T.; Hortobagyi, G. N.; Hung, M. C.; Yu, D. *Cancer Cell* **2004**, *6* (2), 117–127.

(85) Goldman, E. M. and M. **2015**, 1–20.

(86) Nemesh, J. Drop-seq Core Computational Protocol http://mccarrolllab.org/wp-content/uploads/2016/03/Drop-seqAlignmentCookbookv1.2Jan2016.pdf (accessed Sep 1, 2020).

(87) Zappia, L.; Oshlack, A. *Gigascience* **2018**, *7* (7), 1–9.

(88) Sergushichev, A. A. *bioRxiv* **2016**, 060012.

(89) Subramanian, A.; Tamayo, P.; Mootha, V. K.; Mukherjee, S.; Ebert, B. L.; Gillette, M. A.; Paulovich, A.; Pomeroy, S. L.; Golub, T. R.; Lander, E. S.; Mesirov, J. P. *Proc. Natl. Acad. Sci. U. S. A.* **2005**, *102* (43), 15545–15550.

(90) Smith, S. E.; Mellor, P.; Ward, A. K.; Kendall, S.; McDonald, M.; Vizeacoumar, F. S.; Vizeacoumar, F. J.; Napper, S.; Anderson, D. H. *Breast Cancer Res.* **2017**, *19*

(1), 65.

(91) Jernström, S.; Hongisto, V.; Leivonen, S. K.; Due, E. U.; Tadele, D. S.; Edgren, H.; Kallioniemi, O.; Perälä, M.; Mælandsmo, G. M.; Sahlberg, K. K. *Breast Cancer Targets Ther.* **2017**, *9*, 185–198.

(92) Becht, E.; McInnes, L.; Healy, J.; Dutertre, C. A.; Kwok, I. W. H.; Ng, L. G.; Ginhoux, F.; Newell, E. W. *Nat. Biotechnol.* **2019**, *37* (1), 38–47.

(93) Luecken, M. D.; Theis, F. J. *Mol. Syst. Biol.* **2019**, *15* (6).

(94) Li, W.; Freudenberg, J.; Suh, Y. J.; Yang, Y. *Comput. Biol. Chem.* **2014**, *48*, 77–83.

(95) McDermaid, A.; Monier, B.; Zhao, J.; Liu, B.; Ma, Q. *Briefings in Bioinformatics*. Oxford University Press November 1, 2019, pp 2044–2054.

(96) Capaldo, C. T.; Nusrat, A. *Biochim. Biophys. Acta - Biomembr.* **2009**, *1788* (4), 864–871.

(97) Shen, W.-H.; Zhou, J.-H.; Broussard, S. R.; Freund, G. G.; Dantzer, R.; Kelley, K. W. *Cancer Res.* **2002**, 4746–4756.

(98) Yang, J.; Min, K.-W.; Kim, D.-H.; Son, B. K.; Moon, K. M.; Wi, Y. C.; Bang, S. S.; Oh, Y. H.; Do, S.-I.; Chae, S. W.; Oh, S.; Kim, Y. H.; Kwon, M. J. *PLoS One* **2018**, *13* (8), e0202113.

(99) Cai, X.; Cao, C.; Li, J.; Chen, F.; Zhang, S.; Liu, B.; Zhang, W.; Zhang, X.; Ye, L. *Oncotarget* **2017**, *8* (35), 58338–58352.

(100) Mostowy, S.; Shenoy, A. R. *Nat. Rev. Immunol.* **2015**, *15* (9), 559–573.

(101) Wang, W.; Eddy, R.; Condeelis, J. *Nat. Rev. Cancer* **2007**, *7* (6), 429–440.

(102) Nakayama, K. I.; Nakayama, K. *Nat. Rev. Cancer* **2006**, *6* (5), 369–381.

(103) Bassermann, F.; Eichner, R.; Pagano, M. *Biochim. Biophys. Acta - Mol. Cell Res.* **2014**, *1843* (1), 150–162.

(104) Gan, B.; DePinho, R. A. *Cell Cycle* **2009**, *8* (7), 1003–1006.

(105) Laplante, M.; Sabatini, D. M. *J. Cell Sci.* **2009**, *122* (20), 3589–3594.

(106) Kallergi, G.; Tsintari, V.; Sfakianakis, S.; Bei, E.; Lagoudaki, E.; Koutsopoulos, A.; Zacharopoulou, N.; Alkahtani, S.; Alarifi, S.; Stournaras, C.; Zervakis, M.; Georgoulias, V. *Breast Cancer Res.* **2019**, *21* (1), 86.

(107) Hasan, Z.; Koizumi, S. I.; Sasaki, D.; Yamada, H.; Arakaki, N.; Fujihara, Y.; Okitsu, S.; Shirahata, H.; Ishikawa, H. *Nat. Commun.* **2017**, *8*.

(108) Gong, C.; Shen, J.; Fang, Z.; Qiao, L.; Feng, R.; Lin, X.; Li, S. *Biosci. Rep.* **2018**, *38* (4).

(109) Sundqvist, A.; Morikawa, M.; Ren, J.; Vasilaki, E.; Kawasaki, N.; Kobayashi, M.;

Koinuma, D.; Aburatani, H.; Miyazono, K.; Heldin, C. H.; Van Dam, H.; Dijke, P. Ten. *Nucleic Acids Res.* **2018**, *46* (3), 1180–1195.

(110) Mendoza-Rodríguez, M.; Arévalo Romero, H.; Fuentes-Pananá, E. M.; Ayala-Sumuano, J. T.; Meza, I. *Cancer Lett.* **2017**, *390*, 39–44.

(111) Liu, S.; Lee, J. S.; Jie, C.; Park, M. H.; Iwakura, Y.; Patel, Y.; Soni, M.; Reisman, D.; Chen, H. *Cancer Res.* **2018**, *78* (8), 2040–2051.

(112) Korkaya, H.; Kim, G. Il; Davis, A.; Malik, F.; Henry, N. L.; Ithimakin, S.; Quraishi, A. A.; Tawakkol, N.; D'Angelo, R.; Paulson, A. K.; Chung, S.; Luther, T.; Paholak, H. J.; Liu, S.; Hassan, K. A.; Zen, Q.; Clouthier, S. G.; Wicha, M. S. *Mol. Cell* **2012**, *47* (4), 570–584.

(113) Zhang, Z.; Xu, Q.; Song, C.; Mi, B.; Zhang, H.; Kang, H.; Liu, H.; Sun, Y.; Wang, J.; Lei, Z.; Guan, H.; Li, F. *Mol. Cancer Ther.* **2020**, *19* (2), 650–660.

(114) Fagerli, U. M.; Ullrich, K.; Stühmer, T.; Holien, T.; Köchert, K.; Holt, R. U.; Bruland, O.; Chatterjee, M.; Nogai, H.; Lenz, G.; Shaughnessy, J. D.; Mathas, S.; Sundan, A.; Bargou, R. C.; Dörken, B.; Børset, M.; Janz, M. *Oncogene* **2011**, *30* (28), 3198–3206.

(115) Sahoo, S.; Brickley, D. R.; Kocherginsky, M.; Conzen, S. D. *Eur. J. Cancer* **2005**, *41* (17), 2754–2759.

(116) Mistry, P.; Deacon, K.; Mistry, S.; Blank, J.; Patel, R. *J. Biol. Chem.* **2004**, *279* (2), 1482–1490.

(117) Reymond, N.; Im, J. H.; Garg, R.; Cox, S.; Soyer, M.; Riou, P.; Colomba, A.; Muschel, R. J.; Ridley, A. J. *Mol. Oncol.* **2015**, *9* (6), 1043–1055.

(118) Tomaskovic-Crook, E.; Thompson, E. W.; Thiery, J. P. *Breast Cancer Res.* **2009**, *11* (6), 213.

(119) Kalluri, R.; Weinberg, R. A. *J. Clin. Invest.* **2009**, *119* (6), 1420–1428.

(120) Pastushenko, I.; Blanpain, C. *Trends Cell Biol.* **2019**, *29* (3), 212–226.

(121) Chu, P. G.; Weiss, L. M. *Histopathology* **2002**, *40* (5), 403–439.

(122) Xiang, X.; Deng, Z.; Zhuang, X.; Ju, S.; Mu, J.; Jiang, H.; Zhang, L.; Yan, J.; Miller, D.; Zhang, H.-G. *PLoS One* **2012**, *7* (12), e50781.

(123) Schmalhofer, O.; Brabletz, S.; Brabletz, T. *Cancer Metastasis Rev.* **2009**, *28* (1–2), 151–166.

(124) Zhang, S.; Wang, Z.; Liu, W.; Lei, R.; Shan, J.; Li, L.; Wang, X. *Sci. Rep.* **2017**, *7*.

(125) Nasser, M. W.; Qamri, Z.; Deol, Y. S.; Ravi, J.; Powell, C. A.; Trikha, P.; Schwendener, R. A.; Bai, X. F.; Shilo, K.; Zou, X.; Leone, G.; Wolf, R.; Yuspa, S. H.; Ganju, R. K. *Cancer Res.* **2012**, *72* (3), 604–615.

(126) West, N. R.; Watson, P. H. *Oncogene* **2010**, *29* (14), 2083–2092.

(127) Paruchuri, V.; Prasad, A.; McHugh, K.; Bhat, H. K.; Polyak, K.; Ganju, R. K. *PLoS One* **2008**, *3* (3), 1741.

(128) Emberley, E. D.; Murphy, L. C.; Watson, P. H. *Breast Cancer Res.* **2004**, *6* (4), 153–159.

(129) Cancemi, P.; Buttacavoli, M.; Cara, G. Di; Albanese, N. N.; Bivona, S.; Pucci-Minafra, I.; Feo, S. *Oncotarget* **2018**, *9* (49), 29064–29081.

(130) Hua, X.; Zhang, H.; Jia, J.; Chen, S.; Sun, Y.; Zhu, X. *Biomed. Pharmacother.* **2020**, *127*, 110156.

(131) Yuzugullu, H.; Von, T.; Thorpe, L. M.; Walker, S. R.; Roberts, T. M.; Frank, D. A.; Zhao, J. J. *Cell Discov.* **2016**, *2* (1), 1–13.

(132) Sadasivam, S.; DeCaprio, J. A. *Nat. Rev. Cancer* **2013**, *13* (8), 585–595.

(133) Min, M.; Spencer, S. L. *PLOS Biol.* **2019**, *17* (3), e3000178.

(134) Bracken, A. P.; Ciro, M.; Cocito, A.; Helin, K. *Trends Biochem. Sci.* **2004**, *29* (8), 409–417.

(135) Ito, T.; Teo, Y. V.; Evans, S. A.; Neretti, N.; Sedivy Correspondence, J. M. *Cell Rep.* **2018**, *22*, 3480–3492.

(136) Vizán, P.; Gutiérrez, A.; Espejo, I.; García-Montolio, M.; Lange, M.; Carretero, A.; Lafzi, A.; de Andrés-Aguayo, L.; Blanco, E.; Thambyrajah, R.; Graf, T.; Heyn, H.; Bigas, A.; Di Croce, L. *Sci. Adv.* **2020**, *6* (32), eabb2745.

(137) Doyle, L. A.; Ross, D. D. *Oncogene* **2003**, *22* (47 REV. ISS. 6), 7340–7358.

(138) Balaji, S. A.; Udupa, N.; Chamallamudi, M. R.; Gupta, V.; Rangarajan, A. *PLoS One* **2016**, *11* (5).

(139) Lucanus, A. J.; Yip, G. W. *Nat. Publ. Gr.* **2018**.

(140) Mandelkow, E.; Mandelkow, E. M. *Trends Cell Biol.* **2002**, *12* (12), 585–591.

(141) Ivanov, A. I.; McCall, I. C.; Babbin, B.; Samarin, S. N.; Nusrat, A.; Parkos, C. A. *BMC Cell Biol.* **2006**, *7* (1), 12.

(142) Li, T.-F.; Zeng, H.-J.; Shan, Z.; Ye, R.-Y.; Cheang, T.-Y.; Zhang, Y.-J.; Lu, S.-H.; Zhang, Q.; Shao, N.; Lin, Y. .

(143) Hirokawa, N.; Noda, Y.; Tanaka, Y.; Niwa, S. *Nat. Rev. Mol. Cell Biol.* **2009**, *10* (10), 682–696.

(144) Li, B.; Dou, S. X.; Yuan, J. W.; Liu, Y. R.; Li, W.; Ye, F.; Wang, P. Y.; Li, H. *Proc. Natl. Acad. Sci. U. S. A.* **2018**, *115* (48), 12118–12123.

(145) Kwon, M. J.; Park, S.; Choi, J. Y.; Oh, E.; Kim, Y. J.; Park, Y. H.; Cho, E. Y.; Kwon, M. J.; Nam, S. J.; Im, Y. H.; Shin, Y. K.; Choi, Y. L. *Br. J. Cancer* **2012**, *106* (5), 923–930.

(146) Yang, X. H.; Richardson, A. L.; Torres-Arzayus, M. I.; Zhou, P.; Sharma, C.; Kazarov, A. R.; Andzelm, M. M.; Strominger, J. L.; Brown, M.; Hemler, M. E. *Cancer Res.* **2008**, *68* (9), 3204–3213.

(147) Kumar, S.; Park, S. H.; Cieply, B.; Schupp, J.; Killiam, E.; Zhang, F.; Rimm, D. L.; Frisch, S. M. *Mol. Cell. Biol.* **2011**, *31* (19), 4036–4051.

(148) Rasiah, P. K.; Maddala, R.; Bennett, V.; Rao, P. V. *Dev. Biol.* **2019**, *446* (1), 119–131.

(149) Kurozumi, S.; Joseph, C.; Raafat, S.; Sonbul, S.; Kariri, Y.; Alsaeed, S.; Pigera, M.; Alsaleem, M.; Nolan, C. C.; Johnston, S. J.; Aleskandarany, M. A.; Ogden, A.; Fujii, T.; Shirabe, K.; Martin, S. G.; Alshankyty, I.; Mongan, N. P.; Ellis, I. O.; Green, A. R.; Rakha, E. A. *Breast Cancer Res. Treat.* **2019**, *176* (1), 63–73.

(150) Gröger, C. J.; Grubinger, M.; Waldhör, T.; Vierlinger, K.; Mikulits, W. *PLoS One* **2012**, *7* (12), e51136.

(151) Mrouj, K.; Singh, P.; Sobecki, M.; Dubra, G.; Ghoul, E. Al; Aznar, A.; Prieto, S.; Vincent, C.; Pirot, N.; Bernex, F.; Bordignon, B.; Hassen-Khodja, C.; Pouzolles, M.; Zimmerman, V.; Dardalhon, V.; Villalba, M.; Krasinska, L.; Fisher, D. *bioRxiv* **2019**, 712380.

(152) Mani, S. A.; Guo, W.; Liao, M. J.; Eaton, E. N.; Ayyanan, A.; Zhou, A. Y.; Brooks, M.; Reinhard, F.; Zhang, C. C.; Shipitsin, M.; Campbell, L. L.; Polyak, K.; Brisken, C.; Yang, J.; Weinberg, R. A. *Cell* **2008**, *133* (4), 704–715.

(153) Foroni, C.; Broggini, M.; Generali, D.; Damia, G. *Cancer Treat. Rev.* **2012**, *38* (6), 689–697.

(154) Collier, M. P.; Benesch, J. L. P. *Cell Stress Chaperones* **2020**, *25* (4), 601–613.

(155) Gunning, P. W.; Hardeman, E. C.; Lappalainen, P.; Mulvihill, D. P. *J. Cell Sci.* **2015**, *128* (16), 2965–2974.

(156) Chou, D. M.; Elledge, S. J. *Proc. Natl. Acad. Sci. U. S. A.* **2006**, *103* (48), 18143–18147.

(157) Kröger, C.; Afeyan, A.; Mraz, J.; Eaton, E. N.; Reinhardt, F.; Khodor, Y. L.; Thiru, P.; Bierie, B.; Ye, X.; Burge, C. B.; Weinberg, R. A. *Proc. Natl. Acad. Sci. U. S. A.* **2019**, *116* (15), 7353–7362.

(158) Xiao, W.; Zheng, S.; Xie, X.; Li, X.; Zhang, L.; Yang, A.; Wang, J.; Tang, H.; Xie, X. *Mol. Ther. - Oncolytics* **2020**, *17*, 118–129.

(159) Wang, C. Q.; Tang, C. H.; Wang, Y.; Jin, L.; Wang, Q.; Li, X.; Hu, G. N.; Huang, B. F.; Zhao, Y. M.; Su, C. M. *Sci. Rep.* **2017**, *7* (1).

(160) Nami, B.; Wang, Z. *Cancers (Basel).* **2018**, *10* (8), 274.

(161) Ebright, R. Y.; Lee, S.; Wittner, B. S.; Niederhoffer, K. L.; Nicholson, B. T.; Bardia, A.; Truesdell, S.; Wiley, D. F.; Wesley, B.; Li, S.; Mai, A.; Aceto, N.; Vincent-Jordan, N.; Szabolcs, A.; Chirn, B.; Kreuzer, J.; Comaills, V.; Kalinich, M.; Haas,

W.; Ting, D. T.; Toner, M.; Vasudevan, S.; Haber, D. A.; Maheswaran, S.; Micalizzi, D. S. *Science (80-.).* **2020**, *367* (6485), 1468–1473.

(162) Prashar, A.; Schnettger, L.; Bernard, E. M.; Gutierrez, M. G. *Front. Cell. Infect. Microbiol.* **2017**, *7* (SEP), 435.

(163) Barbera, S.; Nardi, F.; Elia, I.; Realini, G.; Lugano, R.; Santucci, A.; Tosi, G. M.; Dimberg, A.; Galvagni, F.; Orlandini, M. *Cell Commun. Signal.* **2019**, *17* (1), 55.

(164) Kim, S. E.; Hinoue, T.; Kim, M. S.; Sohn, K. J.; Cho, R. C.; Cole, P. D.; Weisenberger, D. J.; Laird, P. W.; Kim, Y. I. *Genes Nutr.* **2015**, *10* (1), 1–17.

(165) Maggini, S.; Pierre, A.; Calder, P. C. *Nutrients* **2018**, *10* (10).

(166) MacEyka, M.; Spiegel, S. *Nature* **2014**, *510* (7503), 58–67.

(167) Waumans, Y.; Baerts, L.; Kehoe, K.; Lambeir, A. M.; De Meester, I. *Front. Immunol.* **2015**, *6* (JUL), 387.

(168) Kingsbury, S. R.; Loddo, M.; Fanshawe, T.; Obermann, E. C.; Prevost, A. T.; Stoeber, K.; Williams, G. H. *Exp. Cell Res.* **2005**, *309* (1), 56–67.

(169) Gookin, S.; Min, M.; Phadke, H.; Chung, M.; Moser, J.; Miller, I.; Carter, D.; Spencer, S. L. *PLOS Biol.* **2017**, *15* (9), e2003268.

(170) Kabraji, S.; Solé, X.; Huang, Y.; Bango, C.; Bowden, M.; Bardia, A.; Sgroi, D.; Loda, M.; Ramaswamy, S. *Breast Cancer Res.* **2017**, *19* (1), 88.

(171) Le, X. F.; Lammayot, A.; Gold, D.; Lu, Y.; Mao, W.; Chang, T.; Patel, A.; Mills, G. B.; Bast, R. C. *J. Biol. Chem.* **2005**, *280* (3), 2092–2104.

(172) Sun, H.; Liu, K.; Huang, J.; Sun, Q.; Shao, C.; Luo, J.; Xu, L.; Shen, Y.; Ren, B. *Onco. Targets. Ther.* **2019**, *Volume 12*, 2829–2842.

(173) FAM111B gene - Genetics Home Reference - NIH https://ghr.nlm.nih.gov/gene/FAM111B (accessed Aug 8, 2020).

(174) Chung, V. Y.; Tan, T. Z.; Ye, J.; Huang, R. L.; Lai, H. C.; Kappei, D.; Wollmann, H.; Guccione, E.; Huang, R. Y. J. *Commun. Biol.* **2019**, *2* (1), 1–15.

(175) Jolly, M. K.; Tripathi, S. C.; Jia, D.; Mooney, S. M.; Celiktas, M.; Hanash, S. M.; Mani, S. A.; Pienta, K. J.; Ben-Jacob, E.; Levine, H. *Oncotarget* **2016**, *7* (19), 27067–27084.

(176) Cieply, B.; Riley IV, P.; Pifer, P. M.; Widmeyer, J.; Addison, J. B.; Ivanov, A. V.; Denvir, J.; Frisch, S. M. *Cancer Res.* **2012**, *72* (9), 2440–2453.

(177) Mooney, S. M.; Talebian, V.; Jolly, M. K.; Jia, D.; Gromala, M.; Levine, H.; McConkey, B. J. *J. Cell. Biochem.* **2017**, *118* (9), 2559–2570.

(178) Sánchez-Tilló, E.; De Barrios, O.; Siles, L.; Cuatrecasas, M.; Castells, A.; Postigo, A. *Proc. Natl. Acad. Sci. U. S. A.* **2011**, *108* (48), 19204–19209.

(179) Lee, J.; Ouh, Y.; Ahn, K. H.; Hong, S. C.; Oh, M.; Kim, J.; Cho, G. J. *PLoS One*

2017, *12* (5), 1–8.

(180) Gajria, D.; Chandarlapaty, S. *Expert Rev. Anticancer Ther.* **2011**, *11* (2), 263–275.

(181) Asgari, A.; Sharifzadeh, S.; Ghaderi, A.; Hosseini, A.; Ramezani, A. *Mol. Biol. Rep.* **2019**, *46* (6), 6205–6213.

(182) Dang, C. V. *Cell* **2012**, *149* (1), 22–35.

(183) Stine, Z. E.; Walton, Z. E.; Altman, B. J.; Hsieh, A. L.; Dang, C. V. *Cancer Discov.* **2015**, *5* (10), 1024–1039.

(184) Chen, H.; Liu, H.; Qing, G. *Signal Transduct. Target. Ther.* **2018**, *3* (1), 1–7.

(185) Gabay, M.; Li, Y.; Felsher, D. W. *Cold Spring Harb. Perspect. Med.* **2014**, *4* (6), 1–14.

(186) Richart, L.; Carrillo-de Santa Pau, E.; Río-Machín, A.; de Andrés, M. P.; Cigudosa, J. C.; Lobo, V. J. S.-A.; Real, F. X. *Nat. Commun.* **2016**, *7*, 10153.

(187) Dang, C. V. **2013**, 1–15.

(188) Bouvard, C.; Lim, S. M.; Ludka, J.; Yazdani, N.; Woods, A. K.; Chatterjee, A. K.; Schultz, P. G.; Zhu, S. *Proc. Natl. Acad. Sci. U. S. A.* **2017**, *114* (13), 3497–3502.

(189) Tawani, A.; Mishra, S. K.; Kumar, A. *Sci. Rep.* **2017**, *7* (1), 1–13.

(190) Mathad, R. I.; Hatzakis, E.; Dai, J.; Yang, D. *Nucleic Acids Res.* **2011**, *39* (20), 9023–9033.

(191) Siddiqui-Jain, A.; Grand, C. L.; Bearss, D. J.; Hurley, L. H. *Proc. Natl. Acad. Sci. U. S. A.* **2002**, *99* (18), 11593–11598.

(192) Castell, A.; Yan, Q.; Karin, F.; Hydbring, P.; Zhang, F.; Verschut, V.; Franco, M.; Zakaria, S. M.; Bazzar, W.; Goodwin, J.; Zinzalla, G.; Larson, L.-G. *Sci. Rep.* **2018**, *8* (May), 1–17.

(193) Kiessling, A.; Sperl, B.; Hollis, A.; Eick, D.; Berg, T. *Chem. Biol.* **2006**, *13* (7), 745–751.

(194) Berg, T.; Cohen, S. B.; Desharnais, J.; Sonderegger, C.; Maslyar, D. J.; Goldberg, J.; Boger, D. L.; Vogt, P. K. *Proc. Natl. Acad. Sci. U. S. A.* **2002**, *99* (6), 3830–3835.

(195) Whitfield, J. R.; Beaulieu, M. E.; Soucek, L. *Front. Cell Dev. Biol.* **2017**, *5* (FEB), 10.

(196) Castell, A.; Larsson, L. *Cancer Discov.* **2015**, *5* (7), 701–704.

(197) Carabet, L. A.; Rennie, P. S.; Cherkasov, A. *Int. J. Mol. Sci.* **2019**, *20* (1).

(198) Dang, C. V.; Reddy, E. P.; Shokat, K. M.; Soucek, L. *Nat. Rev. Cancer* **2017**, *17* (8), 502–508.

(199) McKeown, M. R.; Bradner, J. E. *Cold Spring Harb. Perspect. Med.* **2014**, *4* (10).

(200) Thomas, L. R.; Wang, Q.; Grieb, B. C.; Phan, J.; Foshage, A. M.; Sun, Q.; Olejniczak, E. T.; Clark, T.; Dey, S.; Lorey, S.; Alicie, B.; Howard, G. C.; Cawthon, B.; Ess, K. C.; Eischen, C. M.; Zhao, Z.; Fesik, S. W.; Tansey, W. P. *Mol. Cell* **2015**, *58* (3), 440–452.

(201) Thomas, L. R.; Tansey, W. P. *Open Access J. Sci. Technol.* **2015**, *3*, 1–25.

(202) Karatas, H.; Townsend, E. C.; Bernard, D.; Dou, Y.; Wang, S. *J. Med. Chem.* **2010**, *53*, 5179–5185.

(203) Odho, Z.; Southall, S. M.; Wilson, J. R. *J. Biol. Chem.* **2010**, *285* (43), 32967–32976.

(204) Dias, J.; Nguyen, N. Van; Georgiev, P.; Gaub, A.; Brettschneider, J.; Cusack, S.; Kadlec, J.; Akhtar, A. *Genes Dev.* **2014**, *28*, 929–942.

(205) Scott, D. E.; Coyne, A. G.; Hudson, S. A.; Abell, C. *Biochemistry* **2012**, *51*, 4990–5003.

(206) Murray, C. W.; Verdonk, M. L.; Rees, D. C. *Trends Pharmacol. Sci.* **2012**, *33* (5), 224–232.

(207) Huynh, K.; Partch, C. L. *Curr. Protoc. protein Sci.* **2015**, *79*, 28.9.1-28.9.14.

(208) Niesen, F. H.; Berglund, H.; Vedadi, M. *Nat. Protoc.* **2007**, *2* (9), 2212–2221.

(209) Jhoti, H.; Williams, G.; Rees, D. C.; Murray, C. W. *Nat. Publ. Gr.* **2013**, No. July.

(210) Kirsch, P.; Hartman, A. M.; Hirsch, A. K. H.; Empting, M. *Molecules* **2019**, *24* (23).

(211) Aldrich, C.; Bertozzi, C.; Georg, G. I.; Kiessling, L.; Lindsley, C.; Liotta, D.; Merz, K. M.; Schepartz, A.; Wang, S. *J. Med. Chem.* **2017**, *60* (6), 2165–2168.

(212) Zhang, Ji-hu, Chung, Thomas D.Y., Oldenburg, K. R. *J. Biomol. Screen.* **1999**, *4* (2), 67–73.

(213) Jacob, R. T.; Larsen, M. J.; Larsen, S. D.; Kirchhoff, P. D.; Sherman, D. H.; Neubig, R. R. *J. Biomol. Screen.* **2012**, *17* (8), 1080–1087.

(214) Karatas, H.; Townsend, E. C.; Cao, F.; Chen, Y.; Bernard, D.; Liu, L.; Lei, M.; Dou, Y.; Wang, S. *J. Am. Chem. Soc.* **2013**, *135* (2), 669–682.

(215) Cao, F.; Townsend, E. C.; Karatas, H.; Xu, J.; Li, L.; Lee, S.; Liu, L.; Chen, Y.; Ouillette, P.; Zhu, J.; Hess, J. L.; Atadja, P.; Lei, M.; Qin, Z. S.; Malek, S.; Wang, S.; Dou, Y. *Mol. Cell* **2014**, *53* (2), 247–261.

(216) Lea, W. A.; Simeonov, A. *Expert Opin. Drug Discov.* **2011**, *6* (1), 17–32.

(217) Rossi, A. M.; Taylor, C. W. *Nat. Protoc.* **2011**, *6* (3), 365–387.

(218) Hall, M. D.; Yasgar, A.; Peryea, T.; Braisted, J. C.; Jadhav, A.; Simeonov, A.; Coussens, N. P. *Methods Appl. Fluoresc.* **2016**, *4* (2), 022001.

(219) Koh, C. M.; Sabò, A.; Guccione, E. *BioEssays* **2016**, *38* (3), 266–275.

(220) Casey, S. C.; Tong, L.; Li, Y.; Do, R.; Walz, S.; Fitzgerald, K. N.; Gouw, A. M.; Baylot, V.; Gütgemann, I.; Eilers, M.; Felsher, D. W. *Science (80-.).* **2016**, *352* (6282), 227–231.

(221) Polivka, J.; Janku, F. *Pharmacol. Ther.* **2014**, *142* (2), 164–175.

(222) Chacón Simon, S.; Wang, F.; Thomas, L. R.; Phan, J.; Zhao, B.; Olejniczak, E. T.; MacDonald, J. D.; Shaw, J. G.; Schlund, C.; Payne, W.; Creighton, J.; Stauffer, S. R.; Waterson, A. G.; Tansey, W. P.; Fesik, S. W. *J. Med. Chem.* **2020**, *63* (8), 4315–4333.

(223) Macdonald, J. D.; Chacón Simon, S.; Han, C.; Wang, F.; Shaw, J. G.; Howes, J. E.; Sai, J.; Yuh, J. P.; Camper, D.; Alicie, B. M.; Alvarado, J.; Nikhar, S.; Payne, W.; Aho, E. R.; Bauer, J. A.; Zhao, B.; Phan, J.; Thomas, L. R.; Rossanese, O. W.; Tansey, W. P.; Waterson, A. G.; Stauffer, S. R.; Fesik, S. W. *J. Med. Chem.* **2019**, *62* (24), 11232–11259.

Chapter 4: Concluding Remarks

4.1. Summary of Findings

In this dissertation, we presented the characterization of PTEN deficiency and preliminary observations of trastuzumab treatment studies in HER2+ breast cancer cell lines using single cell transcriptomics. We uncovered consequences of intra- and intertumoral heterogeneity by dissecting the effects of PTEN deficiency in HER2+ breast cancer cell lines. Studies towards unraveling how PTEN deficiency affected intratumoral heterogeneity were performed using comparative transcriptomics analyses of subpopulations in parental and shPTEN cell lines. Insights about the intertumoral consequences of PTEN deficiency were extracted from comparative transcriptomic analyses between cell lines. At a single cell resolution, we found that PTEN k.d. increased the global quiescent properties compared to the parental cell line as evidenced by the decreased cell cycle activity. Furthermore, PTEN k.d. expanded a quiescent, epithelial early EMT subpopulation by 84 fold, 120 fold, and 2.4 fold in HCC1954, SKBR3, and BT474, respectively. The phenotype of these expanded subpopulations was characterized as epithelial, early EMT because these expanded subpopulations expressed epithelial keratins, claudins, and EPCAM. However, they expressed low levels of E-cadherin, a critical cell adhesion protein found specifically on the surface of epithelial cells.[119,120,123,157] In addition, they expressed markers that facilitate EMT, such as S100 proteins, MKI67, FN1, and TNFSFR12A.[119,120,123–126,128–130,157] However, expression of traditional mesenchymal markers, such as vimentin and N-cadherin, were not detected by the subpopulations that expanded after PTEN k.d.[119,120,123,157] Interestingly, PTEN k.d. was shown to slightly increase intra-subpopulation heterogeneity by altering the expression of select genes that were critical for the phenotype of the subpopulation, such as cell cycling genes and cell adhesion proteins in HCC1954 and SKBR3 but not BT474. Comparative analyses between cell lines revealed context dependent consequences of PTEN deficiency in HER2+ breast cancer *in vitro*. Altogether, the characterization of

PTEN deficiency in HER2+ breast cancer revealed important clinical implications for cancer management for the subset of HER2+ breast cancer patients with a deficiency in the PTEN tumor suppressor.

In addition, treatment studies were performed to evaluate how the pre-existing transcriptomic profiles shaped by PTEN deficiency in HER2+ breast cancer cell lines would be altered in the presence of trastuzumab. We aimed to gain insight on how reduction of PTEN expression impacted the response of the HER2+ breast cancer cells to trastuzumab. Based on our characterization of the functional consequences of PTEN deficiency, we hypothesized that PTEN k.d. would enrich a quiescent subpopulation with epithelial early EMT characteristics and thus, this subpopulation would exhibit resistance to trastuzumab therapy. Using BT474 and MDA-MB-361, we were unable to observe substantial transcriptomic differences based on trastuzumab treatment. In treatment studies with BT474, we observed small subpopulation level changes between parental and PTEN k.d. cells, and treatment of BT474 PTEN k.d. cells appeared to elicit small subpopulation level changes, but those observations require further studies to yield conclusive results. Furthermore, we did not observe transcriptomic differences in MDA-MB-361 regardless of PTEN status or trastuzumab treatment. Limitations of our treatment studies included the insufficient number of treatment controls and the use of a cell line with a relatively small transcriptomic changes as a result of k.d. of PTEN (i.e. BT474). It is possible that the observations from our treatment studies with BT474 and MDA-MB-361 represented different behaviors of the cancer in response to treatment. In order to evaluate how the PTEN deficiency shapes the response to trastuzumab, it is critical to perform the treatment studies using HER2+ breast cancer cell lines where the transcriptomic changes resulting from k.d. of PTEN is larger than 2-4 fold. We believe appropriate cell lines for treatment studies include HCC1954 and SKBR3 because the transcriptomic changes that resulted from PTEN k.d. were 84 and 120 fold. Therefore, these cell lines represent more appropriate models to study the effect of PTEN loss on trastuzumab response. At this time, we are unable to conclude about the findings from our treatment studies.

4.2. Thoughts for Future Studies

Since PTEN deficiency shows clinical relevance to HER2+ breast cancer in the literature and our data suggested that PTEN deficiency could increase the aggressive cancer phenotype, we propose future studies that could provide more comprehensive characterization of the resultant cancer phenotype after k.d. of PTEN. These studies include additional treatment studies using cell lines that show observable functional consequences arising from k.d. of PTEN, such as HCC1954 and SKBR3. We proposed the use of these cell lines for our treatment analyses because they would be appropriate models to study the effects of PTEN deficiency on trastuzumab response. Our data suggested that those cell lines were very sensitive to k.d. of PTEN as suggested by the large magnitude of subpopulation level changes and the introduction of intra-subpopulation heterogeneity arising in PTEN k.d. cells. Since large, observable effects were found from these cell lines, we inferred that we would be able to observe additional transcriptomic changes after treatment of those cell lines with trastuzumab. These treatment studies are critical steps to understanding how PTEN loss in the 12-40% of HER2+ breast cancer patients affects these patients' inherent ability to respond to trastuzumab.

In addition to understanding how PTEN deficiency shapes the transcriptome to respond to trastuzumab, we are interested in leveraging insight about the consequences of PTEN deficiency to identify biomarkers that could predict trastuzumab response. Our central hypothesis for this work is that PTEN deficiency induces an aggressive cancer phenotype by enriching quiescent, epithelial, early EMT subpopulations and by introducing intra-subpopulation heterogeneity. Thus, it would be very valuable to pursue the identification of biomarkers that could effectively subset HER2+ breast cancer patients based on pre-existing transcriptomic signatures that characterize patients who would inherently respond poorly to therapy or even predict aggressive cancer. The use of biomarkers to subset patients based on pre-existing transcriptomes and to inform about patient response to HER2-directed therapy would help improve personalized medicine strategies for these patients and possibly improve patient outcome. Thus, we strongly believe future studies should include the biological and clinical validation of the subpopulations that were enriched by k.d. of PTEN in order to work towards the discovery

of biomarkers that could detect aggressive subpopulations of HER2+ breast cancer cells in patients. It is important to assess whether the group of HER2+ breast cancer patients with poor patient outcome and aggressive cancer phenotype is linked to the introduction of intra-subpopulation heterogeneity and/or the expansion of a quiescent, early EMT subpopulation, as suggested by our data. It would be ideal if the enriched quiescent early EMT subpopulations could be purified so that their functional properties could be analyzed. Identification of methods for purification of the subpopulation enriched by PTEN k.d. is a critical step prior to performing functional studies. In our studies, we found that subpopulation-specific markers for this quiescent early EMT phenotype was difficult to identify mainly due to its quiescent phenotype and the heterogeneous expression of various genes by this subpopulation. It appeared as though using markers for the subpopulations that did not enrich after PTEN k.d. as negative selection markers for the enriched subpopulations would be the most realistic approach. Alternatively, other routes to identifying biomarkers includes the use BioPortal to leverage RNA-seq data from previously sequenced HER2+ breast cancer tumor data to identify clinically relevant markers that are correlated with PTEN expression status and/or survival of HER2+ breast cancer patients. With the data leveraged from cBioPortal, we could apply a reverse approach where we identify clinically relevant markers to HER2+ breast cancer with PTEN deficiency to identify markers that characterize the enriched subpopulation in our single cell transcriptomics data. In summary, the identification of markers that could enable the purification of the enriched subpopulation that resulted from PTEN k.d. would be critical to working towards the goal of understanding how PTEN deficiency influences trastuzumab response and facilitating the discovery of alternative therapeutic strategies for patients who acquire resistance.

Aside from purifying the quiescent early EMT subpopulation, future studies should include functional studies to test whether or not the enriched subpopulations by PTEN k.d. would undergo additional enrichment and exhibit resistant phenotype. These functional studies include the assessment of the sensitivity of the enriched subpopulation to trastuzumab in cell viability assays (e.g. MTT assays and annexin V assay) to confirm if the enriched subpopulation are resistant to trastuzumab since quiescence and EMT programs are known to be linked to therapy resistance. Cell proliferation studies are

expected to reveal constant cell viability in the presence of trastuzumab treatment, which would support the resistance phenotype of the subpopulations that enriched after PTEN k.d. Additionally, we are interested in evaluating the invasive potential of the enriched subpopulations using matrigel invasion assays. Based on our data, we hypothesize that enriched subpopulations would exhibit invasion characteristics via migrating through the experimental membranes in invasion assay experiments. We also hypothesize that the enriched subpopulations would exhibit greater invasive potential compared to subpopulations that did not enrich after PTEN k.d. and/or the bulk parental cell line. Lastly, we are interested in investigating the tumorigenic potential of these cells using mice xenograft models. In the literature, use of NOD/SCID mice xenografts have been used to assess consequences of PTEN deficiency in HER2+ breast cancer and thus would be appropriate for our studies.[82] In these proposed xenograft studies, subpopulations that were enriched following PTEN k.d. are expected to exhibit greater tumorigenicity compared to parental cells and/or subpopulations that were not enriched by k.d. of PTEN. Enhanced tumorigenicity is expected to be observed by larger tumor size, volumes, and faster growth compared to tumors corresponding to parental cells or cells from subpopulations that were not enriched by PTEN deficiency. Moreover, isolated enriched subpopulations treated with trastuzumab are expected to form larger and faster tumors mice xenograft models compared to the isolated and untreated enriched subpopulations. Collectively, these functional studies of the enriched subpopulations following PTEN k.d. would unequivocally confirm that enriched subpopulations resulting from PTEN deficiency give rise to trastuzumab resistance.

4.3. Clinical Implications of Findings

The cell line models we used aimed to capture the gradual loss of expression of PTEN during the progression of HER2+ breast cancer, which is reflective of real life scenarios of PTEN expression dynamics in HER2+ breast cancer.[55] Ebbesen and coworkers (2015) reported that PTEN loss occurs less at the onset of HER2+ breast cancer but is associated with tumor progression.[55] Thus, the enrichment of a quiescent, epithelial, early EMT subpopulation, as suggested by our findings, is consistent with the resultant cancer phenotype after PTEN loss in HER2+ breast cancer. Importantly, the enrichment of these quiescent, epithelial, early EMT subpopulations hinted that PTEN

deficiency enhances the aggressive cancer phenotype in HER2+ breast cancer that might be linked to trastuzumab resistance. In this dissertation, all of the subpopulations analyzed expressed high levels of HER2, even the subpopulations enriched after PTEN k.d., which suggested that the enriched subpopulations could be targeted by current standard therapies used for HER2+ breast cancer patients. However, based on the phenotype of these enriched subpopulation as suggested by our data, the enriched subpopulations could exhibit resistance to HER2-directed therapy due to the quiescent, early EMT phenotype. Current HER2-targeted therapies (trastuzumab, pertuzumab, trastuzumab drug conjugates) target HER2-overexpressing, proliferative cancer cells and elicits cytostatic effects on those cells or release toxic anti-mitotic payloads to those cells to arrest the cell growth of the HER2-overexpressing cells. Given the mechanism of the HER2-directed therapies, it suggests that the enriched subpopulations by PTEN deficiency would be targeted by HER2-directed therapies but would resist the cytostatic of the first line therapies (trastuzumab and pertuzumab). Additionally, the enriched subpopulations are hypothesized to escape the cytotoxic effects second line therapies and derivatives (trastuzumab emtansine and trastuzumab deruxtecan) since those trastuzumab drug conjugates release anti-mitotic payload, which would be toxic to proliferative cells but not quiescent cells. Thus, as stated above, the identification of markers to isolate these enriched subpopulations from the bulk HER2+ breast cancer cell lines is a critical step to unravelling the consequences of PTEN deficiency and its impact on trastuzumab treatment. In addition to being valuable for technical and functional validation of the enriched subpopulations, the identification of markers could have clinical relevance since it would provide avenues to screen patients for their predicted response to HER2-directed therapies based on their pre-existing transcriptomes rather than solely on the expression of HER2. Effective subset of HER2+ breast cancer patients is necessary for cancer management, especially for metastatic HER2+ breast cancer patients, because the vast majority do not respond to HER2-directed therapies and the fraction of metastatic patients who respond to trastuzumab ultimately acquire resistance within 2 years of treatment. Thus, the use of markers to predict patient response to frontline therapy could improve patient outcome and survival at earlier stages of cancer management for patients with metastatic disease.

It is important to note limitations of our data that derived from our HER2+ breast cancer models, which aims to capture the consequences of PTEN deficiency in HER2 breast cancer. While elucidating the role of PTEN deficiency in HER2+ breast cancer subpopulations is an important feat, it is also possible that PTEN deficiency is a molecular byproduct of oncogenic aberrations such as genetic mutations or epigenetic silencing that is not adequately captured in our data. Thus, it is possible that by studying the consequences of PTEN deficiency, we are not dissecting the primary contribution of the aggressive cancer phenotype or frequent cases of trastuzumab resistance. However, despite these limitations, there have been extensive controversy about the prognostic value of PTEN expression in HER2+ breast cancer. This work presented in this dissertation addresses the controversial role of PTEN and its prognostic value. We showed the inherent heterogeneity that exists within HER2+ breast cancer and that the reduction of PTEN expression could increase intratumoral heterogeneity by changing gene expression programs that governs the phenotype of cancer cells. Collectively, our data provided insight on the dynamic changes of the intratumoral heterogeneity that exists within a given HER2+ breast cancer, which is a critical element to leverage in future cancer management as the clinical importance of intra and intertumoral heterogeneity continues to grow in the field. In sum, our work has great potential to contribute shaping the personalized medicine strategies for HER2+ breast cancer patients in the future.

4.4. References

(1) U.S. Breast Cancer Statistics | Breastcancer.org https://www.breastcancer.org/symptoms/understand_bc/statistics (accessed Jun 1, 2020).

(2) Dai, X.; Li, T.; Bai, Z.; Yang, Y.; Liu, X.; Zhan, J.; Shi, B. *Am. J. Cancer Res.* **2015**, *5* (10), 2929–2943.

(3) Turashvili, G.; Brogi, E. *Front. Med.* **2017**, *4* (DEC).

(4) Wang, J.; Xu, B. *Signal Transduct. Target. Ther.* **2019**, *4* (1).

(5) *Am. Cancer Soc.* **2020**, 1–43.

(6) National Cancer Institute Surveillance, Epidemiology, and E. R. P. (SEER). *Natl. Cancer Inst.* **2019**.

(7) Zhang, L.; Li, J.; Xiao, Y.; Cui, H.; Du, G.; Wang, Y.; Li, Z.; Wu, T.; Li, X.; Tian, J. *Sci. Rep.* **2015**, *5*, 1–14.

(8) Godoy-Ortiz, A.; Sanchez-Muñoz, A.; Parrado, M. R. C.; Álvarez, M.; Ribelles, N.; Dominguez, A. R.; Alba, E. *Front. Oncol.* **2019**, *9* (OCT), 1124.

(9) Loibl, S.; Gianni, L. *Lancet* **2017**, *389* (10087), 2415–2429.

(10) Muller, K. E.; Marotti, J. D.; Tafe, L. J. *Am. J. Clin. Pathol.* **2019**, *152* (1), 7–16.

(11) Vandenberghe, M. E.; Scott, M. L. J.; Scorer, P. W.; Söderberg, M.; Balcerzak, D.; Barker, C. *Sci. Rep.* **2017**, *7* (1), 1–11.

(12) Zhang, X.; Bleiweiss, I.; Jaffer, S.; Nayak, A. *Clin. Breast Cancer* **2017**, *17* (6), 486–492.

(13) Wolff, A. C.; Elizabeth Hale Hammond, M.; Allison, K. H.; Harvey, B. E.; Mangu, P. B.; Bartlett, J. M. S.; Bilous, M.; Ellis, I. O.; Fitzgibbons, P.; Hanna, W.; Jenkins, R. B.; Press, M. F.; Spears, P. A.; Vance, G. H.; Viale, G.; McShane, L. M.; Dowsett, M. *J. Clin. Oncol.* **2018**, *36* (20), 2105–2122.

(14) Mastro, L. Del; Lambertini, M.; Bighin, C.; Levaggi, A.; D'Alonzo, A.; Giraudi, S.; Pronzato, P. *Expert Rev. Anticancer Ther.* **2012**, *12* (11), 1391–1405.

(15) Pernas, S.; Tolaney, S. M. *Ther. Adv. Med. Oncol.* **2019**, *11*, 1–16.

(16) Oh, D. Y.; Bang, Y. J. *Nat. Rev. Clin. Oncol.* **2020**, *17* (1), 33–48.

(17) Swain, S. M.; Kim, S. B.; Cortés, J.; Ro, J.; Semiglazov, V.; Campone, M.; Ciruelos, E.; Ferrero, J. M.; Schneeweiss, A.; Knott, A.; Clark, E.; Ross, G.; Benyunes, M. C.; Baselga, J. *Lancet Oncol.* **2013**, *14* (6), 461–471.

(18) Modi, S.; Saura, C.; Yamashita, T.; Park, Y. H.; Kim, S.-B.; Tamura, K.; Andre, F.; Iwata, H.; Ito, Y.; Tsurutani, J.; Sohn, J.; Denduluri, N.; Perrin, C.; Aogi, K.; Tokunaga, E.; Im, S.-A.; Lee, K. S.; Hurvitz, S. A.; Cortes, J.; Lee, C.; Chen, S.; Zhang, L.; Shahidi, J.; Yver, A.; Krop, I. *N. Engl. J. Med.* **2020**, *382* (7), 610–621.

(19) Murthy, R. K.; Loi, S.; Okines, A.; Paplomata, E.; Hamilton, E.; Hurvitz, S. A.; Lin, N. U.; Borges, V.; Abramson, V.; Anders, C.; Bedard, P. L.; Oliveira, M.; Jakobsen, E.; Bachelot, T.; Shachar, S. S.; Muller, V.; Braga, S.; Duhoux, F. P.; Greil, R.; Cameron, D.; Carey, L. A.; Curigliano, G.; Gelmon, K.; Hortobagyi, G.; Krop, I.; Loibl, S.; Pegram, M.; Slamon, D.; Palanca-Wessels, M. C.; Walker, L.; Feng, W.; Winer, E. P. *N. Engl. J. Med.* **2020**, *382* (7), 597–609.

(20) Kim, C.; Lee, C. K.; Chon, H. J.; Kim, J. H.; Park, H. S.; Heo, S. J.; Kim, H. J.; Kim, T. S.; Kwon, W. S.; Chung, H. C.; Rha, S. Y. *Oncotarget* **2017**, *8* (69), 113494–113501.

(21) Bang, Y. J.; Van Cutsem, E.; Feyereislova, A.; Chung, H. C.; Shen, L.; Sawaki, A.; Lordick, F.; Ohtsu, A.; Omuro, Y.; Satoh, T.; Aprile, G.; Kulikov, E.; Hill, J.; Lehle, M.; Rüschoff, J.; Kang, Y. K. *Lancet* **2010**, *376* (9742), 687–697.

(22) Sims, A. H.; Zweemer, A. J. M.; Nagumo, Y.; Faratian, D.; Muir, M.; Dodds, M.; Um, I.; Kay, C.; Hasmann, M.; Harrison, D. J.; Langdon, S. P. *Br. J. Cancer* **2012**, *106* (11), 1779–1789.

(23) Pohlmann, P. R.; Mayer, I. A.; Mernaugh, R. *Clin. Cancer Res.* **2009**, *15* (24), 7479–7491.

(24) Luque-Cabal, M.; García-Teijido, P.; Fernández-Pérez, Y.; Sánchez-Lorenzo, L.; Palacio-Vázquez, I. *Clin. Med. Insights Oncol.* **2016**, *10*, 21–30.

(25) Nagata, Y.; Lan, K. H.; Zhou, X.; Tan, M.; Esteva, F. J.; Sahin, A. A.; Klos, K. S.; Li, P.; Monia, B. P.; Nguyen, N. T.; Hortobagyi, G. N.; Hung, M. C.; Yu, D. *Cancer Cell* **2004**, *6* (2), 117–127.

(26) Nahta, R. *Int. Sch. Res. Netw.* **2012**, *2012* (428062), 1–16.

(27) Luque-Cabal, M.; García-Teijido, P.; Fernández-Pérez, Y.; Sánchez-Lorenzo, L.; Palacio-Vázquez, I. *Clin. Med. Insights Oncol.* **2016**, *10* (Suppl 1), 21–30.

(28) Pernas, S.; Tolaney, S. M. HER2-Positive Breast Cancer: New Therapeutic Frontiers and Overcoming Resistance.

(29) Chen, S.; Liang, Y.; Feng, Z.; Wang, M. *BMC Cancer* **2019**, *19* (1), 973.

(30) Verma, S.; Miles, D.; Gianni, L.; Krop, I. E.; Welslau, M.; Baselga, J.; Pegram, M.; Oh, D.-Y.; Diéras, V.; Guardino, E.; Fang, L.; Lu, M. W.; Olsen, S.; Blackwell, K. *N. Engl. J. Med.* **2012**, *367* (19), 1783–1791.

(31) Perez, E. A.; Cortés, J.; Gonzalez-angulo, A. M.; Bartlett, J. M. S. *Cancer Treat. Rev.* **2014**, *40* (2), 276–284.

(32) Murthy, P.; Kidwell, K. M.; Schott, A. F.; Merajver, S. D.; Griggs, J. J.; Smerage, J. D.; Van Poznak, C. H.; Wicha, M. S.; Hayes, D. F.; Henry, N. L. *Breast Cancer Res. Treat.* **2016**, *155* (3), 589–595.

(33) Joensuu, H. *Cancer Treat. Rev.* **2017**, *52*, 1–11.

(34) Tolaney, S. M.; Guo, H.; Pernas, S.; Barry, W. T.; Dillon, D. A.; Ritterhouse, L.;

Schneider, B. P.; Shen, F.; Fuhrman, K.; Baltay, M.; Dang, C. T.; Yardley, D. A.; Moy, B.; Kelly Marcom, P.; Albain, K. S.; Rugo, H. S.; Ellis, M. J.; Shapira, I.; Wolff, A. C.; Carey, L. A.; Overmoyer, B.; Partridge, A. H.; Hudis, C. A.; Krop, I. E.; Burstein, H. J.; Winer, E. P. *J. Clin. Oncol.* **2019**, *37* (22), 1868–1875.

(35) Gianni, L.; Pienkowski, T.; Im, Y. H.; Tseng, L. M.; Liu, M. C.; Lluch, A.; Starosławska, E.; de la Haba-Rodriguez, J.; Im, S. A.; Pedrini, J. L.; Poirier, B.; Morandi, P.; Semiglazov, V.; Srimuninnimit, V.; Bianchi, G. V.; Magazzù, D.; McNally, V.; Douthwaite, H.; Ross, G.; Valagussa, P. *Lancet Oncol.* **2016**, *17* (6), 791–800.

(36) Luque-Cabal, M.; García-Teijido, P.; Fernández-Pérez, Y.; Sánchez-Lorenzo, L.; Palacio-Vázquez, I. *Clin. Med. Insights Oncol.* **2016**, *10* (Suppl 1), 21–30.

(37) Andersson, M.; Lidbrink, E.; Bjerre, K. *J Clin Oncol* **2011**, *29* (3), 264–271.

(38) Derakhshani, A.; Rezaei, Z.; Safarpour, H.; Sabri, M.; Mir, A.; Sanati, M. A.; Vahidian, F.; Gholamiyan Moghadam, A.; Aghadoukht, A.; Hajiasgharzadeh, K.; Baradaran, B. *J. Cell. Physiol.* **2020**, *235* (4), 3142–3156.

(39) Valabrega, G.; Montemurro, F.; Sarotto, I.; Petrelli, A.; Rubini, P.; Tacchetti, C.; Aglietta, M.; Comoglio, P. M.; Giordano, S. *Oncogene* **2005**, *24* (18), 3002–3010.

(40) Takuwa, H.; Tsuji, W.; Yotsumoto, F. *Int. J. Surg. Case Rep.* **2018**, *52*, 125–131.

(41) New Treatments Emerge for Metastatic HER2+ Breast Cancer - National Cancer Institute https://www.cancer.gov/news-events/cancer-currents-blog/2020/tucatinib-trastuzumab-deruxtecan-her2-positive-metastatic-breast-cancer (accessed Jun 1, 2020).

(42) Stern, H. M.; Gardner, H.; Burzykowski, T.; Elatre, W.; O'Brien, C.; Lackner, M. R.; Pestano, G. A.; Santiago, A.; Villalobos, I.; Eiermann, W.; Pienkowski, T.; Martin, M.; Robert, N.; Crown, J.; Nuciforo, P.; Bee, V.; Mackey, J.; Slamon, D. J.; Press, M. F. *Clin. Cancer Res.* **2015**, *21* (9), 2065–2074.

(43) Vu, T.; Claret, F. X. *Front. Oncol.* **2012**, *2* (June), 62.

(44) Bartsch, R.; Wenzel, C.; Steger, G. G. *Biologics* **2007**, *1* (1), 19–31.

(45) Gschwantler-Kaulich, D.; Tan, Y. Y.; Fuchs, E.-M.; Hudelist, G.; Köstler, W. J.; Reiner, A.; Leser, C.; Salama, M.; Attems, J.; Deutschmann, C.; Zielinski, C. C.; Singer, C. F. *PLoS One* **2017**, *12* (3), e0172911.

(46) Gajria, D.; Chandarlapaty, S. *Expert Rev. Anticancer Ther.* **2011**, *11* (2), 263–275.

(47) Mercogliano, M. F.; Bruni, S.; Elizalde, P. V.; Schillaci, R. *Front. Oncol.* **2020**, *10*, 584.

(48) Rimawi, M. F.; de Angelis, C.; Contreras, A.; Pareja, F.; Geyer, F. C.; Burke, K. A.; Herrera, S.; Wang, T.; Mayer, I. A.; Forero, A.; Nanda, R.; Goetz, M. P.; Chang, J. C.; Krop, I. E.; Wolff, A. C.; Pavlick, A. C.; Fuqua, S. A. W.; Gutierrez, C.; Hilsenbeck, S. G.; Li, M. M.; Weigelt, B.; Reis-Filho, J. S.; Osborne, C. K.;

Schiff, R. *Breast Cancer Res. Treat.* **2018**, *167* (3), 731–740.

(49) Lebok, P.; Kopperschmidt, V.; Kluth, M.; Hube-Magg, C.; Özden, C.; Taskin, B.; Hussein, K.; Mittenzwei, A.; Lebeau, A.; Witzel, I.; Wölber, L.; Mahner, S.; Jänicke, F.; Geist, S.; Paluchowski, P.; Wilke, C.; Heilenkötter, U.; Simon, R.; Sauter, G.; Terracciano, L.; Krech, R.; Von, A.; Müller, V.; Burandt, E. *BMC Cancer* **2015**, *15* (1–10).

(50) Li, S.; Shen, Y.; Wang, M.; Yang, J.; Lv, M.; Li, P.; Chen, Z.; Yang, J. *Oncotarget* **2017**, *8* (19), 32043–32054.

(51) Kechagioglou, P.; Papi, R. M.; Provatopoulou, X.; Kalogera, E.; Papadimitriou, E.; Grigoropoulos, P.; Nonni, A.; Zografos, G.; Kyriakidis, D. A.; Gounaris, A. *Anticancer Res.* **2014**, *34* (3), 1387–1400.

(52) Chalhoub, N.; Baker, S. J. *Annu. Rev. Pathol. Mech. Dis.* **2009**, *4* (1), 127–150.

(53) Paplomata, E.; O'regan, R. *Ther. Adv. Med. Oncol.* **2014**, *6* (4), 154–166.

(54) Keniry, M.; Parsons, R. *Oncogene* **2008**, *27* (41), 5477–5485.

(55) Ebbesen, S. H.; Scaltriti, M.; Bialucha, C. U.; Morse, N.; Kastenhuber, E. R.; Wen, H. Y.; Dow, L. E.; Baselga, J.; Lowe, S. W. *Proc. Natl. Acad. Sci. U. S. A.* **2016**, *113* (11), 3030–3035.

(56) Luongo, F.; Colonna, F.; Calapà, F.; Vitale, S.; Fiori, M. E.; De Maria, R. *Cancers (Basel).* **2019**, *11* (8), 1076.

(57) Carracedo, A.; Pandolfi, P. P. *Oncogene* **2008**, *27* (41), 5527–5541.

(58) Crowell, J. A.; Steele, V. E.; Fay, J. R. *Mol. Cancer Ther.* **2007**, *6* (8), 2139–2148.

(59) Endersby, R.; Baker, S. J. *Oncogene* **2008**, *27* (41), 5416–5430.

(60) Nuciforo, P. G.; Aura, C.; Holmes, E.; Prudkin, L.; Jimenez, J.; Martinez, P.; Ameels, H.; de la Perna, L.; Ellis, C.; Eidtmann, H.; Piccart-Gebhart, M. J.; Scaltriti, M.; Baselga, J. *Ann. Oncol.* **2015**, *26* (7), 1494–1500.

(61) Carbognin, L.; Miglietta, F.; Paris, I.; Dieci, M. V. *Cancers (Basel).* **2019**, *11* (9), 1–18.

(62) Jones, N.; Bonnet, F.; Sfar, S.; Lafitte, M.; Lafon, D.; Sierankowski, G.; Brouste, V.; Banneau, G.; Tunon de Lara, C.; Debled, M.; MacGrogan, G.; Longy, M.; Sevenet, N. *Int. J. Cancer* **2013**, *133* (2), 323–334.

(63) Zhang, H. Y.; Liang, F.; Jia, Z. L.; Song, S. T.; Jiang, Z. F. *Oncol. Lett.* **2013**, *6* (1), 161–168.

(64) Zhu, Y.; Wloch, A.; Wu, Q.; Peters, C.; Pagenstecher, A.; Bertalanffy, H.; Sure, U. *Stroke* **2009**, *40* (3), 820–826.

(65) Kang, Y. H.; Lee, H. S.; Kim, W. H. *Lab. Investig.* **2002**, *82* (3), 285–291.

(66) Wilks, S. T. *Breast* **2015**, *24* (5), 548–555.

(67) Sangai, T.; Akcakanat, A.; Chen, H.; Tarco, E.; Wu, Y.; Do, K. A.; Miller, T. W.; Arteaga, C. L.; Mills, G. B.; Gonzalez-Angulo, A. M.; Meric-Bernstam, F. *Clin. Cancer Res.* **2012**, *18* (20), 5816–5828.

(68) Hudis, C.; Swanton, C.; Janjigian, Y. Y.; Lee, R.; Sutherland, S.; Lehman, R.; Chandarlapaty, S.; Hamilton, N.; Gajria, D.; Knowles, J.; Shah, J.; Shannon, K.; Tetteh, E.; Sullivan, D. M.; Moreno, C.; Yan, L.; Han, H. S. *Breast Cancer Res.* **2013**, *15* (6), R110.

(69) Xing, Y.; Lin, N. U.; Maurer, M. A.; Chen, H.; Mahvash, A.; Sahin, A.; Akcakanat, A.; Li, Y.; Abramson, V.; Litton, J.; Chavez-MacGregor, M.; Valero, V.; Piha-Paul, S. A.; Hong, D.; Do, K.-A.; Tarco, E.; Riall, D.; Eterovic, A. K.; Wulf, G. M.; Cantley, L. C.; Mills, G. B.; Doyle, L. A.; Winer, E.; Hortobagyi, G. N.; Gonzalez-Angulo, A. M.; Meric-Bernstam, F. *Breast Cancer Res.* **2019**, *21* (1), 78.

(70) Hurvitz, S. A.; Andre, F.; Jiang, Z.; Shao, Z.; Mano, M. S.; Neciosup, S. P.; Tseng, L. M.; Zhang, Q.; Shen, K.; Liu, D.; Dreosti, L. M.; Burris, H. A.; Toi, M.; Buyse, M. E.; Cabaribere, D.; Lindsay, M. A.; Rao, S.; Pacaud, L. B.; Taran, T.; Slamon, D. *Lancet Oncol.* **2015**, *16* (7), 816–829.

(71) Van Swearingen, A. E. D.; Siegel, M. B.; Deal, A. M.; Sambade, M. J.; Hoyle, A.; Hayes, D. N.; Jo, H.; Little, P.; Dees, E. C.; Muss, H.; Jolly, T.; Zagar, T. M.; Patel, N.; Miller, C. R.; Parker, J. S.; Smith, J. K.; Fisher, J.; Shah, N.; Nabell, L.; Nanda, R.; Dillon, P.; Abramson, V.; Carey, L. A.; Anders, C. K. *Breast Cancer Res. Treat.* **2018**, *171* (3), 637–648.

(72) Ramón y Cajal, S.; Sesé, M.; Capdevila, C.; Aasen, T.; De Mattos-Arruda, L.; Diaz-Cano, S. J.; Hernández-Losa, J.; Castellví, J. *J. Mol. Med.* **2020**, *98* (2), 161–177.

(73) Lee, H. J.; Seo, A. N.; Kim, E. J.; Jang, M. H.; Suh, K. J.; Ryu, H. S.; Kim, Y. J.; Kim, J. H.; Im, S.-A.; Gong, G.; Jung, K. H.; Park, I. A.; Park, S. Y. *Am. J. Clin. Pathol.* **2014**, *142* (6), 755–766.

(74) Rye, I. H.; Trinh, A.; Sætersdal, A. B.; Nebdal, D.; Lingjærde, O. C.; Almendro, V.; Polyak, K.; Børresen-Dale, A. L.; Helland, Å.; Markowetz, F.; Russnes, H. G. *Mol. Oncol.* **2018**, *12* (11), 1838–1855.

(75) Ferrari, A.; Vincent-Salomon, A.; Pivot, X.; Sertier, A. S.; Thomas, E.; Tonon, L.; Boyault, S.; Mulugeta, E.; Treilleux, I.; MacGrogan, G.; Arnould, L.; Kielbassa, J.; Le Texier, V.; Blanché, H.; Deleuze, J. F.; Jacquemier, J.; Mathieu, M. C.; Penault-Llorca, F.; Bibeau, F.; Mariani, O.; Mannina, C.; Pierga, J. Y.; Trédan, O.; Bachelot, T.; Bonnefoi, H.; Romieu, G.; Fumoleau, P.; Delaloge, S.; Rios, M.; Ferrero, J. M.; Tarpin, C.; Bouteille, C.; Calvo, F.; Gut, I. G.; Gut, M.; Martin, S.; Nik-Zainal, S.; Stratton, M. R.; Pauporté, I.; Saintigny, P.; Birnbaum, D.; Viari, A.; Thomas, G. *Nat. Commun.* **2016**, *7* (1), 1–9.

(76) Brady, S. W.; McQuerry, J. A.; Qiao, Y.; Piccolo, S. R.; Shrestha, G.; Jenkins, D. F.; Layer, R. M.; Pedersen, B. S.; Miller, R. H.; Esch, A.; Selitsky, S. R.; Parker, J. S.; Anderson, L. A.; Dalley, B. K.; Factor, R. E.; Reddy, C. B.; Boltax, J. P.; Li, D.

Y.; Moos, P. J.; Gray, J. W.; Heiser, L. M.; Buys, S. S.; Cohen, A. L.; Johnson, W. E.; Quinlan, A. R.; Marth, G.; Werner, T. L.; Bild, A. H. *Nat. Commun.* **2017**, *8* (1), 1–15.

(77) Korkaya, H.; Paulson, A.; Iovino, F.; Wicha, M. S. *Oncogene* **2008**, *27* (47), 6120–6130.

(78) Macosko, E. Z.; Basu, A.; Satija, R.; Nemesh, J.; Shekhar, K.; Goldman, M.; Tirosh, I.; Bialas, A. R.; Kamitaki, N.; Martersteck, E. M.; Trombetta, J. J.; Weitz, D. A.; Sanes, J. R.; Shalek, A. K.; Regev, A.; McCarroll, S. A. *Cell* **2015**, *161* (5), 1202–1214.

(79) Andrews, T. S.; Hemberg, M. *Mol. Aspects Med.* **2018**, *59*, 114–122.

(80) Ziegenhain, C.; Vieth, B.; Parekh, S.; Reinius, B.; Guillaumet-Adkins, A.; Smets, M.; Leonhardt, H.; Heyn, H.; Hellmann, I.; Enard, W. *Mol. Cell* **2017**, *65* (4), 631-643.e4.

(81) Ocasio, J.; Babcock, B.; Malawsky, D.; Weir, S. J.; Loo, L.; Simon, J. M.; Zylka, M. J.; Hwang, D.; Dismuke, T.; Sokolsky, M.; Rosen, E. P.; Vibhakar, R.; Zhang, J.; Saulnier, O.; Vladoiu, M.; El-Hamamy, I.; Stein, L. D.; Taylor, M. D.; Smith, K. S.; Northcott, P. A.; Colaneri, A.; Wilhelmsen, K.; Gershon, T. R. *Nat. Commun.* **2019**, *10* (1), 1–17.

(82) Korkaya, H.; Kim, G. Il; Davis, A.; Malik, F.; Henry, N. L.; Ithimakin, S.; Quraishi, A. A.; Tawakkol, N.; D'Angelo, R.; Paulson, A. K.; Chung, S.; Luther, T.; Paholak, H. J.; Liu, S.; Hassan, K. A.; Zen, Q.; Clouthier, S. G.; Wicha, M. S. *Mol. Cell* **2012**, *47* (4), 570–584.

(83) Korkaya, H.; Paulson, A.; Charafe-Jauffret, E.; Ginestier, C.; Brown, M.; Dutcher, J.; Clouthier, S. G.; Wicha, M. S. *PLoS Biol.* **2009**, *7* (6), e1000121.

(84) Nagata, Y.; Lan, K. H.; Zhou, X.; Tan, M.; Esteva, F. J.; Sahin, A. A.; Klos, K. S.; Li, P.; Monia, B. P.; Nguyen, N. T.; Hortobagyi, G. N.; Hung, M. C.; Yu, D. *Cancer Cell* **2004**, *6* (2), 117–127.

(85) Goldman, E. M. and M. **2015**, 1–20.

(86) Nemesh, J. Drop-seq Core Computational Protocol http://mccarrolllab.org/wp-content/uploads/2016/03/Drop-seqAlignmentCookbookv1.2Jan2016.pdf (accessed Sep 1, 2020).

(87) Zappia, L.; Oshlack, A. *Gigascience* **2018**, *7* (7), 1–9.

(88) Sergushichev, A. A. *bioRxiv* **2016**, 060012.

(89) Subramanian, A.; Tamayo, P.; Mootha, V. K.; Mukherjee, S.; Ebert, B. L.; Gillette, M. A.; Paulovich, A.; Pomeroy, S. L.; Golub, T. R.; Lander, E. S.; Mesirov, J. P. *Proc. Natl. Acad. Sci. U. S. A.* **2005**, *102* (43), 15545–15550.

(90) Smith, S. E.; Mellor, P.; Ward, A. K.; Kendall, S.; McDonald, M.; Vizeacoumar, F. S.; Vizeacoumar, F. J.; Napper, S.; Anderson, D. H. *Breast Cancer Res.* **2017**, *19*

(1), 65.

(91) Jernström, S.; Hongisto, V.; Leivonen, S. K.; Due, E. U.; Tadele, D. S.; Edgren, H.; Kallioniemi, O.; Perälä, M.; Mælandsmo, G. M.; Sahlberg, K. K. *Breast Cancer Targets Ther.* **2017**, *9*, 185–198.

(92) Becht, E.; McInnes, L.; Healy, J.; Dutertre, C. A.; Kwok, I. W. H.; Ng, L. G.; Ginhoux, F.; Newell, E. W. *Nat. Biotechnol.* **2019**, *37* (1), 38–47.

(93) Luecken, M. D.; Theis, F. J. *Mol. Syst. Biol.* **2019**, *15* (6).

(94) Li, W.; Freudenberg, J.; Suh, Y. J.; Yang, Y. *Comput. Biol. Chem.* **2014**, *48*, 77–83.

(95) McDermaid, A.; Monier, B.; Zhao, J.; Liu, B.; Ma, Q. *Briefings in Bioinformatics*. Oxford University Press November 1, 2019, pp 2044–2054.

(96) Capaldo, C. T.; Nusrat, A. *Biochim. Biophys. Acta - Biomembr.* **2009**, *1788* (4), 864–871.

(97) Shen, W.-H.; Zhou, J.-H.; Broussard, S. R.; Freund, G. G.; Dantzer, R.; Kelley, K. W. *Cancer Res.* **2002**, 4746–4756.

(98) Yang, J.; Min, K.-W.; Kim, D.-H.; Son, B. K.; Moon, K. M.; Wi, Y. C.; Bang, S. S.; Oh, Y. H.; Do, S.-I.; Chae, S. W.; Oh, S.; Kim, Y. H.; Kwon, M. J. *PLoS One* **2018**, *13* (8), e0202113.

(99) Cai, X.; Cao, C.; Li, J.; Chen, F.; Zhang, S.; Liu, B.; Zhang, W.; Zhang, X.; Ye, L. *Oncotarget* **2017**, *8* (35), 58338–58352.

(100) Mostowy, S.; Shenoy, A. R. *Nat. Rev. Immunol.* **2015**, *15* (9), 559–573.

(101) Wang, W.; Eddy, R.; Condeelis, J. *Nat. Rev. Cancer* **2007**, *7* (6), 429–440.

(102) Nakayama, K. I.; Nakayama, K. *Nat. Rev. Cancer* **2006**, *6* (5), 369–381.

(103) Bassermann, F.; Eichner, R.; Pagano, M. *Biochim. Biophys. Acta - Mol. Cell Res.* **2014**, *1843* (1), 150–162.

(104) Gan, B.; DePinho, R. A. *Cell Cycle* **2009**, *8* (7), 1003–1006.

(105) Laplante, M.; Sabatini, D. M. *J. Cell Sci.* **2009**, *122* (20), 3589–3594.

(106) Kallergi, G.; Tsintari, V.; Sfakianakis, S.; Bei, E.; Lagoudaki, E.; Koutsopoulos, A.; Zacharopoulou, N.; Alkahtani, S.; Alarifi, S.; Stournaras, C.; Zervakis, M.; Georgoulias, V. *Breast Cancer Res.* **2019**, *21* (1), 86.

(107) Hasan, Z.; Koizumi, S. I.; Sasaki, D.; Yamada, H.; Arakaki, N.; Fujihara, Y.; Okitsu, S.; Shirahata, H.; Ishikawa, H. *Nat. Commun.* **2017**, *8*.

(108) Gong, C.; Shen, J.; Fang, Z.; Qiao, L.; Feng, R.; Lin, X.; Li, S. *Biosci. Rep.* **2018**, *38* (4).

(109) Sundqvist, A.; Morikawa, M.; Ren, J.; Vasilaki, E.; Kawasaki, N.; Kobayashi, M.;

Koinuma, D.; Aburatani, H.; Miyazono, K.; Heldin, C. H.; Van Dam, H.; Dijke, P. Ten. *Nucleic Acids Res.* **2018**, *46* (3), 1180–1195.

(110) Mendoza-Rodríguez, M.; Arévalo Romero, H.; Fuentes-Pananá, E. M.; Ayala-Sumuano, J. T.; Meza, I. *Cancer Lett.* **2017**, *390*, 39–44.

(111) Liu, S.; Lee, J. S.; Jie, C.; Park, M. H.; Iwakura, Y.; Patel, Y.; Soni, M.; Reisman, D.; Chen, H. *Cancer Res.* **2018**, *78* (8), 2040–2051.

(112) Korkaya, H.; Kim, G. Il; Davis, A.; Malik, F.; Henry, N. L.; Ithimakin, S.; Quraishi, A. A.; Tawakkol, N.; D'Angelo, R.; Paulson, A. K.; Chung, S.; Luther, T.; Paholak, H. J.; Liu, S.; Hassan, K. A.; Zen, Q.; Clouthier, S. G.; Wicha, M. S. *Mol. Cell* **2012**, *47* (4), 570–584.

(113) Zhang, Z.; Xu, Q.; Song, C.; Mi, B.; Zhang, H.; Kang, H.; Liu, H.; Sun, Y.; Wang, J.; Lei, Z.; Guan, H.; Li, F. *Mol. Cancer Ther.* **2020**, *19* (2), 650–660.

(114) Fagerli, U. M.; Ullrich, K.; Stühmer, T.; Holien, T.; Köchert, K.; Holt, R. U.; Bruland, O.; Chatterjee, M.; Nogai, H.; Lenz, G.; Shaughnessy, J. D.; Mathas, S.; Sundan, A.; Bargou, R. C.; Dörken, B.; Børset, M.; Janz, M. *Oncogene* **2011**, *30* (28), 3198–3206.

(115) Sahoo, S.; Brickley, D. R.; Kocherginsky, M.; Conzen, S. D. *Eur. J. Cancer* **2005**, *41* (17), 2754–2759.

(116) Mistry, P.; Deacon, K.; Mistry, S.; Blank, J.; Patel, R. *J. Biol. Chem.* **2004**, *279* (2), 1482–1490.

(117) Reymond, N.; Im, J. H.; Garg, R.; Cox, S.; Soyer, M.; Riou, P.; Colomba, A.; Muschel, R. J.; Ridley, A. J. *Mol. Oncol.* **2015**, *9* (6), 1043–1055.

(118) Tomaskovic-Crook, E.; Thompson, E. W.; Thiery, J. P. *Breast Cancer Res.* **2009**, *11* (6), 213.

(119) Kalluri, R.; Weinberg, R. A. *J. Clin. Invest.* **2009**, *119* (6), 1420–1428.

(120) Pastushenko, I.; Blanpain, C. *Trends Cell Biol.* **2019**, *29* (3), 212–226.

(121) Chu, P. G.; Weiss, L. M. *Histopathology* **2002**, *40* (5), 403–439.

(122) Xiang, X.; Deng, Z.; Zhuang, X.; Ju, S.; Mu, J.; Jiang, H.; Zhang, L.; Yan, J.; Miller, D.; Zhang, H.-G. *PLoS One* **2012**, *7* (12), e50781.

(123) Schmalhofer, O.; Brabletz, S.; Brabletz, T. *Cancer Metastasis Rev.* **2009**, *28* (1–2), 151–166.

(124) Zhang, S.; Wang, Z.; Liu, W.; Lei, R.; Shan, J.; Li, L.; Wang, X. *Sci. Rep.* **2017**, *7*.

(125) Nasser, M. W.; Qamri, Z.; Deol, Y. S.; Ravi, J.; Powell, C. A.; Trikha, P.; Schwendener, R. A.; Bai, X. F.; Shilo, K.; Zou, X.; Leone, G.; Wolf, R.; Yuspa, S. H.; Ganju, R. K. *Cancer Res.* **2012**, *72* (3), 604–615.

(126) West, N. R.; Watson, P. H. *Oncogene* **2010**, *29* (14), 2083–2092.

(127) Paruchuri, V.; Prasad, A.; McHugh, K.; Bhat, H. K.; Polyak, K.; Ganju, R. K. *PLoS One* **2008**, *3* (3), 1741.

(128) Emberley, E. D.; Murphy, L. C.; Watson, P. H. *Breast Cancer Res.* **2004**, *6* (4), 153–159.

(129) Cancemi, P.; Buttacavoli, M.; Cara, G. Di; Albanese, N. N.; Bivona, S.; Pucci-Minafra, I.; Feo, S. *Oncotarget* **2018**, *9* (49), 29064–29081.

(130) Hua, X.; Zhang, H.; Jia, J.; Chen, S.; Sun, Y.; Zhu, X. *Biomed. Pharmacother.* **2020**, *127*, 110156.

(131) Yuzugullu, H.; Von, T.; Thorpe, L. M.; Walker, S. R.; Roberts, T. M.; Frank, D. A.; Zhao, J. J. *Cell Discov.* **2016**, *2* (1), 1–13.

(132) Sadasivam, S.; DeCaprio, J. A. *Nat. Rev. Cancer* **2013**, *13* (8), 585–595.

(133) Min, M.; Spencer, S. L. *PLOS Biol.* **2019**, *17* (3), e3000178.

(134) Bracken, A. P.; Ciro, M.; Cocito, A.; Helin, K. *Trends Biochem. Sci.* **2004**, *29* (8), 409–417.

(135) Ito, T.; Teo, Y. V.; Evans, S. A.; Neretti, N.; Sedivy Correspondence, J. M. *Cell Rep.* **2018**, *22*, 3480–3492.

(136) Vizán, P.; Gutiérrez, A.; Espejo, I.; García-Montolio, M.; Lange, M.; Carretero, A.; Lafzi, A.; de Andrés-Aguayo, L.; Blanco, E.; Thambyrajah, R.; Graf, T.; Heyn, H.; Bigas, A.; Di Croce, L. *Sci. Adv.* **2020**, *6* (32), eabb2745.

(137) Doyle, L. A.; Ross, D. D. *Oncogene* **2003**, *22* (47 REV. ISS. 6), 7340–7358.

(138) Balaji, S. A.; Udupa, N.; Chamallamudi, M. R.; Gupta, V.; Rangarajan, A. *PLoS One* **2016**, *11* (5).

(139) Lucanus, A. J.; Yip, G. W. *Nat. Publ. Gr.* **2018**.

(140) Mandelkow, E.; Mandelkow, E. M. *Trends Cell Biol.* **2002**, *12* (12), 585–591.

(141) Ivanov, A. I.; McCall, I. C.; Babbin, B.; Samarin, S. N.; Nusrat, A.; Parkos, C. A. *BMC Cell Biol.* **2006**, *7* (1), 12.

(142) Li, T.-F.; Zeng, H.-J.; Shan, Z.; Ye, R.-Y.; Cheang, T.-Y.; Zhang, Y.-J.; Lu, S.-H.; Zhang, Q.; Shao, N.; Lin, Y. .

(143) Hirokawa, N.; Noda, Y.; Tanaka, Y.; Niwa, S. *Nat. Rev. Mol. Cell Biol.* **2009**, *10* (10), 682–696.

(144) Li, B.; Dou, S. X.; Yuan, J. W.; Liu, Y. R.; Li, W.; Ye, F.; Wang, P. Y.; Li, H. *Proc. Natl. Acad. Sci. U. S. A.* **2018**, *115* (48), 12118–12123.

(145) Kwon, M. J.; Park, S.; Choi, J. Y.; Oh, E.; Kim, Y. J.; Park, Y. H.; Cho, E. Y.; Kwon, M. J.; Nam, S. J.; Im, Y. H.; Shin, Y. K.; Choi, Y. L. *Br. J. Cancer* **2012**, *106* (5), 923–930.

(146) Yang, X. H.; Richardson, A. L.; Torres-Arzayus, M. I.; Zhou, P.; Sharma, C.; Kazarov, A. R.; Andzelm, M. M.; Strominger, J. L.; Brown, M.; Hemler, M. E. *Cancer Res.* **2008**, *68* (9), 3204–3213.

(147) Kumar, S.; Park, S. H.; Cieply, B.; Schupp, J.; Killiam, E.; Zhang, F.; Rimm, D. L.; Frisch, S. M. *Mol. Cell. Biol.* **2011**, *31* (19), 4036–4051.

(148) Rasiah, P. K.; Maddala, R.; Bennett, V.; Rao, P. V. *Dev. Biol.* **2019**, *446* (1), 119–131.

(149) Kurozumi, S.; Joseph, C.; Raafat, S.; Sonbul, S.; Kariri, Y.; Alsaeed, S.; Pigera, M.; Alsaleem, M.; Nolan, C. C.; Johnston, S. J.; Aleskandarany, M. A.; Ogden, A.; Fujii, T.; Shirabe, K.; Martin, S. G.; Alshankyty, I.; Mongan, N. P.; Ellis, I. O.; Green, A. R.; Rakha, E. A. *Breast Cancer Res. Treat.* **2019**, *176* (1), 63–73.

(150) Gröger, C. J.; Grubinger, M.; Waldhör, T.; Vierlinger, K.; Mikulits, W. *PLoS One* **2012**, *7* (12), e51136.

(151) Mrouj, K.; Singh, P.; Sobecki, M.; Dubra, G.; Ghoul, E. Al; Aznar, A.; Prieto, S.; Vincent, C.; Pirot, N.; Bernex, F.; Bordignon, B.; Hassen-Khodja, C.; Pouzolles, M.; Zimmerman, V.; Dardalhon, V.; Villalba, M.; Krasinska, L.; Fisher, D. *bioRxiv* **2019**, 712380.

(152) Mani, S. A.; Guo, W.; Liao, M. J.; Eaton, E. N.; Ayyanan, A.; Zhou, A. Y.; Brooks, M.; Reinhard, F.; Zhang, C. C.; Shipitsin, M.; Campbell, L. L.; Polyak, K.; Brisken, C.; Yang, J.; Weinberg, R. A. *Cell* **2008**, *133* (4), 704–715.

(153) Foroni, C.; Broggini, M.; Generali, D.; Damia, G. *Cancer Treat. Rev.* **2012**, *38* (6), 689–697.

(154) Collier, M. P.; Benesch, J. L. P. *Cell Stress Chaperones* **2020**, *25* (4), 601–613.

(155) Gunning, P. W.; Hardeman, E. C.; Lappalainen, P.; Mulvihill, D. P. *J. Cell Sci.* **2015**, *128* (16), 2965–2974.

(156) Chou, D. M.; Elledge, S. J. *Proc. Natl. Acad. Sci. U. S. A.* **2006**, *103* (48), 18143–18147.

(157) Kröger, C.; Afeyan, A.; Mraz, J.; Eaton, E. N.; Reinhardt, F.; Khodor, Y. L.; Thiru, P.; Bierie, B.; Ye, X.; Burge, C. B.; Weinberg, R. A. *Proc. Natl. Acad. Sci. U. S. A.* **2019**, *116* (15), 7353–7362.

(158) Xiao, W.; Zheng, S.; Xie, X.; Li, X.; Zhang, L.; Yang, A.; Wang, J.; Tang, H.; Xie, X. *Mol. Ther. - Oncolytics* **2020**, *17*, 118–129.

(159) Wang, C. Q.; Tang, C. H.; Wang, Y.; Jin, L.; Wang, Q.; Li, X.; Hu, G. N.; Huang, B. F.; Zhao, Y. M.; Su, C. M. *Sci. Rep.* **2017**, *7* (1).

(160) Nami, B.; Wang, Z. *Cancers (Basel).* **2018**, *10* (8), 274.

(161) Ebright, R. Y.; Lee, S.; Wittner, B. S.; Niederhoffer, K. L.; Nicholson, B. T.; Bardia, A.; Truesdell, S.; Wiley, D. F.; Wesley, B.; Li, S.; Mai, A.; Aceto, N.; Vincent-Jordan, N.; Szabolcs, A.; Chirn, B.; Kreuzer, J.; Comaills, V.; Kalinich, M.; Haas,

W.; Ting, D. T.; Toner, M.; Vasudevan, S.; Haber, D. A.; Maheswaran, S.; Micalizzi, D. S. *Science (80-.).* **2020**, *367* (6485), 1468–1473.

(162) Prashar, A.; Schnettger, L.; Bernard, E. M.; Gutierrez, M. G. *Front. Cell. Infect. Microbiol.* **2017**, *7* (SEP), 435.

(163) Barbera, S.; Nardi, F.; Elia, I.; Realini, G.; Lugano, R.; Santucci, A.; Tosi, G. M.; Dimberg, A.; Galvagni, F.; Orlandini, M. *Cell Commun. Signal.* **2019**, *17* (1), 55.

(164) Kim, S. E.; Hinoue, T.; Kim, M. S.; Sohn, K. J.; Cho, R. C.; Cole, P. D.; Weisenberger, D. J.; Laird, P. W.; Kim, Y. I. *Genes Nutr.* **2015**, *10* (1), 1–17.

(165) Maggini, S.; Pierre, A.; Calder, P. C. *Nutrients* **2018**, *10* (10).

(166) MacEyka, M.; Spiegel, S. *Nature* **2014**, *510* (7503), 58–67.

(167) Waumans, Y.; Baerts, L.; Kehoe, K.; Lambeir, A. M.; De Meester, I. *Front. Immunol.* **2015**, *6* (JUL), 387.

(168) Kingsbury, S. R.; Loddo, M.; Fanshawe, T.; Obermann, E. C.; Prevost, A. T.; Stoeber, K.; Williams, G. H. *Exp. Cell Res.* **2005**, *309* (1), 56–67.

(169) Gookin, S.; Min, M.; Phadke, H.; Chung, M.; Moser, J.; Miller, I.; Carter, D.; Spencer, S. L. *PLOS Biol.* **2017**, *15* (9), e2003268.

(170) Kabraji, S.; Solé, X.; Huang, Y.; Bango, C.; Bowden, M.; Bardia, A.; Sgroi, D.; Loda, M.; Ramaswamy, S. *Breast Cancer Res.* **2017**, *19* (1), 88.

(171) Le, X. F.; Lammayot, A.; Gold, D.; Lu, Y.; Mao, W.; Chang, T.; Patel, A.; Mills, G. B.; Bast, R. C. *J. Biol. Chem.* **2005**, *280* (3), 2092–2104.

(172) Sun, H.; Liu, K.; Huang, J.; Sun, Q.; Shao, C.; Luo, J.; Xu, L.; Shen, Y.; Ren, B. *Onco. Targets. Ther.* **2019**, *Volume 12*, 2829–2842.

(173) FAM111B gene - Genetics Home Reference - NIH https://ghr.nlm.nih.gov/gene/FAM111B (accessed Aug 8, 2020).

(174) Chung, V. Y.; Tan, T. Z.; Ye, J.; Huang, R. L.; Lai, H. C.; Kappei, D.; Wollmann, H.; Guccione, E.; Huang, R. Y. J. *Commun. Biol.* **2019**, *2* (1), 1–15.

(175) Jolly, M. K.; Tripathi, S. C.; Jia, D.; Mooney, S. M.; Celiktas, M.; Hanash, S. M.; Mani, S. A.; Pienta, K. J.; Ben-Jacob, E.; Levine, H. *Oncotarget* **2016**, *7* (19), 27067–27084.

(176) Cieply, B.; Riley IV, P.; Pifer, P. M.; Widmeyer, J.; Addison, J. B.; Ivanov, A. V.; Denvir, J.; Frisch, S. M. *Cancer Res.* **2012**, *72* (9), 2440–2453.

(177) Mooney, S. M.; Talebian, V.; Jolly, M. K.; Jia, D.; Gromala, M.; Levine, H.; McConkey, B. J. *J. Cell. Biochem.* **2017**, *118* (9), 2559–2570.

(178) Sánchez-Tilló, E.; De Barrios, O.; Siles, L.; Cuatrecasas, M.; Castells, A.; Postigo, A. *Proc. Natl. Acad. Sci. U. S. A.* **2011**, *108* (48), 19204–19209.

(179) Lee, J.; Ouh, Y.; Ahn, K. H.; Hong, S. C.; Oh, M.; Kim, J.; Cho, G. J. *PLoS One*

2017, *12* (5), 1–8.

(180) Gajria, D.; Chandarlapaty, S. *Expert Rev. Anticancer Ther.* **2011**, *11* (2), 263–275.

(181) Asgari, A.; Sharifzadeh, S.; Ghaderi, A.; Hosseini, A.; Ramezani, A. *Mol. Biol. Rep.* **2019**, *46* (6), 6205–6213.

(182) Dang, C. V. *Cell* **2012**, *149* (1), 22–35.

(183) Stine, Z. E.; Walton, Z. E.; Altman, B. J.; Hsieh, A. L.; Dang, C. V. *Cancer Discov.* **2015**, *5* (10), 1024–1039.

(184) Chen, H.; Liu, H.; Qing, G. *Signal Transduct. Target. Ther.* **2018**, *3* (1), 1–7.

(185) Gabay, M.; Li, Y.; Felsher, D. W. *Cold Spring Harb. Perspect. Med.* **2014**, *4* (6), 1–14.

(186) Richart, L.; Carrillo-de Santa Pau, E.; Río-Machín, A.; de Andrés, M. P.; Cigudosa, J. C.; Lobo, V. J. S.-A.; Real, F. X. *Nat. Commun.* **2016**, *7*, 10153.

(187) Dang, C. V. **2013**, 1–15.

(188) Bouvard, C.; Lim, S. M.; Ludka, J.; Yazdani, N.; Woods, A. K.; Chatterjee, A. K.; Schultz, P. G.; Zhu, S. *Proc. Natl. Acad. Sci. U. S. A.* **2017**, *114* (13), 3497–3502.

(189) Tawani, A.; Mishra, S. K.; Kumar, A. *Sci. Rep.* **2017**, *7* (1), 1–13.

(190) Mathad, R. I.; Hatzakis, E.; Dai, J.; Yang, D. *Nucleic Acids Res.* **2011**, *39* (20), 9023–9033.

(191) Siddiqui-Jain, A.; Grand, C. L.; Bearss, D. J.; Hurley, L. H. *Proc. Natl. Acad. Sci. U. S. A.* **2002**, *99* (18), 11593–11598.

(192) Castell, A.; Yan, Q.; Karin, F.; Hydbring, P.; Zhang, F.; Verschut, V.; Franco, M.; Zakaria, S. M.; Bazzar, W.; Goodwin, J.; Zinzalla, G.; Larson, L.-G. *Sci. Rep.* **2018**, *8* (May), 1–17.

(193) Kiessling, A.; Sperl, B.; Hollis, A.; Eick, D.; Berg, T. *Chem. Biol.* **2006**, *13* (7), 745–751.

(194) Berg, T.; Cohen, S. B.; Desharnais, J.; Sonderegger, C.; Maslyar, D. J.; Goldberg, J.; Boger, D. L.; Vogt, P. K. *Proc. Natl. Acad. Sci. U. S. A.* **2002**, *99* (6), 3830–3835.

(195) Whitfield, J. R.; Beaulieu, M. E.; Soucek, L. *Front. Cell Dev. Biol.* **2017**, *5* (FEB), 10.

(196) Castell, A.; Larsson, L. *Cancer Discov.* **2015**, *5* (7), 701–704.

(197) Carabet, L. A.; Rennie, P. S.; Cherkasov, A. *Int. J. Mol. Sci.* **2019**, *20* (1).

(198) Dang, C. V.; Reddy, E. P.; Shokat, K. M.; Soucek, L. *Nat. Rev. Cancer* **2017**, *17* (8), 502–508.

(199) McKeown, M. R.; Bradner, J. E. *Cold Spring Harb. Perspect. Med.* **2014**, *4* (10).

(200) Thomas, L. R.; Wang, Q.; Grieb, B. C.; Phan, J.; Foshage, A. M.; Sun, Q.; Olejniczak, E. T.; Clark, T.; Dey, S.; Lorey, S.; Alicie, B.; Howard, G. C.; Cawthon, B.; Ess, K. C.; Eischen, C. M.; Zhao, Z.; Fesik, S. W.; Tansey, W. P. *Mol. Cell* **2015**, *58* (3), 440–452.

(201) Thomas, L. R.; Tansey, W. P. *Open Access J. Sci. Technol.* **2015**, *3*, 1–25.

(202) Karatas, H.; Townsend, E. C.; Bernard, D.; Dou, Y.; Wang, S. *J. Med. Chem.* **2010**, *53*, 5179–5185.

(203) Odho, Z.; Southall, S. M.; Wilson, J. R. *J. Biol. Chem.* **2010**, *285* (43), 32967–32976.

(204) Dias, J.; Nguyen, N. Van; Georgiev, P.; Gaub, A.; Brettschneider, J.; Cusack, S.; Kadlec, J.; Akhtar, A. *Genes Dev.* **2014**, *28*, 929–942.

(205) Scott, D. E.; Coyne, A. G.; Hudson, S. A.; Abell, C. *Biochemistry* **2012**, *51*, 4990–5003.

(206) Murray, C. W.; Verdonk, M. L.; Rees, D. C. *Trends Pharmacol. Sci.* **2012**, *33* (5), 224–232.

(207) Huynh, K.; Partch, C. L. *Curr. Protoc. protein Sci.* **2015**, *79*, 28.9.1-28.9.14.

(208) Niesen, F. H.; Berglund, H.; Vedadi, M. *Nat. Protoc.* **2007**, *2* (9), 2212–2221.

(209) Jhoti, H.; Williams, G.; Rees, D. C.; Murray, C. W. *Nat. Publ. Gr.* **2013**, No. July.

(210) Kirsch, P.; Hartman, A. M.; Hirsch, A. K. H.; Empting, M. *Molecules* **2019**, *24* (23).

(211) Aldrich, C.; Bertozzi, C.; Georg, G. I.; Kiessling, L.; Lindsley, C.; Liotta, D.; Merz, K. M.; Schepartz, A.; Wang, S. *J. Med. Chem.* **2017**, *60* (6), 2165–2168.

(212) Zhang, Ji-hu, Chung, Thomas D.Y., Oldenburg, K. R. *J. Biomol. Screen.* **1999**, *4* (2), 67–73.

(213) Jacob, R. T.; Larsen, M. J.; Larsen, S. D.; Kirchhoff, P. D.; Sherman, D. H.; Neubig, R. R. *J. Biomol. Screen.* **2012**, *17* (8), 1080–1087.

(214) Karatas, H.; Townsend, E. C.; Cao, F.; Chen, Y.; Bernard, D.; Liu, L.; Lei, M.; Dou, Y.; Wang, S. *J. Am. Chem. Soc.* **2013**, *135* (2), 669–682.

(215) Cao, F.; Townsend, E. C.; Karatas, H.; Xu, J.; Li, L.; Lee, S.; Liu, L.; Chen, Y.; Ouillette, P.; Zhu, J.; Hess, J. L.; Atadja, P.; Lei, M.; Qin, Z. S.; Malek, S.; Wang, S.; Dou, Y. *Mol. Cell* **2014**, *53* (2), 247–261.

(216) Lea, W. A.; Simeonov, A. *Expert Opin. Drug Discov.* **2011**, *6* (1), 17–32.

(217) Rossi, A. M.; Taylor, C. W. *Nat. Protoc.* **2011**, *6* (3), 365–387.

(218) Hall, M. D.; Yasgar, A.; Peryea, T.; Braisted, J. C.; Jadhav, A.; Simeonov, A.; Coussens, N. P. *Methods Appl. Fluoresc.* **2016**, *4* (2), 022001.

(219) Koh, C. M.; Sabò, A.; Guccione, E. *BioEssays* **2016**, *38* (3), 266–275.

(220) Casey, S. C.; Tong, L.; Li, Y.; Do, R.; Walz, S.; Fitzgerald, K. N.; Gouw, A. M.; Baylot, V.; Gütgemann, I.; Eilers, M.; Felsher, D. W. *Science (80-.).* **2016**, *352* (6282), 227–231.

(221) Polivka, J.; Janku, F. *Pharmacol. Ther.* **2014**, *142* (2), 164–175.

(222) Chacón Simon, S.; Wang, F.; Thomas, L. R.; Phan, J.; Zhao, B.; Olejniczak, E. T.; MacDonald, J. D.; Shaw, J. G.; Schlund, C.; Payne, W.; Creighton, J.; Stauffer, S. R.; Waterson, A. G.; Tansey, W. P.; Fesik, S. W. *J. Med. Chem.* **2020**, *63* (8), 4315–4333.

(223) Macdonald, J. D.; Chacón Simon, S.; Han, C.; Wang, F.; Shaw, J. G.; Howes, J. E.; Sai, J.; Yuh, J. P.; Camper, D.; Alicie, B. M.; Alvarado, J.; Nikhar, S.; Payne, W.; Aho, E. R.; Bauer, J. A.; Zhao, B.; Phan, J.; Thomas, L. R.; Rossanese, O. W.; Tansey, W. P.; Waterson, A. G.; Stauffer, S. R.; Fesik, S. W. *J. Med. Chem.* **2019**, *62* (24), 11232–11259.

Appendix: Towards the Identification of Small Molecule Inhibitors of the Interaction Between Myc and WDR5

Abstract

In approximately 50% of all human cancers, the expression and transcriptional activity of Myc is dysregulated and is closely linked to the onset of tumorigenesis. There have been numerous studies that aimed to inhibit Myc and eradicate its oncogenic activities. Inhibitors resulting from these past studies suffered from poor bioavailability and low target site engagement. A recently discovered interaction between Myc and WDR5 was reported, which showed that the interaction of Myc and WDR5 is critical for Myc to activate the transcription of target genes. The interaction of Myc and WDR5 provided new opportunities for targeting Myc, which we leveraged for our studies. Herein, we describe the use of high throughput screening and fragment based drug discovery identify small molecules and scaffolds with the potential of inhibiting Myc by targeting the interaction between Myc and WDR5. Using fragment based screening, we screened 1,500 fragments and identified 2 candidate fragments. In our high throughput screening campaign, we screened 25,000 small molecules (Z' = 0.61). Small molecule hits were triaged using a negative selection MLL-WDR5 fluorescence polarization based binding assay. Site specificity for the Myc-WDR5 site was evaluated by a Myc-WDR5 fluorescence polarization based binding assay (Z' = 0.68), which yielded 2 small molecules with the potential to engage at the Myc-WDR5 site. Co-crystal studies of validated fragments and small molecules with recombinant WDR5 revealed that none of the fragments nor molecules engaged at the Myc-WDR5 site.

A.1. Introduction

In various cancers, oncogenic c-Myc (hereafter simply referred as Myc) has been linked to the many hallmarks of cancer and has been reported to be dysregulated in approximately 50% of all human cancers.[182–186] Myc is a basic helix loop helix leucine

zipper transcription factor that requires its dimerization with obligate binding partner, Max, in order to influence transcription of target genes.[183,187] It is normally expressed at low levels, and its expression is limited to highly proliferating cells.[182–186] In cancers, the oncogenic potential of Myc is linked to its function as a transcription factor and drives tumorigenesis by increasing the transcription that is essential to proliferation, metabolism, and biosynthetic pathways.[182–186]

Because Myc plays a critical part to tumorigenesis, there have been numerous efforts to inhibit Myc.[188–194] Both direct and indirect approaches have been pursued. Direct approaches targeting processes that impair the gene expression of Myc, which included the stabilization of G-quadruplex structures proximal to the promoter of Myc gene.[188–191] The stabilization of these G-quadruplex structures consequently repress the transcription of Myc genes.[188–191] Other direct approaches to targeting Myc includes impairing the co-localization of Myc on chromatin and inhibiting its heterodimerization with its binding partner Max.[192–194] These approaches yielded small molecule inhibitors that had poor tumor accumulation, poor bioavailability, and poor target site engagement, and thus, had limited clinical success.[195] Indirect approaches to targeting Myc included interfering with the protein translation of the Myc mRNA and stabilization of the Myc protein.[195,196] Despite these various approaches to target Myc, many of them have been unsuccessful in producing an efficacious inhibitor with high bioavailability profiles.[184,195] The crux of this problem is due to the intrinsic disordered structure of Myc; it takes on various and transient secondary structures and does not have any discernible pockets amendable for drug discovery.[197–199] Because of these physical properties, Myc has been long deemed an “undruggable” target.[197–199]

Interestingly, Tansey and Fesik laboratories proposed a new model regarding the recruitment of Myc to chromatin.[200,201] They showed that the activity of Myc is mediated by WD40 protein, WDR5, which functions as a transcriptional activator in various protein complexes, such as MLL, RbBP5, KANSL1, and KANSL2.[200,202–204] In regards to Myc, it facilitates recruits Myc to the promoter region of target genes and activate the transcription of those genes.[200] Biochemical and *in vivo* studies from Tansey and coworkers demonstrated that Myc associates with a groove on the surface of WDR5 through key hydrogen bonds and electrostatic interactions.[200] Scrutiny of the publically

available protein structure of WDR5 and the Myc peptide (PDB: 4Y7R) revealed key resides on WDR5 near the Myc interacting site (e.g. K52, K220, H178 and F263), which could be leveraged to generate high affinity chemical probes or small molecule inhibitors targeting the Myc-WDR5 site. Thus, the interaction of Myc and WDR5 presented a new opportunity for targeting Myc by targeting a druggable protein-protein interaction.

Herein, we described our approach to identifying small molecule inhibitors for the interaction of Myc and WDR5 by using high throughput screening and fragment based drug discovery campaigns. Both campaigns yielded 2-5 small molecules and fragments after screening and validation. However, none of the small molecules and scaffolds identified in our screens were shown to engage at the Myc-WDR5 interface by co-crystal studies.

A.2. Materials and Methods

A.2.1. Fragment-Based Screening of ChemDiv and Life893 Fragment Libraries Against WDR5

Plates consisting of fragments at 1 mM in DMSO were removed from -20°C freezer, equilibrated to room temperature, and centrifuged at 1500 rpm for 2 min prior to addition of fragments to 384 well plates. To screen 1,350 fragments from the ChemDiv and Life893 fragment libraries against recombinant N-terminal truncated WDR5Δ23 (residues 24-334), 1 µL of DMSO or 1 mM fragment in DMSO was added to 384 well plates, followed by the addition of 9 µL of 6.67 µM WDR5 and 10 µL of 2X Sypro Orange dye from Protein Thermal Shift™ Dye Kit (Thermo Fischer cat. no. 461146). The final concentrations for this assay were 3 µM WDR5, 1X Sypro Orange, and 50 µM of each fragment in 50 mM HEPES. Plates were centrifuged using a benchtop centrifuge for 1 min prior to the assay. Total concentration of DMSO was 5% (v/v). The negative control used was 3 µM of WDR5 and 1X Sypro Orange (“WDR5+Sypro Orange control”). “Active fragments” were defined as fragments that increased the melting temperature of WDR5 by 2°C relative to the melting temperature (T_m) of WDR5 in absence of the fragment, resulting in 10 fragments. To increase the quantity of “active fragments,” fragments were then selected if they induced an increase in the melting temperature of 2 standard deviations relative to the negative control. To screen fragments in the presence of MM-401, a final concentration of 5 µM of MM-401 was used. To determine if these were non-

specific binders, we performed the dose-dependent thermal shift assays using different concentrations of the fragments to assess whether concentration-dependent changes in the T_m of WDR5 occurred in the presence and absence of the WDR5-MLL inhibitor. Plates were assayed using Applied Biosystems ViiA7 Real-Time PCR system. Plates were heated from 25 – 95°C with a heating rate of 0.5°C/min Measurements were made in with excitation and emission wavelengths set at 580 nm and 623 nm, respectively.

A.2.2. Multiplexed High-Throughput Screening of Small Molecules Against WDR5

Multiplexed high-throughput screening of compounds deposited at the Center of Chemical Genomics of the University of Michigan was performed in collaboration with Dr. Aaron Robida. Libraries screened included LOPAC, Prestwick, and MB 24K. All thermal stability assays of recombinant ΔN_{1-23} WDR5 were performed using Applied Biosystems ViiA7 Real-Time PCR system. Plates were heated from 25 – 95°C with a heating rate of 0.5°C/min. Measurements were made in with excitation and emission wavelengths set at 580 nm and 623 nm, respectively. The thermal unfolding of WDR5 was monitored using Sypro Orange dye from Protein Thermal Shift™ Dye Kit (Thermo Fisher cat. no. 4461146) or using SYPRO™ Orange Protein Gel Stain 5000X Concentrate in DMSO (Thermo Fischer cat. no. S6650). Assays were performed using Applied Biosystems™ MicroAmp™ Optical 384-Well Reaction Plate with Barcode (Fisher Scientific cat. no. 4309849). For these assays, 5 µL of 50 mM HEPES were added to the wells reserved for the negative control and multiplexed compounds (4 compounds per well). The combination of compounds to be multiplexed was predetermined by personnel at the Center of Chemical Genomics. To wells reserved for 4-plex was added 50 µL of selected compounds for a total of 200 nL of 4-plexed compounds per well. Compounds were added using Sciclone ALH3000 pintool (Perkin Elmer). To negative and positive control wells was added 1 µL of 20% DMSO (v/v). Following, to entire plate was added 14 µL of the master mix consisting of 15 µM of WDR5 in 50 mM HEPES and 2X Sypro Orange or 10X SYPRO Orange dye in 50 mM HEPES. The master mix consisting of 15 µM WDR5 and 2X Sypro Orange or 10X SYPRO Orange was prepared fresh prior to each assay and was placed on the shaker for 10 minutes prior to addition. Plate was covered with Applied Biosystems™ MicroAmp™ Optical Adhesive Film (Fisher Scientific cat. no. 43-119-71), centrifuged at 1500 rpm for 2 min, and then, the thermal stability assay was performed.

The total concentration of DMSO was 1% (v/v). Final concentrations were 3 μM WDR5, 1X Sypro Orange or 5X SYPRO Orange dye, and 10 – 25 μM of each compound in 50 mM HEPES or 10 μM Myc peptide (sequence: H-DEEEIDVVSV-NH_2). The negative control for this assay was 3 μM WDR5 + 1X Sypro Orange or 5X SYPRO Orange dye, and the positive control was 3 μM WDR5 + 1X Sypro Orange control (or 5X SYPRO Orange) + 10 μM Myc peptide. "Active wells" were defined as wells that showed an increase in the melting temperature by 3 standard deviations relative to the negative control. Deconvolution of 4-plexed "hits" were performed as dose-dependent thermal stability assays using Mosquito X1 (TTP Labtech) to select compounds from "active wells" and deliver to 384-well plate to provide a final concentration of 2-5 μM in DMSO. Measurements for deconvolution studies were performed as duplicates and thermal stability assays were performed using the Applied Biosystems ViiA7 Real-Time PCR system as noted above.

A.2.3. Quality Control Studies for Ordered "Hit" Compounds Identified by HTS

Ordered compounds (49) were analyzed for purity using ESI-MS dissolved in 1:1 acetonitile:water, and peaks corresponding to $M+H^+$ were analyzed. Activity of ordered compounds were analyzed using Thermal Shift Assay with same parameters as noted above to confirm that these compounds induce a change in T_m that is greater than 3 standard deviations relative to the T_m of WDR5 alone. Assay conditions of "retest" studies were identical to conditions used for HTS.

A.2.4. MLL-WDR5 Fluorescence Polarization Assay (Negative Selection)

MLL-WDR5 competition assay was performed as previously described with some modifications, which were detailed here.[202] To 15 mL Falcon tube was added 3.8 mL of 8.42 nM of recombinant WDR5 in FP buffer and 3.8 mL of 1.26 nM MLL probe in FP buffer. Mixture was equilibrated at RT for 3 hours in dark with agitation. After 3 hours, aliquots of 3x20 μL were used to assess formation of WDR5-MLL probe complex. Fluorescence polarization values of complex were approximately 91 $\pm$ 9.9. Following the evaluation of WDR5-MLL probe complex, competitive binding assay was prepared. To a black 384 well plate was added 19 μL of WDR5-MLL probe complex solution and 1 μL of either 20 mM, 10 mM, 5 mM, or 2.5 mM of HTS compound in DMSO. To wells corresponding to probe only positive controls was added 9.5 μL of 1.26 nM of MLL probe

in FP buffer, 9.5 µL of FP buffer, and 1 µL of DMSO. To wells corresponding to MM-401 positive controls was added 19 µL of WDR5-MLL probe complex solution and 1 µL DMSO. To wells corresponding to WDR5-MLL probe negative controls was added 19 µL WDR5-MLL probe complex solution and 1 µL DMSO. Final assay conditions were 4 nM WDR5, 0.6 nM MLL probe, 5 µM MM-40l, and one of the following concentrations of HTS compounds: 1 mM, 500 µM, 250 µM, or 125 µM. Final volume of competitive binding assay per well was 20 µL. Competitive binding assays was incubated for 12 hours at RT in dark to ensure complete competition between HTS compounds and MLL probe. Titrations of HTS compounds were performed using the following concentrations of working solutions: 20 mM, 10 mM, 5 mM, 2.5 mM, 1.25 mM, 62.5 µM, 31.3 µM, and 15.65 µM. Final assay concentrations for HTS compounds in titrations were 1 mM, 500 µM, 250 µM, 125 µM, 62.5 µM, 31.3 µM, 15.65 µM, and 7.8 µM. Fluorescence polarization was read using the following spectrophotometric parameters: λ_{ex} = 485 nm and λ_{em} = 528 nm. FP buffer was prepared fresh prior to each assay and had final pH = 6.5. Henderson–Hasselbalch equation (below) was used to determine amounts of sodium phosphate (monobasic and dibasic) for buffer. For 15 mL of FP buffer, 121 mg NaH_2PO_4 and 68 mg Na_2HPO_4 and 215 µL of Triton X-100 was mixed in MilliQ water. Competitive assay was performed with 4 technical replicates and 2 biological replicates.

$$pH = pK_a + log\frac{[dibasic]}{[monobasic]}$$

In Henderson-Hasselbalch equation, pK_a was 6.82, dibasic corresponds to Na_2HPO_4, and monobasic corresponds to NaH_2PO_4.

A.2.5. Myc-WDR5 Fluorescence Polarization Assay

To 5 mL Eppendorf tube was added 1.57 mL of 111.11 µM of recombinant WDR5 in FP buffer and 875 µL of Myc probe in FP buffer. Binding of WDR5 and Myc probe was equilibrated for 4 hours at RT in dark with agitation. After 4 hours, fluorescence polarization readings were obtained to ensure formation of WDR5-Myc probe complex. Fluorescence polarization readings for WDR5-Myc peptide complex was 80$\pm$9.6 and free Myc probe was 23.7$\pm$6.5. To a black 384 well plate was added 14 µL of WDR5-Myc probe complex solution, 5 µL of FP buffer, and 1 µL of HTS compound in DMSO. Final concentrations of HTS compounds were 1 mM, 500 µM, 250 µM, or 125 µM. To wells

corresponding to Myc probe positive control was added 20 µL of probe master mix (135 µL of FP buffer and 75 µL of 400 nM Myc probe solution). To wells corresponding to Myc peptide positive control was added 14 µL of WDR5-Myc probe complex solution and 6 µL of 647 µM Myc solution in FP buffer. Follow-up studies of the quick titration of the HTS compounds was performed using an extended titration with the following final concentrations of HTS compounds: 750 µM, 375 µM, 187.5 µM, 93.75 µM, and 46.87 µM in DMSO. Concentrations for the follow-up studies were as noted for the quick titration. For each well, the following assay conditions were used 9 µL of 100 µM recombinant WDR5, 5 µL of 400 nM Myc probe solution, 1 µL of compound in DMSO, and 5 µL of FP buffer (final volume 20 µL). Final assay concentrations were 45 µM WDR5, 40 nM Myc probe, 200 µM Myc peptide, and the final concentrations for the HTS compounds were noted above. Fluorescence polarization was read using the following spectrophotometric parameters: λ_{ex} = 485 nm and λ_{em} = 528 nm. FP buffer was prepared fresh prior to each assay and based on the buffer used to study the interaction of WDR5 and KANSL2, which also is an overlapping interaction at the Myc-WDR5 site.[204] The FP buffer for the Myc-WDR5 FP assay consisted of 20 mM Tris and 200 mM NaCl (pH 7.0). For 15 mL of FP buffer, 34 mg of Tris base and 177 mg NaCl was combined in 15 mL of MilliQ water. Resultant pH was acidified using 162 µL of 1M HCl to pH 7.0.

A.2.6. Peptide Synthesis of Myc Probes

Peptides were synthesized manually using NovaRink resin (loading capacity 0.44 mmol/g). To sealed vessel was added 227 mg NovaRink (0.1 mmol) in 10 mL of NMP. In a separate vessel was added Fmoc-AA (Fmoc protected amino acid, 0.5 mmol) in 2.6 nL NMP and 87 µL of DIPEA (0.5 mmol). Basic amino acid mixture was mixed at RT until clear and yellow in color. Then, 54 mg of HOAT (0.4 mmol) and 152 mg of HATU (0.4 mmol) were added to basic amino acid mixture and sonicated until reaction mixture was clear. Activated Fmoc-AA mixture was added to NovaRink resin. Coupling reaction proceeded at RT for 1 hour with agitation. Double coupling was performed for bulky aliphatic amino acids, such as Fmoc-Val, Fmoc-Ile, and Fmoc-Ahx. Following coupling reaction, reaction supernatant was decanted, washed with 3x10 mL NMP, 3x10 mL DCM, and 3x10 mL NMP. Deprotection of Fmoc was performed using 20% piperidine/NMP (in XS) for 30 min at RT with agitation. Sample of deprotected resin was removed and added

to ninhydrin stain to assess complete deprotection prior to the start of the subsequent coupling step. Final unlabeled Myc peptide consisted of following amino acid sequence: Fmoc-Ahx-DEEEDIDVVSV-NH_2 (M+H = 1466.68 Da).

Bioconjugation of Myc peptides was performed using 5/6-FAM-NHS (Thermo cat. # 44610). To scintillation vial was added 100 mg of 5/6-FAM-NHS (0.1 mmol, 3 eq) in 4 mL NMP and 70 µL of DIPEA (0.4 mmol, 4 eq). Mixture was swirled to afford a bright red, clear mixture. Mixture was added to resin. Labeling reaction proceeded for 12 hours at RT in dark and with agitation. Following 12 hours, resin was washed with 3x10 mL NMP, 3x10 mL DCM, and 3x10 mL NMP. Global deprotection and resin cleavage was performed in TFA/H_2O (9.5: 0.5, v/v) for 1 hour at RT with agitation. TFA was removed *in vacuo*. Azeotrope of DCM and TFA was used to quicken evaporation of TFA. Peptide was precipitated using 10 mL Et_2O at 0°C for 1 hour, which yielded white, cloudy mixture with precipitate. Precipitate was filtered using Hirsch funnel, retained, and dried in desiccator for 3 hours. Crude peptide (2 mg) was used for reverse phase (C18) purification using HPLC. Crude peptide was dissolved in 0.1 M NH_4HCO_3 (*aq*) to yield a clear, bright green solution. Crude peptide solution was filtered by syringe (25 µm filter) prior to injecting onto HPLC for purification. Optimized purification method was the following: 20% ACN/H_2O (isocratic for first 15 minutes), 20-40% ACN/H_2O for 20 minutes, 40-75% ACN/H_2O for 15 minutes, and finally 40-75% ACN/H_2O for final 5 minutes. Fractions of purified peptide eluted at 40% ACN/H_2O and were detected with λ = 210 nm and λ = 254 nm. Peptide fractions were combined and solvent was removed *in vacuo*. Peptides were then resuspended in 3 mL of water, frozen in -80°C for 3 days, and lyophilized for 3 days.

A.3. Results and Discussion

For this drug discovery project, we used a high throughput screening (HTS) approach to screen libraries consisting of small molecules with drug-like properties and contain pharmacophores that have been selected by medicinal chemists for their structural diversity and bioactivity. The affinities of small molecule “hits” from the HTS screening campaign are typically in the micromolar range. We also used a fragment-based drug discovery (FBDD) approach. Molecules from fragment libraries are smaller than small molecules and thus, bind to the protein with affinities ranging from micromolar to millimolar.[205] However, due to their small size, these fragments are able to overcome

the entropic barrier to binding and can make “high quality interactions,” which permits their binding to be detected.[205,206] Thus, screening fragments would facilitate the discovery of chemical scaffolds that are essential to the interaction with the target protein. These two screening approaches are summarized in Figure A.1. By using both of these libraries, we were able to sample a larger chemical space to search for molecules capable of binding to WDR5 so that it could be a candidate for blocking the interaction of Myc and WDR5.

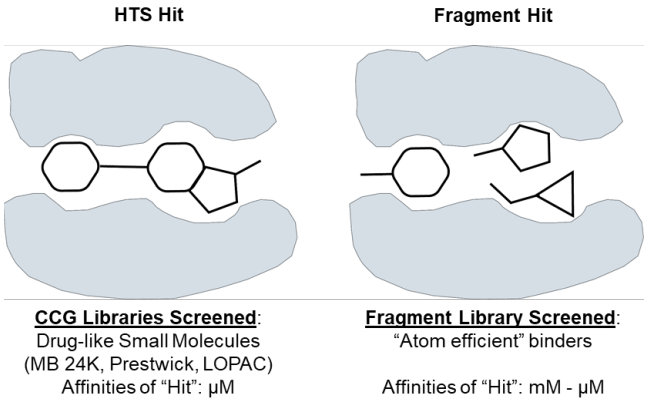

Figure A.1. Complementary Approaches to Drug Discovery Approaches: High Throughput Screening and Fragment-Based Screening.

A.3.1. Fragment Based Drug Discovery for Scaffolds That Interact with WDR5

In order to screen compounds against WDR5, we used the Thermal Shift assay, which is an assay based on differential scanning fluorimetry.[207] This assay measures the melting temperature (T_m) of WDR5 in the presence of a hydrophobic dye (commercially available Thermal Shift assay kit can be used or SYPRO Orange can also be used).[208] The quantum yield of this dye is very low in aqueous buffers, but as the thermal shift assay progresses, WDR5 heats and undergoes thermal denaturation, which exposes the hydrophobic core of the protein.[208] When the hydrophobic dye interacts with the hydrophobic core of WDR5, the quantum yield increases and facilitates the measurement of the T_m, which is the temperature at which half of the population of the protein is denatured and half remains properly folded.[208] In the presence of a small molecule that binds to the protein, protein receives additional stabilization from the interaction with the small molecule, which shifts the T_m to higher temperature (Figure A.2).[208] The shift in T_m facilitates the identification of compounds or fragments with binding activity. This general thermal shift assay was used as the screening method in this project due to the lack of

availability of an effective direct binding assay between Myc and WDR5. Thomas and coworkers developed a fluorescent polarization (FP) competitive assay for the WDR5/Myc interface using a FP probe constructed from consisting of a 10mer amino acid sequence of Myc that interacts with WDR5 and labeled with fluorescein (FAM).[200] However, the narrow dynamic range of this assay prevents its use as a screening method and therefore, we elected to perform a general screen of fragments and small molecules against WDR5, which were followed by validation studies to substantiate the binding of those "hit" molecules and to evaluate the site-specificity of those "hits."

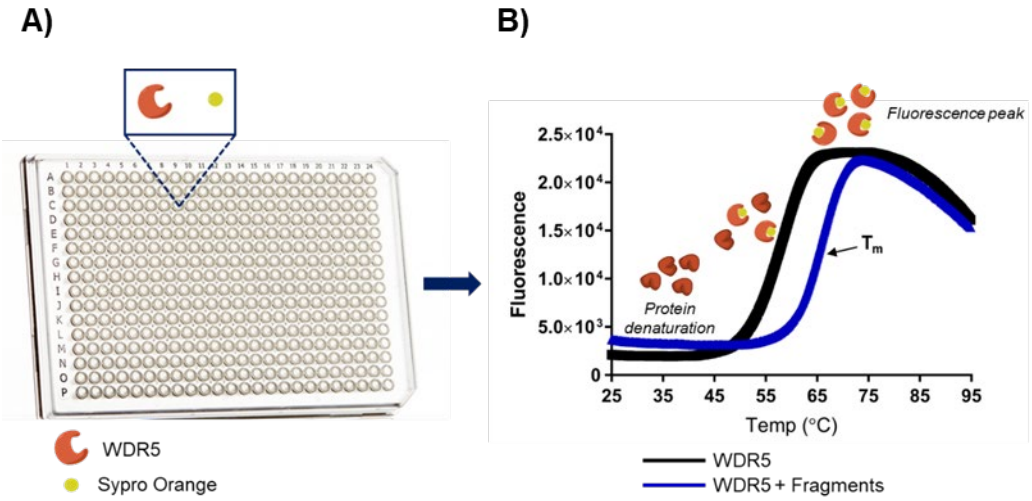

Figure A.2. Cartoon of Thermal Shift Assay Using Sypro Orange for Fragment-Based Drug Discovery Approach.

Prior to screening experiments using fragment libraries or small molecule libraries, optimal conditions were screened. Parameters for assay conditions were: optimal WDR5:thermal shift dye ratio, buffer, DMSO concentration, and detergent concentration. We also determined the optimal concentration of MLL-WDR5 inhibitor so that it could be used as a positive control for binding. We performed cross-titration of the thermal shift dye (1:500, 1:1000) and WDR5 (1 μM, 3 μM, 5 μM) to determine the pair of the concentration of the thermal shift dye and WDR5 that provided a melt curve with a distinct sigmoidal shape, a S/N = 10, and the variance around the calculated T_m. From this cross-titration, we found that the use of 3 μM WDR5 and 1:1000 Sypro Orange dye was optimal and resulted in a baseline T_m for WDR5 as 57 degs. Following, we screened for the optimal buffer (1X PBS, 50 mM Tris, 50 mM HEPES) and selected 50 mM HEPES as the buffer for this assay. Tris contains a primary amine, and thus, was not selected as the

assay buffer for its potential to participate in solvolysis with electrophilic small molecules or fragments in the screen. The detergent screen showed that the presence of detergents (Triton X-100 and Tween-20) resulted in high background through the putative interactions of the detergents with the aromatic framework of the Sypro Orange dye, and therefore, detergents were excluded from the assay conditions. Lastly, we determined the optimal concentration of dimethyl sulfoxide (DMSO) to be included in the assay conditions so that it could assist in the solubilization of organic fragments and compounds. From this DMSO screen, I determined that the optimal concentration of DMSO was 5% (v/v); higher concentrations of DMSO decreases the T_m, which is associated with a destabilization of WDR5 at these concentrations. From these studies, we determined the optimal conditions for fragment and small molecule screening campaigns using the thermal shift assay.

Fragments screened against WDR5 were obtained from Dr. Shaomeng Wang's laboratory at the University of Michigan; these fragments came from the ChemDiv and Life Chemical fragment libraries. Fragments from these libraries have been certified to abide by the "Rule of 3," which is similar to Lipinski's "Rule of 5" for small molecules.[209,210] This property is a defining characteristic of fragment libraries because they provide control over the physiochemical properties during the optimization of the "hit" fragment to a molecule with more drug-like properties (Rule of 5). [209,210] The initial design for the fragment screens is to perform the thermal shift assay in the presence of a MLL-WDR5 inhibitor to occlude the MLL-WDR5 site and thus, to maximize the discovery of fragments capable of interacting at the Myc-WDR5 site. However, due to the low-throughput nature of this assay set-up, we elected to identify fragments that increased the T_m of WDR5 in absence of the MLL-WDR5 inhibitor and validate the identified fragment for its ability to induce an additional increase in the T_m of WDR5 in the presence of the MLL-WDR5 inhibitor. In order to identify "hit" fragments from these libraries, we screened these fragments at 50 μM against 3 μM of WDR5 and 1:1000 Sypro Orange dye in 50 mM HEPES buffer with 5% DMSO (v/v), and "hit" fragments were defined as fragments that increased the baseline T_m of WDR5 by 2°C to identify highly tight binders of WDR5 (Figure A.3). Fragments fitting these criteria were then validated in a dose-dependent thermal shift assay, which resulted in 10 fragments displaying a dose-dependent increase in the baseline T_m of WDR5 (Figure A.3B). In order to further substantiate the binding of these

fragments, we assayed them in a dose-dependent thermal shift assay in the presence of 5 μM of an MLL-WDR5 inhibitor, LC-045 (provided by Dr. Yangbing Li from Dr. Shaomeng Wang's lab). By including the MLL-WDR5 inhibitor, the new baseline T_m for WDR5 was 72 degs, and fragments that were considered as "real binders" of WDR5 were ones that increased the T_m of WDR5 beyond 72 degs, which resulted in 2 fragments. The increase in Tm caused by LS.6.4.3 is likely to be caused by aggregation of WDR5 since only flat melt curves were observed for WDR5 in the presence of LS.6.4.3 and LC-045 (Figure A.3C). Two of the 10 fragments, LS.3.6.3 and LS.7.8.2 (Figure A.3C and D) were sent to the Center of Chemical Genomics at the University of Michigan for co-crystal studies, but these studies revealed that these fragments do not bind near the WDR5/Myc interface (data not shown). After performing this round of fragment screening, we realized that the use of a 2 deg shift as the selection criteria might have been too stringent and thus, hindered the opportunity to identify scaffolds that truly bind to WDR5 albeit with lower affinities.

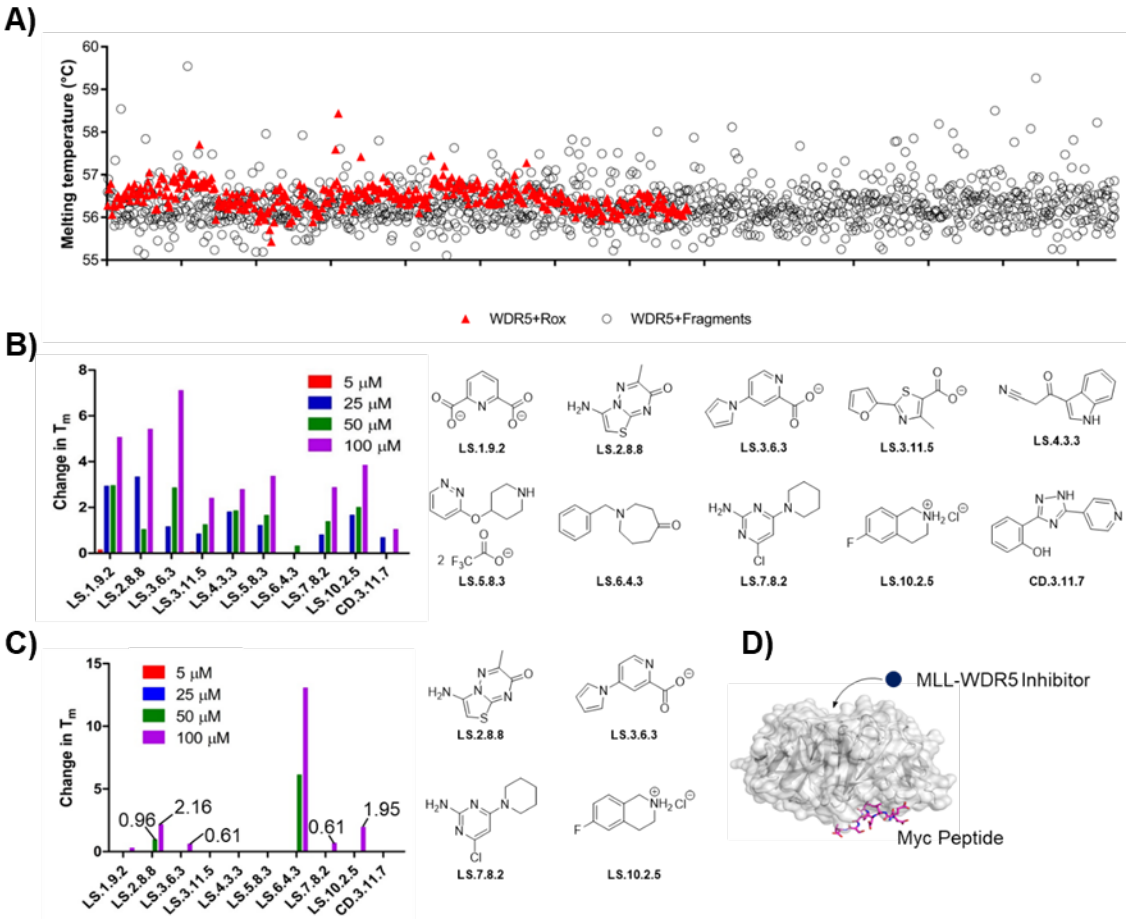

Figure A.3. Fragment Based Screening Approach to Identify Inhibitors of Myc-WDR5 Protein Interaction. A) Campaign view of thermal shift screen of 1,500 fragments against recombinant WDR5 depicting the change in melting temperature (Tm) of WDR5. X-axis depicts all of compounds by library identifier. B) Dose dependent thermal shift assay for fragments that elicited a change in Tm ≥ 2°C. Structures of fragments shown on right. C) Dose dependent thermal shift assay for fragments shown in B. Assay conducted in presence of MLL-WDR5 inhibitor, LC-045. Change in Tm of WDR5 in presence of LC-045 and fragment depicted on graph. Structures of framgents that elicited additional change in Tm in WDR5 shown on right. D) Cartoon depicting the interactions between WDR5 and MLL and WDR5 and Myc peptide. Aim of fragment based screen was to identify fragments that occupy near the interaction between WDR5 and Myc. Protein structure of WDR5 interacting with Myc peptide obtained from PDB (4Y7R).

To continue with the quest to identify potential fragment binders, we reanalyzed the thermal shift data (completed in absence of the MLL-WDR5 inhibitor, LC-045) for fragments that increased the T_m of WDR5 by 2 standard deviations (SD) relative to the Tm of WDR5 alone, which is commonly used in FBDD. The use of 2SD as the selection parameter resulted in 68 fragments and after assaying those 68 fragments in a dose-dependent thermal shift assay, 35 fragments exhibited a dose-dependent increase in the Tm of WDR5 (Figure A.4). Akin to the validation approach previously described, we screened the 35 fragments against WDR5 in the presence of MLL-WDR5 inhibitor, MM-401, for their ability to provide an additional thermal stability and determined that 17 of

these fragments increased the T_m of WDR5 from 0.6 – 3°, depending on the concentration of the fragment used (Figure A.4). These 17 fragments have been identified from the primary screening campaign of Life Chemicals and Chem Div fragment libraries as true potential binders of WDR5 and will require further validation using co-crystal studies to ascertain the location and binding modes of these fragments to the surface of WDR5.

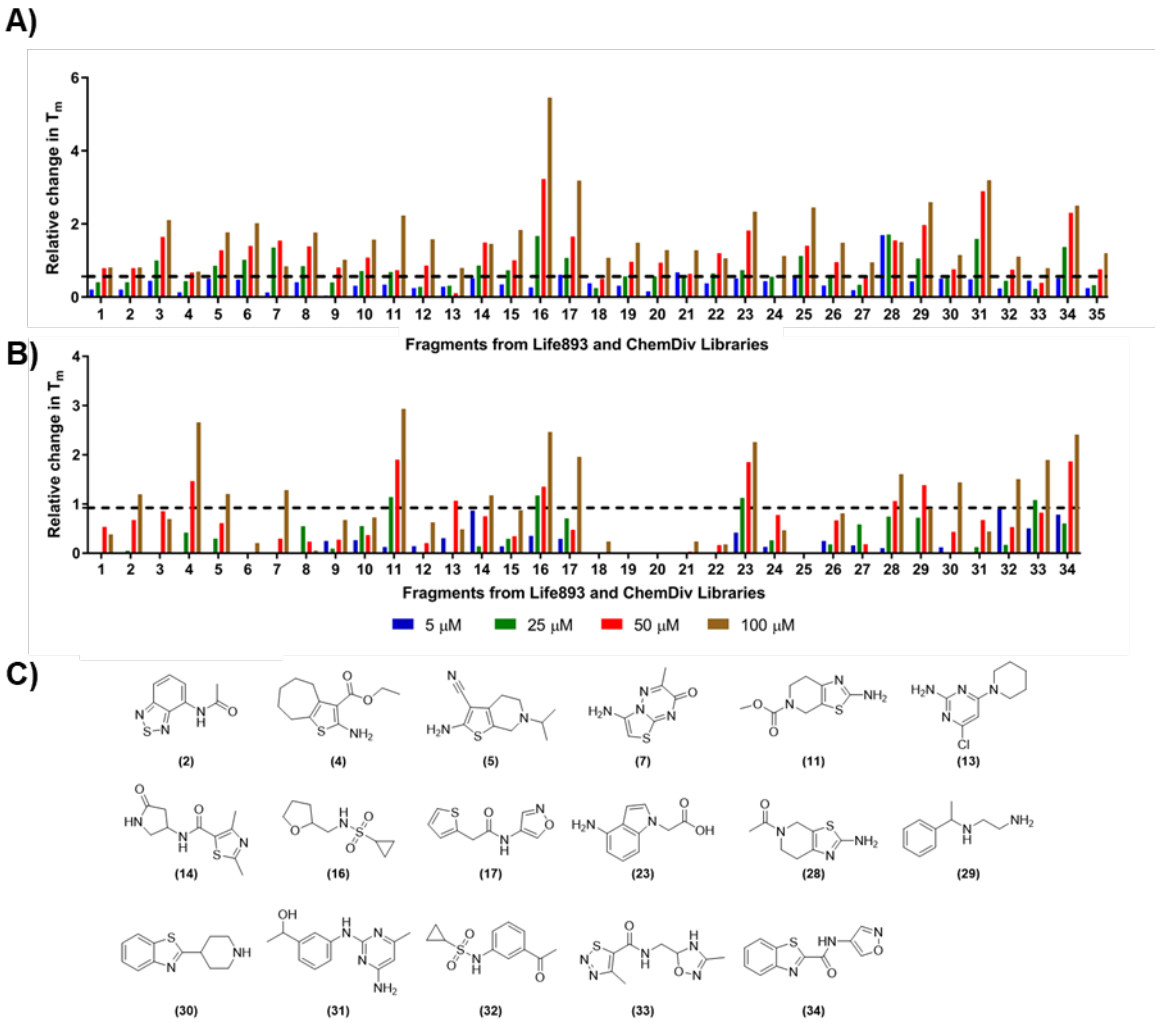

Figure A.4. Validation of Fragments Identified From Fragment Based Screening. A) Campaign view of dose-dependent thermal shift assay of 35 fragments that increased Tm of WDR5 ≥ 2 standard deviations. B) Campaign view of dose-dependent thermal shift of WDR5 in presence of 35 fragments shown in A and WDR5-MLL inhibitor, MM-401. C) Structures of fragments that increased Tm of WDR5 ≥ 2 standard deviations even in presence of MM-401.

At the end of the fragment-based screening campaign, 4 fragments were identified using the thermal shift assay. These fragments increased the T_m of WDR5, even in the presence of a MLL-WDR5 inhibitor, suggesting these fragments could be real binders of WDR5. These fragments were sent to the Center of Structural Biology at the University

of Michigan for crystallization studies to elucidate the site-specificity of these fragments. From the crystallization and crystal soaking studies performed by Dr. Jeanne Stuckey from the Center of Structural Biology, these fragments were found to bind to WDR5 on the face opposite of the WDR5-Myc interaction (data not shown). Based on this finding, these fragments were not proceeded to further analyses, such as structural-activity relationship (SAR) analyses or chemical modifications to improve binding potency. Additional fragment libraries could be screened to continue the discovery of chemical scaffolds capable of interacting near the interface of WDR5 and Myc.

A.3.2. High Throughput Screening of Drug-Like Compounds Against WDR5

In addition to using the fragment-based approach to identify novel inhibitors for the interaction between WDR5 and Myc, we also performed multiplexed high throughput screening. This approach is complementary to the fragment-based approach because unlike the fragment-based approach, HTS features small molecules, which are much larger than fragments and harbor more moieties and atoms that could interact with WDR5. Thus, compounds identified from HTS would have a higher binding affinity than fragments identified from fragment-based screening. Despite this advantage, compounds identified from HTS could be promiscuous binders, that is, compounds that bind to an array of proteins with little specificity.[211] This limitation was minimized in this study because the assayed compounds were selected from commercially available libraries of drug-like compounds that have been curated to exclude these promiscuous ligands and assay interfering compounds (e.g. PAINS, pan-assay interference compounds[211]). Compounds assayed in this high throughput screening campaign were from the LOPAC, Prestwick, and Maybridge 24K libraries. The LOPAC library feature compounds with pharmacologically active compounds. The Prestwick library is a collection of FDA approved drugs and small molecules that were selected for their pharmacological diversity and verified bioavailability in humans. Lastly, the Maybridge 24K library features chemically diverse compounds and scaffolds. From these libraries yielded 25,000 small molecules for the HTS screening campaign, which was performed in collaboration with the Center of Chemical Genomics at the University of Michigan.

The Thermal Shift screening assay was used to screen the 25,000 compounds in a 384-well plate format, where each well consisted of recombinant WDR5 proteins, Sypro

Orange dye, and 4 drug-like compounds. Prior to the HTS, it was imperative to perform quality control studies to optimize the dynamic range of the assay and minimize the assay variability, especially since 80-100% of all initial "hits" (i.e. compounds that exhibit activity during a screening assay) could result from artefacts if controls and assay parameters are unoptimized.[211] The Z' score is a statistical parameter used to assess the dynamic range of the assay and the assay variability and is expressed as the following:

$$Z' = 1 - \frac{3SD_{control,neg} + 3SD_{control,pos}}{\left|mean_{control,neg} - mean_{control,pos}\right|}$$

Thus, an assay with a wide dynamic range and minimal variability would exhibit a Z-factor > 0.5.[212] This statistic is based on the assumption that all of the activities in a chemical library during a HTS campaign will exhibit a normal distribution, where the vast majority of the compounds will exhibit little to no biological activity.[212] Thus, the threshold for identifying "hits" (i.e. compounds that exhibit significant activity in a HTS campaign) has been widely accepted to be 3 standard deviations from the average signal of the controls.[212]

For these studies, quality control screening experiments yielded a Z' score of 0.6, which confirmed that the HTS conditions yielded a wide dynamic range between the positive and negative controls as well as minimal assay variation. The positive control used in this HTS campaign consists of WDR5, Sypro Orange dye, and a 10mer peptide of Myc that consists of the amino acids that interact with WDR5. The negative control used in this HTS campaign consists of WDR5 and the Sypro Orange dye. Using the conditions optimized for HTS during the quality control studies, multiplexed (4-plex) HTS was performed to screen 25,000 compounds against WDR5 at a single concentration (1-20 μM, Figure A.5). The threshold of 3SD relative to the negative control (i.e. WDR5 with Sypro Orange) yielded 581 active wells, which corresponded to 2,324 compounds (9.5% hit rate, Figure A.5).

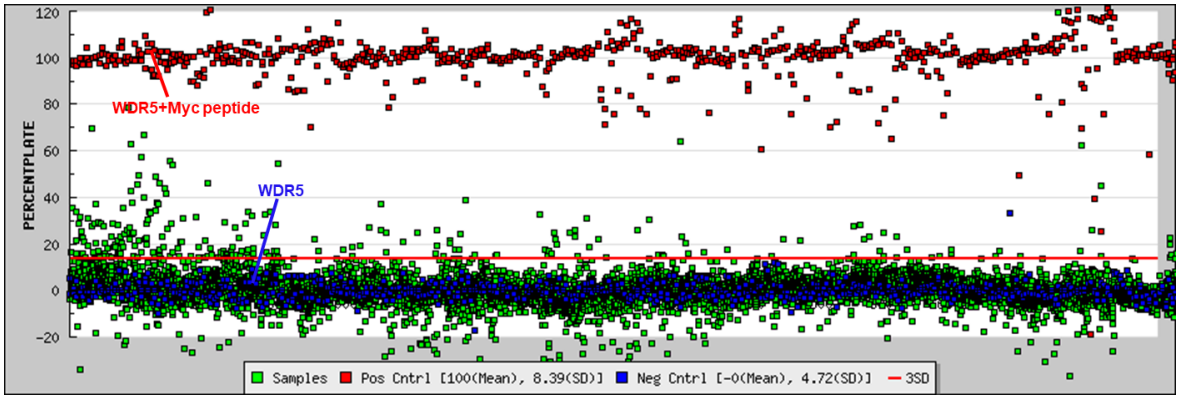

Figure A.5. Campaign View of HTS of 25,000 Compounds Against WDR5. Signals were normalized to signal of positive control (100%, red dots) and negative control (0%, blue dots). Signal from WDR5 in presence of multiplexed compounds are denoted in green and are normalized to the controls. Red line denotes 3 standard deviations (SD) above the negative control. Primary screen resulted in 581 active wells (9.5% "hit" rate). Z' score for HTS primary screen: 0.61. Image retrieved from MScreen.

Since the HTS campaign was performed in a multiplexed format (4-plex), it was necessary to perform a deconvolution step to determine which one of the 4 multiplexed compounds that raised the T_m of WDR5 by more than 3SD relative to the negative control (Figure A.6). For the deconvolution studies, compounds in active wells were screened individually at a concentration of 10 μM against WDR5. Due to the large number of active wells from the initial screen, the top 1,000 compounds were prioritized for deconvolution screening studies, which identified 207 active compounds. These 207 active compounds underwent additional filtering steps, which involved removal of compounds predicted to exhibit reactive chemical functionality (i.e. exhibits behaviors of PAINS[211]) and lack of drug-like properties. Specifically, active compounds that were considered to be promiscuous binders, defined as a "hit" in more than 10 assays recorded on MScreen[213], were removed. Additionally, compounds with chemical structures predicted to be reactive as defined by NIH Molecular Libraries Small Molecule Repository and compounds with chemical structures predicted to be cytotoxic in biological assays were also removed from further studies. The resultant quantity of active compounds from the deconvolution screen was 101 compounds.

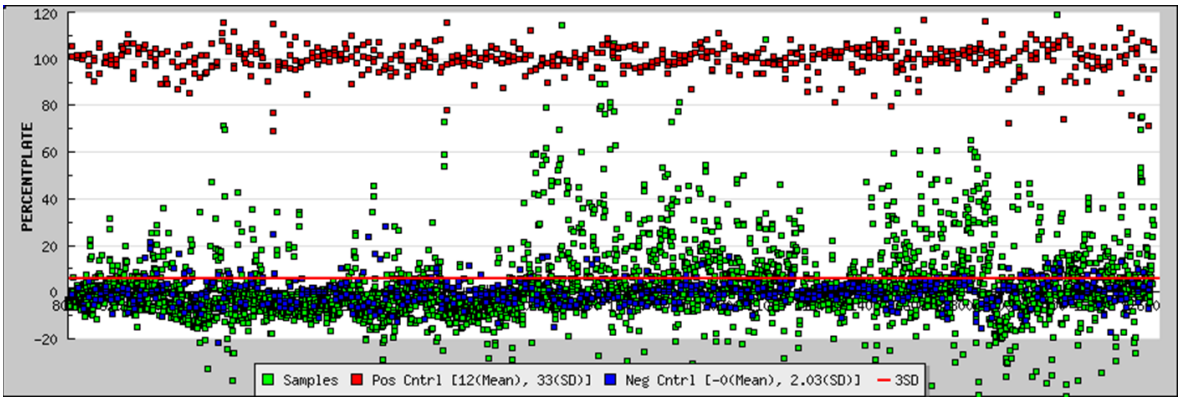

Figure A.6. Campaign View of HTS Deconvolution of Active Compounds. Signals were normalized to signal of positive control (100%, red dots) and negative control (0%, blue dots). Signal from WDR5 in presence of multiplexed compounds are denoted in green and are normalized to the controls. Red line denotes 3 standard deviations (SD) above the negative control. Deconvolution studies resulted in 207 active compounds (8.7% "hit" rate). Z' score for HTS deconvolution screen: 0.64. Image retrieved from MScreen.

Active compounds identified from the deconvolution studies were processed using concentration dependent thermal shift assays. Compounds considered "hits" from HTS were those that induced dose dependent changes in the T_m of WDR5. Concentration dependent thermal shift studies resulted in 49 compounds. These compounds resulted in a change in T_m that ranged from 0.5° to greater than 5°. Following the HTS of 25,000 small molecules against WDR5, 49 were considered "hits," which corresponded to a "hit" rate of 0.2%. These 49 compounds were ordered and retested in singleton using identical conditions as the primary screen to confirm their activity. This retest assay identified 7 compounds that did not increase the T_m of WDR5 and therefore were removed from downstream studies. The final number of compounds that proceeded to downstream studies was 42.

After confirming the activity of the 42 compounds in the retest assay, we next evaluated the site specificity of these compounds. We leveraged the previously characterized protein-protein interaction of WDR5 and MLL to eliminate compounds that engage at the WDR5-MLL site via negative selection.[202,214,215] In collaboration with the Wang Lab at the University of Michigan, we employed a competitive fluorescence polarization based assay targeting the protein-protein interaction of WDR5 and MLL for negative selection. Fluorescence polarization is a chemical technique that relies on the fluorescence properties of a fluorophore to evaluate protein-ligand binding.[216–218] Fluorescence polarization can be calculated from the following equation[218]:

$$P = \frac{F_{||} - F_{\perp}}{F_{||} + F_{\perp}}$$

In the equation shown above, $F_{||}$ denotes the parallel fluorescence intensity, and $F_{\perp}$ denotes the perpendicular fluorescence intensity.[218] Both parallel and perpendicular fluorescence intensity contribute the polarization of light.[216–218] Therefore, a fluorescence polarization based assay leverages the polarizability of a chemical probe, which is a small (10mer) peptide labeled with a fluorophore.[216–218] Upon excitation with polarized light, a free probe (i.e. a probe not interacting with any protein) tumbles rapidly in solution, which results in the depolarization of both the perpendicular and parallel fluorescence intensity and thus, ultimately results in a low polarization signal.[216–218] In contrast, if the probe binds to a protein (which is larger in molecular weight than the probe), the probe-protein complex will tumble slowly in solution and thus, retain the polarized light and results in a high polarization signal.[216–218] In context of the negative selection MLL-WDR5 assay, we used this assay as an approach to eliminate compounds that reduce the polarization of MLL-WDR5 complex (Figure A.7A). Such compounds compete with the MLL probe for the MLL-WDR5 interaction site and thus would be deprioritized (Figure A.7A). Since some of the 42 compounds identified from the HTS campaign have conjugated systems and have the potential to exhibit fluorescence, these 42 compounds were screened for auto-fluorescence. The auto-fluorescence screen identified 9 compounds that exhibited intrinsic fluorescence at concentrations greater than 50 μM, which overlapped with the concentration range used for the negative selection assay. The remaining 33 compounds were screened in the negative selection assay were initially evaluated in the MLL-WDR5 FP assay at 500 μM and 1 mM (Figure A.7B). These concentrations were selected because the binding affinity of WDR5 to the MLL probe was 100 nM, and therefore, high concentrations of the HTS compounds were required to evaluate any displacement of the MLL probe. Compounds that competed with the MLL probe for WDR5 at 500 μM and 1 mM were analyzed in a follow-up study using a concentration range of 7 μM to 1 mM (Figure A.7C). This negative selection assay identified 2 compounds that displaced the MLL probe in a concentration-dependent manner, suggesting they interacted near the site of MLL-WDR5 rather than Myc-WDR5. These 2 compounds were removed from downstream analyses, resulting in 31 compounds.

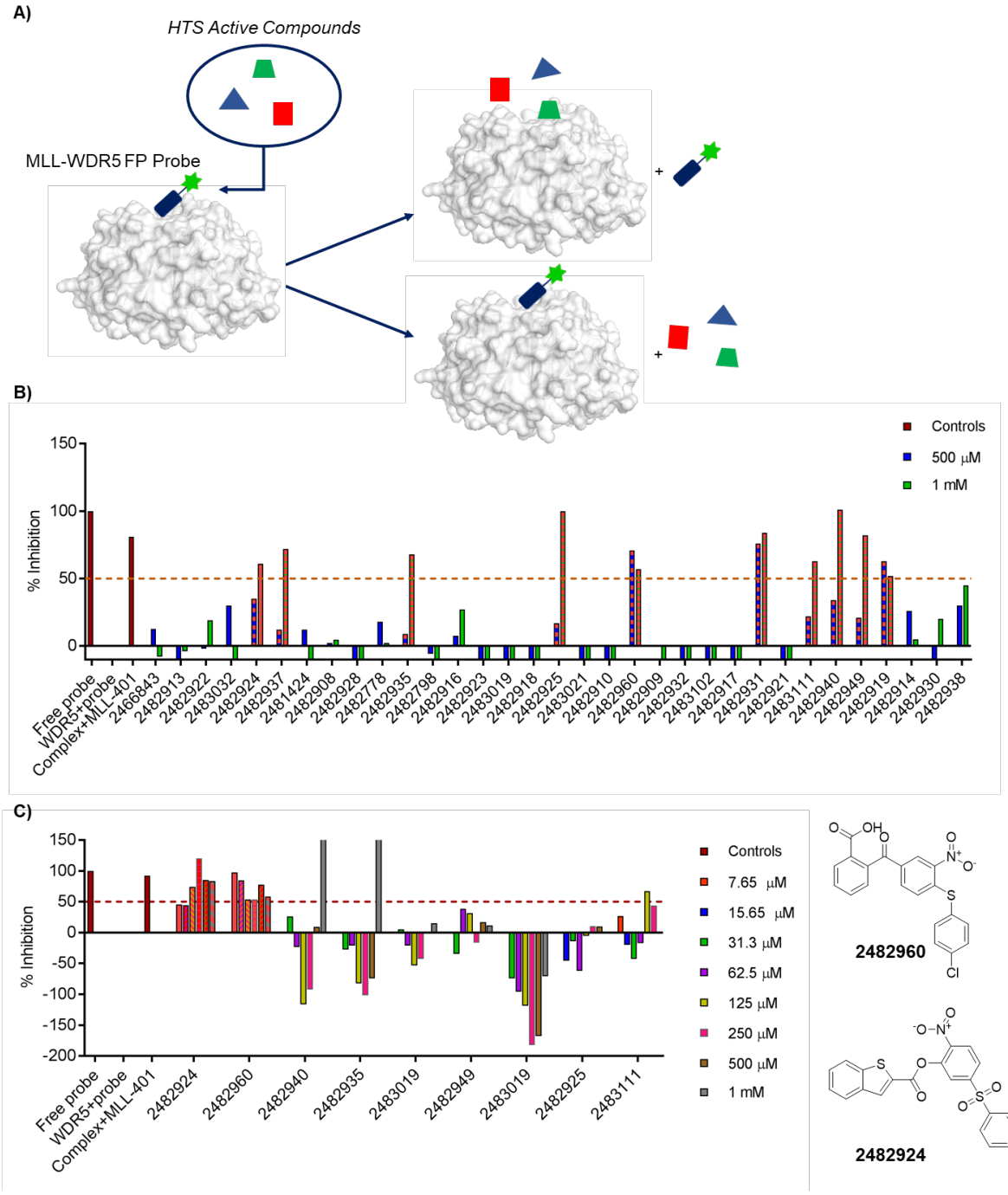

Figure A.7. Negative Selection of HTS Compounds Using MLL-WDR5 Competitive Binding Assay. A) Cartoon of competitive binding assay to eliminate compounds that engage at MLL-WDR5 site. KD of MLL probe and WDR5 is 100 nM. Amino acid sequence of MLL probe is Ac-ARTEVHLRKS-Ahx-Ahx-K(5-FAM)-NH2.. Protein structure of WDR5 obtained from PDB (4Y7R). B) Identification of binders at the MLL-WDR5 site by screening HTS compounds at 500 µM and 1 mM. C) Concentration dependent binding assay to validate competitors of MLL probe. Structures of compounds that displaced MLL probe in concentration dependent manner are shown.

After triaging the compounds using MLL-WDR5 assay as a negative selection tool, we sought to evaluate if these compound engaged at the WDR5-Myc interaction site.

Since our ultimate goal was to identify small molecule inhibitors of the protein-protein interaction of WDR5 and Myc, determining if these compounds interact with WDR5 at the Myc interacting site was a critical step to discovering potential WDR5-Myc inhibitors. To assess whether these compounds engaged at the WDR5-Myc site, we used a fluorescence polarization based competition assay using the previously published amino acid sequence of Myc that interacts with WDR5.[200] The binding affinity of the Myc probe to recombinant WDR5 was 10 μM.[200] We synthesized the Myc probe, reevaluated this binding affinity, and obtained a comparable binding affinity (K_D = 13 μM, Figure SA.1). We attempted to rationally design and synthesize Myc probes with higher binding affinity to WDR5 by maximizing π stacking interactions between V264 of the Myc peptide and nearby aromatic residues of WDR5 to improve the dynamic range of the Myc/WDR5 FP assay (Figure SA.1). However, we were unable to rationally design a Myc probe with a stronger binding affinity than 10 μM. Therefore, we leveraged the previously published amino acid sequence of Myc for the fluorescence polarization based competitive binding assay. The goal of using the competitive Myc/WDR5 assay was to identify compounds that competed with the Myc probe to displace it from WDR5 in a concentration-dependent manner (Figure A.8A). The 31 compounds were initially screened at 125 μM and 250 μM or 500 μM and 1 mM, depending on the solubility of those compounds (Figure A.8B). Again, these concentrations were selected because they were approximately $10K_D$ of Myc-WDR5 and therefore were deemed appropriate concentrations for the HTS compounds to displace the Myc probe. Under the assay conditions for the Myc-WDR5 competitive binding assay, 6 compounds were exhibited solubility issues which were evidenced by high scattering of light by the colloids of those compounds. Thus, those 6 compounds were removed from the Myc-WDR5 competitive binding assay and left 25 compounds for site specificity analyses. Screening these 25 compounds at 125 μM, 250 μM, 500 μM, or 1 mM identified 3 compounds that displaced the Myc probe from WDR5. The inhibitory activities of these 3 compounds were screened from a range of 50 μM – 1 mM ($5K_D$ – $100K_D$), which confirmed the concentration-dependent displacement of the Myc probe for 2 compounds (Figure A.8C). Concentration-dependent displacement of the Myc probe suggested these two compounds engaged at/near the Myc-WDR5 interaction site (Figure A.8C).

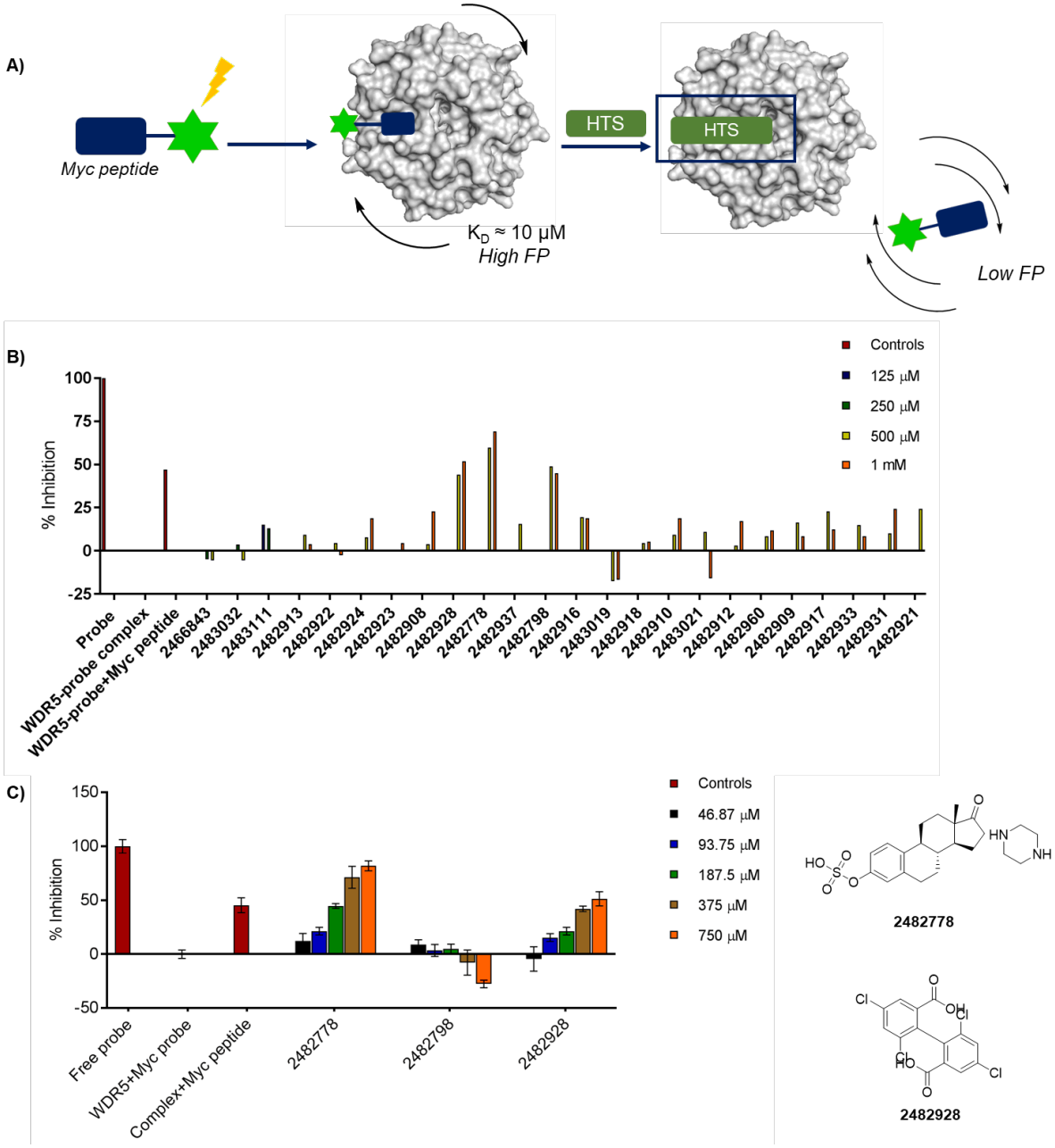

Figure A.8. Site Specificity Evaluation of HTS Compounds Using Myc-WDR5 Competitive Binding Assay. A) Cartoon of competitive binding assay to evaluate site specificity of HTS binding to WDR5 in presence of Myc peptide probe. KD of Myc probe and WDR5 is 13 µM. Amino acid sequence of Myc probe is FAM-Ahx-DEEEIDVVSV-NH2..Protein structure of WDR5 obtained from PDB (4Y7R). Z' of Myc-WDR5 FP assay was 0.68. B) Identification of binders at the Myc-WDR5 site by screening HTS compounds at 125 µM, 250 µM, 500 µM, and 1 mM. C) Concentration dependent binding assay to validate competitors of Myc probe. Structures of compounds that displaced Myc probe in concentration dependent manner are shown.

Co-crystallization studies were performed in collaboration with Dr. Jeanne Stuckey at the Center of Structural Biology to determine if these 2 compounds exhibited site-specifity for the WDR5-Myc interaction site. These co-crystallization studies revealed

neither 2928 nor 2778 interacted with WDR5 since the solved structure of WDR5 did not include neither of these compounds.

A.4. Concluding Remarks

The protein-protein interaction of Myc and WDR5 is a critical driver to early tumorigenesis events. There have been numerous reports aiming to inhibit Myc for Myc-driven cancers.[184,195,219–221] However, these efforts had limited success for clinical applicability, and only therapeutics that indirectly target Myc (i.e. to inhibit Myc translation and targeting via immunotherapy) have been approved.[220,221] To overcome previously reported shortcomings in targeting Myc, we pursued a drug discovery program targeting the Myc-WDR5 protein-protein interaction using HTS and FBDD as a means to directly target Myc. These two screening approaches are complementary and were intended to facilitate the discovery of diverse compounds and scaffolds that could serve as parent compounds to future inhibitors of the interaction of Myc and WDR5.

Both approaches identified 2-5 compounds/fragments at the end of the screening and validation stages. However, structural elucidation of these compounds and fragments using co-crystallization studies revealed that none of those compounds and fragments targeted the Myc-WDR5 site. Recently, nanomolar inhibitors of the interaction between Myc and WDR5 were identified by Fesik and coworkers.[222,223] These potent inhibitors were identified through a NMR-based fragment based screen of libraries containing 14,000 fragments and a FP based HTS campaign of 250,000 small molecules.[222,223] Simon and coworkers leveraged characterized chemical shifts from ^{15}N labeled apo WDR5 and ^{15}N labeled WDR5 with a peptide of Myc that engages with WDR5.[222] In our studies, we were unable to leverage characterized chemical shifts of ^{15}N labeled WDR5 with Myc, which would have been needed as a critical positive control to screen for fragments or small molecules. The lack of this positive control hindered our pursuit of NMR studies for our primary screens because we would not have had a reference for chemical shifts that signified engagement with WDR5 at the Myc binding site. MacDonald and coworkers from the Fesik Lab also identified potent leads using their FP based Myc-WDR5 competitive binding assay as their HTS screen.[221] Both of these reports from the Fesik Lab emphasized the importance of leveraging structure-based screens to guide the discovery of fragment hits and small molecule hits. In our studies, our hypothesis was

based on the discovery of weak binders to the largely hydrophobic cleft where WDR5 interacts with Myc and thus used thermal shift as the primary screen for both our fragment based screen and HTS campaigns. Evaluation of the current literature surrounding the discovery of small molecule inhibitors of the protein interaction between WDR5 and Myc revealed that our primary screening assay was not optimal for the discovery of potent inhibitors for this interaction. Opportunities for identifying inhibitors for this interaction could have been improved by heavier investment in the biophysical characterization of the protein interaction between Myc and WDR5 and leveraging this biophysical insight to guide the development of a structure-based screening assay. Such structure-based screening assay could have improved the opportunities to finding site-specific binders at the onset of our primary screens.

Future studies for the drug discovery could involve leverage of those recently identified compounds to attenuate the deregulated cell growth, metabolism, survival, and/or differentiation of cancer cells in Myc-driven cancers. Screens of these compounds or derivatives of these compounds could be performed to identify subsets of specific Myc-driven cancers that could profit from the treatment of these Myc-WDR5 inhibitors. Such studies could provide novel chemical tools and small molecule therapeutics for Myc-driven cancers.

A.5. Additional Figure

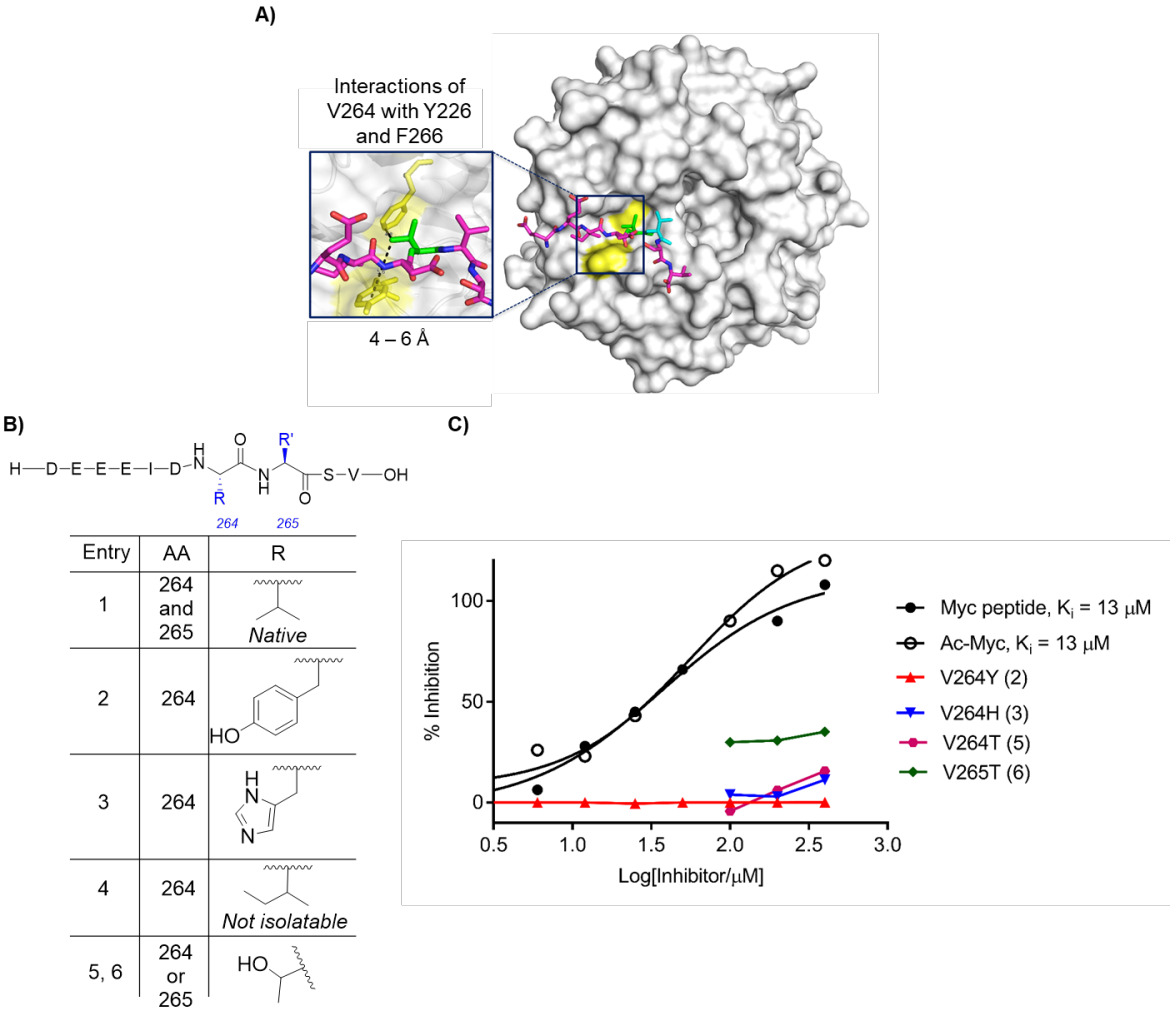

Entry	AA	R
1	264 and 265	*Native*
2	264	HO
3	264	
4	264	*Not isolatable*
5, 6	264 or 265	HO

Figure SA.1. Approach for Rational Design of Myc Probes for Myc-WDR5 Competitive Binding Assay. A) Previously solved protein structure of WDR5 (grey) interacting with Myc peptide (magenta). Interactions between the aromatic residues of WDR5 (F266, yellow) and aliphatic residues of Myc (V264 and Y226, green and cyan) were targeted. Structure of WDR5 and Myc peptide obtained from PDB (4Y7R). B) Aromatic residue substitution at 264 or 265 position on Myc peptide. C) Competitive binding of synthesized Myc peptides against Myc probe (FAM-Ahx-DEEEIDVVSV-NH2).

A.6. References

(1) U.S. Breast Cancer Statistics | Breastcancer.org https://www.breastcancer.org/symptoms/understand_bc/statistics (accessed Jun 1, 2020).

(2) Dai, X.; Li, T.; Bai, Z.; Yang, Y.; Liu, X.; Zhan, J.; Shi, B. *Am. J. Cancer Res.* **2015**, *5* (10), 2929–2943.

(3) Turashvili, G.; Brogi, E. *Front. Med.* **2017**, *4* (DEC).

(4) Wang, J.; Xu, B. *Signal Transduct. Target. Ther.* **2019**, *4* (1).

(5) *Am. Cancer Soc.* **2020**, 1–43.

(6) National Cancer Institute Surveillance, Epidemiology, and E. R. P. (SEER). *Natl. Cancer Inst.* **2019**.

(7) Zhang, L.; Li, J.; Xiao, Y.; Cui, H.; Du, G.; Wang, Y.; Li, Z.; Wu, T.; Li, X.; Tian, J. *Sci. Rep.* **2015**, *5*, 1–14.

(8) Godoy-Ortiz, A.; Sanchez-Muñoz, A.; Parrado, M. R. C.; Álvarez, M.; Ribelles, N.; Dominguez, A. R.; Alba, E. *Front. Oncol.* **2019**, *9* (OCT), 1124.

(9) Loibl, S.; Gianni, L. *Lancet* **2017**, *389* (10087), 2415–2429.

(10) Muller, K. E.; Marotti, J. D.; Tafe, L. J. *Am. J. Clin. Pathol.* **2019**, *152* (1), 7–16.

(11) Vandenberghe, M. E.; Scott, M. L. J.; Scorer, P. W.; Söderberg, M.; Balcerzak, D.; Barker, C. *Sci. Rep.* **2017**, *7* (1), 1–11.

(12) Zhang, X.; Bleiweiss, I.; Jaffer, S.; Nayak, A. *Clin. Breast Cancer* **2017**, *17* (6), 486–492.

(13) Wolff, A. C.; Elizabeth Hale Hammond, M.; Allison, K. H.; Harvey, B. E.; Mangu, P. B.; Bartlett, J. M. S.; Bilous, M.; Ellis, I. O.; Fitzgibbons, P.; Hanna, W.; Jenkins, R. B.; Press, M. F.; Spears, P. A.; Vance, G. H.; Viale, G.; McShane, L. M.; Dowsett, M. *J. Clin. Oncol.* **2018**, *36* (20), 2105–2122.

(14) Mastro, L. Del; Lambertini, M.; Bighin, C.; Levaggi, A.; D'Alonzo, A.; Giraudi, S.; Pronzato, P. *Expert Rev. Anticancer Ther.* **2012**, *12* (11), 1391–1405.

(15) Pernas, S.; Tolaney, S. M. *Ther. Adv. Med. Oncol.* **2019**, *11*, 1–16.

(16) Oh, D. Y.; Bang, Y. J. *Nat. Rev. Clin. Oncol.* **2020**, *17* (1), 33–48.

(17) Swain, S. M.; Kim, S. B.; Cortés, J.; Ro, J.; Semiglazov, V.; Campone, M.; Ciruelos, E.; Ferrero, J. M.; Schneeweiss, A.; Knott, A.; Clark, E.; Ross, G.; Benyunes, M. C.; Baselga, J. *Lancet Oncol.* **2013**, *14* (6), 461–471.

(18) Modi, S.; Saura, C.; Yamashita, T.; Park, Y. H.; Kim, S.-B.; Tamura, K.; Andre, F.; Iwata, H.; Ito, Y.; Tsurutani, J.; Sohn, J.; Denduluri, N.; Perrin, C.; Aogi, K.; Tokunaga, E.; Im, S.-A.; Lee, K. S.; Hurvitz, S. A.; Cortes, J.; Lee, C.; Chen, S.; Zhang, L.; Shahidi, J.; Yver, A.; Krop, I. *N. Engl. J. Med.* **2020**, *382* (7), 610–621.

(19) Murthy, R. K.; Loi, S.; Okines, A.; Paplomata, E.; Hamilton, E.; Hurvitz, S. A.; Lin, N. U.; Borges, V.; Abramson, V.; Anders, C.; Bedard, P. L.; Oliveira, M.; Jakobsen, E.; Bachelot, T.; Shachar, S. S.; Muller, V.; Braga, S.; Duhoux, F. P.; Greil, R.; Cameron, D.; Carey, L. A.; Curigliano, G.; Gelmon, K.; Hortobagyi, G.; Krop, I.; Loibl, S.; Pegram, M.; Slamon, D.; Palanca-Wessels, M. C.; Walker, L.; Feng, W.; Winer, E. P. *N. Engl. J. Med.* **2020**, *382* (7), 597–609.

(20) Kim, C.; Lee, C. K.; Chon, H. J.; Kim, J. H.; Park, H. S.; Heo, S. J.; Kim, H. J.; Kim, T. S.; Kwon, W. S.; Chung, H. C.; Rha, S. Y. *Oncotarget* **2017**, *8* (69), 113494–113501.

(21) Bang, Y. J.; Van Cutsem, E.; Feyereislova, A.; Chung, H. C.; Shen, L.; Sawaki, A.; Lordick, F.; Ohtsu, A.; Omuro, Y.; Satoh, T.; Aprile, G.; Kulikov, E.; Hill, J.; Lehle, M.; Rüschoff, J.; Kang, Y. K. *Lancet* **2010**, *376* (9742), 687–697.

(22) Sims, A. H.; Zweemer, A. J. M.; Nagumo, Y.; Faratian, D.; Muir, M.; Dodds, M.; Um, I.; Kay, C.; Hasmann, M.; Harrison, D. J.; Langdon, S. P. *Br. J. Cancer* **2012**, *106* (11), 1779–1789.

(23) Pohlmann, P. R.; Mayer, I. A.; Mernaugh, R. *Clin. Cancer Res.* **2009**, *15* (24), 7479–7491.

(24) Luque-Cabal, M.; García-Teijido, P.; Fernández-Pérez, Y.; Sánchez-Lorenzo, L.; Palacio-Vázquez, I. *Clin. Med. Insights Oncol.* **2016**, *10*, 21–30.

(25) Nagata, Y.; Lan, K. H.; Zhou, X.; Tan, M.; Esteva, F. J.; Sahin, A. A.; Klos, K. S.; Li, P.; Monia, B. P.; Nguyen, N. T.; Hortobagyi, G. N.; Hung, M. C.; Yu, D. *Cancer Cell* **2004**, *6* (2), 117–127.

(26) Nahta, R. *Int. Sch. Res. Netw.* **2012**, *2012* (428062), 1–16.

(27) Luque-Cabal, M.; García-Teijido, P.; Fernández-Pérez, Y.; Sánchez-Lorenzo, L.; Palacio-Vázquez, I. *Clin. Med. Insights Oncol.* **2016**, *10* (Suppl 1), 21–30.

(28) Pernas, S.; Tolaney, S. M. HER2-Positive Breast Cancer: New Therapeutic Frontiers and Overcoming Resistance.

(29) Chen, S.; Liang, Y.; Feng, Z.; Wang, M. *BMC Cancer* **2019**, *19* (1), 973.

(30) Verma, S.; Miles, D.; Gianni, L.; Krop, I. E.; Welslau, M.; Baselga, J.; Pegram, M.; Oh, D.-Y.; Diéras, V.; Guardino, E.; Fang, L.; Lu, M. W.; Olsen, S.; Blackwell, K. *N. Engl. J. Med.* **2012**, *367* (19), 1783–1791.

(31) Perez, E. A.; Cortés, J.; Gonzalez-angulo, A. M.; Bartlett, J. M. S. *Cancer Treat. Rev.* **2014**, *40* (2), 276–284.

(32) Murthy, P.; Kidwell, K. M.; Schott, A. F.; Merajver, S. D.; Griggs, J. J.; Smerage, J. D.; Van Poznak, C. H.; Wicha, M. S.; Hayes, D. F.; Henry, N. L. *Breast Cancer Res. Treat.* **2016**, *155* (3), 589–595.

(33) Joensuu, H. *Cancer Treat. Rev.* **2017**, *52*, 1–11.

(34) Tolaney, S. M.; Guo, H.; Pernas, S.; Barry, W. T.; Dillon, D. A.; Ritterhouse, L.;

Schneider, B. P.; Shen, F.; Fuhrman, K.; Baltay, M.; Dang, C. T.; Yardley, D. A.; Moy, B.; Kelly Marcom, P.; Albain, K. S.; Rugo, H. S.; Ellis, M. J.; Shapira, I.; Wolff, A. C.; Carey, L. A.; Overmoyer, B.; Partridge, A. H.; Hudis, C. A.; Krop, I. E.; Burstein, H. J.; Winer, E. P. *J. Clin. Oncol.* **2019**, *37* (22), 1868–1875.

(35) Gianni, L.; Pienkowski, T.; Im, Y. H.; Tseng, L. M.; Liu, M. C.; Lluch, A.; Starosławska, E.; de la Haba-Rodriguez, J.; Im, S. A.; Pedrini, J. L.; Poirier, B.; Morandi, P.; Semiglazov, V.; Srimuninnimit, V.; Bianchi, G. V.; Magazzù, D.; McNally, V.; Douthwaite, H.; Ross, G.; Valagussa, P. *Lancet Oncol.* **2016**, *17* (6), 791–800.

(36) Luque-Cabal, M.; García-Teijido, P.; Fernández-Pérez, Y.; Sánchez-Lorenzo, L.; Palacio-Vázquez, I. *Clin. Med. Insights Oncol.* **2016**, *10* (Suppl 1), 21–30.

(37) Andersson, M.; Lidbrink, E.; Bjerre, K. *J Clin Oncol* **2011**, *29* (3), 264–271.

(38) Derakhshani, A.; Rezaei, Z.; Safarpour, H.; Sabri, M.; Mir, A.; Sanati, M. A.; Vahidian, F.; Gholamiyan Moghadam, A.; Aghadoukht, A.; Hajiasgharzadeh, K.; Baradaran, B. *J. Cell. Physiol.* **2020**, *235* (4), 3142–3156.

(39) Valabrega, G.; Montemurro, F.; Sarotto, I.; Petrelli, A.; Rubini, P.; Tacchetti, C.; Aglietta, M.; Comoglio, P. M.; Giordano, S. *Oncogene* **2005**, *24* (18), 3002–3010.

(40) Takuwa, H.; Tsuji, W.; Yotsumoto, F. *Int. J. Surg. Case Rep.* **2018**, *52*, 125–131.

(41) New Treatments Emerge for Metastatic HER2+ Breast Cancer - National Cancer Institute https://www.cancer.gov/news-events/cancer-currents-blog/2020/tucatinib-trastuzumab-deruxtecan-her2-positive-metastatic-breast-cancer (accessed Jun 1, 2020).

(42) Stern, H. M.; Gardner, H.; Burzykowski, T.; Elatre, W.; O'Brien, C.; Lackner, M. R.; Pestano, G. A.; Santiago, A.; Villalobos, I.; Eiermann, W.; Pienkowski, T.; Martin, M.; Robert, N.; Crown, J.; Nuciforo, P.; Bee, V.; Mackey, J.; Slamon, D. J.; Press, M. F. *Clin. Cancer Res.* **2015**, *21* (9), 2065–2074.

(43) Vu, T.; Claret, F. X. *Front. Oncol.* **2012**, *2* (June), 62.

(44) Bartsch, R.; Wenzel, C.; Steger, G. G. *Biologics* **2007**, *1* (1), 19–31.

(45) Gschwantler-Kaulich, D.; Tan, Y. Y.; Fuchs, E.-M.; Hudelist, G.; Köstler, W. J.; Reiner, A.; Leser, C.; Salama, M.; Attems, J.; Deutschmann, C.; Zielinski, C. C.; Singer, C. F. *PLoS One* **2017**, *12* (3), e0172911.

(46) Gajria, D.; Chandarlapaty, S. *Expert Rev. Anticancer Ther.* **2011**, *11* (2), 263–275.

(47) Mercogliano, M. F.; Bruni, S.; Elizalde, P. V.; Schillaci, R. *Front. Oncol.* **2020**, *10*, 584.

(48) Rimawi, M. F.; de Angelis, C.; Contreras, A.; Pareja, F.; Geyer, F. C.; Burke, K. A.; Herrera, S.; Wang, T.; Mayer, I. A.; Forero, A.; Nanda, R.; Goetz, M. P.; Chang, J. C.; Krop, I. E.; Wolff, A. C.; Pavlick, A. C.; Fuqua, S. A. W.; Gutierrez, C.; Hilsenbeck, S. G.; Li, M. M.; Weigelt, B.; Reis-Filho, J. S.; Osborne, C. K.;

Schiff, R. *Breast Cancer Res. Treat.* **2018**, *167* (3), 731–740.

(49) Lebok, P.; Kopperschmidt, V.; Kluth, M.; Hube-Magg, C.; Özden, C.; Taskin, B.; Hussein, K.; Mittenzwei, A.; Lebeau, A.; Witzel, I.; Wölber, L.; Mahner, S.; Jänicke, F.; Geist, S.; Paluchowski, P.; Wilke, C.; Heilenkötter, U.; Simon, R.; Sauter, G.; Terracciano, L.; Krech, R.; Von, A.; Müller, V.; Burandt, E. *BMC Cancer* **2015**, *15* (1–10).

(50) Li, S.; Shen, Y.; Wang, M.; Yang, J.; Lv, M.; Li, P.; Chen, Z.; Yang, J. *Oncotarget* **2017**, *8* (19), 32043–32054.

(51) Kechagioglou, P.; Papi, R. M.; Provatopoulou, X.; Kalogera, E.; Papadimitriou, E.; Grigoropoulos, P.; Nonni, A.; Zografos, G.; Kyriakidis, D. A.; Gounaris, A. *Anticancer Res.* **2014**, *34* (3), 1387–1400.

(52) Chalhoub, N.; Baker, S. J. *Annu. Rev. Pathol. Mech. Dis.* **2009**, *4* (1), 127–150.

(53) Paplomata, E.; O'regan, R. *Ther. Adv. Med. Oncol.* **2014**, *6* (4), 154–166.

(54) Keniry, M.; Parsons, R. *Oncogene* **2008**, *27* (41), 5477–5485.

(55) Ebbesen, S. H.; Scaltriti, M.; Bialucha, C. U.; Morse, N.; Kastenhuber, E. R.; Wen, H. Y.; Dow, L. E.; Baselga, J.; Lowe, S. W. *Proc. Natl. Acad. Sci. U. S. A.* **2016**, *113* (11), 3030–3035.

(56) Luongo, F.; Colonna, F.; Calapà, F.; Vitale, S.; Fiori, M. E.; De Maria, R. *Cancers (Basel).* **2019**, *11* (8), 1076.

(57) Carracedo, A.; Pandolfi, P. P. *Oncogene* **2008**, *27* (41), 5527–5541.

(58) Crowell, J. A.; Steele, V. E.; Fay, J. R. *Mol. Cancer Ther.* **2007**, *6* (8), 2139–2148.

(59) Endersby, R.; Baker, S. J. *Oncogene* **2008**, *27* (41), 5416–5430.

(60) Nuciforo, P. G.; Aura, C.; Holmes, E.; Prudkin, L.; Jimenez, J.; Martinez, P.; Ameels, H.; de la Perna, L.; Ellis, C.; Eidtmann, H.; Piccart-Gebhart, M. J.; Scaltriti, M.; Baselga, J. *Ann. Oncol.* **2015**, *26* (7), 1494–1500.

(61) Carbognin, L.; Miglietta, F.; Paris, I.; Dieci, M. V. *Cancers (Basel).* **2019**, *11* (9), 1–18.

(62) Jones, N.; Bonnet, F.; Sfar, S.; Lafitte, M.; Lafon, D.; Sierankowski, G.; Brouste, V.; Banneau, G.; Tunon de Lara, C.; Debled, M.; MacGrogan, G.; Longy, M.; Sevenet, N. *Int. J. Cancer* **2013**, *133* (2), 323–334.

(63) Zhang, H. Y.; Liang, F.; Jia, Z. L.; Song, S. T.; Jiang, Z. F. *Oncol. Lett.* **2013**, *6* (1), 161–168.

(64) Zhu, Y.; Wloch, A.; Wu, Q.; Peters, C.; Pagenstecher, A.; Bertalanffy, H.; Sure, U. *Stroke* **2009**, *40* (3), 820–826.

(65) Kang, Y. H.; Lee, H. S.; Kim, W. H. *Lab. Investig.* **2002**, *82* (3), 285–291.

(66) Wilks, S. T. *Breast* **2015**, *24* (5), 548–555.

(67) Sangai, T.; Akcakanat, A.; Chen, H.; Tarco, E.; Wu, Y.; Do, K. A.; Miller, T. W.; Arteaga, C. L.; Mills, G. B.; Gonzalez-Angulo, A. M.; Meric-Bernstam, F. *Clin. Cancer Res.* **2012**, *18* (20), 5816–5828.

(68) Hudis, C.; Swanton, C.; Janjigian, Y. Y.; Lee, R.; Sutherland, S.; Lehman, R.; Chandarlapaty, S.; Hamilton, N.; Gajria, D.; Knowles, J.; Shah, J.; Shannon, K.; Tetteh, E.; Sullivan, D. M.; Moreno, C.; Yan, L.; Han, H. S. *Breast Cancer Res.* **2013**, *15* (6), R110.

(69) Xing, Y.; Lin, N. U.; Maurer, M. A.; Chen, H.; Mahvash, A.; Sahin, A.; Akcakanat, A.; Li, Y.; Abramson, V.; Litton, J.; Chavez-MacGregor, M.; Valero, V.; Piha-Paul, S. A.; Hong, D.; Do, K.-A.; Tarco, E.; Riall, D.; Eterovic, A. K.; Wulf, G. M.; Cantley, L. C.; Mills, G. B.; Doyle, L. A.; Winer, E.; Hortobagyi, G. N.; Gonzalez-Angulo, A. M.; Meric-Bernstam, F. *Breast Cancer Res.* **2019**, *21* (1), 78.

(70) Hurvitz, S. A.; Andre, F.; Jiang, Z.; Shao, Z.; Mano, M. S.; Neciosup, S. P.; Tseng, L. M.; Zhang, Q.; Shen, K.; Liu, D.; Dreosti, L. M.; Burris, H. A.; Toi, M.; Buyse, M. E.; Cabaribere, D.; Lindsay, M. A.; Rao, S.; Pacaud, L. B.; Taran, T.; Slamon, D. *Lancet Oncol.* **2015**, *16* (7), 816–829.

(71) Van Swearingen, A. E. D.; Siegel, M. B.; Deal, A. M.; Sambade, M. J.; Hoyle, A.; Hayes, D. N.; Jo, H.; Little, P.; Dees, E. C.; Muss, H.; Jolly, T.; Zagar, T. M.; Patel, N.; Miller, C. R.; Parker, J. S.; Smith, J. K.; Fisher, J.; Shah, N.; Nabell, L.; Nanda, R.; Dillon, P.; Abramson, V.; Carey, L. A.; Anders, C. K. *Breast Cancer Res. Treat.* **2018**, *171* (3), 637–648.

(72) Ramón y Cajal, S.; Sesé, M.; Capdevila, C.; Aasen, T.; De Mattos-Arruda, L.; Diaz-Cano, S. J.; Hernández-Losa, J.; Castellví, J. *J. Mol. Med.* **2020**, *98* (2), 161–177.

(73) Lee, H. J.; Seo, A. N.; Kim, E. J.; Jang, M. H.; Suh, K. J.; Ryu, H. S.; Kim, Y. J.; Kim, J. H.; Im, S.-A.; Gong, G.; Jung, K. H.; Park, I. A.; Park, S. Y. *Am. J. Clin. Pathol.* **2014**, *142* (6), 755–766.

(74) Rye, I. H.; Trinh, A.; Sætersdal, A. B.; Nebdal, D.; Lingjærde, O. C.; Almendro, V.; Polyak, K.; Børresen-Dale, A. L.; Helland, Å.; Markowetz, F.; Russnes, H. G. *Mol. Oncol.* **2018**, *12* (11), 1838–1855.

(75) Ferrari, A.; Vincent-Salomon, A.; Pivot, X.; Sertier, A. S.; Thomas, E.; Tonon, L.; Boyault, S.; Mulugeta, E.; Treilleux, I.; MacGrogan, G.; Arnould, L.; Kielbassa, J.; Le Texier, V.; Blanché, H.; Deleuze, J. F.; Jacquemier, J.; Mathieu, M. C.; Penault-Llorca, F.; Bibeau, F.; Mariani, O.; Mannina, C.; Pierga, J. Y.; Trédan, O.; Bachelot, T.; Bonnefoi, H.; Romieu, G.; Fumoleau, P.; Delaloge, S.; Rios, M.; Ferrero, J. M.; Tarpin, C.; Bouteille, C.; Calvo, F.; Gut, I. G.; Gut, M.; Martin, S.; Nik-Zainal, S.; Stratton, M. R.; Pauporté, I.; Saintigny, P.; Birnbaum, D.; Viari, A.; Thomas, G. *Nat. Commun.* **2016**, *7* (1), 1–9.

(76) Brady, S. W.; McQuerry, J. A.; Qiao, Y.; Piccolo, S. R.; Shrestha, G.; Jenkins, D. F.; Layer, R. M.; Pedersen, B. S.; Miller, R. H.; Esch, A.; Selitsky, S. R.; Parker, J. S.; Anderson, L. A.; Dalley, B. K.; Factor, R. E.; Reddy, C. B.; Boltax, J. P.; Li, D.

Y.; Moos, P. J.; Gray, J. W.; Heiser, L. M.; Buys, S. S.; Cohen, A. L.; Johnson, W. E.; Quinlan, A. R.; Marth, G.; Werner, T. L.; Bild, A. H. *Nat. Commun.* **2017**, *8* (1), 1–15.

(77) Korkaya, H.; Paulson, A.; Iovino, F.; Wicha, M. S. *Oncogene* **2008**, *27* (47), 6120–6130.

(78) Macosko, E. Z.; Basu, A.; Satija, R.; Nemesh, J.; Shekhar, K.; Goldman, M.; Tirosh, I.; Bialas, A. R.; Kamitaki, N.; Martersteck, E. M.; Trombetta, J. J.; Weitz, D. A.; Sanes, J. R.; Shalek, A. K.; Regev, A.; McCarroll, S. A. *Cell* **2015**, *161* (5), 1202–1214.

(79) Andrews, T. S.; Hemberg, M. *Mol. Aspects Med.* **2018**, *59*, 114–122.

(80) Ziegenhain, C.; Vieth, B.; Parekh, S.; Reinius, B.; Guillaumet-Adkins, A.; Smets, M.; Leonhardt, H.; Heyn, H.; Hellmann, I.; Enard, W. *Mol. Cell* **2017**, *65* (4), 631-643.e4.

(81) Ocasio, J.; Babcock, B.; Malawsky, D.; Weir, S. J.; Loo, L.; Simon, J. M.; Zylka, M. J.; Hwang, D.; Dismuke, T.; Sokolsky, M.; Rosen, E. P.; Vibhakar, R.; Zhang, J.; Saulnier, O.; Vladoiu, M.; El-Hamamy, I.; Stein, L. D.; Taylor, M. D.; Smith, K. S.; Northcott, P. A.; Colaneri, A.; Wilhelmsen, K.; Gershon, T. R. *Nat. Commun.* **2019**, *10* (1), 1–17.

(82) Korkaya, H.; Kim, G. II; Davis, A.; Malik, F.; Henry, N. L.; Ithimakin, S.; Quraishi, A. A.; Tawakkol, N.; D'Angelo, R.; Paulson, A. K.; Chung, S.; Luther, T.; Paholak, H. J.; Liu, S.; Hassan, K. A.; Zen, Q.; Clouthier, S. G.; Wicha, M. S. *Mol. Cell* **2012**, *47* (4), 570–584.

(83) Korkaya, H.; Paulson, A.; Charafe-Jauffret, E.; Ginestier, C.; Brown, M.; Dutcher, J.; Clouthier, S. G.; Wicha, M. S. *PLoS Biol.* **2009**, *7* (6), e1000121.

(84) Nagata, Y.; Lan, K. H.; Zhou, X.; Tan, M.; Esteva, F. J.; Sahin, A. A.; Klos, K. S.; Li, P.; Monia, B. P.; Nguyen, N. T.; Hortobagyi, G. N.; Hung, M. C.; Yu, D. *Cancer Cell* **2004**, *6* (2), 117–127.

(85) Goldman, E. M. and M. **2015**, 1–20.

(86) Nemesh, J. Drop-seq Core Computational Protocol http://mccarrolllab.org/wp-content/uploads/2016/03/Drop-seqAlignmentCookbookv1.2Jan2016.pdf (accessed Sep 1, 2020).

(87) Zappia, L.; Oshlack, A. *Gigascience* **2018**, *7* (7), 1–9.

(88) Sergushichev, A. A. *bioRxiv* **2016**, 060012.

(89) Subramanian, A.; Tamayo, P.; Mootha, V. K.; Mukherjee, S.; Ebert, B. L.; Gillette, M. A.; Paulovich, A.; Pomeroy, S. L.; Golub, T. R.; Lander, E. S.; Mesirov, J. P. *Proc. Natl. Acad. Sci. U. S. A.* **2005**, *102* (43), 15545–15550.

(90) Smith, S. E.; Mellor, P.; Ward, A. K.; Kendall, S.; McDonald, M.; Vizeacoumar, F. S.; Vizeacoumar, F. J.; Napper, S.; Anderson, D. H. *Breast Cancer Res.* **2017**, *19*

(1), 65.

(91) Jernström, S.; Hongisto, V.; Leivonen, S. K.; Due, E. U.; Tadele, D. S.; Edgren, H.; Kallioniemi, O.; Perälä, M.; Mælandsmo, G. M.; Sahlberg, K. K. *Breast Cancer Targets Ther.* **2017**, *9*, 185–198.

(92) Becht, E.; McInnes, L.; Healy, J.; Dutertre, C. A.; Kwok, I. W. H.; Ng, L. G.; Ginhoux, F.; Newell, E. W. *Nat. Biotechnol.* **2019**, *37* (1), 38–47.

(93) Luecken, M. D.; Theis, F. J. *Mol. Syst. Biol.* **2019**, *15* (6).

(94) Li, W.; Freudenberg, J.; Suh, Y. J.; Yang, Y. *Comput. Biol. Chem.* **2014**, *48*, 77–83.

(95) McDermaid, A.; Monier, B.; Zhao, J.; Liu, B.; Ma, Q. *Briefings in Bioinformatics*. Oxford University Press November 1, 2019, pp 2044–2054.

(96) Capaldo, C. T.; Nusrat, A. *Biochim. Biophys. Acta - Biomembr.* **2009**, *1788* (4), 864–871.

(97) Shen, W.-H.; Zhou, J.-H.; Broussard, S. R.; Freund, G. G.; Dantzer, R.; Kelley, K. W. *Cancer Res.* **2002**, 4746–4756.

(98) Yang, J.; Min, K.-W.; Kim, D.-H.; Son, B. K.; Moon, K. M.; Wi, Y. C.; Bang, S. S.; Oh, Y. H.; Do, S.-I.; Chae, S. W.; Oh, S.; Kim, Y. H.; Kwon, M. J. *PLoS One* **2018**, *13* (8), e0202113.

(99) Cai, X.; Cao, C.; Li, J.; Chen, F.; Zhang, S.; Liu, B.; Zhang, W.; Zhang, X.; Ye, L. *Oncotarget* **2017**, *8* (35), 58338–58352.

(100) Mostowy, S.; Shenoy, A. R. *Nat. Rev. Immunol.* **2015**, *15* (9), 559–573.

(101) Wang, W.; Eddy, R.; Condeelis, J. *Nat. Rev. Cancer* **2007**, *7* (6), 429–440.

(102) Nakayama, K. I.; Nakayama, K. *Nat. Rev. Cancer* **2006**, *6* (5), 369–381.

(103) Bassermann, F.; Eichner, R.; Pagano, M. *Biochim. Biophys. Acta - Mol. Cell Res.* **2014**, *1843* (1), 150–162.

(104) Gan, B.; DePinho, R. A. *Cell Cycle* **2009**, *8* (7), 1003–1006.

(105) Laplante, M.; Sabatini, D. M. *J. Cell Sci.* **2009**, *122* (20), 3589–3594.

(106) Kallergi, G.; Tsintari, V.; Sfakianakis, S.; Bei, E.; Lagoudaki, E.; Koutsopoulos, A.; Zacharopoulou, N.; Alkahtani, S.; Alarifi, S.; Stournaras, C.; Zervakis, M.; Georgoulias, V. *Breast Cancer Res.* **2019**, *21* (1), 86.

(107) Hasan, Z.; Koizumi, S. I.; Sasaki, D.; Yamada, H.; Arakaki, N.; Fujihara, Y.; Okitsu, S.; Shirahata, H.; Ishikawa, H. *Nat. Commun.* **2017**, *8*.

(108) Gong, C.; Shen, J.; Fang, Z.; Qiao, L.; Feng, R.; Lin, X.; Li, S. *Biosci. Rep.* **2018**, *38* (4).

(109) Sundqvist, A.; Morikawa, M.; Ren, J.; Vasilaki, E.; Kawasaki, N.; Kobayashi, M.;

Koinuma, D.; Aburatani, H.; Miyazono, K.; Heldin, C. H.; Van Dam, H.; Dijke, P. Ten. *Nucleic Acids Res.* **2018**, *46* (3), 1180–1195.

(110) Mendoza-Rodríguez, M.; Arévalo Romero, H.; Fuentes-Pananá, E. M.; Ayala-Sumuano, J. T.; Meza, I. *Cancer Lett.* **2017**, *390*, 39–44.

(111) Liu, S.; Lee, J. S.; Jie, C.; Park, M. H.; Iwakura, Y.; Patel, Y.; Soni, M.; Reisman, D.; Chen, H. *Cancer Res.* **2018**, *78* (8), 2040–2051.

(112) Korkaya, H.; Kim, G. Il; Davis, A.; Malik, F.; Henry, N. L.; Ithimakin, S.; Quraishi, A. A.; Tawakkol, N.; D'Angelo, R.; Paulson, A. K.; Chung, S.; Luther, T.; Paholak, H. J.; Liu, S.; Hassan, K. A.; Zen, Q.; Clouthier, S. G.; Wicha, M. S. *Mol. Cell* **2012**, *47* (4), 570–584.

(113) Zhang, Z.; Xu, Q.; Song, C.; Mi, B.; Zhang, H.; Kang, H.; Liu, H.; Sun, Y.; Wang, J.; Lei, Z.; Guan, H.; Li, F. *Mol. Cancer Ther.* **2020**, *19* (2), 650–660.

(114) Fagerli, U. M.; Ullrich, K.; Stühmer, T.; Holien, T.; Köchert, K.; Holt, R. U.; Bruland, O.; Chatterjee, M.; Nogai, H.; Lenz, G.; Shaughnessy, J. D.; Mathas, S.; Sundan, A.; Bargou, R. C.; Dörken, B.; Børset, M.; Janz, M. *Oncogene* **2011**, *30* (28), 3198–3206.

(115) Sahoo, S.; Brickley, D. R.; Kocherginsky, M.; Conzen, S. D. *Eur. J. Cancer* **2005**, *41* (17), 2754–2759.

(116) Mistry, P.; Deacon, K.; Mistry, S.; Blank, J.; Patel, R. *J. Biol. Chem.* **2004**, *279* (2), 1482–1490.

(117) Reymond, N.; Im, J. H.; Garg, R.; Cox, S.; Soyer, M.; Riou, P.; Colomba, A.; Muschel, R. J.; Ridley, A. J. *Mol. Oncol.* **2015**, *9* (6), 1043–1055.

(118) Tomaskovic-Crook, E.; Thompson, E. W.; Thiery, J. P. *Breast Cancer Res.* **2009**, *11* (6), 213.

(119) Kalluri, R.; Weinberg, R. A. *J. Clin. Invest.* **2009**, *119* (6), 1420–1428.

(120) Pastushenko, I.; Blanpain, C. *Trends Cell Biol.* **2019**, *29* (3), 212–226.

(121) Chu, P. G.; Weiss, L. M. *Histopathology* **2002**, *40* (5), 403–439.

(122) Xiang, X.; Deng, Z.; Zhuang, X.; Ju, S.; Mu, J.; Jiang, H.; Zhang, L.; Yan, J.; Miller, D.; Zhang, H.-G. *PLoS One* **2012**, *7* (12), e50781.

(123) Schmalhofer, O.; Brabletz, S.; Brabletz, T. *Cancer Metastasis Rev.* **2009**, *28* (1–2), 151–166.

(124) Zhang, S.; Wang, Z.; Liu, W.; Lei, R.; Shan, J.; Li, L.; Wang, X. *Sci. Rep.* **2017**, *7*.

(125) Nasser, M. W.; Qamri, Z.; Deol, Y. S.; Ravi, J.; Powell, C. A.; Trikha, P.; Schwendener, R. A.; Bai, X. F.; Shilo, K.; Zou, X.; Leone, G.; Wolf, R.; Yuspa, S. H.; Ganju, R. K. *Cancer Res.* **2012**, *72* (3), 604–615.

(126) West, N. R.; Watson, P. H. *Oncogene* **2010**, *29* (14), 2083–2092.

(127) Paruchuri, V.; Prasad, A.; McHugh, K.; Bhat, H. K.; Polyak, K.; Ganju, R. K. *PLoS One* **2008**, *3* (3), 1741.

(128) Emberley, E. D.; Murphy, L. C.; Watson, P. H. *Breast Cancer Res.* **2004**, *6* (4), 153–159.

(129) Cancemi, P.; Buttacavoli, M.; Cara, G. Di; Albanese, N. N.; Bivona, S.; Pucci-Minafra, I.; Feo, S. *Oncotarget* **2018**, *9* (49), 29064–29081.

(130) Hua, X.; Zhang, H.; Jia, J.; Chen, S.; Sun, Y.; Zhu, X. *Biomed. Pharmacother.* **2020**, *127*, 110156.

(131) Yuzugullu, H.; Von, T.; Thorpe, L. M.; Walker, S. R.; Roberts, T. M.; Frank, D. A.; Zhao, J. J. *Cell Discov.* **2016**, *2* (1), 1–13.

(132) Sadasivam, S.; DeCaprio, J. A. *Nat. Rev. Cancer* **2013**, *13* (8), 585–595.

(133) Min, M.; Spencer, S. L. *PLOS Biol.* **2019**, *17* (3), e3000178.

(134) Bracken, A. P.; Ciro, M.; Cocito, A.; Helin, K. *Trends Biochem. Sci.* **2004**, *29* (8), 409–417.

(135) Ito, T.; Teo, Y. V.; Evans, S. A.; Neretti, N.; Sedivy Correspondence, J. M. *Cell Rep.* **2018**, *22*, 3480–3492.

(136) Vizán, P.; Gutiérrez, A.; Espejo, I.; García-Montolio, M.; Lange, M.; Carretero, A.; Lafzi, A.; de Andrés-Aguayo, L.; Blanco, E.; Thambyrajah, R.; Graf, T.; Heyn, H.; Bigas, A.; Di Croce, L. *Sci. Adv.* **2020**, *6* (32), eabb2745.

(137) Doyle, L. A.; Ross, D. D. *Oncogene* **2003**, *22* (47 REV. ISS. 6), 7340–7358.

(138) Balaji, S. A.; Udupa, N.; Chamallamudi, M. R.; Gupta, V.; Rangarajan, A. *PLoS One* **2016**, *11* (5).

(139) Lucanus, A. J.; Yip, G. W. *Nat. Publ. Gr.* **2018**.

(140) Mandelkow, E.; Mandelkow, E. M. *Trends Cell Biol.* **2002**, *12* (12), 585–591.

(141) Ivanov, A. I.; McCall, I. C.; Babbin, B.; Samarin, S. N.; Nusrat, A.; Parkos, C. A. *BMC Cell Biol.* **2006**, *7* (1), 12.

(142) Li, T.-F.; Zeng, H.-J.; Shan, Z.; Ye, R.-Y.; Cheang, T.-Y.; Zhang, Y.-J.; Lu, S.-H.; Zhang, Q.; Shao, N.; Lin, Y. .

(143) Hirokawa, N.; Noda, Y.; Tanaka, Y.; Niwa, S. *Nat. Rev. Mol. Cell Biol.* **2009**, *10* (10), 682–696.

(144) Li, B.; Dou, S. X.; Yuan, J. W.; Liu, Y. R.; Li, W.; Ye, F.; Wang, P. Y.; Li, H. *Proc. Natl. Acad. Sci. U. S. A.* **2018**, *115* (48), 12118–12123.

(145) Kwon, M. J.; Park, S.; Choi, J. Y.; Oh, E.; Kim, Y. J.; Park, Y. H.; Cho, E. Y.; Kwon, M. J.; Nam, S. J.; Im, Y. H.; Shin, Y. K.; Choi, Y. L. *Br. J. Cancer* **2012**, *106* (5), 923–930.

(146) Yang, X. H.; Richardson, A. L.; Torres-Arzayus, M. I.; Zhou, P.; Sharma, C.; Kazarov, A. R.; Andzelm, M. M.; Strominger, J. L.; Brown, M.; Hemler, M. E. *Cancer Res.* **2008**, *68* (9), 3204–3213.

(147) Kumar, S.; Park, S. H.; Cieply, B.; Schupp, J.; Killiam, E.; Zhang, F.; Rimm, D. L.; Frisch, S. M. *Mol. Cell. Biol.* **2011**, *31* (19), 4036–4051.

(148) Rasiah, P. K.; Maddala, R.; Bennett, V.; Rao, P. V. *Dev. Biol.* **2019**, *446* (1), 119–131.

(149) Kurozumi, S.; Joseph, C.; Raafat, S.; Sonbul, S.; Kariri, Y.; Alsaeed, S.; Pigera, M.; Alsaleem, M.; Nolan, C. C.; Johnston, S. J.; Aleskandarany, M. A.; Ogden, A.; Fujii, T.; Shirabe, K.; Martin, S. G.; Alshankyty, I.; Mongan, N. P.; Ellis, I. O.; Green, A. R.; Rakha, E. A. *Breast Cancer Res. Treat.* **2019**, *176* (1), 63–73.

(150) Gröger, C. J.; Grubinger, M.; Waldhör, T.; Vierlinger, K.; Mikulits, W. *PLoS One* **2012**, *7* (12), e51136.

(151) Mrouj, K.; Singh, P.; Sobecki, M.; Dubra, G.; Ghoul, E. Al; Aznar, A.; Prieto, S.; Vincent, C.; Pirot, N.; Bernex, F.; Bordignon, B.; Hassen-Khodja, C.; Pouzolles, M.; Zimmerman, V.; Dardalhon, V.; Villalba, M.; Krasinska, L.; Fisher, D. *bioRxiv* **2019**, 712380.

(152) Mani, S. A.; Guo, W.; Liao, M. J.; Eaton, E. N.; Ayyanan, A.; Zhou, A. Y.; Brooks, M.; Reinhard, F.; Zhang, C. C.; Shipitsin, M.; Campbell, L. L.; Polyak, K.; Brisken, C.; Yang, J.; Weinberg, R. A. *Cell* **2008**, *133* (4), 704–715.

(153) Foroni, C.; Broggini, M.; Generali, D.; Damia, G. *Cancer Treat. Rev.* **2012**, *38* (6), 689–697.

(154) Collier, M. P.; Benesch, J. L. P. *Cell Stress Chaperones* **2020**, *25* (4), 601–613.

(155) Gunning, P. W.; Hardeman, E. C.; Lappalainen, P.; Mulvihill, D. P. *J. Cell Sci.* **2015**, *128* (16), 2965–2974.

(156) Chou, D. M.; Elledge, S. J. *Proc. Natl. Acad. Sci. U. S. A.* **2006**, *103* (48), 18143–18147.

(157) Kröger, C.; Afeyan, A.; Mraz, J.; Eaton, E. N.; Reinhardt, F.; Khodor, Y. L.; Thiru, P.; Bierie, B.; Ye, X.; Burge, C. B.; Weinberg, R. A. *Proc. Natl. Acad. Sci. U. S. A.* **2019**, *116* (15), 7353–7362.

(158) Xiao, W.; Zheng, S.; Xie, X.; Li, X.; Zhang, L.; Yang, A.; Wang, J.; Tang, H.; Xie, X. *Mol. Ther. - Oncolytics* **2020**, *17*, 118–129.

(159) Wang, C. Q.; Tang, C. H.; Wang, Y.; Jin, L.; Wang, Q.; Li, X.; Hu, G. N.; Huang, B. F.; Zhao, Y. M.; Su, C. M. *Sci. Rep.* **2017**, *7* (1).

(160) Nami, B.; Wang, Z. *Cancers (Basel).* **2018**, *10* (8), 274.

(161) Ebright, R. Y.; Lee, S.; Wittner, B. S.; Niederhoffer, K. L.; Nicholson, B. T.; Bardia, A.; Truesdell, S.; Wiley, D. F.; Wesley, B.; Li, S.; Mai, A.; Aceto, N.; Vincent-Jordan, N.; Szabolcs, A.; Chirn, B.; Kreuzer, J.; Comaills, V.; Kalinich, M.; Haas,

W.; Ting, D. T.; Toner, M.; Vasudevan, S.; Haber, D. A.; Maheswaran, S.; Micalizzi, D. S. *Science (80-.).* **2020**, *367* (6485), 1468–1473.

(162) Prashar, A.; Schnettger, L.; Bernard, E. M.; Gutierrez, M. G. *Front. Cell. Infect. Microbiol.* **2017**, *7* (SEP), 435.

(163) Barbera, S.; Nardi, F.; Elia, I.; Realini, G.; Lugano, R.; Santucci, A.; Tosi, G. M.; Dimberg, A.; Galvagni, F.; Orlandini, M. *Cell Commun. Signal.* **2019**, *17* (1), 55.

(164) Kim, S. E.; Hinoue, T.; Kim, M. S.; Sohn, K. J.; Cho, R. C.; Cole, P. D.; Weisenberger, D. J.; Laird, P. W.; Kim, Y. I. *Genes Nutr.* **2015**, *10* (1), 1–17.

(165) Maggini, S.; Pierre, A.; Calder, P. C. *Nutrients* **2018**, *10* (10).

(166) MacEyka, M.; Spiegel, S. *Nature* **2014**, *510* (7503), 58–67.

(167) Waumans, Y.; Baerts, L.; Kehoe, K.; Lambeir, A. M.; De Meester, I. *Front. Immunol.* **2015**, *6* (JUL), 387.

(168) Kingsbury, S. R.; Loddo, M.; Fanshawe, T.; Obermann, E. C.; Prevost, A. T.; Stoeber, K.; Williams, G. H. *Exp. Cell Res.* **2005**, *309* (1), 56–67.

(169) Gookin, S.; Min, M.; Phadke, H.; Chung, M.; Moser, J.; Miller, I.; Carter, D.; Spencer, S. L. *PLOS Biol.* **2017**, *15* (9), e2003268.

(170) Kabraji, S.; Solé, X.; Huang, Y.; Bango, C.; Bowden, M.; Bardia, A.; Sgroi, D.; Loda, M.; Ramaswamy, S. *Breast Cancer Res.* **2017**, *19* (1), 88.

(171) Le, X. F.; Lammayot, A.; Gold, D.; Lu, Y.; Mao, W.; Chang, T.; Patel, A.; Mills, G. B.; Bast, R. C. *J. Biol. Chem.* **2005**, *280* (3), 2092–2104.

(172) Sun, H.; Liu, K.; Huang, J.; Sun, Q.; Shao, C.; Luo, J.; Xu, L.; Shen, Y.; Ren, B. *Onco. Targets. Ther.* **2019**, *Volume 12*, 2829–2842.

(173) FAM111B gene - Genetics Home Reference - NIH https://ghr.nlm.nih.gov/gene/FAM111B (accessed Aug 8, 2020).

(174) Chung, V. Y.; Tan, T. Z.; Ye, J.; Huang, R. L.; Lai, H. C.; Kappei, D.; Wollmann, H.; Guccione, E.; Huang, R. Y. J. *Commun. Biol.* **2019**, *2* (1), 1–15.

(175) Jolly, M. K.; Tripathi, S. C.; Jia, D.; Mooney, S. M.; Celiktas, M.; Hanash, S. M.; Mani, S. A.; Pienta, K. J.; Ben-Jacob, E.; Levine, H. *Oncotarget* **2016**, *7* (19), 27067–27084.

(176) Cieply, B.; Riley IV, P.; Pifer, P. M.; Widmeyer, J.; Addison, J. B.; Ivanov, A. V.; Denvir, J.; Frisch, S. M. *Cancer Res.* **2012**, *72* (9), 2440–2453.

(177) Mooney, S. M.; Talebian, V.; Jolly, M. K.; Jia, D.; Gromala, M.; Levine, H.; McConkey, B. J. *J. Cell. Biochem.* **2017**, *118* (9), 2559–2570.

(178) Sánchez-Tilló, E.; De Barrios, O.; Siles, L.; Cuatrecasas, M.; Castells, A.; Postigo, A. *Proc. Natl. Acad. Sci. U. S. A.* **2011**, *108* (48), 19204–19209.

(179) Lee, J.; Ouh, Y.; Ahn, K. H.; Hong, S. C.; Oh, M.; Kim, J.; Cho, G. J. *PLoS One*

2017, *12* (5), 1–8.

(180) Gajria, D.; Chandarlapaty, S. *Expert Rev. Anticancer Ther.* **2011**, *11* (2), 263–275.

(181) Asgari, A.; Sharifzadeh, S.; Ghaderi, A.; Hosseini, A.; Ramezani, A. *Mol. Biol. Rep.* **2019**, *46* (6), 6205–6213.

(182) Dang, C. V. *Cell* **2012**, *149* (1), 22–35.

(183) Stine, Z. E.; Walton, Z. E.; Altman, B. J.; Hsieh, A. L.; Dang, C. V. *Cancer Discov.* **2015**, *5* (10), 1024–1039.

(184) Chen, H.; Liu, H.; Qing, G. *Signal Transduct. Target. Ther.* **2018**, *3* (1), 1–7.

(185) Gabay, M.; Li, Y.; Felsher, D. W. *Cold Spring Harb. Perspect. Med.* **2014**, *4* (6), 1–14.

(186) Richart, L.; Carrillo-de Santa Pau, E.; Río-Machín, A.; de Andrés, M. P.; Cigudosa, J. C.; Lobo, V. J. S.-A.; Real, F. X. *Nat. Commun.* **2016**, *7*, 10153.

(187) Dang, C. V. **2013**, 1–15.

(188) Bouvard, C.; Lim, S. M.; Ludka, J.; Yazdani, N.; Woods, A. K.; Chatterjee, A. K.; Schultz, P. G.; Zhu, S. *Proc. Natl. Acad. Sci. U. S. A.* **2017**, *114* (13), 3497–3502.

(189) Tawani, A.; Mishra, S. K.; Kumar, A. *Sci. Rep.* **2017**, *7* (1), 1–13.

(190) Mathad, R. I.; Hatzakis, E.; Dai, J.; Yang, D. *Nucleic Acids Res.* **2011**, *39* (20), 9023–9033.

(191) Siddiqui-Jain, A.; Grand, C. L.; Bearss, D. J.; Hurley, L. H. *Proc. Natl. Acad. Sci. U. S. A.* **2002**, *99* (18), 11593–11598.

(192) Castell, A.; Yan, Q.; Karin, F.; Hydbring, P.; Zhang, F.; Verschut, V.; Franco, M.; Zakaria, S. M.; Bazzar, W.; Goodwin, J.; Zinzalla, G.; Larson, L.-G. *Sci. Rep.* **2018**, *8* (May), 1–17.

(193) Kiessling, A.; Sperl, B.; Hollis, A.; Eick, D.; Berg, T. *Chem. Biol.* **2006**, *13* (7), 745–751.

(194) Berg, T.; Cohen, S. B.; Desharnais, J.; Sonderegger, C.; Maslyar, D. J.; Goldberg, J.; Boger, D. L.; Vogt, P. K. *Proc. Natl. Acad. Sci. U. S. A.* **2002**, *99* (6), 3830–3835.

(195) Whitfield, J. R.; Beaulieu, M. E.; Soucek, L. *Front. Cell Dev. Biol.* **2017**, *5* (FEB), 10.

(196) Castell, A.; Larsson, L. *Cancer Discov.* **2015**, *5* (7), 701–704.

(197) Carabet, L. A.; Rennie, P. S.; Cherkasov, A. *Int. J. Mol. Sci.* **2019**, *20* (1).

(198) Dang, C. V.; Reddy, E. P.; Shokat, K. M.; Soucek, L. *Nat. Rev. Cancer* **2017**, *17* (8), 502–508.

(199) McKeown, M. R.; Bradner, J. E. *Cold Spring Harb. Perspect. Med.* **2014**, *4* (10).

(200) Thomas, L. R.; Wang, Q.; Grieb, B. C.; Phan, J.; Foshage, A. M.; Sun, Q.; Olejniczak, E. T.; Clark, T.; Dey, S.; Lorey, S.; Alicie, B.; Howard, G. C.; Cawthon, B.; Ess, K. C.; Eischen, C. M.; Zhao, Z.; Fesik, S. W.; Tansey, W. P. *Mol. Cell* **2015**, *58* (3), 440–452.

(201) Thomas, L. R.; Tansey, W. P. *Open Access J. Sci. Technol.* **2015**, *3*, 1–25.

(202) Karatas, H.; Townsend, E. C.; Bernard, D.; Dou, Y.; Wang, S. *J. Med. Chem.* **2010**, *53*, 5179–5185.

(203) Odho, Z.; Southall, S. M.; Wilson, J. R. *J. Biol. Chem.* **2010**, *285* (43), 32967–32976.

(204) Dias, J.; Nguyen, N. Van; Georgiev, P.; Gaub, A.; Brettschneider, J.; Cusack, S.; Kadlec, J.; Akhtar, A. *Genes Dev.* **2014**, *28*, 929–942.

(205) Scott, D. E.; Coyne, A. G.; Hudson, S. A.; Abell, C. *Biochemistry* **2012**, *51*, 4990–5003.

(206) Murray, C. W.; Verdonk, M. L.; Rees, D. C. *Trends Pharmacol. Sci.* **2012**, *33* (5), 224–232.

(207) Huynh, K.; Partch, C. L. *Curr. Protoc. protein Sci.* **2015**, *79*, 28.9.1-28.9.14.

(208) Niesen, F. H.; Berglund, H.; Vedadi, M. *Nat. Protoc.* **2007**, *2* (9), 2212–2221.

(209) Jhoti, H.; Williams, G.; Rees, D. C.; Murray, C. W. *Nat. Publ. Gr.* **2013**, No. July.

(210) Kirsch, P.; Hartman, A. M.; Hirsch, A. K. H.; Empting, M. *Molecules* **2019**, *24* (23).

(211) Aldrich, C.; Bertozzi, C.; Georg, G. I.; Kiessling, L.; Lindsley, C.; Liotta, D.; Merz, K. M.; Schepartz, A.; Wang, S. *J. Med. Chem.* **2017**, *60* (6), 2165–2168.

(212) Zhang, Ji-hu, Chung, Thomas D.Y., Oldenburg, K. R. *J. Biomol. Screen.* **1999**, *4* (2), 67–73.

(213) Jacob, R. T.; Larsen, M. J.; Larsen, S. D.; Kirchhoff, P. D.; Sherman, D. H.; Neubig, R. R. *J. Biomol. Screen.* **2012**, *17* (8), 1080–1087.

(214) Karatas, H.; Townsend, E. C.; Cao, F.; Chen, Y.; Bernard, D.; Liu, L.; Lei, M.; Dou, Y.; Wang, S. *J. Am. Chem. Soc.* **2013**, *135* (2), 669–682.

(215) Cao, F.; Townsend, E. C.; Karatas, H.; Xu, J.; Li, L.; Lee, S.; Liu, L.; Chen, Y.; Ouillette, P.; Zhu, J.; Hess, J. L.; Atadja, P.; Lei, M.; Qin, Z. S.; Malek, S.; Wang, S.; Dou, Y. *Mol. Cell* **2014**, *53* (2), 247–261.

(216) Lea, W. A.; Simeonov, A. *Expert Opin. Drug Discov.* **2011**, *6* (1), 17–32.

(217) Rossi, A. M.; Taylor, C. W. *Nat. Protoc.* **2011**, *6* (3), 365–387.

(218) Hall, M. D.; Yasgar, A.; Peryea, T.; Braisted, J. C.; Jadhav, A.; Simeonov, A.; Coussens, N. P. *Methods Appl. Fluoresc.* **2016**, *4* (2), 022001.

(219) Koh, C. M.; Sabò, A.; Guccione, E. *BioEssays* **2016**, *38* (3), 266–275.

(220) Casey, S. C.; Tong, L.; Li, Y.; Do, R.; Walz, S.; Fitzgerald, K. N.; Gouw, A. M.; Baylot, V.; Gütgemann, I.; Eilers, M.; Felsher, D. W. *Science (80-.).* **2016**, *352* (6282), 227–231.

(221) Polivka, J.; Janku, F. *Pharmacol. Ther.* **2014**, *142* (2), 164–175.

(222) Chacón Simon, S.; Wang, F.; Thomas, L. R.; Phan, J.; Zhao, B.; Olejniczak, E. T.; MacDonald, J. D.; Shaw, J. G.; Schlund, C.; Payne, W.; Creighton, J.; Stauffer, S. R.; Waterson, A. G.; Tansey, W. P.; Fesik, S. W. *J. Med. Chem.* **2020**, *63* (8), 4315–4333.

(223) Macdonald, J. D.; Chacón Simon, S.; Han, C.; Wang, F.; Shaw, J. G.; Howes, J. E.; Sai, J.; Yuh, J. P.; Camper, D.; Alicie, B. M.; Alvarado, J.; Nikhar, S.; Payne, W.; Aho, E. R.; Bauer, J. A.; Zhao, B.; Phan, J.; Thomas, L. R.; Rossanese, O. W.; Tansey, W. P.; Waterson, A. G.; Stauffer, S. R.; Fesik, S. W. *J. Med. Chem.* **2019**, *62* (24), 11232–11259.